Identification of components and substrates of Snf1-related kinase 1 (SnRK1) complexes in *Arabidopsis thaliana*

Dissertation

Zur Erlangung des Doktorgrades (Dr. rer. nat.)

der

Mathematisch-Naturwissenschaftlichen Fakultät

der

Rheinischen Friedrich-Wilhelms-Universität Bonn

vorgelegt von

Bing Bai

aus ChangChun, Jilin, China

Bonn, 2018

Angefertigt mit Genehmigung der Mathematisch-Naturwissenschaftlichen Fakultät der Rheinischen Friedrich-Wilhelms-Universität Bonn

Gedruckt mit Unterstützung des Deutschen Akademischen Austauschdienstes

1. Gutachter: Prof. Dr. Dorothea Bartels

2. Gutachter: Dr. Csaba Koncz

Tag der mündlichen prüfung: Feburary 06, 2019
Erscheinungsjahr: 2019

ERKLÄRUNG

Hiermit erkläre ich an Eides statt, dass ich für meine Promotion keine anderen als die angegebenen Hilfsmittel benutzt habe, und dass die inhaltlich und wörtlich aus anderen Werken entnommenen Stellen und Zitate als solche gekennzeichnet sind.

Bing Bai

Bonn, November 2018 **----------**

Contents

Figures

Tables

Abbreviations and symboles

A	adenine
ABA	abscisic acid
Ac	acetate
ACC	1-aminocyclopropanol-1-carboxylic acid
ADP	adenosine 5'-diphosphate
amiRNA	artificial microRNA
AMP	adenosine 5'-monophosphate
A. thaliana	*Arabidopsis thaliana*
ATP	adenosine 5'-triphosphate
ATPase	adenosine 5'-triphosphatase
bp	base pair
BR	brassinosteroids
BSA	bovine serum albumin
C	cytosine
°C	grad Celsius
CaMV	Cauliflower Mosaic Virus
cDNA	complementary DNA
C-terminal	carboxyl terminal
DAPI	4,6-diamine-2-phenylindole dihydrochloride
DMSO	dimethyl sulfoxide
DNA	deoxyribonucleic acid
dNTP	deoxyribonucleotide triphosphate
DTT	dithiotreitol
E. coli	*Escherichia coli*
EDTA	ethylenediaminetetraacetic acid
EtBr	ethidium bromide
EtOH	ethanol
G	guanine
GA	gibberellin
g	gram
g	relative centrifugal field unit
GST	glutathione-S-transferase
h	hour
IAA	indole-3-acetic acid
IgG	immunoglobuline G
JA	jasmonate
kb	kilobase
kDa	kilo Dalton (1,000 Da)
l	liter
M	Molar
µg	microgram

µl	microliter
µM	micromolar
mA	milliampere
mg	milligram
min.	minute
ml	milliliter
mM	millimolar
mRNA	messenger RNA
nt	nucleotide
N-terminal	amino terminal
N-terminus	amino terminus
OD	optical density
O/N	overnight
PAGE	polyacrylamide gel electrophoresis
PCR	polymerase chain reaction
PEG	polyethylene glycol
pH	negative logarithm of the proton concentration
PRL1	*PLEIOTROPIC REGULATORY LOCUS 1*
RNA	ribonucleic acid
RNase	ribonuclease
ROS	reactive oxygen species
rpm	revolution per minute
RT	room temperature
S. cerevisiae	*Saccharomyces cerevisiae*
SA	salicylic acid
SDS	sodium dodecylsulfate
TAE	Tris-acetate (40 mM); EDTA (1mM)
TE	Tris.HCl (10mM); EDTA (1mM)
TEMED	N,N,N',N' tetramethylenethylendiamine
Tris	Tris(hydroxymethyl) aminomethane
U	unit
Ub	ubiquitin
UTR	untranslated region
UV	ultraviolet light
V	Volt
vol.	volume
wt	wild type

Aminoacids

A	Ala	Alanine
C	Cys	Cysteine
D	Asp	Aspartic acid
E	Glu	Glutamic acid
F	Phe	Phenylalanine
G	Gly	Glycine
H	His	Histidine

I	Ile	Isoleucine
K	Lys	Lysine
L	Leu	Leucine
M	Met	Methionine
N	Asn	Asparagine
P	Pro	Proline
Q	Gln	Glutamine
R	Arg	Arginine
S	Ser	Serine
T	Thr	Threonine
V	Val	Valine
W	Trp	Trptophan
Y	Tyr	Tyrosine

Summary

Similarly to yeast Sucrose nonfermenting 1 (Snf1) and animal AMP-activated protein kinases (AMPKs), plant Snf1-related (SnRK1) kinases play a central role in the regulation of cellular energy homeostasis and responses to carbon source availability. Members of the Snf1/SnRK1/AMPK family are differentially activated by carbon source depletion and increasing AMP/ATP ratio to confer down-regulation of energy consuming anabolic pathways and parallel activation of energy producing processes by phosphorylation of key metabolic enzymes and transcription factors. Inhibition of photosynthetic CO_2 fixation and ATP production stimulates plant SnRK1 activation in leaves, which provide sucrose as main transported sugar for developing sink organs. Sensing of sucrose availability by conversion of its metabolic products to trehalose-6-phosphate (T6P) is reported to inhibit SnRK1 through a yet unknown protein factor. As Snf1 and AMPKs, Arabidopsis SnRK1 enzymes form trimeric complexes with activating γ/SNF4 and substrate targeting β1/2/3-subunits. SnRK1 activity is stimulated by T-loop phosphorylation of catalytic α-subunits AKIN10/11 by upstream activating kinases and inhibited through dephosphorylation by PP2C protein phosphatases acting in ABA/sugar signaling. Our current knowledge on plant SnRK1 kinases is largely based on protein-protein interaction assays in heterologous systems, and transcriptomics and phosphoproteomics studies using antisense inhibition and overexpression of SnRK1 catalytic subunits in leaf protoplasts and seedlings carrying various mutations in metabolic and hormonal pathways.

A major goal of this Ph.D. work was to use precisely modified native gene constructs for expression of SnRK1 subunits in fusion with suitable tags, such as green and red fluorescent proteins (GFP and mCherry) in plants, and exploit this technology for purification of SnRK1 complexes and identification of their interacting partners. By enlarging the ATP-binding pocket of SnRK1α1 subunit AKIN10, an analog-sensitive AS-kinase carrying a combined affinity tag (GFPPIPL) was constructed by recombineering-based site-directed mutagenesis and expressed in plants. Unlike other kinases in Arabidopsis, the AS-AKIN10 kinase can catalyze phosphorylation of substrates with bulky N^6-substituted thioATP derivatives, which can be specifically detected, enriched and identified by mass spectrometry.

Our study demonstrates that exchange of the phosphorylated T-loop Thr175 residue of AKIN10 to A and D/E residues results only in partial inactivation and limited stimulation of substrate phosphorylation activity of SnRK1 *in vitro* and, upon ectopic expression of cDNA constructs by a CaMV35S promoter *in vivo*, respectively. Ectopic expression of wild type and T-loop mutant versions of AKIN10 resulted only in minor developmental changes, including earlier flowering on short day, and enhanced root and hypocotyl elongation in the case of T175D T-loop AKIN10 derivative. Expression of AKIN10-GFP/PIPL and SNF4-YFP constructs by native genes provided suitable materials for affinity purification of SnRK1 complexes and identification of their interacting partners by mass spectrometry. In addition to previously described two-hybrid interacting partners, such as the HSPRO2 and DUF581

domain proteins, these studies confirmed reciprocal co-immunoprecipitation and association of class II trehalose synthase/ phosphatase (TPS) enzymes with SnRK1. Dimerization of trimeric SnRK1 enzymes was detected in cytoplasmic complexes. Association of SnRK1 with TPS partners, such as TPS8, was found to confer UDP-glucose and T6P mediated inhibition of SnRK1. This indicated that class II TPS enzymes might serve as metabolic sensors, which negatively regulate SnRK1 in response to the availability of sucrose-derived metabolic signals. However, using a nuclear protein purification approach optimized for the isolation of NTC spliceosome-activating complex and associated spliceosome components, we failed to identify novel interacting partners of SnRK1. Optimization of *in situ* kinase reactions in isolated nuclei and nuclear extracts, as well as enrichment of thiophosphorylated substrates of the analog-sensitive AS-AKIN10 kinase, nevertheless resulted in the identification of several novel candidate SnRK1 substrates. One of these, the nuclear NAP57/CBF5/DYSKERIN pseudouridine synthase involved in the regulation of telomere length and ribosome biogenesis was found to be phosphorylated in its catalytic domain by SnRK1. Further analysis of AS-kinase substrates and components of nuclear kinase complexes is expected to provide deeper insight into transcription targets and regulatory roles of plant SnRK1.

Zusammenfassung

Pflanzliche Snf1-verwandte (SnRK1)-Kinasen, wie Sucrose Non-fermenting 1 (Snf1) in Hefe und AMP-aktivierten Proteinkinasen (AMPKs) in Säugetieren, spielen eine zentrale Rolle bei der Regulation der zellulären Energiehomöostase und steuern die Reaktionen auf die Verfügbarkeit von Kohlenstoffquellen. Mitglieder der Snf1/SnRK1/AMPK-Familie werden sowohl durch die Abnahme von Kohlenstoffquellen als auch durch die Erhöhung des AMP/ATP-Verhältnisses differentiell aktiviert, um die Herabregulierung energieverbrauchender anabolischer Stoffwechselwege und die parallele Aktivierung energieerzeugender Prozesse durch Phosphorylierung von wichtigen metabolischen Enzymen und Transkriptionsfaktoren zu ermöglichen. Inhibierung der photosynthetischen CO_2-Fixierung und der ATP-Produktion stimulieren die Aktivierung der pflanzlichen SnRK1 in Blättern, welche Saccharose als Haupttransportzucker für die Entwicklung von Sinkorganen bereitstellen. Studien zufolge führt die Erfassung der Saccharoseverfügbarkeit durch Umwandlung seiner Stoffwechselprodukte in Trehalose-6-phosphat (T6P) zu Inhibierung von SnRK1 durch einen noch unbekannten Proteinfaktor. Ebenso wie Snf1 und AMPKs bilden Arabidopsis-SnRK1-Enzyme trimere Komplexe mit aktivierenden γ / SNF4- und Substrat-Targeting-β1 / 2/3-Untereinheiten. Die SnRK1-Aktivität wird durch T-Loop-Phosphorylierung der katalytischen α-Untereinheiten AKIN10 / 11 durch Upstream-Aktivierungskinasen stimuliert und durch Dephosphorylierung durch PP2C-Proteinphosphatasen, die in ABA und Zuckersignalisierung agieren, inhibiert. Unser aktueller Wissenstand bezüglich pflanzlicher SnRK1-Kinasen basiert weitgehend auf Protein-Protein-Interaktionstests in heterologen Systemen und Transkriptom- und Phosphoproteomik-Analysen unter Verwendung von Antisense-Inhibierung und Überexpression von SnRK1-katalytischen Untereinheiten in Blattprotoplasten und Keimlingen, die verschiedene Mutationen in Stoffwechsel- und Hormonpfaden tragen. Das Hauptziel dieser Doktorarbeit bestand in der Applikation von genau modifizierten nativen Genkonstrukten zur Expression von SnRK1-Untereinheiten in Fusion mit geeigneten Markierungen wie grünen und roten Fluoreszenzproteinen (GFP und mCherry) in Pflanzen und folglich in der Identifikation ihrer interagierenden Partner. Durch Vergrößerung der ATP-Bindungstasche der SnRK1α1-Untereinheit AKIN10 wurde eine analog-sensitive AS-Kinase, die einen kombinierten Affinitätsmarker (GFPPIPL) trug, mit zielgerichteter Mutagenese durch Recombineering entwickelt und in Pflanzen exprimiert. Im Gegensatz zu anderen Kinasen in Arabidopsis kann die AS-AKIN10-Kinase die Phosphorylierung von Substraten mit sperrigen N6-substituierten ThioATP-Derivaten katalysieren, die durch Massenspektrometrie spezifisch nachgewiesen, angereichert und identifiziert werden können. Unsere Studie zeigt, dass der Austausch des phosphorylierten T-Loop-Thr175-Rests von AKIN10 gegen A- und D/E-Reste nur zu einer partiellen Inaktivierung und begrenzten Stimulation der Substratphosphorylierungsaktivität von SnRK1 *in vitro* führt, selbst bei ektopischer Expression von cDNA-Konstrukten durch einen CaMV35S-Promotor *in vivo*. Die ektopische Expression von Wildtyp- und T-Loop-Mutantenversionen von AKIN10 führte nur zu geringfügigen Entwicklungsänderungen,

einschließlich früherer Blüte unter Kurztagsbedingungen, und verstärkte Wurzel- und Hypocotyl-Verlängerung im Fall des T175D-T-Loop-AKIN10-Derivats. Die Expression von AKIN10-GFP / PIPL- und SNF4-YFP-Konstrukten durch native Gene lieferte geeignete Materialien für die Affinitätsreinigung von SnRK1-Komplexen und die Identifizierung ihrer interagierenden Partner durch Massenspektrometrie. Zusätzlich zu den zuvor beschriebenen Zwei-Hybrid-Interaktionspartnern, wie den HSPRO2- und DUF581-Domänenproteinen, bestätigten diese Studien die gegenseitige Co-Immunopräzipitation und die Assoziation von Klasse-II-Trehalosesynthase / Phosphatase (TPS) -Enzymen mit SnRK1. Dimerisierung von trimeren SnRK1-Enzymen wurde in zytoplasmatischen Komplexen nachgewiesen. Zudem wurde aufgedeckt, dass die Assoziation von SnRK1 mit TPS-Partnern wie TPS8 UDP-Glucose und T6P-vermittelte die Hemmung von SnRK1 zur Folge hat. Dies deutet darauf hin, dass TPS-Enzyme der Klasse II als metabolische Sensoren dienen könnten, die SnRK1 als Reaktion auf die Verfügbarkeit von Sucrose und denen daraus abgeleiteten metabolischen Signalen negativ regulieren. Bei der Verwendung eines nuklearen Proteinreinigungsansatzes, der für die Isolierung des NTC-Spliceosomen-Aktivierungskomplexes und der zugehörigen Spliceosomenkomponenten optimiert wurde, konnten jedoch keine neuen interagierenden Partner von SnRK1 identifiziert werden. Die Optimierung von In-situ-Kinase-Reaktionen in isolierten Kernen und Kernextrakten sowie die Anreicherung thiophosphorylierter Substrate der analogempfindlichen AS-AKIN10-Kinase führten dennoch zur Identifizierung mehrerer neuartiger Kandidaten für SnRK1-Substrate. Eines davon, die nukleare NAP57 / CBF5 / DYSKERIN-Pseudouridinsynthase, die an der Regulation der Telomerlänge und der Ribosomenbiogenese beteiligt ist, wurde in ihrer katalytischen Domäne durch SnRK1 phosphoryliert. Es ist annehmbar, dass die weitere Analysen von AS-Kinase-Substraten und -Komponenten von Kernkinase-Komplexen tiefere Einblicke in die Transkriptionsziele und die regulatorischen Rollen von SnRK1 in Pflanzen ermöglichen.

1. Introduction

In all living organisms, adenosine triphosphate (ATP) is the major carrier and storage form of cellular energy, which is utilized in growth promoting anabolic reactions, intracellular transport, cell motility, division and many other pathways supporting cell viability. Maintenance of energy homeostasis is thus tightly linked to monitoring ATP consumption resulting in ultimate accumulation of AMP. In cells of non-photosynthetic organisms, the major source of energy is glucose. All carbohydrates are converted to glucose and catabolic intermediates, which are generated during its degradation producing ATP under either anaerobic or aerobic condition. By acquiring mitochondria of prokaryotic origin during evolution, glucose degradation was linked to ATP producing oxidative phosphorylation in eukaryotes. Cellular catabolism of alternative carbon sources (e.g., polysaccharides, lipids, proteins etc.) coupled to the citrate/Krebs cycle of mitochondria offered an alternative mode for higher rate of ATP production and gluconeogenesis under aerobic conditions. Under anaerobic condition however glucose remained a preferred substrate which, when present, acts as signaling molecule conferring transcriptional repression of genes and post-translational inactivation of enzymes involved in the utilization of alternative carbon sources and respiration.

Through evolutionary incorporation of chloroplasts via likely symbiosis with primitive cyanobacteria, plant cells acquired the capability to utilize light energy for CO_2 fixation to triose-phosphates (i.e., dihydroxyacetone phosphate [DHAP] and glyceraldehyde-3-phosphate [GAP]) by the Calvin cycle. Triose-phosphates are converted through the chloroplast fructose-1,6-bisphosphate aldolase (FBA), fructose 1,6-bisphosphatase (FBPase), phosphoglucose isomerase (PGI), phosphoglucomutase (PGM) and ADP-glucose pyrophosphorylase (AGPase) to ADP-glucose, which is then used for starch synthesis in chloroplasts of light-exposed leaves during the day. In addition to AGPase, the export of triose-phosphates into the cytoplasm by triose-phosphate/Pi translocators secures the inorganic phosphate supply for maintenance of photosynthetic ATP production and Calvin cycle. Triose-phosphates in the cytoplasm are analogously converted by cytoplasmic FBA, FBPase, PGI and PGM enzymes to fructose-6-P (F6P) and glucose-1-P (G1P). Upon conversion of G1P to UDP-glucose by UDP-glucose pyrophosphorylase (UGPase), sucrose-phosphate synthases (SPS) condense it with F6P to sucrose-6-P, which is then dephosphorylated by sucrose phosphatase. The resulting sucrose is compartmentalized and stored in vacuoles of photosynthesizing leaves. Thus, both starch synthesis in the chloroplasts and removal of sucrose from the cytoplasm secures photosynthetic activity. Sucrose is a major form of carbohydrate, which is transported in higher plants from leaves to developing young sink organs through the night, where it is either split by sucrose synthase (SUSY) to UDP-glucose and fructose, or by cell wall invertases to glucose and fructose. The latter are converted to G1P and F6P by hexokinases, providing substrates for the reversal of above pathway in glycolysis. In addition, UDP-glucose and G1P is utilized for the synthesis of trehalose-6-P, which is an important molecule signalling the availability of sucrose e.g., for starch synthesis in sink tissues. It has been noted long ago that

inhibition of phloem transport of sucrose to sink tissues or accumulation of free sucrose or its hexose-phosphate cleavage products in leaves inhibits photosynthesis and leads to the repression of many light-induced genes (Paul and Foyer, 2001; Lemoine et al., 2013; Figueroa and Lunn, 2016). In contrast to other eukaryotes, it is thus important to distinguish between the opposing regulatory effects of sugars (i.e., chiefly, sucrose and derived hexoses) between photosynthetic leaves and other non-photosynthetic organs, such as roots, in which the availability of carbohydrates is a major source of energy as in all other nonphotosynthetic organism. As nonparasitic plants in their natural environment do not meet with significant carbohydrate resources, their viability and growth is entirely dependent on photosynthetic carbon fixation, a process which is negatively regulated by sugar signalling (Granot et al., 2014). With other words, while starvation for carbon source correlating with lower energy balance promotes utilization of alternative nutrient supplies in other organisms, low free sugar status in the cytoplasm of photosynthetic cells of plants is a prerequisite for efficient photosynthetic ATP production and carbon fixation to sugars.

1.1 Carbon catabolic

The recognition that glucose is a preferred carbon source in comparison to other sugars dates back to the early observation that glucose is preferentially catabolised by bacteria and inhibits the uptake and metabolism of other sugars (e.g., lactose) by a mechanism known as Carbon Catabolite Repression (CCR) or glucose effect. In *Enterobacteria*, a phosphoenolpyruvate (PEP):carbohydrate phosphotransferase system (PTS), that transports and phosphorylates carbohydrates controls CCR. A central regulator of glucose specific PTS system is Enzyme II A (EIIA), which is unphosphorylated in the presence of glucose and inhibits the transporters of alternative sugars. When glucose is fully consumed, EIIA becomes phosphorylated, which relieves the inhibition of alternative sugar transporters. At the same time, phosphorylated EIIA activates the adenylate cyclase (CyaA) producing cAMP, which then allows transcriptional activation of genes involved in alternative sugar catabolism, e.g., the lactose (Lac) operon, by the catabolite activator protein (CAP/Crp), and by inactivation of LacR repressor through stimulation of lactose uptake (Deutscher, 2008; Görke and Stülke, 2008).

Cyclic AMP signaling is also essential for glucose sensing and CCR/glucose repression in the budding yeast *Saccharomyces cerevisiae.* In the central growth promoting cAMP/PKA signaling pathway, extracellular glucose and sucrose are sensed by the seven-transmembrane G protein–coupled receptor (GPCR) Gpr1, which activates the small GTPase Gpa2, a homolog of animal Gα subunit of trimeric GTPases. In turn, Gpa2 stimulates the activation of adenylate cyclase Cyr1 resulting in cAMP-mediated stimulation of protein kinase A (PKA), a central activator of glycolysis, fermentative growth, ribosome biogenesis, cell expansion and division etc., and a repressor of genes involved in respiratory metabolism, gluconeogenesis and stress responses. Activation of Cyr1 is also controlled independently of Gpr1/Gpa2 by the small GTPases Ras1 and Ras2, their guanine exchange factors (GEFs) Cdc25 and Sdc25, and GTPase Activating Proteins (GAPs) Ira1 and Ira2. Ras1/2 respond to intracellular glucose

as their activation, similarly to GPCR, is dependent on sugar phosphorylation, which leads to downregulation of their Ira1/2 inhibitors (for review see: Busti et al., 2010). GPRC stimulates Ras1/2 expression, whereas binding of Ras1/2 to Cyr1 is essential for cAMP synthesis and PKA activation. Glucose signaling stimulates transcription of ribosomal protein and biogenesis genes by PKA-mediated activation of their key transcription factors Rap1 and Sfp1, respectively. At the same time, PKA inhibits the functions of Msn2/4 zinc-finger transcription activators of stress responses that recognize conserved STRE (stress responsive elements) in the promoters of their target genes.

As activation of the cAMP/PKA signalling pathway is strictly dependent on intracellular sugar phosphorylation, it is also tightly linked to the regulation of sugar uptake by sugar transporters. The uptake of glucose as preferred sugar is controlled by low and high affinity hexose transporters (HXTs), the expression of which is regulated by two glucose sensors, Snf3 and Rgt2. In the absence of glucose, expression of the *HXT* genes is repressed by the Rgt1 transcriptional repressor and its co-repressors Mth1 and Std1, which recruit the general transcription repressors Ssn6 and Tup1 to *HXT* promoters. Mth1 (acting in the presence of other carbon sources than glucose) and Std1 (activated by exhaustion of glucose) also block the function of Snf3 (high affinity sensor of low glucose concentration) and Rgt2 (low affinity sensor of higher glucose levels) by binding to their C-termini. Activation of Snf3 and/or Rgt2 by glucose stimulates ubiquitination of Mth1 and Std1 by the SCF^{Grr1} E3 ligase and their subsequent proteasomal degradation. This allows phosphorylation and inactivation of the Rgt1 repressor by glucose/cAMP-activated PKA, stimulating the expression of *HXT* genes of glucose transporters.

Glucose sensing, uptake and subsequent phosphorylation confer transcriptional repression of genes (i.e., glucose repression) involved in the utilization of alternative carbon sources and respiration, stimulating at the same time the activation genes in the glycolytic and fermentative pathways. Yeast has three glucokinases: hexokinase 1 and 2 (HXK1 and Hxk2) and glucokinase (Glc1). Inactivation of all three of these genes is required for complete abolishment of glucose repression. Glucose repression is also induced by 2-deoxyglucose, which is phosphorylated but cannot enter into glycolysis. This indicates that phosphorylated sugars or their immediate derivatives could play a role as signalling molecules in glucose repression. Initial studies of transcriptional regulation of *SUC2* gene encoding an extracellular invertase revealed a special requirement for Hxk2 in conferring glucose repression of *Suc2*. These studies uncovered that Hxk2, including its catalytically inactive form, is imported in a glucose-inducible fashion into nuclei in complex with the Mig1 transcription repressor that together with the Ssn6/Tup1 general repressors inhibits transcription of *SUC2* and other glucose repressed genes. Hxk2 and Mig1 thus represent central regulators of catabolite/glucose repression in yeast (for reviews see Gancedo, 1998; Carlson, 1999; Moreno et al., 2005; Conrad et al., 2014; Kayikci and Nielsen, 2015).

Screening for yeast mutations that prevent *Suc2* activation by abolishing sucrose utilization and causing a *s*ucrose *n*on*f*ermenting phenotype identified the Snf1 kinase as a key regulator required for alleviation of glucose repression (Celenza and Carlson, 1984). Snf1 is activated by exhaustion of cellular

glucose causing carbon starvation and during yeast growth on ethanol and alternative carbon sources. Activation of Snf1 is essential for stimulation of respiratory metabolism, glyoxylate cycle, peroxisome biogenesis, gluconeogenesis, lipid degradation, autophagy and other catabolic pathways and inhibition of amino acid, protein and lipid biosynthesis and other energy consuming anabolic processes in cross-talk with other signalling pathways (for reviews see Hedbacker and Carlson, 2006; Usaite et al., 2009, Conrad et al., 2014). Snf1 phosphorylates Hxk2 preventing its nuclear localization and interaction with Mig1, as well as Mig1 at the Ser311 residue of its Hxk2-binding domain abolishing its nuclear localization and thus relieving glucose-induced transcriptional repression (Ahuatzi et al., 2007).

1.2 Control of energy homeostasis by conserved AMP-activated protein kinases in eukaryotes

Biochemical studies of the regulation of human sterol/isoprenoid synthesis by its rate-limiting HMG-CoA reductase enzyme uncovered the role of a specific protein kinase, which inactivated this enzyme in an AMP-inducible fashion. Following its first identification in 1973, the same AMP-activated kinase was found to regulate the activity of acetyl-CoA carboxylases (ACC1 and 2) in the first step of fatty acid biosynthesis. Protein kinases with similar activities were also detected in Drosophila and Arabidopsis (Hardie and MacKintosh, 1992). It has been hypothesized early on that the HMG-CoAR and ACC kinases are linked to monitoring cellular ATP consumption, which through the adenylate kinase reaction (2ADP ->ATP and AMP) leads to the production of the kinase allosteric activator AMP. Heat shock, hypoxia, muscle exercise and other stresses were found to stimulate the AMP-activated kinase (AMPK), which also required a second kinase for enhancing its activity to inhibit key enzymes of lipid and sterol biosynthesis. Cloning of the cDNA of human AMPK by Carling et al. (1994) demonstrated a close relationship between the human enzyme and yeast Snf1, though the human AMPK cDNA failed to complement the yeast *Δsnf1* mutation. By contrast, several plant Snf1-related kinases (SnRKs) were identified earlier in rye, barley and Arabidopsis, which complemented the *Δsnf1* mutation and showed close relationship with human AMPK (Alderson et al., 1991; Halford et al., 1992; Le Guen et al., 1992). At the same time, yeast mutant screens identified Snf4, an essential activator γ subunit of Snf1, whereas two-hybrid protein interaction studies uncovered association of Snf1 and Snf4 with one of the three substrate targeting scaffold β-subunits, SIP1, SIP2 and Gal83 in a trimeric enzyme holocomplex. Subsequent identification of mammalian and plant homologs of yeast Snf1 kinase subunits, genetic dissection of their functional and interacting domains, *in vitro* assembly and crystallization of their components, and identification of their upstream and downstream signalling partners contributed to our current understanding of regulation and signalling functions of conserved eukaryotic Snf1/AMPK/SnRK kinase family (Hardie et al., 1998; Carlson, 1999; Hardie and Carling, 1999; Kemp et al., 1999; Carlin, 2004; Hardie, 2004; Hardie, 2007; Scott et al., 2009; Hardie et al., 2011; Carling et al., 2011; Crozet et al., 2014; Broeckx et al., 2016; Hardie et al., 2016; Margalha et al., 2016; Ross et al., 2016; Garcia and Shaw, 2017; Craig et al., 2018).

1.3 The structure and activation of Snf1/SnRK1/AMPK protein kinases

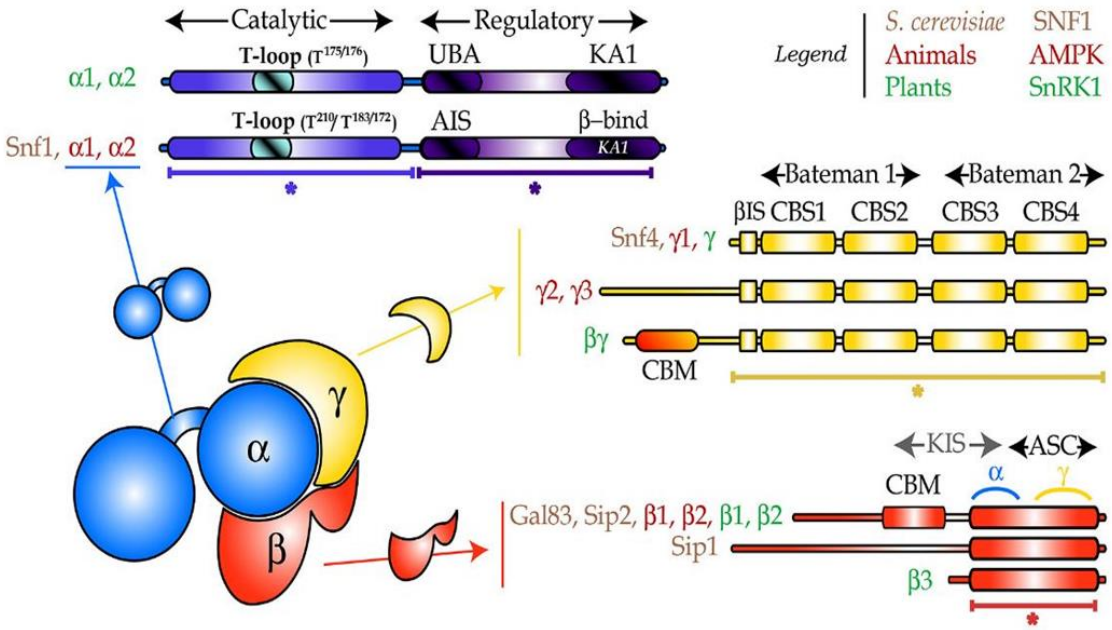

Figure 1. Conservation of functional domains of Snf1/SnRK1/AMPK subunits (according to Crozet et al., 2014).
The α-subunits carry highly conserved N-terminal catalytic kinase domains including the ATP-binding site and activation T-loop (blue circles). A conserved T-loop threonine (T210 in Snf1, T175/176 in AKIN10/AKIN11, T172 in AMPKα1) is phosphorylated by upstream activating kinases. The C-terminal segments of α-subunits carry an autoinhibitory domain (AIS/αAID), which overlaps in Snf1 and SnRK1s with a UBA (ubiquitin associated) domain that probably plays a role in degradation of the kinase and/or in binding to polyubiquitinated partners or substrates. A so-called α-linker region separates the UBA from the kinase associated (KA1, αCTD) domain, which interacts with the C-terminal domains of β and N-termini of γ subunits. The KA1 domain is followed by a serine/threonine-rich loop in the AMPKα-subunits, which is phosphorylated by inhibitory upstream kinases, and adjacent to C-terminal nuclear localization sequences (NLS). The activating γ subunits carry an N-terminal beta-interacting sequences (βIS) followed by four adenylate-binding CBS (cystathionine-β-synthase) repeats forming two so-called Bateman domains. Human AMPKγ2 and 3 carry longer N-terminal extensions, whereas the N-terminus of plant SNF4 (called also AKINβγ) harbours a carbohydrate binding module (CBM), which is found only in the β-subunits of yeast Snf1 and animals AMPKs. N-termini of the β-subunits vary in length and except for Arabidopsis β3 and yeast SIP1 carry conserved CBM sequences that located in the vicinity of catalytic domain (α-KD) and T-loop of α-subunits, and thus were designated earlier as kinase-interacting sequences (KIS). C-termini (β-CTD) of the β subunits carry the ASC (association to the complex) domains, which interact with α and γ subunits. Brown letters mark yeast Snf1 subunits, purple letters the subunits of human AMPK, and green letters the Arabidopsis SnRK1 subunits. In contrast to the review Crozet et al. (2104), Arabidopsis has only one SNF4/AKINβγ gene, the γ form marked in the adapted figure corresponds to an incomplete cDNA, which was first isolated and shown to complement the yeast *Δsnf4* mutation by Kleinow et al. (2000). The full-length gene product corresponds to βγ with the N-terminal CBM also complements the yeast *Δsnf4* mutation as was shown by Lumbreras et al. (2001).

Members of the Snf1/SnRK1/AMPK kinase family were isolated as heterotrimeric enzymes composed of catalytic α, targeting β and activating γ subunits (Figure 1; Crozet et al., 2014; Craig et al., 2018). In yeast, the Snf1 kinase catalytic α and Snf4 activating γ subunits occur in different complexes with three β-subunits Gal83p, Sip1p and Sip2p that carry N-terminal myristoylation signal sequences promoting their membrane localization. In comparison, human AMPK may form 12 different complexes by the combination of two catalytic subunits α1 and α2, two substrate-targeting β-subunits (β1 and β2) and three activating γ-subunits (γ1, γ2 and γ3). The Arabidopsis genome codes for three SnRK1 catalytic by a single gene, which is also designated as AKINβγ because it carries an N-terminal CBM

(carbohydrate-binding module) that is only present in the β-subunits of yeast and mammalian Snf1/AMPK homologs. From the three AKINβ1, AKINβ2 and AKINβ3 Arabidopsis SnRK1 subunits, AKINβ3 is atypical because it lacks the N-terminal CBM domain but can still interact with α and γ subunits, and was reported to complement the triple yeast *gal83 sip1 sip2* mutation, as the AKINβ1 and AKINβ2 subunits (Gissot et al., 2004). Arabidopsis SNF4 with and without its N-terminal CBM domain can also functionally replace yeast Snf4 in genetic complementation experiments (Kleinow et al., 2000; Lubreras et al., 2001). Catalytic subunits of rye, tobacco, potato and Arabidopsis SnRK1 kinases complement the yeast *Δsnf1* mutation stimulating the utilization of alternative carbon sources, such as glycerol and ethanol (Alderson et al., 1991; Muranaka et al.,1994; Bhalerao et al.,1999; Lovas et al., 2003).

Despite close sequence, structural and functional similarities, studies of yeast, plant and mammalian kinases revealed significant differences in their regulation. Purified catalytic subunits of AMPK do not show autophosphorylation *in vitro* and are not activated by AMP unless their T-loops were previously phosphorylated by upstream activating kinases (for review see Lin and Hardie, 2018). Activation of yeast Snf1 is also dependent on T-loop phosphorylation, however, it is insensitive to AMP. Nonetheless, ADP prevents inactivation of Snf1 by the protein phosphatase Glc7 (Mayer et al., 2011). In comparison, purified spinach SnRK1 is not activated by either AMP or ADP, but AMP was reported to inhibit its dephosphorylation by recombinant mammalian PP2C (Sugden et al. 1999a).

These differences in the regulation of yeast Snf1, plant SnRK1 and mammalian AMPK are likely related to characteristic differences of carbon metabolic pathways controlled by their functions, and also reflect evolutionary changes in the regulatory domains of their subunits. Thus, yeast Snf1 is required to promote gluconeogenesis from ethanol, when glucose is exhausted by fermentation, as well as for synthesis of storage carbohydrates glycogen and trehalose to promote cell survival under starvation (i.e., when carbon source is completely exhausted). By contrast, human AMPK inhibits glycogen synthesis and itself is inhibited by glycogen-binding. In higher plants, except for some desiccation tolerant species, no trehalose accumulation is detected, while starch is synthesized in the chloroplasts and etio-/amyloplasts. Plant SnRK1 is required for starch mobilization in the dark in source leaves, but promotes starch accumulation in sink organs, such as potato tubers (see for review Wurzinger et al., 2018). Furthermore, SnRK1 is activated by photosynthesis inhibitors (Baena-González et al., 2007) in leaves, and suggested to be inhibited by trehalose-6-phophate (T6P) in sink tissues, down-regulating photosynthesis-related gene expression (Zhang et al., 2009; Wingler et al., 2012).

Comparison of partial crystal structures of Snf1 and AMPK indicates largely similar interaction between the three subunits, although the role of carbohydrate-binding CBD domain is still enigmatic (Amodeo et al., 2007; Sanz et al., 2016; Li et al., 2017). Yeast Snf1 requires T-loop phosphorylation and Snf4-binding for its activation. In its inactive form, the Snf1 catalytic domain (KD) interacts with the autoinhibitory AID domain. The activation of T-loop is located in a cleft of the KD, which might be

available for phosphorylation. However, ultimate activation of Snf1 requires binding of the activating Snf4/γ subunit, which results in a conformational change of the KD. Similarly to the γ-subunits of AMPKs, Snf4 carries four CBS (cystathionine-β-synthase) repeats, which show less than 40% sequence homology to the AMPK γ-subunits. From the two Bateman domains formed by the CBS repeats, domain 2 (CBS3 and 4) promotes dimerization (i.e., formation of dimeric 2x αβγ complex) by forming a pocket proposed to function in AMP or ADP binding (Rudolph et al., 2007). The CBS4 site was fund to show higher affinity for binding of NADH, which might play a role in redox regulation of the kinase, while the CBS2 site is suggested to bind ADP triggering a further conformational change of KD that closes the cleft protecting the T-loop from dephosphorylation (Mayer et al., 2011).

In comparison, the activation of human AMPK requires three events: T-loop phosphorylation, interaction with the activating γ-subunit and AMP/ADP-binding to the CBS repeats for further allosteric activation. In the γ-subunit of crystallised human AMPK, an Asn residue required form AMP/ADP-binding in the CBS2 site is mutated. From the other three CBS repeats, 3 and 4 are required for the conformational change protecting dephosphorylation of the T-loop. Site 4 is stably bound by AMP. Thus, site 3 is critical for allosteric regulation (Xiao et al., 2011, Li et al., 2017). In addition to chemicals inhibiting ATP production by mitochondrial oxidative phosphorylation and AMP analogues binding to the CBS-repeats, several small molecule drugs, such as salicylic acid (SA), can remarkably activate AMPK independently of T-loop phosphorylation. These molecules bind either to the CBM module or the allostreric drug and metabolite-binding site (ADaM), which is found in a small lobe formed by the kinase active site and the closely located CBM domain. Activation of AMPK by SA and other drugs at this site also requires the phosphorylation of Ser108 residue of β1 subunit, which is thought to happen by autophosphorylation. Intriguingly, association of the β-subunits with Snf1-Snf4 is reported to play a negative regulatory role because mutations in and close to the Snf4 CBS2 domain, which relieve Snf4 interaction with the CBM domain of Gal83, largely abolish glucose inhibition of Snf1 (Momcilovic et al., 2008). Finally, AMPK (and likely Snf1 also) is inactivated by several signalling kinases (e.g., PKA, and AKT/S6K), which phosphorylate a conserved C-terminal Ser residue (Ser 485 in AMPKα1) in the catalytic α-subunits (i.e., probably abolishing interaction with the activating γ-subunits; for review see Guigas and Viollet, 2016; Garcia and Shaw, 2017).

In comparison, much less is known about the structure and activation of plant SnRK1 enzymes, which were not yet crystallized. Recent study of *in vitro* assembled Arabidopsis SnRK1 complexes indicates that they are resistant to T-loop dephosphorylation, cannot be activated by AMP and ADP, and the CBM domains of their β-subunits cannot bind starch or glycogen (Emanuelle et al., 2015). Furthermore, CBS repeats of Arabidopsis SNF4 are divergent for the conserved residues required for AMP/ADP/ATP binding (Emanuelle et al., 2016). Finally, in the catalytic AKIN10/11 subunits of Arabidopsis SnRK1, the autoinhibitory (AID) domain appears to be replaced by an UBA domain, which is reported to enhance their phosphorylation by the upstream kinase GIRK2, but does not seem to

influence the kinase activity despite enhancing degradation of α-subunits (Farrás et al., 2001; Emanuelle et al., 2018). Zhang et al. (2009) and Emanuelle et al. (2015) reported that unknown protein factors might inhibit the kinase in photosynthetic leaves and sink tissues in connection with T6P, but the molecular mechanisms underlying these observations are unknown. How SnRK1 activation (i.e., T-loop phosphorylation) is affected by AMP analogs, inhibitors of mitochondrial oxidative phosphorylation, SA and other small molecule activators is also unclear.

1.4 Yeast Snf1 signaling: alleviation of glucose repression

Snf1 plays roles in nutrient responses, cellular development, including meiosis and sporulation, aging, haploid invasive growth, diploid pseudohyphal growth, cell cycle and transcription (Honigberg and Lee, 1998; Carlson, 1999; Cullen and Sprague, 2000; Hedbacker and Carlson, 2008). Phosphorylated T-loop of Snf1 is recognized by the Reg1 regulatory subunit of the PP1 protein phosphatase Glc7 and its paralog Reg2. The activity of Glc7 is increased by the glucose sensing cAMP/PKA pathway within minutes resulting in T-loop dephosphorylation and inactivation of Snf1 (Castermans et al., 2012). Reg1-Glc7 also dephosphorylates the Ser14 residue of hexokinase Hxk2 stimulating its nuclear import and complex formation with Mig1, preventing its Snf1-mediated phosphorylation and stimulating glucose repression (Fernández-García et al., 2012). Reg1-Glc7 controls dephosphorylation of Mig1 promoting its nuclear localization. Due regulatory interplay between Reg1-Glc7 and regulatory subunits of PP2A phosphatases, activation of the latter is also thought to contribute to inactivation of Snf1 (Castermans et al., 2012). The *Δreg1* mutation alleviates glucose repression of Snf1 resulting in enhanced glycogen accumulation similarly to the *sit4* mutation of PP2A catalytic subunit (Ruiz et al., 2011). In addition, the lethality of *Δreg1Δsit4* mutations conferred by constitutive activation of Snf1 is suppressed by overexpression of the PP2C phosphatase Ptc1, which can dephosphorylate the T-loop of trimeric Snf1, although it acts as MAP-kinase phosphatase in the high osmolarity and cell wall integrity pathway (Ruiz et al., 2013). In contrast to Ptc1, Reg1-Glc7 and Sit4 dephosphorylate the T-loop of monomeric Snf1. Thus, Snf4 or the β-subunits are not required for T-loop phosphorylation or dephosphorylation of Snf1. Salt stress leads to Snf1 T-loop phosphorylation without affecting glucose signalling (McCartney and Schmidt, 2001), whereas Snf1 carrying deletion of its β/γ-binding C-terminal domain still undergoes T-loop phosphorylation in response to glucose limitation (Ruiz et al., 2011; García-Salcedo et al., 2014). However, similarly to the *Δreg1* mutant, C-terminally truncated Snf1 does not respond to glucose repression. Glucose inhibition of interaction between Snf1 and Snf4 demonstrates that formation of trimeric kinase complex (i.e., in addition to T-loop phosphorylation) is necessary for Snf1 activation and signalling (Carlson, 1999; Hedbacker and Carlson, 2008). Deletion of the carbohydrate-binding CBM domain of Gal83 β-subunit decreases glucose inhibition of Snf1 indicating a role for this domain in conveying glucose repression (Momcilovic et al., 2008). Similarly, the SIP2 β-subunit acts as an inhibitor of Snf1 in aging yeast cells. SIP2 acetylation by the NuA4 acetyl transferase complex enhances its interaction with Snf1 by reducing its

activity to phosphorylate Sch9/S6K, which is a downstream effector of both TORC1 and cAMP/PKA pathways promoting protein synthesis and DNA replication. Thus, SIP2 inhibition of Snf1 prolongs replication time slowering aging (Lu et al., 2011).

When glucose is limiting and the cAMP/PKA pathway is downregulated leading to decreased Reg1-Glc7 activity (but also in response to envinmental stresses, such as alkaline pH, high sodium chloride, oxidative agents or inhibition of TORC1 by nitrogen starvation). Snf1 is then activated through phosphorylation of its T-loop by three partially redundant upstream kinases Sak1, Elm and Tos1 (Hong et al., 2003a). Of these, Sak1 plays a dominant role and represents the sole kinase, which mediates the activation of Gal83-containing Snf1 in response to glucose limitation (Hedbacker et al., 2004a; McCartney et al., 2005). Whereas Reg1-Glc7 dephosphorylates and activates Gpa1, the G-protein activator of cAMP/PKA signaling, phosphorylation by Sak1, Elm1 and Tos1 is reported to inactivate Gpa1 (Clement et al., 2013). By contrast, activation of PKA in the *ire1/2* (Ras inhibitor) and *bcy1* (PKA inhibitor) mutants hampers Snf1 activation suggesting potential regulation of Snf1-activating kinases by PKA-mediated phosphorylation (Castermans et al., 2012). Upon T-loop phosphorylation, Gal83-Snf1 relocalizes to the nucleus and Sip1-Snf1 to the vacuolar membrane, while Sip2-Snf1 remains cytoplasmic. N-terminal myristoylation of Sip1 is required for its relocalization, similarly to that of Sip2, which is located in the plasma-membrane but relocated to the cytoplasm in glucose-deprived aging cells. Sequestration of Snf1 and Snf4 to cell membrane by the N-terminally myristoylated β-subunits may thus also play a role in the regulation of Snf1-activity, in addition to targeting the kinase to various cellular substrates (Vincent et al., 2001; Hedbacker et al., 2004b).

Snf1 regulates hundreds of genes involved in alternative carbon source utilization by controlling the activity of key transcription factors, and promotes repression of TORC1-regulated genes in amino acid metabolims by repressing GCN4 (see for reviews Broach, 2012; Conrad et al., 2014; Rødkaer and Faergeman, 2014). Genes acting in the metabolism of alternative sugars (e.g., sucrose, galactose, maltose etc.) are activated through inactivation of Mig1/2 repressors by Snf1 as described above. Genes involved in gluconeogenesis, TCA cycle and glyoxylate shunt are induced by the Snf1-regulated transcription factors Cat8, Sip4 and Rds2. Snf1 phorphorylates Cat8, which then activates SIP4 that binds through Gal83 to Snf1. Both transcription activators recognize carbon source response elements (CSRE) in the promoters of their traget genes and peform partially overlapping functions. Cat8 is repressed by Mig1, but activated by the Hap2/3/4 transcription activator complex of mitochondrial respiratory genes, from which the Hap4 activator of other Hap genes is stimulated by the Rds2 substrate of Snf1. In addition, Snf1 phosphorylates the heat-shock transcription factor Hsf1, which binds to HSE elements of target genes conferring heat tolerance. Consequently, *Δsnf1/snf4* mutants are heat sensitive. Another Snf1 substrate is Msn2, which together with its partner Msn4 is a key regulator of genes that carry conserved stress response elements (STREs). Msn2 and 4 are activated through Rim15-mediated phosphorylation, which is inhibited by PKA and TORC1 under glucose repression. Rim15 controls cell wall

integrity/synthesis and entry into the G_0 phase of the cell cycle and probably requires Snf1 as upstream kinase for its activity. Snf1 also phosphorylates Rgt1 conferring repression of some *HXT* genes under glucose starvation. In addition to phosphorylating numerous transcription factors, Snf1 plays a more general role in the regulation of RNA polymerase II (RNAPII) transcription. Through interaction with the SRB/Mediator complex, SNF1 regulates the activity of RNA polymerase II (Vincent et al., 2001). By phosphorylation of Ser10 residue of histone H3, Snf1 recruits the SAGA complex and phosphorylates its GCN5 histone H3K14 acetyltransferase subunit stimulating transcription initiation on many genes including e.g. *INO1*, and the hexose transporter genes *HXT2* and *4* (Lo et al., 2001, 2005).

Regulatory interactions between Snf1 and the rapamycin-sensitive TORC1 kinase complex involved in sensing cellular nitrogen/amino acid availability control coordinate responses to glucose and nitrate availability. Under amino acid limitation in the presence of glucose, Snf1 activates the Gcn2 protein kinase of translation initiation factor eIF2α, which slows down translation but selectively allows the synthesis of Gcn4 transcription activator of genes involved in amino acid biosynthesis and nitrogen utilization (Cherkasova et al., 2010). Under glucose deprivation, Snf1 downregulates both transcription and translation of Gcn4 (Kayikci and Nielsen, 2015). The vacuole/lysosomal membrane-associated TORC1 complex regulates phosphorylation of Gln3 and Gat1 transcription activators of genes controlled by nitrogen catabolite repression (NCR). Phosphorylated Gln3 and Gat1 are sequestered in the cytoplasm by the scaffold protein Ure2 are released by Snf1-mediated phosphorylation stimulating their nuclear import under glucose starvation. Thus, Snf1 and TORC1 coordinately control responses to carbon and nitrate starvation (for review see Shimobayashi and Hall, 2014).

1.5 The roles of trehalose-6-phosphate synthase and Snf1 in regulation of cell death and aging in yeast

Similarly to animal AMPKs, Snf1 phosphorylates and inhibits acetyl CoA carboxylase (ACC1) in the first committed step of fatty acid biosynthesis by decreasing the concentration of malonyl CoA, which stimulates fatty acid oxidation and ATP production in mitochondria. As ACC1 activation results in downregulation of *INO1* (inositol 1-phosphate synthase), *snf1* mutants cannot synthesize inositol-1-phosphate supporting phosphoinositol signalling. Another important signalling molecular in yeast is trehalose-6-phosphate (T6P), synthesis of which requires the function of Snf1. Originally, T6P was reported to inhibit Hxk2, the central activator of glucose repression, and accumulation of trehalose was demonstrated to confer heat stress tolerance, which is abolished in *snf1* mutants (Blazquez et al., 1993; François and Parrou, 2001; Walther et al., 2013). Yeast *tps1* (trehalose-6-P synthase) mutants cannot grown on glucose; show reduced growth on nonfermentative carbon sources, cannot synthesize ethanol, accumulate glycolytic sugar phosphate intermediates and inosine, and display rapid depletion of adenine nucleotides. However, inactivation of Tpp1 (Trehalose-6-P phosphatase), expected to result in T6P accumulation, does not enhance the inhibition of Hxk2. Furthermore, the *tpp1* mutation does not

completely abolish trehalose accumulation, indicating that other sugar phosphatases can also convert T6P to trehalose. In addition, Hxk2 mutations alleviating T6P inhibition *in vitro* do not abolish glucose repression, although deletion of the *Hxk2* gene suppresses the defects caused by the *tps1* mutation (Bonini et al., 2003). In addition to the *Δhxk2* mutation, inactivation of Snf1 also restores the defects of the *tsp1* mutant growing on glucose. The *Δtps1* mutation does not alter T-loop phosphorylation of Snf1, indicating that T6P is not an inhibitor of the Snf1 kinase. Tps1/T6P is suggested to repress gluconeogenesis in the presence of glucose, independently of inhibiting Snf1 (which promotes gluconeogenesis from alternative carbon sources), downstream of the Snf1-stimulated Cat8 and SIP4 activators of this pathway (Deroover et al., 2016). Intriguingly, the TPS1 protein itself and not trehalose is reported to be essential for activation of thermotolarance in the absence of Snf1-mediated phosphorylation of Hsf1 activator of heat shock response (Petitjean et al., 2015). In addition, the glycolysis intermediate fructose-1,6-bisphosphate (Fru-1,6bisP) accumulating in the *Δtps1* mutant is demonstrated to bind the Cdc25 activator of Ras1/2 resulting in its hyperactivation stimulating cell death (Peeters et al., 2017). Recently, Petitjean et al. (2017) provided evidence for that a catalytically inactive Tps1 is sufficient to inhibit the induction of cell death when growing yeast on glucose or other fermentable carbon sources. Similarly, Snf1 also inhibits Ras-dependent induction of programmed cell death by either acetate or deregulation of mitochondrial respiration resulting in ROS overproduction (Laera et al., 2016; Knupp et al., 2017). Snf1 is required to maintain mitochondrial respiration during glucose starvation and prevents cell death by regulating controlled respiratory autophagy (Yi et al., 2018). Similarly, Tps1 is reported to confer hypoxia tolerance in Drosophila, and to be required for maintenance of mitochondrial respiratory functions in yeast (Chen et al., 2003; Noubhani et al., 2009). Extension of chronological life span (ECL) of yeast by trehalose production (i.e., activation of Tps1) is controlled by the Yak1, Rim15 and Mck1 kinases, which are stimulated by Snf1 but negatively regulated by the TORC1 and cAMP/PKA pathways controlling the activation of oxidative stress defense in yeast (Cao et al., 2016). This indicates that Snf1 and downstream acting TPS1 act analogously as cell death repressors in the same cell survival pathways but their regulatory interaction, if any, is so far largely unclear.

1.6 Mammalian AMP-activated protein kinases

In mammals, the major form of transported sugar in the blood is glucose. In humans, glucose homeostasis is controlled by glucose sensing and readjusted by glycogen and fatty acid synthesis promoted by insulin and inhibited by glucagon signalling in the liver. One of the major function of AMPK is to stimulate glucose uptake/glycolysis e.g., in muscles (i.e., upon exercise-induced AMPK activation), and to promote of glucose production and secretion in the liver by inhibiting of insulin secretion from pancreatic β cells (see for review Rourke et al., 2018). In general, at the cell level AMPK promotes glucose uptake, glycolysis, fatty acid oxidation, mitochondrial biogenesis (mitofission and mitophagy) and autophagy but inhibits gluconeogenesis, synthesis of fatty acids, sterols, glycogen,

proteins and rRNA, and thereby the increase of cell size and division. In humans, defective regulation of AMPK is associated with metabolic disorders, obesity, type 2 diabetes and cancer (for reviews see Hardie, 2007; Cordero and Violett, 2016; Garcia and Shaw, 2017).

As discussed in section 1.3, T-loop phosphorylation is obligatory for activation of AMPK (Hong et al., 2003a). In humans, the major AMPK-activating kinase is LKB1, a tumour suppressor mutated in patients of Peutz–Jeghers syndrome, which was identified based on its similarity to the Snf1-activating kinases (Hawley et al., 2003). Whereas monomeric LKB1 is nuclear, cytoplasmic LKB1 is found in a complex with the pseudokinase (STE20-related adaptor) and armadillo repeat adaptor protein MO25 (mouse protein 25), and targeted to membranes by its C-terminal CaaX prenylation motive. LKB1 activates 14 AMPK-related kinases, and functions as a tumour suppressor by inhibiting cell proliferation and controlling cell polarity (Alessi et al., 2006; Williams and Brenman, 2008). Similarly to the Snf1-activating kinase Sak1, LKB1 is inhibited by cAMP-dependent PKA and TOR1-activated S6 protein kinase (RSK) phosphorylation, whereas LKB1 phosphorylation inhibits TOR1. Phosphorylation by the DNA damage sensing ATM kinase activates LKB1, which interacts with the p53 tumour suppressor promoting apoptosis (Zeng and Berger, 2006). Activation of LKB1 is unaffected by the ATP/AMP ratio and is thought to be maintained by autophosphorylation.

Remarkably, Oakhill et al. (2010) found that mutation of the myristoylation site of β1 subunit preventing membrane localization of AMPK, compromised LKB1-mediated phosphorylation of Thr172 residue of AMPKα1 subunit. Subsequent studies of cellular co-localization of LKB1-AMPK complex led to the recognition that AMPK interacts in an AMP-stimulated fashion with AXIN1, a component of the Wnt signalling pathway, which targets AMPK to LKB1, as well as potentially to some other partners, such as catenin β1, the tumour suppressor APC (adenomatosis polyposis coli, involved in the induction of apoptosis) and protein phosphatase PP2A (Zhang et al., 2013; Zhang et al., 2016). Subsequent studies revealed that the AXIN1-AMPK-LKB1 complex contains LAMTOR1, a component of the pentameric RAGULATOR (Rag) GTPase complex, which triggers relocalization of activated human mTORC1 complex to lysosomal membranes through interaction with its RAPTOR subunit. The AXIN-AMPK-Rag-mTORC1 supercomplex is targeted to the vacuolar v-ATPase that plays a key role of mTORC1 sensing of amino acid and glucose availability. Glucose starvation was found to promote lysosomal assembly of the AXIN-AMPK-LKB supercomplex, which is abolished by inactivation of AXIN1 and LKB1. In contrast with the widely accepted canonical AMP-mediated activation mechanism, Zhang et al. (2017) found that in several human cell types subjected to glucose deprivation the AMP/ATP ratio remains unchanged, yet AMPK is activated by T-loop phosphorylation. The glucose sensing mechanism, which activates the lysosomal AXIN-AMPK complex independently of a change in the ATP/AMP ratio employs a v-ATPase-binding fructose-1,6-bisphophate (Fru-1,6bisP) aldolase. Binding of Fru-1,6bisP, as glycolysis intermediate indicating glucose availability, to catalytically active or inactive forms of the aldolase is reported to promote dissociation of AXIN-LKB1 from the supercomplex preventing AMPK

activation by T-loop phosphorylation. Under glucose starvation, aldolase is uncharged with substrate and mTORC1 is released, while the AXIN-LKB1-AMPK complex is stabilized leading to AMPK activation (see for review Carroll and Dunlop, 2017; Lin and Hardie, 2017).

Inhibition of AMPK activation by Fru-1,6bisP is particularly interesting because AMPK inhibits fructose-1,6-bisphosphatase, the rate limiting enzyme of gluconeogenesis (producing Fru-6P). At the same time, AMPK activation stimulates the kinase activity of 6-phosphofructo-2-kinase/fructose-2,6-bisphosphatase (PFK2/3/FBPase-2/3) resulting in the accumulation of Fru-2,6-P, an activator of phosphofructokinase 1 (PFK-1) promoting glycolysis. Remarkably, inactive form of the PFK2 enzyme itself is sufficient to perform this function (Arden et al., 2008). By contrast, glucagon activation of cAMP/PKA signalling stimulates though phosphorylation the function of FBPase, which leads to inhibition of glycolysis and stimulation of gluconeogenesis (in parallel with stimulation of glycogen degradation in the liver). In addition to insulin and glucagon, the regulation of AMPK activity is linked to signalling pathways of several other hormones and cytokines, such as ghrelin, leptin resistin, adiponectin, inflammatory mediators, glucocorticoids and thyroid hormoneT3 and T4 (Lim et al., 2010; Hardie, 2010).

The second activating kinase, which phosphorylates the T-loop of AMPK independently of the AMP/ATP ratio and complements the yeast *sak1 elm tos1* mutation is the calcium/calmodulin-dependent kinase kinase 2 CAMKK2 that acts in specific tissues and is activated by Ca^{2+}-signalling in various hormonal pathways (Hawley et al., 2005; Hurley et al., 2005; Woods et al., 2005). In contrast to LKB1, CAMKK2 can also phosphorylate the T-loop of monomeric AMPKα. As mentioned above, AMPKα is inhibited through phosphorylation of its C-terminal S/T-rich loop by the cAMP-activated PKA (Hurley et al., 2006), mTORC1/insulin-activated AKT/S6K (Horman et al., 2008), GSK3 (glycogen synthesis kinase 3; Suzuki et al., 2013), PKD1 (protein kinase D; Coughlan et al., 2016), and PKC (protein kinase C; Heathcote et al., 2016) kinases. Phosphorylation of S/T-loop is proposed to target AMPKα to phosphatases dephosphorylating the activation T-loop (Hawley et al., 2016), as well as for ubiquitination by e.g. the TRIM28 ubiquitin ligase (Pineda et al., 2015) and UBE20 (ubiquitin-conjugating enzyme E20; Vila et al., 2017) in various tumours, and by the WWP1 ubiquitin ligase under high glucose condition in muscle cells (Lee et al., 2013).

AMPK plays a key role in safe-guarding the functionality of mitochondria, and is activated by ROS signalling, as well as by oxidation and S-glutathionylation of cysteines 299 and 304 in the α-subunit (Hawley et al., 2010; Zmijewski et al., 2010). On the other hand, oxidation of the highly conserved cysteine residues 130 and 174 in the catalytic domain leads to AMPKα inactivation in heart muscles during ischemia, which is reversed by thioredoxin 1 (Shao et al., 2014).

During metabolic stress, AMPK restores ATP levels by inhibiting ATP-consuming biosynthetic pathways though phosphorylation of key rate-limiting enzymes and numerous transcription factors

acting in different signalling pathways (Mouchiroud et al., 2014). As mentioned above, AMPK stimulates glucose uptake by phosphorylating TBC1D1 (TBC domain family 1) and TXNIP (thioredoxin-interacting protein), which promote plasma-membrane localization of GLUT4 and GLUT1 glucose transporters (Wu et al., 2013). In addition to stimulating glycolysis by activation of the PFKFB2/3 enzymes, AMPK phosphorylates and inhibits the liver glycogen synthases GYS1 and GYS2 by decreasing their affinity for both UDP-glucose and glucose-6-P (Bultot et al., 2012). Similarly, AMPK phosphorylation inhibits the activities of ACC1/2 (acetyl-CoA carboxylase 1) and HMGCR (3-hydroxy-3-methyl-glutaryl-coA reductase) co-ordinately downregulating fatty acid and sterol biosynthesis, respectively (Hardie, 2014). AMPK also phosphorylates GFAT1 (fructose-6-phosphate amidotransferase 1) inhibiting hexosamine synthesis and O-linked protein glycosylation by β-N-acetylglucosamine (O-GlcNAc; Eguchi et al., 2009; Zibrova et al., 2017). In the nucleus, AMPK phosphorylation inhibits the functions of SREBP1 (sterol regulatory element binding protein 1; Li et al., 2011), HNF4a (hepatocyte nuclear factor-4a; Hong et al., 2003b) and ChREBP (carbohydrate-responsive element binding protein; Kawaguchi et al., 2002) representing key activators of genes involved in gluconeogenesis, and sterol and fatty acid biosynthesis. Furthermore, AMPK promotes nuclear exclusion of CRTC2 (cyclic-AMP-regulated transcriptional co-activator 2) and class II HDACs (histone deacetylases), which act as co-activators of genes in gluconeogenesis (Koo et al., 2005; Mihaylova et al., 2011).

As yeast Sn1f (Zhang and Cao, 2017), AMPK interaction with the mTORC1 complex inhibits TOR1-signaling (Garcia and Shaw, 2017). By phosphorylation of TSC2, AMPK activates the GTPase-activating TSC1:TSC2 complex inhibiting the mTORC1-activating Rheb G-protein, (Inoki et al., 2003). AMPK also phosphorylates and inhibits the function of RAPTOR, which targets the mTORC1 complex to the RAGULATOR at the lysosomal membrane (Gwinn et al., 2008; Sancak et al., 2010). Intriguingly, Rheb was found to directly interact with the glycolytic enzyme glyceraldehyde-3-phosphate dehydrogenase (GAPDH), which inhibits mTORC1 activation unless GAPDH is bound by its substrate glyceraldehyde-3-phosphate (Lee et al., 2009). Thus, in addition to aldolase probably a second glycolytic enzyme controls as metabolic sensor the regulatory interaction between mTORC1 and AMPK. As seen in yeast, through activation of ribosomal S6 protein kinase AKT/S6K, mTORC1 stimulates protein synthesis, which is inhibited by Snf1/AMPK downregulation of mTORC1. AMPK also inhibits ribosomal RNA synthesis by phosphorylation of RNA polymerase I transcription initiation factor IA (TIF-IA; Hoppe et al., 2009), as well as ribosomal translation by phosphorylation of eukaryotic elongation factor 2 kinase (eEF2K, yeast Gcn2), an inhibitor of translation, which is downregulated by mTORC1 and AKT/S6K (Leprivier et al., 2013; Faller et al., 2015). In addition to inhibition of protein synthesis, AMPK promotes autophagy (i.e., lysosomal degradation of proteins, cell organelles etc.), which is inhibited by mTORC1. By phosphorylation, AMPK activates ULK1 (unc-51-like autophagy-activating kinase 1) stimulating the autophagy cascade, as well as Atg9 and Beclin 1 to promote the formation of autophagosomes and recruitment of VPS34 (vacuolar protein sorting 34)-containing

complexes (Kim et al., 2011; 2013; Mack et al., 2012). AMPK inhibition of mTORC1 prevents inactivation of Tfeb (transcription factor EB), a key transcription activator of genes in lysosomal autophagy. In addition, AMPK activates FOXO3a (Forkhead boxO3) to increase transcription of Tfeb-interacting CARM1 (co-activator-associated arginine methyltransferase 1) stimulating the expression of autophagy genes (Greer et al., 2007; Shin et al., 2016; Young et al., 2016). By promoting autophagy, AMPK also aids the removal of damaged mitochondria. More importantly, AMPK activates PGC1α (peroxisome proliferator activated receptor gamma, coactivator 1α), a key regulator of mitochondrial biogenesis, by phosphorylation and also promotes NAD^+-dependent activation of PGC1α by Sirtuin 1 (Sirt1; Jäger et al., 2007; Cantó et al., 2009). Furthermore, AMPK phosphorylates and activates MFF (mitochondrial fission factor), a receptor of DRP1 (dynamin-related protein 1) promoting mitochondrial fission (Toyama et al., 2016). By these means, AMPK secures the maintenance of oxidative phosphorylation and effective ATP generation through the TCA cycle.

Inactivation of LKB1 and AMPK impairs mitochondrial respiration, which is compensated by so called anaplerotic utilization of glutamate that by reductive carboxylation converts α-ketoglutarate to isocitrate available for lipid synthesis. This anaplerotic shift is frequently observed in pancreatic cancer cells, in which mutations of LBK1 result in enhanced glucose-induced insulin secretion, fatty acid synthesis (i.e., due to ACC1 activation) and deregulated growth (Swisa et al., 2015). Finally, AMPK also counteracts mitochondrial ROS production and oxidative stress signalling as it phosphorylates and promotes nuclear localization of activated Nrf2 (nuclear factor erythroid 2-related factor 2), which is a key regulator of genes acting in anti-oxidative defence (Joo et al., 2016).

These and many other observations support the conclusion that AMPK negatively controls cell growth and division. Few direct AMPK substrates in the mitogenic pathways were identified. AMPK is reported promote cell-cycle arrest at the G1 phase via phosphorylation of tumour suppressors p53 (Imamura et al., 2001; Jones et al., 2005), Rb (Retinoblastoma, Dasgupta and Milbrandt, 2009), and p27Kip1 (CDK-inhibitor, Liang et al., 2007). AMPK phosphorylation also inhibits MDMX (mouse double minute X), a negative regulator of p53 tumour suppressor leading to p53-mediated cell-cycle arrest (He et al., 2014). Similarly, AMPK-mediated phosphorylation targets for destruction GLI1 (Glioma-associated oncogene 1) in the Hedgehog signalling pathway (Li et al., 2015b), inhibits the Hippo-YAP pathway by stabilization of AMOTL1 (angiomotin-like 1; DeRan et al., 2014), a negative regulator of YAP (Yes-associated protein), and directly inhibits the YAP oncoprotein (Mo et al., 2015; Wang et al., 2015).

As yeast Snf1, human AMPK appears to participate in general regulation of RNAP II transcription. AMPK is reported to phosphorylate and inhibit interaction of p300 histone acetyltransferase with nuclear receptors (Yang et al., 2001). AMPK also regulates histone H3K27 trimethylation by phosphorylation of the T311 residue of histone methyltransferase EZH2 (Enhancer of zeste homolog 2), which inhibits its interaction SUZ12 in the core of Polycomb Repressor Complex 2

(PRC2; Wan et al., 2018). AMPK phosphorylation abolishes the interaction of Cry1/2 cryptochrome blue-light receptors as repressors with several nuclear hormone receptors. Cry1 and Cry2 also function as repressors of CLOCK and BMAL1 transcription activators of the circadian clock, which are negatively regulated by the PERIOD (PER1/2/3) proteins. AMPK-mediated phosphorylation targets the Cry1/2 and PER proteins for degradation (Um et al., 2007; Lamia et al., 2009; 2011).

1.7 Identification of AMPK substrates using engineered analogue-sensitive (AS) kinases in chemical genetic screens

Due to central regulatory significance of AMPKs in controlling type 2 diabetes, obesity and cancer, specific identification of their substrates and regulatory partners became of central importance. To facilitate the identification of AMPK phosphorylated substrates in various signalling pathways and nuclear transcription regulatory complexes, Banko et al. (2011) exploited a novel mass spectrometry-based chemical genetic approach (Alaimo et al., 2001). This approach is based on the identification of so-called‘‘gatekeeper’’ amino acid residues in the ATP-binding pockets of protein kinases which are located close to the N^6 position of the adenine ring of ATP. By exchanging these gatekeeper amino acid residues for smaller amino acids, the engineered “analogue specific (AS)” protein kinases are enabled to use ATP analogs that carry bulky N^6-substitutions, such as benzyl, phenethyl, cyclopentenyl etc. groups (Allen et al., 2007, Figure 2A). Due to the steric hindrance of the gatekeeper residue, these bulky ATP analogs are poor substrates for wild-type kinases. To specifically label the substrates phosphorylated by AS-kinases, bulky N^6-modified ATPγS nucleotides are used, which transfer thiophosphate residues to the kinase phosphorylation sites. These thiophosphate residues can then be alkylated with para-nitrobenzyl mesylate (PNBM) and detected using a specific monoclonal antibody recognizing the P-S-PNMB hapten structure (Allen et al., 2005). Using the same approach, the PNBM-alkylated thiophosphorylated kinase substrates can be purified by binding to the immobilized monoclonal antibody and then identified upon trypsin digestion by MS/MS or LC/MS mass spectrometry. Alternatively, tryptic peptides of thiophosphate labelled kinase substrates can be covalently captured and more efficiently enriched by binding to iodoacetyl-agarose resin, and selectively released by strong oxidative agents, such as oxone for large scale analysis of AS-kinase substrates compared to samples containing the wild type kinase versions (Blethrow et al., 2008; Hertz et al., 2010; Carlson and White, 2012; Figure 2).

Using this technology, Banko et al. (2011) transiently expressed AS-AMPKα2 in human cells, and following AMPK stimulation with 2-deoxyglucose performed *in situ* thiophosphorylation followed by capture of PNBM-alkylated thiophophorylated substrates with immobilized monoclonal antibody (Figure 2B). Compared to wild type AMPKα2 control, 32 AS-AMPK α2 candidate substrates were identified, including known AMPK targets, such as ACC1 and CARM1. The majority of newly identified AMPK substrates represented proteins involved in the control of mitosis, including CDC27,

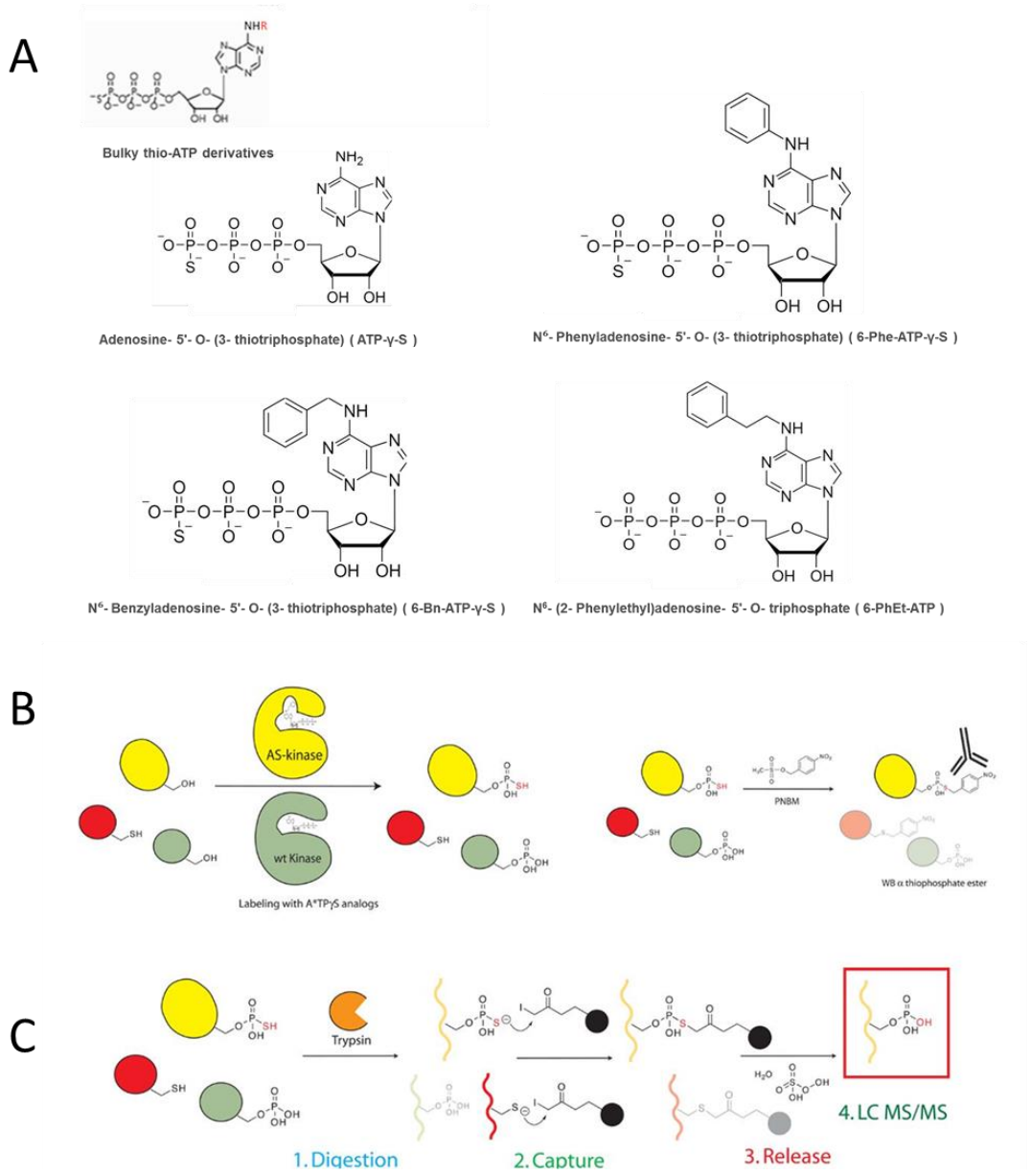

Figure 2. Identification of AS-kinase substrates by PNBM detection and enrichment of thiophosphorylated substrates.
A) Exchange of the "gatekeeper" amino acid for smaller amino acid residues (e.g. Gly) in the conserved ATP-binding pockets of protein kinases is used for engineering of analogue sensitive AS-kinases, which can utilize ATP-analogues carrying bulky N^6-substitutions, such as benzyl, phely or phenethyl groups. For detection of phosphorylation, ATP is replaced by thioγP-ATP (thioATP or ATPγS), which transfer thiophosphate (P-SH) groups to the kinase substrates. **B)** Wild type kinases present in protein extracts cannot use bulky N^6-substituted thioAPT analogues which in contrast are utilized by the AS-kinases. Thus, AS-kinase substrates thiophosphorylated by these bulky thioATP analogues can be specifically detected by alkylation of proteins with p-nitrobenzyl mesylate at pH 4.0 following the kinase reaction (Lee et al., 2011). The PNBM-alkylated proteins can be detected by a monoclonal antibody (ABCAM ab92570) developed by Allen et al. (2005). **C)** For large-scale enrichment of AS-kinase substrates, total cell or nuclear protein extracts are thiophopshorylated with either endogeneously produced or externally added AS-kinases in the presence of bulky thioATP, and upon desalting and trypsin digestion the thiophosphorylated peptides are bound through alkylation to iodoacetyl-agarose beads. Peptides carrying alkylated cysteine residues (i.e., thiol groups) stay stably bound, while peptides with alkylated thiophosphate residues can be selectively oxidized to sulfoxide by oxone and released from the beads for subsequent mass spectrometry identification (Blethrow et al., 2008; Hertz et al., 2010).

APC1 subunit of anaphase promoting complex, regulatory subunit 12A of protein phosphatase 1 and others. Schaffer et al. (2017) stably expressed the AS-AMPKα1 and α2 kinase subunits in the human cancer cell line U2OS and performed *in situ* thiophosphorylation reactions in AMPK-stimulated DMSO permeabilized cells followed by application of the iodoacetyl-agarose enrichment method (Figure 2C; Blethrow et al., 2008; Hertz et al., 2010). This approach resulted in the identification of 50 candidate AMPK substrates including 29 previously characterized ones, such as ACC1, RAPTOR, TBC1D1 etc., and 14 AMPK substrates involved in cellular motility, adhesion, or invasion. These and other applications illustrate that the use of AS-kinases and enrichment of their specific thiophosphorylated substrates is a powerful tool in further analysis of Snf1/SnRK1/AMPK regulated signalling pathways.

1.8 Plant SnRK1 kinases

In comparison to yeast Snf1 and animal AMPKs, so far less is known about the regulatory functions of plant SnRK1 enzymes and molecular mechanisms linking them to various signalling pathways (Crozet et al., 2014; Margalha et al., 2016; Broeckx et al., 2016; Wurzinger et al., 2018). The Snf1-related class of plant protein kinases belong to three clads, which include the SnRK1, SnRK2 and SnRK3 families that show sequence relationships between their catalytic domains but considerable divergence in their regulatory domains, subunits and interacting partners (Hrabak et al., 2003). Only subunits of the SnRK1 family can genetically complement the corresponding yeast mutations. The SnRK2 subfamily contains 10 divergent plant-specific kinases, which are regulated by the ABA receptor-PP2C complexes and control the activities of transcription factors in osmotic stress and abscisic acid (ABA) signalling (Cutler et al., 2010; Umezawa et al., 2010). The SnRK3 subfamily contains 25 members, which interact with calcineurin B-like (CBL) calcium-binding proteins involved in salt (e.g., SOS, salt overly sensitive) and osmotic stress signalling (Steinhorst and Kudla, 2013).

In contrast to members of the SnRK2 and SnRK3 families, studies of the functions of plant SnRK1 enzymes is hampered by the lack of null mutations in the SnRK1α1/2 subunit genes *AKIN10/11*. In the moss *Physcomitrella patens*, double knockout of *Snf1a/b* genes prevents growth, starch accumulation and viability unless the mutant is maintained in the presence of externally provided sugars under continuous illumination (Thelander et al., 2004). Inducible artificial microRNA silencing of *SnRK1α1/2* in Arabidopsis was reported to cause ultimate lethality, which cannot be compensated by sugar feeding or continuous illumination. Partial SnRK1α silencing apparently prevents starch mobilization through the night and promotes activation of stress responses and anthocyanin accumulation (Baena-González et al., 2007; Margalha et al., 2016). Silencing of barley SnRK1α results in binucleated pollens suggesting a meiotic defect resulting in male sterility (Zhang et al., 2001). Recently, Gao et al. (2016) reported that inactivation of the sole of Arabidopsis SNF4/SnRK1γ subunit gene in the SALK_074210 and GABI 346E09 T-DNA insertion mutants did not prevent *in vitro* pollen germination but inhibited pollen growth on the stigma surface due to reduced ROS generation and

defective mitochondrion and peroxisome biogenesis (Gao et al., 2016). Genetic analysis of the same mutants in our laboratory shows that the *snf4* mutant alleles segregate at 1:1 ratio due to a defect in male meiosis II. Similarly to *AKIN10/11*, no T-DNA null mutations exist in the atypical *AKINβ3* gene, and so far there is no report on the effects of existing insertion mutations in the *AKINβ1/2* genes.

Based on Affymetrix transcript profiling, Baena González et al. (2007) found that numerous dark-induced transcripts controlled by the S1-group of bZIP transcription factors are upregulated following transient overexpression of SnRK1α1/2 in leaf protoplasts cultured in 0.4M mannitol-containing carbon and nitrogen source free medium. Because the transcript profiling data showed an overlap with a number of genes that are oppositely regulated by glucose and sucrose feeding in Arabidopsis seedlings, but indicated similar regulation with genes induced by extended dark-treatments, it was concluded that SnRK1 is activated similarly to yeast Snf1 and mammalian AMPKs by sugar starvation. In contrast, Bhalerao et al., (1999) and Jossier et al. (2009) found that in Arabidopsis seedlings grown *in vitro* with proper N-supply in the presence of high concentration of glucose or sucrose (i.e., inhibiting source to sink phloem transport), SnRK1 phosphorylation activity is increased. In addition, glucose-1-phosphate (G-1P) and G-6P were reported to inhibit *in vitro* the activity of partially purified SnRK1 enzymes (Toroser et al., 2000; Zhang et al., 2009; Nunes et al., 2013). However, none of the studies demonstrated that sugar treatments alter the activating T-loop phosphorylation of SnRK1.

Zhang et al., (2009) found that overexpression of the *E. coli otsA* trehalose-6-phosphate (T6P) synthase (TPS1) in Arabidopsis confers largely opposing transcriptomics changes compared to the protoplast data of Baena-González et al. (2007). The same authors reported that T6P inhibits the activity of SnRK1 in protein extracts of developing seedlings, but T6P inhibition was not detected in mature leaf extracts. The SnRK1 inhibitory activity could be separated by anion-exchange chromatography from the kinase and reconstituted by a size separated protein fraction suggesting the existence of a protein factor, which associates with SnRK1 and mediates its inhibition by T6P-sensing. According to Nunes et al. (2013), the same protein fraction is possibly responsible for SnRK1 inhibition by G-1P and G-6P. Given these data, it is now generally thought that SnRK1 is negatively regulated by T6P, although yeast Snf1 and animal AMPKs are unaffected by this compound. This model became attractive, since the levels of T6P appear to faithfully correlate with cellular availability of sucrose (Paul et al., 2008; Lunn et al., 2014; Figueroa and Lunn, 2016). Therefore, T6P was proposed to mediate sugar-induced repression of SnRK1. This model is certainly applicable to sucrose, which is split by sucrose synthase (SuSy) to fructose and UDP-glucose, where the latter compound is a direct substrate for T6P synthesis from G-6P and UDP-glucose. However, T6P was found not to inhibit plant HXK1 (GIN2, GLUCOSE INSENSITIVE 2), which is similarly to its yeast counterpart is a key activator of glucose repression (Moore et al., 2003). Thus, it is still unclear how sugar phosphorylation through HXK1 regulates *in vivo* the activity of SnRK1.

2-deoxyglucose (2-DG, phosphorylation of which is thought to decrease ATP levels) was demonstrated to activate SnRK1 similarly to mammalian AMPK (Harthill et al., 2006). 2-DG-mediated activation of SnRK1 was reported to induce phosphorylation of TPS5, which is a bifunctional class II trehalose-6-phosphate synthase/phosphatase enzyme carrying a fusion of TPS and TPP catalytic domains. In Arabidopsis, TPS5 to 11 belong to this class II family, while TPS1 to 4 represent monomeric trehalose-6-phosphate synthase, and TPPA to J monomeric T6P-phosphatase enzymes (Vandesteene et al., 2012). All Arabidopsis TPPs can complement the yeast *tpp* mutation, and TPS1, 2 and 4 are also active enzymes complementing the yeast *Δtps1Δtpp* mutation (Delorge et al., 2015). Despite a contradictory report (Chary et al., 2008), it appears that none of the class II TPS-TPP enzymes complement the yeast *Δtps1Δtpp* mutant, although they appear to carry functional catalytic domains (Ramon et al., 2009). Similarly to the yeast *tps1* mutation, inactivation of Arabidopsis *TPS1* results in severe growth arrest, embryo arrest, accumulation of soluble sugars and starch, and elevated expression of genes related to ABA signalling. Partial loss of function *tps1* mutants show enhanced ABA sensitivity and delayed flowering (Gómez et al., 2010). Given these observations, Wahl et al. (2013) reported that T6P production by TPS1 plays a central role in induction of flowering suggesting a correlation with T6P-mediated inhibition of SnRK1.

Overexpression of yeast Tps1 in Arabidopsis leads to pleiotropic developmental defects (Miranda et al., 2007), similarly to overexpression of Arabidopsis TPS1 homolog, which confers ABA insensitive seed germination and reduced inhibition of photosynthesis by glucose. However, Avonce et al. (2004) found that TPS1 overexpression results in late flowering, sterility and downregulation of ABI4 in ABA signalling. Furthermore, they reported that TPS1 is repressed by glucose and derepressed by antisense inhibition of HXK1, which would suggest that TPS1 transcription is inhibited by HXK1-dependent glucose repression. Remarkably, Miranda et al. (2007) showed that overexpression a translational fusion of yeast TPS1 to TPP does not result in any of these defects but confers drought, freezing and heat stress tolerance. In contrast to TPS1, Arabidopsis class II TPS5 is reported to be upregulated by sugar (Baena-González et al., 2007), while TPS8-11 are induced by sugar starvation (Usadel et al., 2008). However, all class II TPS transcripts are suggested to be destabilized upon sucrose feeding (Yadav et al., 2014). So, if class II TPS-TPP enzymes would act as potential T6P sensors as hypothesised (Broeckx et al., 2016), it is predicted that their functions would be differentially regulated by sugar availability at the level of transcription and/or mRNA stability. Recent studies of transcriptomics changes in response to extended night (defined in plants as sugar starvation condition, but influenced by activation of numerous stress response pathways) followed by recurrent sugar supply also indicate that only part of observed effects are related to SnRK1. Thus, in analogy to yeast Tps1 and Snf1 (Deroover et al., 2016), Cookson et al. (2016) raised the possibility that TPS1/T6P and SnRK1 might regulate sucrose-dependent and sugar starvation responses independently, such that T6P accumulation inhibits SnRK1 solely when sucrose is available.

Similarly to yeast Snf1 and animal AMPKs, plant SnRK1 enzymes are regulated by T-loop phosphorylation of their catalytic α-subunits. Based on complementation of yeast *sak1 elm1 tos1* triple mutant, two putative Arabidopsis SnRK1 activating kinases SnAK1/GIRK2 and SnAK2/GIRK1 (GEMINIVIRUS REP INTERACTING KINASE 1) were identified (Hey et al. 2007), which were previously reported to interact with and phosphorylate the geminivirus replicator protein AL2 (Kong and Hanley-Bowdoin, 2002; Shen and Hanley-Bowdoin, 2006). SnAK1/2 undergo autoactivation by autophosphorylation of their T-loop Thr residues (SnAK Thr153; SnAK2 Thr154) and phosphorylate the T-loops of SnRK1α subunits by increasing their kinase activities *in vitro* (Shen et al., 2009; Crozet et al., 2010; Robertlee et al., 2010). At the same time, SnRK1 can phosphorylate the T-loop Ser residues of SnAK kinases (SnAK1 S260 and SnAK2 S261) by inhibiting their activity *in vitro*. This might indicate a negative feedback loop by which SnRK1 inhibits virus replication through inactivating the geminivirus-induced SnAK kinases to phosphorylate the viral replicator protein AL1 (Crozet et al., 2010). Double T-DNA knockout of *SnAK1/2* results in arrested seedling development unless seeds are germinated on glucose-containing medium, on which the double mutant grows as miniature infertile plant. In the *snak1snak2* mutant, the T-loop phosphorylation of SnRKα1 is highly reduced (Glab et al., 2017) suggesting that despite *in vitro* autoactivation of SnRK1α kinases, SnAK1/2 is required for their *in vivo* activation. N-terminal deletion retaining the active kinase domain of SnAK2 in another combination of T-DNA insertion alleles was used to construct a partial loss of function double *snak1snak2*, mutant, which shows normal development but enhanced sensitivity to glucose and salt. In correlation with this phenotype, SnAK2/GIRK1 was found to phosphorylate the T-loop of the SOS2 (Salt overly sensitive 2) SNRK3.11 kinase, which plays a key role in the regulation of salt tolerance (Liu et al., 2000; Barajas-Lopez et al., 2018). SnAK1/2 levels are low in most plant organs except for the apical meristem of developing seedlings. It was therefore concluded earlier that SnAKs are likely not essential suggesting the existence of alternative upstream kinases (Crozet et al., 2014, Margalha et al., 2016). The recent genetic data now challenge this conclusion. Finally, it is worth to note that the closest yeast homologs of Arabidopsis SnAKs are not Elm, Pak1 or Tos1 but the fission yeast Ssp1 kinase involved in the regulation of cell polarity (Lee et al., 2018).

Similarly to SnAK1/2, SnRK1α2/AKIN11 was also found to interact in yeast 2H assays with the geminivirus AL2 and L2 proteins and their homologs, AL2 of tomato golden mosaic virus (TGMV) and L2 of beet curly top virus (BCTV), and these interactions were reported to inhibit AKIN11 (Hao et al., 2003). The same viral proteins were observed to interact with and inactivate adenosine kinase (ADK), which recycles ADP to ATP and AMP maintaining energy homeostasis (Wang et al., 2003). AL2/L2 expression results in enhanced viral susceptibility and was found to inhibit ADK and T-loop phosphorylation of AKIN11 (Wang et al., 2003; Mohannath et al., 2014). Remarkably, AKIN11 also interacts with and phosphorylates ADK by stimulating its activity, while AKIN11 overexpression confers tolerance to viral infection (Hao et al., 2003; Mohannath et al., 2014). SNRK1 is also reported to phosphorylate the cabbage leaf curlvirus (CalCuV) and tomato mottle virus (ToMoV) AL2/L2

proteins thereby delaying viral infection (Shen et al., 2014). The stress-induced plasma-membrane-bound remorin proteins, which enhance geniminivirus infection also interact with and are phosphorylated by SnRK1 (Son et al., 2014). In pepper, SnRK1 interacts with and phosphorylates the AvrBST resistance protein, which recognizes the AvrBS1 elicitor of *Xanthomonas campestr*is pv. *vesicatoria* (Xcv) that induces SnRK1-dependent hypersensitive defence response (HR; Szczesny et al., 2010). Finally, interaction of Arabidopsis SNF4/AKINβγ with the HSPRO1/2 LRR proteins implicated in resistance responses to *Pseudomonas syringae* corroborate the observations that SnRK1 plays an important role in the regulation of pathogen defence responses (Gissot et al., 2006; Murray et al., 2007; Schuck et al., 2013).

It was found early on that the T-loop of purified spinach SnRK1 kinase can be dephosphorylated with human PP2C phosphatase *in vitro*, which is prevented by low concentration of AMP (Sugden et al., 1999a). In fact, SnRK1 is dephosphorylated and inactivated by the ABI1 and PP2C protein phosphatases (Rodrigues et al., 2018), as well as by the myristolyted putative membrane-bound PP2C74 enzyme (Tsugama et al., 2012). Notably, the SnAK-activated membrane-bound SOS2/SnRK3.11 kinase similarly interacts with the PP2C phosphatase ABI2, which together with ABI1 represent central inhibitors of ABA signalling that are responsible also for inactivation of members of the SnRK2 family in the absence of ABA signal. These PP2Cs form a complex with ABA receptors and are inactivated upon ABA-binding to the PYL/PYR receptors (Cutler et al., 2010; Umezawa et al., 2010). Inactivation of SnRK1 and SnRK2 enzymes confer ABA insensitivity (Radchuk et al., 2006; Fujii et al., 2011), whereas their overexpression results in enhanced ABA sensitivity (e.g., Jossier et al., 1999; promoting sucrose accumulation in case of SnRK2.6; Zheng et al., 2010).

Thus far, it is unknown how myristoylation of SnRK1 β-subunits affect the kinase activity, localization and substrate specificity. Mutation of the canonical MG glycine residue and inactivation of NMT1 myristyltransferase were reported to enhance nuclear localization of AKINβ1 and to increase SnRK1 activity (Pierre et al., 2017). Several sites of human AMPKβs are phosphorylated *in vivo*, out of which Ser108 phosphorylation is required for AMPK activation by salicylic acid that prevents its T-loop dephosphorylation (Warden et al., 2001). Tomato Adi3, a nuclear suppressor of programmed cell death interacts with SnRK1α and SnRK1β1, and phosphorylates the S26 residue of the β1 subunit, which might contribute to inhibition of the kinase activity (Avila et al., 2012).

Various environmental queues, such as low nutrient conditions and phosphate starvation were reported to promote SnRK1 ubiquitination and proteasomal degradation. SnRK1 interacts with the Skp1 subunit of SCF E3 ubiquitin ligases and the proteasome α4 subunit suggesting its possible involvement in the control of ubiquitination in association with the proteasome (Farrás et al., 2001). SnRK1α1/2 (AKIN10/11) also interacts in yeast two-hybrid (2H) assays with the PRL1 WD40 protein which, in addition to its role in the NTC spliceosome activating complex (Koncz et al., 2012), functions as substrate targeting subunit of Cul4-DDB1 ubiquitin E3 ligase mediating degradation of SnRK1α1

subunit (Németh et al., 1998; Bhalerao et al., 1999; Lee et al., 2008). SnRK1α1/AKIN10 interacts also with the SUMO-conjugating (E2) enzyme SCE1 (Elrouby and Coupland, 2010) and polySUMOylation of its lysine residues K34, K63 and K390 by SIZ1 (a key regulator of phosphate starvation, SA-dependent pathogen response and ABI5-dependent ABA responses; Datta et al., 2018), targets the active kinase for ubiquitination-dependent degradation (Crozet et al., 2016).

The SnRK1α subunits interact with a range of potential partners in yeast 2H screens. One of the 2H partners includes the family of ABA-induced SKIN (SnRK1 inhibitor) proteins that prevent SnRK1-mediated activation of starch degrading α-amylase by the MYBS1 transcription factor in rice (Lu et al., 2007). Homologs of rice SKINs have been recently identified in Arabidopsis, but their functions remained so far uncharacterized (Nietzsche et al., 2016). Another WD-40 protein, which interacts with the C-terminal regulatory domain of Arabidopsis SnRK1α1/AKIN10 is the myo-inositol polyphosphate 5-phosphatase (5PTase13, inactivates the second messenger inositol 1,4,5-triphosphate, InsP3), which is suggested to modulate SnRK1 stability in response to phsosphoinositol signaling and sugar availability (Ananieva et al., 2008). SnRK1 also interacts in 2H screens with members of a DUF581 domain protein family of unknown function. The DUF581 factors are suggested to act as SnRK1 targeting subunits based on their 2H interactions with TCP transcription factors and DELLA repressors of gibberellin signaling (Nietzsche et al., 2014; 2016).

Similarly to their yeast and animal counterparts, plant SnRK1 kinases modulate the activity of key enzymes of anabolic and catabolic pathways in cell metabolism, as well as several hormonal and stress pathways controlling plant growth, development, abiotic/biotic stress tolerance, autophagy and cell death (for reviews see Hey et al., 2010; Broeckx et al., 2016; Hulsmans et al., 2016). As mentioned above, SnRK1 kinases purified from various plant species were shown to phosphorylate and confer dark-induced inactivation of sucrose- phosphate synthase (SPS; Winter and Huber, 2000) and nitrate reductase (NR, Lillo et al., 2004). Phosphorylated SPS (i.e., at Ser 158) and NR undergo proteolytic degradation under low sugar conditions, but might be stabilized by phosphoserine-binding 14-3-3 adaptor proteins in response to sugar availability. In turn, the stability of 14-3-3 proteins appears to be oppositely regulated by the ATL31 ubiquitin E3 ligase in response to C/N availability (Yasuda et al., 2014). In addition, overexpression of membrane-associated SnRK1β1 subunit was reported to decrease the activity of NR (Li et al., 2009). Sugden et al (1999b) found early on that in addition to SPS and NR, SnRK1 purified from spinach leaves can phosphorylate the Ser577 residue of HMGR (3-hydroxy-3-methylglutaryl-coenzyme a reductase) and inactivate this first rate-limiting enzyme in the mevalonate pathway. Downregulation of HMGR by Arabidopsis SnRK1α1 phosphorylation was confirmed by Robertlee et al. (2017). Flores-Pérez et al. (2010) observed that increased sugar accumulation in the *prl1* mutant stimulates the accumulation mevalonate pathway derived isoprenoid products (i.e., which suggests that SnRK1 is likely more stable in the *prl1* mutant and thus shows somewhat higher activity in leaf extracts where it is not inhibited by T6P). In maize leaves, SnRK1 stimulates the phosphorylation

of S15 residue of sucrose synthase promoting its ubiquitination and proteasomal degradation (Hardin et al., 2003). Similarly to human AMPK, Arabidopsis SnRK1 also phosphorylates 6-phosphofructo-2-kinase/fructose-2,6-bisphosphatase stimulating its PFK2 kinase activity (McCormick and Kruger, 2015). On this way, SnRK1 probably enhances glycolysis in sink tissues (Kulma et al., 2014). In leaves during photosynthesis, sucrose accumulates and stored in vacuoles, and PFK2 activity and F-2,6-bisP levels are low during the day. Kulma et al. (2014) showed that PF2K/F2KP is phosphorylated by SnRK1 in the light and bound to 14-3-3 proteins, which probably inhibit its activity. Cho and Yoo (2011) provided evidence for that fructose-1,6-bisphosphatase acts independently of its catalytic function as fructose (i.e., fructose-6-P) sensor conferring glucose repression downstream of hexokinase 1 (HXK1) and the ABA receptor-PP2C-SnRK2 pathway. Hypoxia and extended night/darkness (i.e., often defined as starvation condition) were reported to stimulate SnRK1-mediated phosphorylation of SPS, NR, PFK2/F2KP and also TPS7/8 to stimulate glycolysis and mitochondrial respiration or gluconeogenesis under hypoxia (Cho et al., 2016; Nukarinen et al., 2016). Nonphosphorylating glyceraldehyde-3-phosphate dehydrogenase (np-Ga3PDHase) acting in an alternative route of glycolysis in heterotrophic sink tissues is also a substrate of wheat SnRK1, which is reported to be allosterically inhibited by ribose-5-phosphate, fructose-1,6-bisphosphate and 3-phosphoglycerate but not by glucose-6-P and T6P (Piattoni et al., 2011).

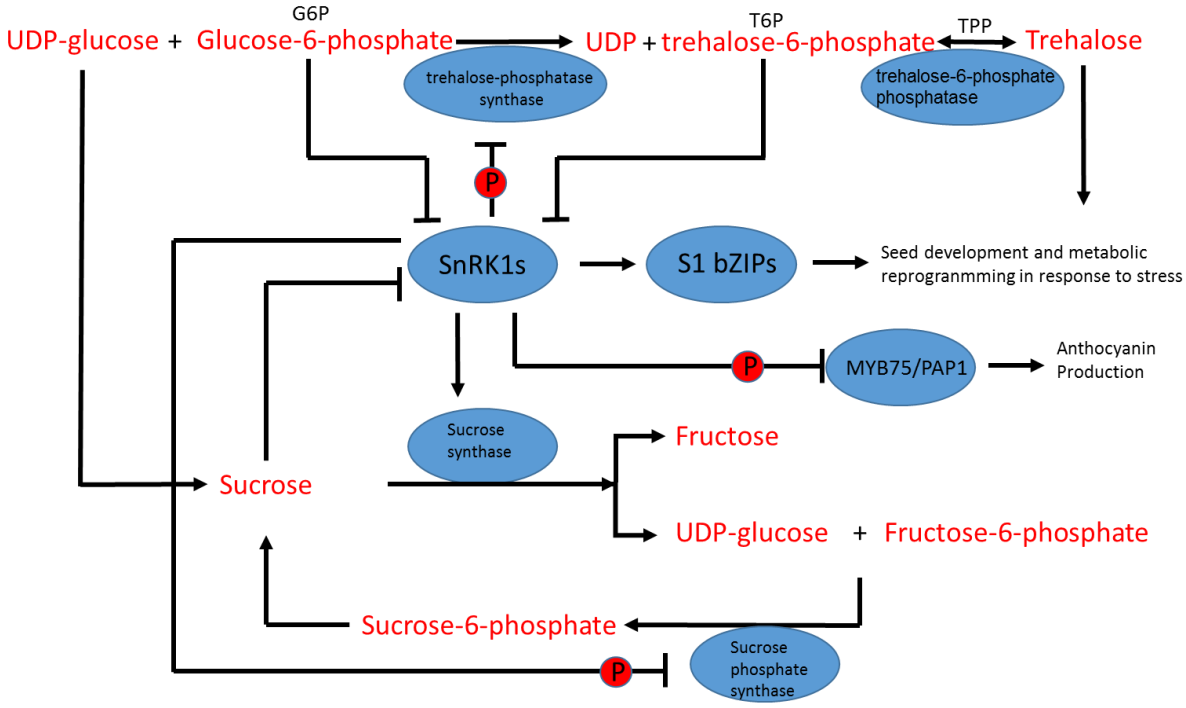

Figure 3. Schematic model for SnRK1 regulation of sucrose metabolism and signalling pathways.
Regulation of key enzymes in the pathways and SnRK1-mediated control of dimerization and activation of C/S1-group of bZIP TFs are described is the text.

Finally, pyruvate kinase (PK), another rate-limiting enzyme of glycolysis (producing pyruvate and ATP from phosphoenolpyruvate (PEP) and ADP), is found to interact with potato StubSnRK1 in

yeast 2H assays. Antisense inhibition of StubSnRK1 decreases the activity of cytosolic PK activity (Beczner et al., 2010), while in C/N-limited Arabidopsis protoplasts overexpression of AKIN10 up-regulates mRNA levels of cytosolic PK (Baena-González et al., 2007). In summary, these data indicate that plant SnRK1 regulates the glycolysis at several steps by phosphorylating various enzymes, and that this regulation differs in photosynthetic source leaves and developing sink organs (Figure 3).

Transcript profiling studies performed with SnRK1α1/AKIN10 overexpressing Arabidopsis protoplasts identified over 1000 SnRK1 regulated genes (Baena-González et al., 2007). This study indicates that SnRK1 overexpression enhances the expression of genes acting in cell wall, starch, sucrose, amino acid, lipid, and protein degradation, and autophagy but downregulates genes involved in ribosome biogenesis and other anabolic processes. Recently, Cookson et al., (2016) compared the dataset of Baena-González et al. (2007) to transcript profiling studies performed with continuous light-grown plants shifted for various times into darkness and re-exposed to light or sugar feeding excluding the effect of circadian clock regulation (Usadel et al., 2008). This study identified two clusters of SnRK1 regulated genes based on their altered expression during early phase of light to dark shift and upon exhaustion of leaf starch reserves. The latter cluster is enriched for genes, which are also modulated by redox changes, ABA and ethylene.

Baena-González et al. (2007) identified several dark-induced *DIN* genes, such as DIN6/ASN1 (ASPARAGINE SYNTHASE 1), which are upregulated by SnRK1 overexpression in protoplasts. Activation of *DIN6/ASN1* is controlled by the S1-class of bZIP transcription factors (bZIP1, bZIP2/GBF5, bZIP11/GBF6/ATB2, bZIP44 and bZIP53). Co-expression of S1-bZIPs with SnRK1α1/AKIN10 stimulated the transcription of *DIN6/ASN1* similarly to the C-group bZIP63 transcription factor (TF), a heterodimerization partner of S1-bZIPs. While translation of S1-bZIPs is stalled by upstream short open reading frames (i.e., uORFs) when sugar is available, overexpression several S-bZIPs is reported to cause growth defects resulting in accumulation of sucrose and hexose-phosphates (see for review Lastdrager et al., 2014). At the same time, transcription of S1-bZIP1 and C-bZIP9/63 are repressed, while S1-bZIP11 is induced by sugar availability. S1-bZIP11 overexpression is reported to induce *TPP-F/G* and trehalase expression lowering the level of T6P, and suggested to confer thus activation of SnRK1 (Ma et al., 2011). While the S1-group bZIP44 and bZIP53 TFs influence ABA/sugar modulated seed development and germination (Alonso et al., 2009; Iglesias-Fernández et al., 2013), bZIP1 appears to mediate sugar repression (Kang et al., 2010). bZIP11 interacts with the ADA2b adaptor protein to recruit the SAGA/GCN5 histone acetylase complex to auxin-regulated promoters (Weiste and Droge-Laser, 2014). SnRK1 phosphorylates *in vitro* and likely *in vivo* the C-group bZIP63 TF in contrast to members of the S1-group, and is thus suggested to control their functions by SnRK1-stimulated heterodimerization (Mair et al., 2015).

Recently, silencing of bZIP2/11/44 in a *bzip1bzip53* mutant and silencing of SnRK1α2/AKIN11 in the weak GABI_579E09 *akin10* mutant was reported to inhibit transcription of several genes involved

in the catabolism of branched chain amino acids (BCAAs: Leu, iLeu, and Val), which are induced by darkness and hypoxia. SnRK1 silencing also downregulates transcription ETF/ETFQ electron acceptor of mitochondrial electron transport chain, which receives electrons from the BCAA degrading mitochondrial enzymes (Pedrotti et al., 2018). Based on direct binding of bZIP2 to the *ETF/ETFQ* promoter and dimerization of bZIP2 with bZIP63, it was concluded that SnRK1 activation of S1/C-bZIP1 plays a key role in activation of amino acid, especially BCAA degradation pathways in response to starvation. In addition, SnRK1α1 was found to be recruited to the *ETF/ETFQ* promoter at which histone acetylation is reduced in the SnRK1α silenced plants suggesting the SnRK1 stimulates histone H3-acetylation and thereby transcription initiation (Pedrotti et al., 2018; Dröge-Laser and Weiste, 2018). These results support the view that C/S1-bZIPs are important downstream transcription regulators in plant SnRK1 signaling pathways (Dröge-Laser et al., 2018).

Dephosphorylation of SnRK1 by PP2C phosphatases, enhanced ABA sensitivity of SnRK1α overexpressing lines and ABA insensitivity conferred by SnRK1α silencing indicate that SnRK1 acts downstream of the PYL/PYR ABA receptor-PP2C complex in ABA hormone signalling. Whether there is any regulatory interaction between SnRK1 and SnRK2 kinases in ABA signalling is still unclear. The ABI5 and DPBF/EIL/bZIP12 transcription factors representing downstream activators of ABA signalling in seed maturation and germination are equally phosphorylated by the SnRK2.6/Ost1 and SnRK1α1/AKIN10 kinases *in vitro* (Shukla, 2005; Bitrián et al., 2011). SnRK2 kinases phosphorylate and inactivate the RAV1 transcription repressor of *ABI3*, *ABI4* and *ABI5* genes acting as positive effectors of ABA signalling (Feng et al., 2014). ABI3 (SIS10; SUGAR INSENSITIVE 10) is a transcription activator, which binds to RY motives [CATGCA(TG)] of seed specific genes involved in embryo maturation and early seedling development (Mönke et al., 2012). ABI3 is activated by the homologous AP2/B3 domain transcription factor FUS3 and its partner LEC1, which are key regulators of late embryogenesis specific gene expression and vegetative phase transitions, and also control the stability of ABI3, while repressing ethylene signalling (Lumba et al., 2012). SnRK1α1/AKIN10 is reported to interact with and phosphorylate FUS3 conferring its stabilization and thereby inhibiting the embryonic-to-vegetative phase transition (Tsai and Gazzarrini, 2012). In comparison, ABI4 (SIS5; SUCROSE UNCOUPLED 6; SUGAR-INSENSITIVE 5; SUN6) belonging to the DREB subfamily A-3 of ERF/AP2 transcription factors, is an important downstream activator of HXK1-dependent glucose repression and sugar-induced ABA biosynthesis. In addition, ABI4 is a transcription repressor of COP1, which mediates ubiquitination and degradation of HY5 (H-group bZIP56), a key regulator of photomorphogenesis and anthocyanin biosynthesis (Xu et al., 2016). In addition, ABI4 is a repressor of ACS4/8 genes involved in ethylene synthesis, and thus like FUS3 inhibits ethylene signalling (Dong et al., 2016).

In the ethylene signalling pathway EIN2 and EIN3 act as positive regulators of SnRK1 antagonized leaf senescence, which stimulate the expression of NAC2 transcription factor, a target of

microRNA 164 (Li et al., 2013). Inactivation of EIN2 and the ethylene receptor ETR1 results in hypersensitivity to glucose (Zhou et al., 1998; Cheng et al., 2002), whereas inactivation of CTR1 (GIN4, GLUCOSE INSENSITIVE 4; SIS1; SUGAR-INSENSITIVE 1) repressor of ethylene signalling results in sugar insensitivity. Cheng et al. (2002) showed that ethylene signalling represses HXK1-dependent glucose-induced transcription of ABSCISIC ACID DEFICIENT2 (ABA2) resulting in downregulation of ABA production. Yanagisawa et al. (2003) found that glucose signalling through HXK1 enhances the degradation of EIN3 transcription factor, a canonical transcription activator of ethylene responsive genes (e.g., *ERF1*). Recently, Kim et al. (2017) reported that SnRK1α1 interacts with, phosphorylates and enhances glucose-induced degradation of EIN3. These data suggests that induction of leaf senescence and starch degradation by ethylene could lead to hexose accumulation and activation of HXK1 signalling (i.e., glucose repression), which in turn would inhibit photosynthesis and stimulate ABA production. Subsequent activation of ABA signalling then might trigger activation of SnRK1 (and SnRK2s) and inhibition of ethylene signalling by destabilization of EIN3. It is currently unknown how ethylene-induced proteolysis of EIN2 and activation of ethylene-induced gene expression through histone acetylation by nuclear import of EIN2-C-terminus (Ju et al., 2012; Qiao et al., 2012; Zhang et al., 2017) is affected by SnRK1. This model also implies that the CTR1 repressor of ethylene signalling could play a positivity regulatory role in ABA signalling, and possibly in the stimulation of SnRK1 and/or SnRK2 kinases. According to Yasumura et al., (2015), indeed this is the case in the moss *Physcomitrella patens*, but probably in higher plants this function is replaced by another CTR1-related kinase.

As mentioned above, ethylene signalling activates transcription of NAC2 TF (also called ANAC092 or ORE1) stimulating leaf senescence (Balazadeh et al., 2010). In our laboratory, Kleinow et al. (2009) showed that SnRK1α1/2 (AKIN10/11) interact with and phosphorylate another NAC (NO APICAL MERISITEM) TF, ATAF1. Silencing of ATAF1 confers dramatic growth reduction and developmental defects, while ATAF1 overexpression stimulates starch metabolism, authopagy, amino acid catabolism and directly activates *TRE1* (TREHALASE 1), which reduces the levels of trehalose and T6P (i.e., likely enhancing SnRK1 activity; Garapati et al., 2015). SnRK1α1/AKIN10 was also found to phosphorylate two Ser residues of IDD8/NUC (INDETERMINATE DOMAIN/ NUTCRACKER) transcription activator of sucrose synthase genes *SUS1* and *SUS4* (Seo et al., 2011), which modulate photoperiodic flowering in response to sugar availability. Inactivation of IDD8 results in delayed flowering under long day. Jeong et al. (2015) reported that AKIN10-mediated phosphorylation reduces the activity of IDD8 resulting in a similar effect. AKIN10 was found to interact with the PTL (PETALOSS) trihelix TF and suggested to control thereby cell division and growth in the boundaries between developing flower petals (O'Brien et al., 2015). Furthermore, SnRK1 is reported to phosphorylate and promote degradation of WRINKLED1, a member of AP2 TF family, which stimulates glycolysis and lipid biosynthesis (Zhai et al., 2017). In barley, SnRK1 interacts with and phosphorylates a class I heat-shock protein suggesting its possible involvement in the regulation of protein folding and/or heat tolerance (Slocombe et al., 2004). Another putative SnRK1 interacting

partner and likely substrate is MYC2, which is apparently destabilized by SnRK1 phosphorylation inhibiting its central function in the integration of light and hormonal signalling pathways to control stress (e.g. salt) tolerance (Kazan and Manners, 2013; Im et al., 2014).

Transcript profiling data of Baena-González et al. (2007) suggests the SnRK1 overexpression confers transcriptional downregulation of numerous ribosomal protein genes. Similarly to the roles of yeast Snf1 and animal AMPK in inhibition of translation, the translation initiation factor eIFiso4G1 was reported to be phosphorylated by SnRK1 in response to hypoxia and dark-treatment (Cho et al., 2016). In analogy to Snf1 and AMPK, SnRK1 appears to repress translation by negative regulation of mTORC1 signalling (Xiong and Sheen, 2014; Dobrenel et al., 2016). As mentioned above, mammalian mTORC1 controls protein synthesis by inhibition of eIF4E-binding proteins and activation of S6 kinases that stimulate translation initiation, elongation, and ribosome biogenesis (Ma and Blenis, 2009). Arabidopsis TORC1 is also associated with the RAPTOR and LST8 subunits, and interacts with and activates the S6 kinases S6K1/2 (Mahfouz et al., 2006; Xiong and Sheen, 2012; 2014). Similarly to human mTORC1, Arabidopsis TORC1 appears to inhibit autophagy probably through downregulating the activity of ATG1-ATG13 kinase complex (Liu and Bassham, 2010; Suttangkakul et al., 2011). By contrast, SnRK1 overexpression inhibits autophagy by inhibition of TORC1 (Soto-Burgos and Bassham, 2017). Accordingly to Xiong et al. (2013), activation of TORC1 by leaf-derived sugars stimulates meristem growth via TORC1-mediated phosphorylation and stimulation of E2F transcription activators of genes involved in DNA replication and entry into the G1/S phase of cell cycle. In comparison, S6K1 was found to phosphorylate the E2F-binding pocket of RBR tumour suppressor, which binds and thus inactivates the E2F TFs (Henriques et al., 2010). In addition, sugar/auxin-mediated activation of TORC1 and subsequent phosphorylation of S6K on Thr499 was found to stimulate phosphorylation of translation initiation factor eIF3h, which is required for reinititation of translation on mRNAs carrying inhibitory upstream open reading frame (uORF, Schepetilnikov et al., 2013). How TORC1 and S6K control the translation of uORF-containing S1-group bZIP mRNAs is unclear but this observation apparently contradicts the previous reports on sucrose repressed translation of S1 bZIP mRNAs. Like mammalian AMPKs, SnRK1 is reported to phosphorylate the RAPTOR regulatory subunit of Arabidopsis TORC1 (Nukarinen et al., 2016). Glucose–TORC1 signalling stimulates transition of young germinating seedlings to photoautropic growth, including the activation stem cell inducer WUSCHEL (Pfeiffer et al., 2016), and many other genes involved in ribosome biogenesis, DNA replication, cell cycle control, transcription and RNA processing (Xiong et al., 2013). Although several key regulators of mTORC1 signalling, such as TSC2 (tuberous sclerosis complex 2) and AXIN are not present in plants and so far no information is available about possible existence of membrane-bound fructose aldolase sensor in TORC1 complexes, these studies indicate that antagonistic regulation of cellular pathways by regulatory interactions between TORC1 and Snf1/AMPK/SnRK1 complexes are largely conserved in plants. Further studies of these regulatory interactions are expected to provide a deeper insight into mechanisms underlying the control of plant growth and stress responses by nutrient availability.

Finally, it is important note that so far all results on the regulation of metabolic enzymes and transcription factors (see below) by SnRK1-mediated phosphorylation are based on *in vitro* kinase assays and phosphopeptide analyses using total protein extracts or partially purified enzymes from wild type, SnRK1 overexpressing or SnRK1 silenced plants, tissues and protoplasts. Thus, even by using known AMPK/SnRK1 substrates, such as the SAMS or AMARA peptides (Davies et al., 1989), it cannot be always safely concluded that the observed changes are directly due to SnRK1 and not to some other SnRK1-regulated protein kinases and/or phosphatases, or SnRK2/3 kinases potentially recognizing the same substrates. Unlike for human AMPK (section 1.7), no AS-version of SnRK1α kinase subunits are available so far for *in vivo* confirmation and identification of SnRK1 substrates.

1.9 Aims of the present work

Major goals of the present work were

- The construction of an analogue-sensitive SnRK1α1/AKIN10 kinase and confirmation of its activity *in vitro* and *in vivo* using kinase reactions with ATPγS and optimization of detection of thiophosphorylated substrates by PNBM,
- Comparison of activities of T-loop mutant (nonphosphorylatable and phosphomimetic constitutively active) versions of AKIN10 kinases, and assessment of their effects on plant development,
- Expression of GFP-tagged wild type and analogue-sensitive AKIN10 in transgenic plants for purification and comparative analysis of their interacting protein partners by mass spectrometry,
- Optimization of thiophosphorylation reactions in isolated nuclei and nuclear extracts of AS-AKIN10 expressing plants for enrichment and identification of thiophosphorylated SnRK1 substrates.

2. Materials and methods

2.1 Materials

2.1.1. Chemicals, enzymes and laboratory supplies

Chemicals and laboratory supplies	
Company	**Product**
Amersham Biosciences GmbH, Germany	ECL blotting detection reagents
Baker chemicals, Netherland	Ethanol
Biomol GmbH, Germany	Caesium chloride
Bio-rad, Germany	Bradford reagent
Biozym, Germany	LE Agarose
Boehringer Mannheim, Germany	Hygromycin B
Calbiochem Corporation, Germany	Ethidium bromide
Difco Laboratories, USA	Bacto agar
	Bacto-peptone
	Bacto-tryptone
Duchefa, Netherland	Carbenicillin disodium salt
	Cefotaxime sodium salt
	Phytoagar
	Ticarcillin
Eastman Kodak Company, USA	Kodak X-Omat AR-5 Film
Gibco BRL, Germany	1kb DNA molecular marker
Heirler Cenovis GmbH, Germany	Milk powder
Invitrogen GmbH, Germany	Oligonucleotides
	Trizol
Merck, Germany	2-propanol
	Chloroform
	D-glucose
Millipore, USA	Sterivex 0.22µM filter units
Promega, USA	pGemT vector kit
Qiagen GmbH, Germany	QIAEX II Gel Extraction Kit
Roth GmbH, Germany	Acrylamide
	dNTPs
Serva GmbH, Germany	SDS
	Ponceau S solution
Sigma-Aldrich Co., USA	Ampicillin
	Kanamycin
	Rifampicin
	Bromophenol blue
	Coomassie-Blue R250
	DEPC (diethylpyrocarbonate)
	DTT (dithiothreitol)
	IPTG (Isopropyl β-D-galactoside)
	β-mercaptoethanol
	TEMED

	TritonX-100
	Sucrose
	Tween-20
	Ca-hypochlorit
	Protease Inhibitor Cocktail
	PMSF (Phenylmethylsulphonyl fluoride)
	Oxone
Whatman, USA	3MM paper
Enzymes	
New England Biolabs, Germany	DNase and RNase
	Restriction endonucleases
	T4 DNA ligase
	Q5 High Fidelity DNA Polymerase
	Antarctic phosphatase
Invitrogen GmbH, Germany	Accuprime Taq HIFI
	SuperscriptII reverse transcriptase
	Taq DNA polymerase
Chromatography resins	
GE Healthcare	Glutathion Sepharose 4B
Qiagen	Ni-NTA resin
Thermo Fisher Scientific	UltraLink Iodoacetyl Resin
Chromo Tek	GFP Trap
Sigma-Aldrich	HA affinity matrix
Radiochemicals	
GE Healthcare	$\gamma(^{32}P)ATP$
Pipette tips and tubes	
Eppendorf, Germany	Pipette tips
	PCR, 1.5 mL and 2 mL reaction tubes
Beckman Instruments Inc., USA	Centrifuge tubes
Corning Inc., USA	Falcon tubes

2.1.2. Bacterial strains

Escherichia coli strains	
DH5α	F^- endA1 glnV44 thi-1 recA1 relA1 gyrA96 deoR nupG purB20 φ80dlacZΔM15 Δ(lacZYA-argF)U169, hsdR17(rK–mK+), λ^-
BL21(DE3) pLysS	E. coli B F^- ompT gal dcm lon hsdSB(rB^-mB^-) λ(DE3 [lacI lacUV5-T7p07 ind1 sam7 nin5]) [$malB^+$]K-12(λS) pLysS[T7p20 orip15A](CmR)
JKE201	MFDpir ΔT IV lacIq (JKE201) MG1655 RP4-2-Tc::[ΔMu1:: Δaac(3)IV::lacIq-Δ$aphA^-$ Δnic35-ΔMu2::zeo] ΔdapA::(erm-pir) ΔrecA ΔmcrA Δ(mrr-hsdRMS-mcrBC) Zeocin, Erythromycin resistant
DH10B	F^- mcrA Δ(mrr-hsdRMS-mcrBC) Φ80dlacZΔM15 ΔlacX74 endA1 recA1 deoR Δ(ara,leu)7697 araD139 galU galK nupG rpsL λ^-
SW102	F^- mcrA Δ(mrr-hsdRMS-mcrBC) Φ80dlacZ M15 ΔlacX74 deoR recA1 endA1 araD139 Δ(ara, leu) 7649 galU galK rspL nupG [λcI857 (cro-bioA) <> tet]
Agrobacterium tumefaciens	
GV3101(pMP90RK)	C58C1 RifR, pMP90RK (pTiC58 ΔT-DNA) GmR, KmR (Koncz and Schell,1986)

2.1.3. Plant materials

Plant materials	
Arabidopsis thaliana, ecotype Columbia (Col-0), wildtype	Koncz and Rédei, 1994
PIN1-GFP	Benková et al., 2003
PIN2-GFP	Xu and Scheres, 2005
DR5-GFP	Liao et al., 2015
akin10 GABI mutant	GABI_579E09

2.1.4. BAC clones

Gene	AGI Gene number	BAC clone name
AKIN10	At3g01090	T4P13

(Data from TAIR [www.arabidopsis.org])

2.1.5. Plasmid vectors and construct

2.1.5.1. Plasmid vectors

Plasmid vectors	Reference
pET201	Bhalerao et al. (1999)
pPCV702	Koncz et al. (1994)
pGemT	Promega
pGemT-Km-araC-ccdB	kindly provided by Mihály Horváth
pGAP-Hyg	Bitrián et al. (2011)
pGAP-Km	Bitrián et al. (2011)
pBSKII-GFPPIPL	kindly provided by Sabine Schaefer

2.1.5.2. Plasmid constructs

Plasmid constructs	Bacterial resistance	Plant resistance
pET201-AKIN10-His	AmpR	
pET201-M119G-His	AmpR	
pET201-T175A-His	AmpR	
pET201-T175D-His	AmpR	
pET201-M119G-His NO AID	AmpR	
pET201-T175A-His NO AID	AmpR	
pET201-T175D-His NO AID	AmpR	
pET201-T175E-His NO AID	AmpR	
pPCV702-AKIN10-HA	AmpR	KmR
pPCV702-M119G-HA	AmpR	KmR
pPCV702-T175A-HA	AmpR	KmR
pPCV702-T175D-HA	AmpR	KmR
pPCV702-AKIN10-HA NO AID	AmpR	KmR
pPCV702-T175A-HA NO AID	AmpR	KmR
pPCV702-T175D-HA NO AID	AmpR	KmR
pPCV702-T175E-HA NO AID	AmpR	KmR
pGAP-AKIN10-GFPPIPL	AmpR	KmR/HygR
pGAP-AKIN10M119G-GFPPIPL	AmpR	KmR/HygR

pGAP-AKIN10T175A-GFPPIPL	AmpR	KmR/HygR
pGAP-AKIN10T175D-GFPPIPL	AmpR	KmR/HygR
pGAP-AKIN10-mCherry	AmpR	KmR/HygR
pGAP-AKIN10M119G-mCherry	AmpR	KmR/HygR
pET201-NAP57-His	AmpR	
pET201-DEAD-box-His	AmpR	
pET201-TRH1-His	AmpR	
pET201-Thioesterase-His	AmpR	
pET201-Ribosomal protein S5-His	AmpR	

2.1.5.3. Oligonucleotides

2.1.5.3.1. Oligonucleotides for site-directed mutagenesis

AKIN10-5Short	ggtacaaggatccgATGGATGGATCAGGCACAGGCAG
AKIN10M119G-3	CTCACCAGAGTTCACATACTCtccGACAAGATAAATATCTGTGGG
AKIN10T175A-3	GGACTTCCACAACTagcCTTCAAAAAATGACCATCTC
AKIN10T175D-3	GGACTTCCACAACTatcCTTCAAAAAATGACCATCTC
AKIN10T175E-3	GGACTTCCACAACTctcCTTCAAAAAATGACCATCTC
AKIN10-3 long	gtggtggtgatcaaagcttgtcgacTCAGTGATGGTGATGGTGATGGAGGAC
AKIN10-3 short No AID	gtggtggtgatcaagcttgtcgacTCATTTTGCCTGTTGCACAGTATCTGGAG

2.1.5.3.2. Oligonucleotides for recombineering

Replacement of Stop codon with Km-ccdB	
AKIN10KmccdB-STOP FW	TCTTGTTCTTGGATCTGTGTGCTGCTTTTCTTGCTCAGCTCCGAGT CCTCgccgccatgaccgtcccgtc
AKIN10KmccdB-STOP RW	AAAAAAAAGGAATAAGTGGGGATTATTCTTGAAGAGGTCCGGTT TAGTATgagctcttatattccccagaacatcagg
Replacement of M119 with Km-ccdB	
AKIN10KmccdBM119Fw	TCATCCGTCTCTATGAGGTTATAGAGACTCCCACAGATATTTATC TTGTCgccgccatgaccgtcccgtc
AKIN10KmccdBM119Rw	CTACCCTTCTCAACAATATAGTCAAATAGCTCACCAGAGTTCACA TACTCgagctcttatattccccagaacatcagg
Replacement of T175 with Km-ccdB	
AKIN10KmccdBT175Fw	TTGCTGATTTTGGCCTGAGCAACATAATGCGAGATGGTCATTTTT TGAAGgccgccatgaccgtcccgtc
AKIN10KmccdBT175Rw	agggctgaagcacttacCTCTGGAGCGGCATAATTTGGACTTCCACAACTga gctcttatattccccagaacatcagg
PCR amplification of GFPPIPL	
AKIN10GFPPIPL5	TCTTGTTCTTGGATCTGTGTGCTGCTTTTCTTGCTCAGCTCCGAGT CCTCatggtgagcaagggcgaggag
AKIN10GFPPIPL3	TCTTGTTCTTGGATCTGTGTGCTGCTTTTCTTGCTCAGCTCCGAGT CCTCatgggtcatgatgatcatcaccatg
PCR amplification of mCherry	
AKIN10mCherKm5	TCTTGTTCTTGGATCTGTGTGCTGCTTTTCTTGCTCAGCTCCGAGT CCTCatggtgagcaagggcgaggag
AKIN10mCherKm3	AAAAAAAAGGAATAAGTGGGGATTATTCTTGAAGAGGTCCGGTT TAGTATTACGCTAGGGATAACAGGGTAATATAGggtaa
Mutating M119 to G by replacing Km-ccdB	
AKIN10M119GFw	TCATCCGTCTCTATGAGGTTATAGAGACTCCCACAGATATTTATC TTGTCGGAGAGTATGTGAACTCTGGTGAGCTATTTGAC

AKIN10M119GRw	CTACCCTTCTCAACAATATAGTCAAATAGCTCACCAGAGTTCACA TACTCTCCGACAAGATAAATATCTGTGGGAGTCTC
Mutating T175 to A by replacing Km-ccdB	
AKIN10T175AFw	TTGCTGATTTTGGCCTGAGCAACATAATGCGAGATGGTCATTTTT TGAAGgctAGTTGTGGAAGTCCAAATTATGCCG
AKIN10T175ARw	agggctgaagcacttacCTCTGGAGCGGCATAATTTGGACTTCCACAACTag cCTTCAAAAAATGACCATCTCGCATT
Mutating T175 to D by replacing Km-ccdB	
AKIN10T175DFw	TTGCTGATTTTGGCCTGAGCAACATAATGCGAGATGGTCATTTTT TGAAGgatAGTTGTGGAAGTCCAAATTATGCCG
AKIN10T175DRw	agggctgaagcacttacCTCTGGAGCGGCATAATTTGGACTTCCACAACTat cCTTCAAAAAATGACCATCTCGCATT
Gap repair primers	
AKIN10FLANK1 EcoRI 5’	ggggtgttgGAATTCCTTTTGCCTACTGCTGGTTGGGTC
AKIN10FLANK1 SalI 3’	gggttgtggGTCGACGCTATTGCAGCACCATGTCTTGTCC
AKIN10FLANK2 SalI 5’	ggaacaccgGTCGACCACGCCAGAGAACAACAACACATCAG
AKIN10FLANK2 BamHI 3’	ccgttgtggGGATCCGTTGTGTCTTCGCCGAGATTCTTACC
PCR for sequencing the M119G,T175A/D replacement	
AKIN10-5A	AAGGTTGCTATCAAGATCCTCAATCGTC
AKIN10-3A	CACAGCTCCAGACATCTACTTCAGGG
PCR for sequencing the stop codon replacement	
AKIN10seq5	GAAGCAGCTGTTAAGTCGCCCAA
AKIN10seq3	TTGGTGGCATGATGCACTACAAGTTATG
PCR for sequencing the GFP junctions	
GFP5seqR :	CCGGACACGCTGAACTTGTGG
GFP3seqF :	TGCTGCCCGACAACCACTACCT

2.1.5.3.3. Oligonucleotides for CaMV 35S promoter driven expression of modified AKIN10 cDNA constructs in plants

AKIN10-5F	ggtacaaggatccgATGGATGGATCAGGCACAGGCAG
AKIN10HA-long-3	gtggtggtgatcaaagcttgtcgacTCAagcataatctggaacatcgtatggataGTGATGGTGATGGTGATGGAGGAC
AKIN10HA-short-3	gtggtggtgatcaTCAagcataatctggaacatcgtatggataGTGGTGGTGGTGGTGGTGCTC
Primers for Sequencing	
AKIN10seq1F	ATGGATGGATCAGGCACAGGCAG
AKIN10seq2F	TGCAGGAGGATGAGGCGAGGAAC
AKIN10seq3R	GTTTCGATGGCAGTATTCCACTCCTG
AKIN10seq4F	GTTGCACAGTATCTGGAGGAGGAACAG
AKIN10seq5F	ATGACGGAAGTCCTGAAAGCCCTG
AKIN10seq6R	AGCATAATCTGGAACATCGTATGGATAGTG

2.1.5.3.4. Oligonucleotides for putative SnRK1 substrates

NAP57-5	taacgtggatccATGGCGGAGGTCGACATCTC
NAP57-3	tgaactctcgagTCATTCCTCATCATCCTCACTGTC
DEADBamHI-5	taacgtggatccATGGAATCCATCATGGAAGA
DEADSalI -3	tgaactgtcgacTTATATTTCTCCTCTGTAGCCACCCG
TRH1BamHI-5	taacgtggatccATGGCTGATAGGAGAAACAG
TRH1SalI -3	tgaactgtcgacCAAGTAATAGTTCATGCCCACTT

Thioesterase BamHI-5	taacgtggatccATGTTTCTTCAGGTTACCGG
Thioesterase Xho1-3	tgaactctcgagAACGGCGTCGTCTTGGCGTA
RibosoSalI S5-5	taacgtgtcgacATGGATGAATCTGAAGGTAG
RibosoNotI S5-3	tgaactgcggccgcAACTTTACGAGCCAAGGTTCT

2.1.5.3.5. Oligonucleotides for qRT-PCR

Primer	**Sequence**
10F1	GCTCAGTAACTCGATGCACGATAACAAC
10R1	TGCAAATCCAGTAGATACTTGTCGTCCC
10F2	GGACTGATGGAATATCAAGGAGTTGGCT
10R2	ATTCAAATCTTGCAGGGCTTTCAGG
10-1F1	TTTTTGAGAATGGATGGATCAGGCACA
10-2F1	AAAAGTAGAATGGATGGATCAGGCACA
10-3F1	ATCGGAGAATGGATGGATCAGGCACA
10R3	CAATGCATGCTCAGCTATCTTCACCCTA
11F1	CAGAGATGAATCCAGCATCATTGAGG
11R1	AGAAACTGCGGACCGTTAACTCTCTGTAT
11-1F	CCCATCAATCTGATTCTCCTTGTTTCTGTA
11-2F	CAGATTACATCGAAATGGATCATTCATCAA
11-13F	GCTTTTCAGGAAATGGATCATTCATCAA
11R2	TGATAGCAACCTTATGCCCTGTGACAA
11-3F2	CCGAGTTTCAGGAGACAACATGGTTC
11-3R2	GAGACTGAAGTCCAAGAGCCCATTTTC
12F1	CCATCATCTTACCGACCGTCATCAAA
12R1	GACACCTAGCTCTCTGAGAAACGCAAC
B1F1	CTCGATGTTCATAACTTTGTGCCAGAA
B1R1	GGAGTCCATCCTTGCTCTATGAACACAT
B1-1F	CTCCTCAGGTTCCCGTGGCTC
B1-2F	CTCCTCAGCCCACATTGTTATTCCAC
B1-3F	CGAGTAAATTTCTGAGTCTACTGTTGCTATATTCAT
B1R2	CACCGCCACATCATTACCTCCTTG
B2F1	TGGGATAATTGGAAGACAAGAAGTCGG
B2R1	GTTGAAAGTGTTCCCAGCATCATCTCTA
B3Fx	GCAGTACCGCCACACCTTCAACAC
B3Rnew	CACCACAGTGACAAACTTAGTCCTGAACC
B3-1F	CAATCATTGAGCTAATCATATTCTAGGTTTTTG
B3-2F	GCGACTGATTCCTCAATTTTGATTTTCC
B3-3F	ACGAAATTTGCATTGATATCGAAGTTTTTG
B3-4F	CATTGAGCTAATCATATTCTAGGTTAAGTAAAAACAGAGTT
B3R2	TGGATAAGATTGCCACCTAGTGCCTTT
SNF4F	GACAGTTCACCAGGCGCTACAGTTG
SNF4R	ATTCGCCAACCGCTCCATCACTT

2.1.6. Culture media

2.1.6.1. LB medium

Bacto-tryptone	10g/L
Bacto-yeast extract	5g/L
NaCl	10g/L
Bacto-Agar (for solid medium)	20g/L
Adjust pH to 7.5 with NaOH	Autoclave for 20min at 120ºC

2.1.6.2. YEB medium:

Beef extract	5g/L
Bacto yeast extract	1g/L
Bacto-peptone	1g/L
Sucrose	5g/L
Bacto-agar (for solid medium)	15g/L
Adjust pH to 7.4 with NaOH	2mL of 1M $MgSO_4$ is added after sterilization

2.1.6.3. MSAR Arabidopsis medium (Koncz et al., 1994)

MSAR medium	
Macro-elements	25mL/L
Micro-element	1mL/L
Fe-Na_2-EDTA	5mL/L
$CaCl_2.2H_2O$	5.8mL/L
KI	2mL/L
Sucrose	5g/L
Vitamins	2.2mL/L
phytoagar	7 g/L
Adjust pH to 5.8 with KOH. Autoclave for 20 min at 120ºC	

2.1.6.4. MSAR stock solutions

2.1.6.4.1. Macro-elements stocks

Macro-elements:	1L Stock Solution
NH_4NO_3	20g
KNO_3	40g
KH_2PO4	7.4g
$MgSO4$	5g
$(NH3)2SO4$	3g

2.1.6.4.2. Micro-elements stocks

Micro-elements:	1L Stock Solution
H_3BO_3	6.2g
$MnSO_4.4H_2O$	16.9g
$ZnSO_4.7H_2O$	8.6g

Na_2MoO_4	250mg
$CuSO_4.5H_2O$	50mg
$CoCl_2.6H_2O$	250mg

2.1.6.4.3. Fe-Na_2-EDTA

Fe-Na2-EDTA:	1L Stock Solution
$FeSO_4.7H_2O$	5.56 g
Na2-EDTA	7.45g
Dissolve chemicals independently, mix the two solutions. Heat for 10-15min at 70-80°C	

2.1.6.4.4. Vitamins

Vitamins:	1L Stock Solution
myo-inositol	50g/L
L thiamine-HCl	2.5g/L
nicotinic acid	0.5g/L
pyridoxine.HCl	0.2g/L

2.1.7. Antibiotics

Antibiotics	Stock solution	Working concentration (mg/L)		
		E. coli	Agrobacterium	Arabidopsis
Ampicillin	50mg/mL in water	100	-	-
Carbenicillin	50mg/mL in water	100	100	-
Claforan	200mg/mL in water	-	-	300
Cloramphenicol	25mg/mL in ethanol	25	50	-
Hygromycin	15mg/mL in water	-	-	15
Kanamycin	100mg/mL in water	25	25	100
Rifampicin	25mg/mL in methanol	100	100	-
Ticarcillin	150mg/mL in water	-	-	150
All antibiotics were filtered sterilized and stored at -20ºC				

2.1.8. Plant hormones

Plant hormones	**Stock solution**	**Working concentration**
Abscisic acid (ABA)	10mM in methanol	0.1 to 2µM
ACC (1-aminocyclopropane-1-carboxylic acid)	1mM in H2O	from 10 up to 50µM
Indole 3-acetic acid (IAA)	2mg/ml dissolved in 0.5N KOH	2mg/l

2.1.9. General solutions and buffers

2.1.9.1. DNA electrophoresis solutions

2.1.9.1.1. 10 x TBE buffer

Tris-base	107.78 g/L (0.89 M)
EDTA-Na2-salt	7.44 g/L (0.02 M)
Boric acid	55.0 g/L (0.89 M)

2.1.9.1.2. 10 x TAE buffer

Tris.HCl (pH 8.0)	1M
EDTA-Na2-salt	10mM
Sodium acetate	1M

2.1.9.1.3. 10 x DNA Loading dye

Glycerol	50%
Tris.HCl (pH 8.0)	200mM
EDTA	500mM
Bromophenol blue	0.25%

2.1.9.1.4. DNA extraction & visualization

Phenol:chloroform:i-amylalcohol:	Mix at ratio 25:24:1	
EtBr	10mg/ml in water	500µg/l

2.1.9.1.5. Protease & phosphatase inhibitors, IPTG and β-estradiol stocks

General solutions and buffers	Stock solution	Working concentration
β-estradiol	10mM in DMSO	5-20 µM
MG-132	50mM in DMSO	5-20 µM
IPTG	1M in water	1mM
Na_3VO_4 phosphatase inhibitor	100 mM	1.0 mM
NaF phosphatase inhibitor	0.5 M	20 mM
Protease inhibitor cocktail (Sigma)	1 tablet in 1ml H_2O	100x dilution

2.1.10. Antibodies

Antibodies		Manufacturer	Host species	Working Dilution
Primary	Anti-GFP	Chromotek	Rat	1:2000
	Anti-His	Roche	Mouse	1:2000
	Anti-HA	Roche	Mouse	1:2000
	Anti-thio-estar	Abcam	Rabbit	1:5000
	Anti-AKIN10	Agrisera	Rabbit	1:1000
	Anti-AKIN11	Agrisera	Rabbit	1:1000
	Anti-AKINβ1	Agrisera	Rabbit	1:1000
	Anti-AKINβ2	Agrisera	Rabbit	1:1000
	Anti-SNF4	Agrisera	Rabbit	1:1000
	Anti-Thr172	Merck Millipore	Rabbit	1:1000
	Anti-actin	Abcam	Rabbit	1:500
Secondary	Anti-Rabbit IgG(H+L)	Sigma-Aldrich	Goat	1:10000
	Anti-mouse IgG(H+L)	Agrisera	Goat	1:10000
	Anti-Rat IgG(H+L)	Thermo	Goat	1:5000

2.2. Methods

2.2.1. General molecular biology methods

2.2.1.1. Mini-preparation of plasmid DNA from E.coli by alkaline lysis with SDS (Birnboim and Doly, 1979)

A single bacterial colony is inoculated into in 4 ml LB-medium with antibiotics and grown overnight (O/N) at 37°C with shaking (250 rpm). Cells from 1.5 ml culture are pelleted in Eppendorf tubes by centrifugation at 13 krpm for 3 min in an Eppendorf centrifuge followed by removal of the supernatant. The cells are resuspended in 150 µl Solution I and incubated at room temperature for 15 min, and then lysed with 150 µl Solution II by inverting the tubes several times until obtaining a water clear lysate within 5 min. The lysate is then neutralized with 300 µl Solution III and incubated for 30 min on ice to precipitate proteins and cell debris, which are removed by centrifugation at13 krpm for 10 min at 4°C. Circular plasmid (or BAC) DNA is precipitated by addition of 0.7 or 1 volume of ice cold i-propanol and incubation of the samples for at least 30 min on ice. The precipitated DNA is collected by centrifugation at 13 krpm at 4°C for 10 min. After removal of the supernatant, the DNA pellet is washed with 100 to 200 µl 70% ethanol (-20°C) and dried in a vacuum desiccator for 1 to 5 min. The DNA pellet is dissolved in 50 µl low TE (20 mM Tris.HCl (pH 8.0), 1 mM EDTA) containing 400 µg/ml RNase I (from 4 mg/l heat-treated bovine pancreatic RNase I stock) and subjected to fingerprinting by restriction endonuclease digestions. Alternatively, the DNA is dissolved in 100 µl low TE containing RNase I, incubated for 2h at 37°C and then subjected to digestion at 37°C with 500 µg/ml proteinase K (Merck, freshly made 5mg/ml stock predigested for 10 min at 37°C) for 2h or O/N. Subsequently, the DNA is extracted by equal volume of high TE (50mM Tris.HCl (pH 7.5), 20mM EDTA) saturated phenol. After centrifugation the supernatant (i.e., upper water phase) is reextracted similarly twice with equal volume of phenol:chloroform-i-amylalcohol (25:24:1), and then with equal volume of ice cold chloroform.i-amylalcohol. The supernatant is supplemented with 0.1 vol 3M Na-acetate (pH 5.6) and 0.7 vol. i-propanol, mixed, incubated on ice for at least 30 min to precipitate the DNA. Finally, the DNA is pelleted by centrifugation, washed with 70% ethanol and dried as described above, then dissolved in 20 to 50 µl sterile ddH_20 and subjected to Sanger sequencing or used as template in PCR reactions.

Solution I 50mM glucose, 50 mM Tris.HCl [pH7.5], 10mM EDTA, 2mg/ml lysozyme

Solution II 1% SDS, 0.2N NaOH (freshly made from 20%SDS and 0.4M NaOH)

Solution III 3M sodium acetate pH 4.8 (pH was adjusted with glacial acetic acid)

2.2.1.2. DNA digestion with restriction endonucleases

Digestions of DNA samples were performed with restriction endonucleases according to the manufacturers' instructions (New England Biolabs). Reactions were carried out in 1.5 ml Eppendorf tubes in a final volume of 20 to 50 µl using 1-5 U enzyme/µg DNA.

2.2.1.3. Agarose gel electrophoresis

DNA fragments are size separated by agarose gel electrophoresis. The concentration of agarose gel depends on the size of DNA fragments to be separated.

DNA fragments ≥ 10Kb	0.5% agarose
DNA fragments 0.5-10Kb	1.0% agarose
DNA fragments ≤ 500bp	2.0% agarose

The agarose powder is mixed with necessary volume of 1xTBE or 1xTEA buffer in an Erlenmeyer bottle and boiled in a microwave oven until a water clear solution is obtained. After cooling down to about 40-45°C, ethidium bromide is added to a final concentration of 0.5μg/ml, and the gel is casted in an electrophoresis tray with a slot former comb. DNA samples are mixed with 0.1 vol. of 10 x DNA loading dye and pipetted into the gel wells along a size marker, such as 1kb DNA ladder or HindIII digested λ-phage DNA. The samples are separated in TBE gels by 120-150V and in TEA gels by max. 80V current, and then the DNA bands are visualized under UV light (254nm) and photographed (e.g., using a Kodak DC-120 digital camera and a Kodak Digital Science 1D V 3.0.2. software).

2.2.1.4. Isolation of DNA fragments from agarose gel

For isolation of DNA fragments, the gel is illuminated by an UV source of 365nm, the DNA bands are excised by a scalpel and transferred into dialysis tubes (Serva Wisking MWCO 12 000 -14 000, boiled in 10mM EDTA) and filled up bubble free with 100-150μl electrophoresis buffer before closing the tubes with clamps (Sigma-Aldrich). The dialysis tubes are placed in electrophoresis chambers with just enough buffer to cover them, and then the DNA is eluted to the wall of dialysis tubes by applying current (as for electrophoresis). By reversing the current polarity for 1min, the DNA is released from the wall of dialysis tube, and then pipetted over into an Eppendorf tube and purified by phenol-chloroform extraction as described in 2.2.1.2. Alternatively, the DNA fragments can also be purified using the QIAEX II Gel Extraction Kit according to the recommended protocol, but the yield is gradually decreased by increasing the fragment size above 5kb in this case.

2.2.1.5. Measurement of nucleic acid concentration

DNA and RNA concentrations were measured at OD_{260} using Nanodrop 1000 spectrophotometer. OD_{260} 1.0 equals with 50 μg/mL of dsDNA, 33 μg/mL of ssDNA, 20-30 μg/mL of oligonucleotide, and 40 μg/mL RNA solution. The purity of nucleic acids is sufficient when the OD_{260}/OD_{280} is ~1.8 for DNA and ~2.0 for RNA.

2.2.1.6. Dephosphorylation of DNA 5' ends by Antarctic calf-intestine alkaline phosphatase (CIAP)

CIAP catalyzes the removal of 5'-phosphate groups from DNA and RNA, which is essential for preventing self-ligation of linearized plasmid DNAs used for cloning of DNA fragments. 2 units of CIAP

is added to dephosphorylate 1 µg linear DNA by incubation for 30 min at 37°C in 50 mM Tris.HCl (pH 8.0), 10 mM $MgCl_2$, 100 mM NaCl, 1 mM dithiothreitol, or 100 mM Tris-HCl (pH 8.0).

2.2.1.7. DNA ligation and filling out the DNA ends with Klenow fragment of DNA polymerase I or T4 DNA polymerase

Ligation of linearized plasmid vectors and DNA fragments carrying compatible restriction endonuclease cleaved or blunt ends is performed in 10µl final volume with 1µl of T4 DNA ligase (5U; New England Biolabs, NEB) in ligase buffer (50 mM Tris-HCl (pH 7.5), 10 mM $MgCl_2$, 1 mM ATP and 10 mM DTT) using an approximate vector to insert concentration ratio of 1:5 at 16°C overnight. In case of blunt-end ligations, the ligation is performed at room temperature O/N and the ligation mix is supplemented with 2 to 5U of T4 RNA ligase. Incompatible sticky ends of DNA fragments are filled-in with 1-2U of Klenow fragment of DNA polymerase I in fill-in buffer (500mM Tris-HCl (pH 7.2), 100 mM $MgSO_4$, 1 mM DTT, 0.5 mM dNTPs) or with 1 to 5U of T4 DNA polymerase in buffer (33 mM Tris-acetate (pH 7.5), 66 mM potassium acetate, 10 mM magnesium acetate, 5 mM DTT and 0.5mM dNTPs) at room temperature for 30 min. T4 DNA polymerase is similarly used for removal of single stranded 3' overhangs.

2.2.1.8. PCR (Polymerase Chain Reaction

2.2.1.8.1. PCR with recombinant Taq DNA polymerase

20 µl final volume	
10X PCR buffer	2 µl
10 mM dNTP mixture	1 µl
primer 1 (10 µM)	2 µl
primer 2 (10 µM)	2 µl
Template DNA	10-20 ng
Taq DNA polymerase (5 U/µl)	0.2 µl
Autoclaved distilled water	X to 20 µl

2.2.1.8.2. PCR with Q5 high fidelity DNA polymerase (NEB)

100 µl final volume	
Q5 PCR buffer 5X	20 µl
Q5 PCR Enhancer 5X	20 µl
10 mM dNTP mixture	4 µl
primer 1 (10 µM)	5 µl
primer 2 (10 µM)	5 µl
Template DNA	10-20 ng
Q5 DNA polymerase (5 U/µl)	1 µl
Autoclaved distilled water	X to 100 µl

2.2.1.8.3. The PCR program

The PCR program in a Bio Rad Multi-cycler PTC 240 Tetrad TM 2 machine:

1. initial denaturation	95°C	5 min
2. denaturation	95°C	30sec
3. primer annealing	T_m	30 sec
4.chain extension	68 or 72°C	1min/kb DNA fragment length
5.final extension	72°C	10min
6. storage	4°C	forever

The cycles of PCR (usually 35) are performed from step 2 to step 4. The Tm value of primers are calculated by the manufacturer and also estimated by using the following calculation: Tm = 4x (G+C) +2x (A+T) or using the DNA Star Laser Gene Primer Select software.

2.2.1.9. Transformation of bacteria

2.2.1.9.1. Preparation of *E.coli* and Agrobacterium GV3101 (pMP90RK) electro-competent cells

Electrocompetent *E. coli* and *Agrobacterium tumefaciens* cells were prepared according to Dower et al. (1988). *E. coli* strains were streaked out onto LB medium containing appropriate antibiotics (if necessary) and grown for 12h at 37°C. Agrobacterium GV3101 (pMP90RK) was grown on YEB plates containing either rifampicin (100mg/L) and kanamycin (25mg/L), or rifampicin and gentamycin (25mg/L) at 28°C. Single *E. coli* colony was inoculated into 5ml LB medium and grown for 12h at 37°C with shaking (200 rpm), while Agrobacterium starter culture was prepared similarly in YEB medium and grown for 2 days at 28°C. The *E. coli* starter culture was used for inoculation of 1L LB culture and grown at 37°C until reaching a density OD_{600} 0.4-0.6. The Agrobacterium starter was similarly used for inoculation of 1L YEB culture and grown at 28°C to OD_{600} 0.4-0.6. Subsequently, the *E. coli* and Agrobacterium cultures were treated similarly. The cells were pelleted by centrifugation (6,000 g) for 10-15 min at 4°C, and washed three times with at least 150 ml of ice cold sterile ddH_20. Next, the pelleted cells were resuspended in 2 ml 10% glycerol and 100 µl aliquots were frozen in liquid nitrogen and stored at -80°C, or used for immediately for electroporation.

For transformation of *E. coli* strain SW102, the electro-competent cells were always prepared freshly. From a 5 mL starter culture grown O/N at 32°C with the appropriate antibiotics, 100 µl were used to inoculate a 10 mL secondary culture. The secondary culture was grown until OD_{600} 0.4-0.6, distributed into five 2 mL Eppendorf tubes, and pelleted in a tabletop centrifuge at 8,000 rpm for 1 minute. The cell pellets from the five tubes were resuspended in 1 mL final volume of LB and incubated at 42°C by shaking in a thermoblock for 15 minutes in order to activate the heat inducible genes of Red proteins for BAC recombineering. Subsequently, the cells were transferred onto ice and washed three times with 1 mL ice-cold sterile ddH2O. The pellet was ultimately resuspended in 50 µL H_2O and DNA was added.

2.2.1.9.2. Electroporation of bacterial cells

100µl aliquots of electrocompetent cells were thawed on ice and mixed with 2.5µl ligation mix or 100-200 ng plasmid DNA. If ligation mixes were transformed, they were first dialyzed against water on a Millipore membrane filter (MFTM 0.025µm VSWP) to remove salts. The mixture of *E. coli* electro-competent cells and added DNA was transferred into a pre-chilled electroporation cuvette (BioBudget, 2mm) and subjected to an electropulse (at 2.5 kV (i.e., 12.5 kV/cm cuvette with), 25 µF, and 200 Ω) for 4-5 milliseconds in a Bio-Rad Gene Pulser. Agrobacterium cells were similarly transformed using electroporation at 400Ω with a primary capacitance of 25µF for 8.0-9.0 msec. Thereafter, *E. coli* cells were resuspended in 1 mL LB and transferred into a centrifuge tube for incubation at 32°C (SW102) or 37°C (DH5α) for 1-1.5 hours while shaking at 500 rpm. Agrobacterium cells were diluted with 1ml YEB medium and incubated for 3h at 28°C. Then, cells were streaked onto LB-agar or YEB-agar plates containing the necessary antibiotics and grown O/N at 37°C for *E.coli* or for two days at 28°C for Agrobacterium.

2.2.1.10.Conjugation of binary vectors from E. coli to Agrobacterium and backwards

The binary vectors used in our laboratory (pPCV= plant cloning vectors and pGAP= GAP repair vectors) carry the oriT (conjugational transfer origin) and oriV (vegetative replication origin) of the broad-host range plasmid RK2/RP4. These plasmids can be transferred to other bacteria from *E. coli* strains, which carry defective (non-replicating) RK2 derivatives integrated into their chromosome. The Agrobacterium host GV3101 (C58C1 RifR) (pMP90RK) carries an RK2-segment of 48kb from pRK2014 integrated into the T-DNA-less helper Ti-plasmid pMP90 (Koncz and Schell, 1984). This RK2 segment provides the *trfA* (trans replicator function A) gene for replication of pPCV and pGAP plasmids by the RK2 oriV, as well as Tra operons producing all components of the RK2 plasmid conjugation system. Therefore, the pPCV and pGAP vectors can also be back-conjugated into any *E. coli* strain, to test whether their plant DNA inserts are stably maintained in Agrobacterium.

For conjugation, the pPCV and pGAP vectors are transformed by electroporation into the *E. coli* donor strain MFDpir ΔTIV lacIq (JKE201, kindly provided by C. Dehio, Biozentrum, University of Basel), which is auxotrophic for the production of 2,6-diaminopimelic acid (DAP). 10 ml culture of *E. coli* JKE201 carrying the pPCV or pGPA binary vectors is grown O/N in LB containing 0.3 mM DAP at 37°C, while the recipient Agrobacterium GV3101 (pMP90RK) strain is grown for 1 day in 10ml LB on 28°C. Next morning, the cultures are diluted back to OD_{600} 0.2-0.3 (*E. coli* in LB_DAP, Agro in LB) and grown up to OD_{600} 0.5 at 28°C. This takes about 60 to 90 min. Then, 2 ml of *E. coli* and 2 ml of Agrobacterium is mixed in a sterile test tube, and 20-30 µl drops from the conjugation mix are placed onto a LB-DAP agar plate, dried and incubated at 28°C for 1-2 days. Subsequently, a loop from the conjugation mixes is streaked out on YEB-agar containing 100 mg/L rifampicin (Rif100) and 100 mg/l carbenicillin (Cb100) to isolate GV3101 (pMP90RK) transconjugants carrying the binary vector from *E. coli*.

The binary vectors can be back-conjugated from GV3101 (pMP90RK) into any *E. coli* recipient, such as DH5α. The binary vector containing Agrobacterium GV3101 (pPM90RK) donor is grown in 10ml LB-Cb100 liquid, whereas the *E. coli* DH5α recipient in 10 ml LB O/N at 28°C. The cultures are diluted back to OD_{600} 0.2-0.3, and then grown until OD_{600} 0.5. After mixing equal volumes of Agrobacterium donor and *E. coli* recipient, 20-30 µl drops from the conjugation mix are dried onto LB agar plate and incubated at 28°C for 1-2 days. Then a loop from the conjugation spots is streaked out onto LB-Cb100 plates to grow up single *E. coli* colonies at 37°C, where Agrobacterium growth is inhibited.

2.2.1.11.Construction of bacterial and plant expression vectors

The AKIN10 cDNA isoform AT3G01090.1 was cloned by Bhalerao et al. (1999) into the BamHI-SalI sites of polylinker of pET201 bacterial expression vector between coding sequences of N-terminal thioredoxin (Trx) and a C-terminal His6 tags. This pET201-AKIN10 clone was used as template for introducing the M119G (ATP-binding pocket modification for AS kinase), and T-loop Thr175A, Thr175D and Thr175E amino acid exchanges by PCR-based site-directed mutagenesis into the coding sequence of AKIN10. The 3' mutagenesis primers (AKIN10M119G-3 and AKINT175A/D/E-3) were used in combination with the AKIN10-5' primer to PCR amplify mutagenized fragments of the 5' cDNA coding region. After gel purification, these fragments were used as primers in combination with the AKIN10-3' primer to PCR amplify the mutagenized versions of full length AKIN10 cDNA, which were then digested by BamHI (at the 5'-end) and SalI (at the 3'-end), gel isolated and cloned into BamHI and SalI sites of pET201. The same mutagenized 5'-fragments were used in combination with the AKIN10-3 short No AID primer (2.1.4.3.1) to PCR amplify mutagenized versions of a short form of AKIN10 cDNA, which carried a deletion of coding sequences for the C-terminal regulatory domain starting from the nucleotide position of 873 in the cDNA isoform AT3G01090.1. The resulting pET201-AKIN10 expression constructs were used for purification of wt and mutagenized forms of AKIN10 kinase from *E. coli*.

To overexpress both full-length and C-terminally truncated forms of AKIN10 carrying Thr175A/D/E amino acid exchanges in plants, the modified cDNAs were PCR amplified from the pET201 plasmid templates with the AKIN10-5 and AKIN10HA-long-3 or AKIN10HA-short-3 primers (2.1.4.3.3), which added coding sequences of a HA-epitope tag and a stop codon in frame to the 3' end of mutagenized AKIN10 cDNA sequences. The PCR products were isolated as BamHI and SalI fragments and upon filling in their ends were cloned into filled-in BamHI site located between a CaMV35S promoter and nopaline synthase polyadenylation sequences in the plant expression vector pPCV702 (Koncz et al., 1994). All AKIN10 constructs were confirmed by full-length Sanger sequencing using the primers listed in 2.1.4.3.3.

2.2.1.12.BAC Recombineering

BAC recombineering utilizes bacterial artificial chromosomes (BACs) carrying chromosomal segments with 20 to 100 intact genes for targeted gene modifications. Precise modification of genes without endonuclease or Gateway aided cloning is achieved by homologous recombination between BACs and PCR-amplified DNA fragments that are flanked by 50 nucleotide segments homologous to flanks of targeted BAC positions (e.g., start or stop codon of a gene). The BAC recombineering uses the λ-Red Exo, Gam, and Beta recombinase proteins for promotion of recombination between short homologous sequences. The 5'-3' exonuclease Exo encoded by Redα generates short single-stranded overhangs at the ends of linear double-stranded DNA fragments. Together with Redβ (Beta), which promotes annealing of these single-stranded overhangs to complementary sequences, this system allows to insert, delete or modify any desired sequence – thus generating simple SNPs or complex gene fusions. Additionally, the Gam (γ) protein inhibits the RecBCD nuclease and prevents the degradation of the linear dsDNA substrates.

The *E. coli* host SW102 used in our experiments for BAC recombineering carries a defective prophage with the Redαβγ genes under the control of the λ phage pL promoter, which is regulated by the temperature sensitive cI857 (cIts) repressor. Conditional expression of the recombination proteins is initiated by inactivation of the heat-labile repressor at 42°C (Warming et al., 2005). Plant genes modified in BACs are transferred by gap-repair into to binary vectors, which are suitable for high-frequency Agrobacterium-mediated plant transformation (Bitrián et al., 2011). This latter technology developed in our lab originally employed the *E. coli galK* positive/negative selectable marker gene described by Warming et al. (2005). However, the selection for galactose utilization and insensitivity to 2-deoxygalactose on minimal medium requires couple of weeks lowering the efficiency and speed of BAC recombineering. Therefore, the *galK* positive-negative selectable marker was replaced with an antibiotic resistance gene linked to a conditional negative selection marker in our laboratory. M. Horváth inserted a PCR amplified fragment of a CmR gene linked to an I-SceI recognition site from the pEL04 vector (Lee et al., 2001) into the NaeI site of pGEM-T Easy (Promega Co.) as NgoMIV fragment. Subsequently, this was linked to an araC-pAra-ccdB gene cassette, which was inserted into the adjacent SpeI-SacI sites of pGEM-T as XbaI-SacI fragment from the plasmid pSW8197 (Le Roux et al., 2007). In this construct, the araC repressor controls an arabinose-inducible promoter-diven *ccdB* DNA gyrase inhibitor "killer" gene. Subsequently, the NaeI/NgoMIV CmR fragment was deleted to yield pGEM-T-araC-ccdB, and a kanamycin resistance (KmR) gene from pACYC177 (Chang and Cohen, 1978) was cloned as BspHI fragment into the NcoI site of this intermediate vector, such that an I-SceI cleavage site was incorporated between the KmR and araC-ccdB gene cassettes.

The BAC recombineering technology based on the use of KmR-araC-ccdB positive/negative selection marker includes three steps (Figure 4). First, the KmR-araC-ccdB cassette is PCR amplified by two primers, which carry 50 nucleotide homology to sequences flanking the target site, such as the

stop codon of AKIN10 gene carried by BAC T4P13 (CmR). The amplified KmR-araC-ccdB cassette is electroporated into the BAC containing *E. coli* strain SW102 upon brief heat-shock induction of the λ-Red recombinase proteins. Cells, in which the KmR-araC-ccdB cassette is recombined by double cross-over into the BAC by replacing the AKIN10 codon are selected in the presence of kanamycin and 0.2% glucose to suppress the expression of arabinose-inducible promoter driven lethal *ccdb* gene.

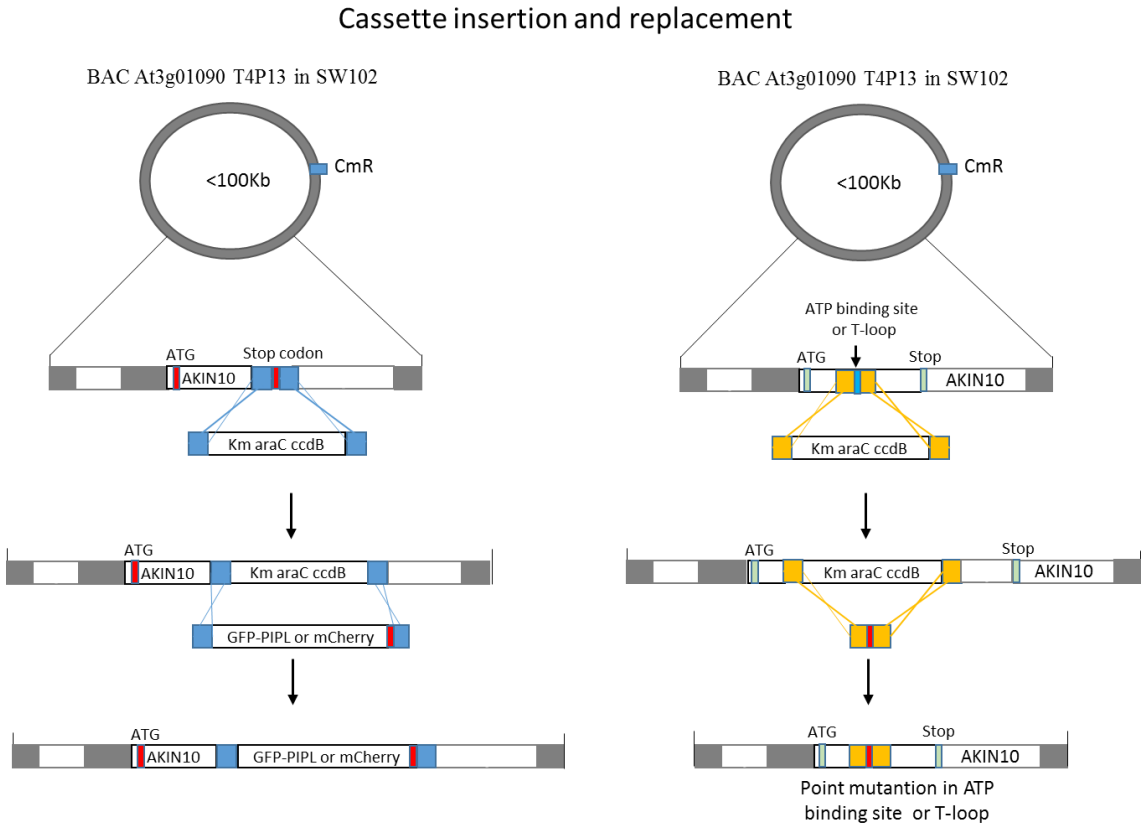

Figure 4. Schematic work flow of cassette insertion and exchange steps in recombineering experiments with the *AKIN10* gene containing BAC T4P13.

Because the copy number of BACs is 2 to 5 in *E. coli* and the selectable cassette is usually incorporated only in one of the BACs, the transformed colonies are grown in the presence of kanamycin and absence of chloramphenicol to select for the modified BACs. Because BACs do not carry a plasmid partitioning function, they are lost from the cells in the absence of selection for their antibiotic (CmR) resistance marker. Using primers flanking the stop codon, which is replaced by the KmR-araC-ccdB cassette, the loss of unmodified original BACs is screened for, using colony PCR. On this way, we obtained *E. coli* SW102 clones, which carried only BACs with the KmR-araC-ccdB cassette replacing the AKIN10 stop codon.

In the second step, the KmR-araC-ccdB cassette insertion is replaced with the DNA sequence of a suitable tag, such as green fluorescent protein (GFP) or mCherry version of the red fluorescent protein (RFP). In our case, we used a modified GFP tag, which was fused to the PIPL tag consisting of

coding sequences of 38 histidine residues from Arabidopsis CobW homolog PIP-L protein, 2 copies of Strep-II tag and a C-terminal HA-tag (PIPL tag). The PIPL tag provides the advantage that the tagged proteins can be purified by multiple methods, such as by GFT-Trap, Ni-agarose, streptactin-agarose and HA immunoaffity pull-down. Coding sequences of the GFP-PIPL tag were PRC amplified with primers, which carried 50 nucleotide homology arms for recombining with sequences flanking the KmR-araC-ccdB cassette in the *AKIN10* gene. This purified PCR fragment was transformed into SW102 carrying the modified AKIN10 BAC. To select for replacement of the KmR-araC-ccdB cassette by GFP-PIPL sequences, the transformed *E. coli* SW102 strain was grown in the presence of 0.2% arabinose, which induces the expression of *ccdB* gene causing cell lethality. On this way, colonies carrying the replacement of KmR-araC-ccdB cassette with the GFP-PIPL tag in the AKIN10 BAC were obtained and verified by colony PCR using primers, which flank the position of the stop codon.

Finally, the GFP-PIPL tagged *AKIN10* gene was moved by gap-repair into Agrobacterium pGAP-Km and pGAP-Hyg plant transformation vectors (Bitrián et al., 2011, Figure 5). For this, two DNA segments of about 1kb in length (Flank 1 and Flank 2), located in neighbouring genes upstream and downstream of *AKIN10* in the BAC, were PCR amplified and cloned as EcoRI-SalI and SalI-BamHI fragments into the EcoRI and BamHI sites of pGAP vectors. Subsequently, the resulting pGAP plasmids were linearized by SalI, treated by Antarctic phosphatase (CIAP, to prevent self-ligation) and transformed into *E. coli* SW102 carrying the BAC with the AKIN10-GFP-PIPL gene fusion. Recombination between Flank1 and Flank2 sequences of pGAP and BAC was selected for by growing the transformants on LB-medium with ampicillin (100mg/l) or carbenicillin (100mg/L). Finally, the recombinant pGAP clones harbouring the AKIN10-GFP-PIPL construct were isolated, retransformed into *E. coli* DH5α, and followed plasmid DNA isolation were verified by restriction endonuclease fingerprinting and Sanger DNA sequencing.

For expression of an analogue-sensitive version of AKIN10 in Arabidopsis, the gatekeeper Met119 codon in the ATP-binding pocket of AKIN10-GFP-PIPL was exchanged for glycine by reiterating the above described recombineering procedure. First, the Met119 codon was replaced by the KmR-araC-ccdB cassette.

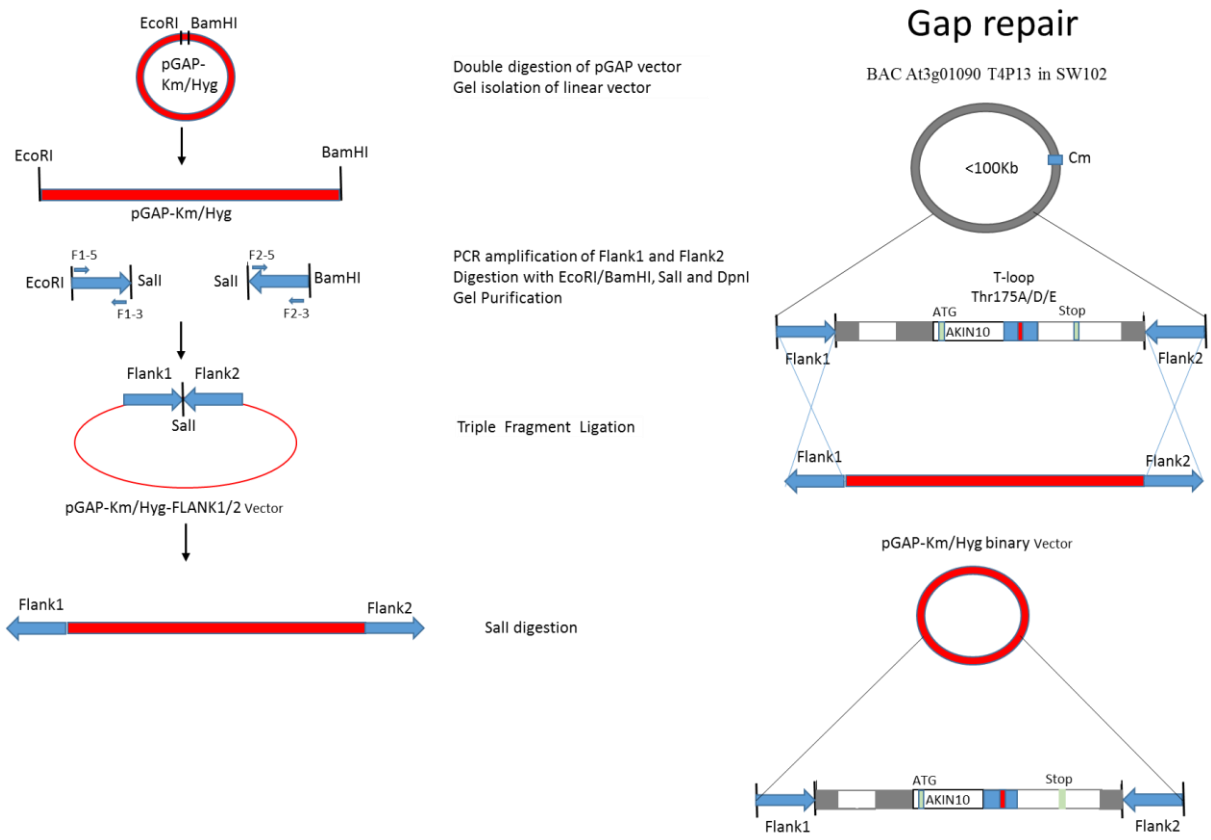

Figure 5. Work flow of gap repair step of recombineering.

For replacement of the KmR-araC-ccdB cassette inserted into the place of Met119 codon, we used two synthetic oligonucleotides that carried a Met119G codon exchange, about 25 bp overlap with each other and 50 nucleotide homology to the left and right of Met119 codon. These oligonucleotides were denatured at 100°C for 10 min, and allowed to anneal by cooling down onto room temperature. Then, the single-stranded ends of annealed oligonucleotide pair were filled out by T4 DNA polymerase mediated DNA synthesis. Finally, the oligonucleotides were transformed into *E. coli* SW102 carrying the AKIN10-GFP-PIPL BAC with the KmR-araC-ccdB at the position of the Met119 codon. Following selection for the loss of KmR-araC-ccdB cassette, the AS-AKIN10-GFP-PIPL gene was rescued by gap repair in the pGAP vectors and the codon exchange was confirmed by sequencing. Finally, we have used the latter approach for replacing the T-loop Thr175 codon in AKIN10-GFP-PIPL by alanine (A), aspartate (D) and glutamate (E) codons. Some necessary details of laboratory protocols of individual steps are described below.

2.2.1.12.1. Cassette insertion

The BAC T4P13-containing *E. coli* strain SW102 was grown overnight in LB medium with 50 µg/mL kanamycin at 32°C to avoid the induction of cI^{ts} repressor controlled λ-phage Red recombinase. Preparation of electrocompetent SW102 cells for transformation is described in section 2.2.1.9.2. The Km-araC-ccdB cassette (2.6 kb) was PCR amplified (section 2.2.1.8.2 and 3) with primers listed in

section 2.1.5.3.2 and gel purified before electroporation (with 1 to 5 µg PCR fragment). The transformed cells were plated on LB-agar medium containing 25 µg/mL kanamycin and 0.2% glucose and grown at 32°C for subsequent screening with colony PCR with Taq DNA polymerase (sections 2.2.1.8.1 and 3) using specific sequencing primers flanking the targeted *AKIN10* gene positions (section 2.1.5.3.2). For PCR, single bacterial colonies are picked with a flat toothpick, swirled in 10-15 µl water and replicated on LB plates. 1-2 µl of bacterial suspension is used in the PCR reactions.

2.2.1.12.2. Cassette replacement

The GFP-PIPL cassette (1.05 kb) was PCR amplified with the primers AKIN10GFPPIPL5 and AKIN10GFPPIPL3 (section 2.1.5.3.2) using pBSKII-GFP-PIPL plasmid DNA as template and proof-reading Q5 High-Fidelity DNA polymerase (NEB, section 2.2.1.8.2). After gel purification, the GFP-PIPL PCR fragment (1 to 5 µg) was electroporated into *E. coli* SW102 carrying the BAC with the Km-araC-ccdB cassette replacement of *AKIN10* stop codon. The transformants were plated onto LB medium containing 25 µg/mL chloramphenicol and 0.1% arabinose, and grown overnight at 32°C. In the presence of arabinose, the growth of cells containing the Km-araC-ccdB cassette is inhibited, in contrast to transformants in which the Km-araC-ccdB cassette was replaced with the GFP-PIPL cassette. The exchange of Km-araC-ccdB (2.6kb) for the GFL-PIPL (1.05 kb) cassette was monitored by the expected change in the size of DNA fragments monitored by colony PCR.

2.2.1.12.3. Gap repair

Amplification of flanking fragments was performed with oligonucleotide primers that contained added EcoRI and SalI sites for Flank1, and SalI and BamHI sites for Flank2. The PCR fragments of Flanks1/2 were digested with the corresponding restriction endonucleases, gel purified and ligated into Antarctic phosphatase-treated EcoRI and BamHI sites within the T-DNA of binary vectors pGAP-Hyg or pGAP-Km. These gap repair vectors carry a bacterial ampicillin resistance marker, and in their T-DNAs a kanamycin (Km) or hygromycin (Hyg) selectable marker for plant transformation (Bitrián et al., 2011). Triple ligation of vector and flanks was electroporated into *E. coli* DH10B. The cells were plated on LB medium containing ampicillin (100mg/L). Plasmid DNA prepared from the transformants was subjected to control EcoRI-SalI, SalI-BamHI and EcoRI-BamHI digestions. To perform gap repair, the pGAP-Flank1/2 plasmid DNAs were linearized with SalI between the Flank1 and Flank2 segments, and treated with Antarctic phosphatase. A portion of plasmids was then self-ligated and tested for lack of transformation by electroporation of *E. coli* DH10α. Subsequently, the SalI linearized pGAP-Flank1/2 plasmids (500 ng/2.5 µL) were transformed into electrocompetent SW102 cells carrying the modified AKIN10-GFP-PIPL genes in the BAC. Upon electroporation, the transformed culture was incubated in 1 mL LB for 1h at 32ºC in a shaking thermoblock and then 150µL aliquots were plated on LB medium containing ampicillin and incubated at 30ºC for approx. 20h. The appearing transformed colonies were screened for the predicted gap repair recombination event by diagnostic EcoRI and BamHI restriction endonuclease digestions. All pGAP constructs were then sequenced to verify in frame fusion of the GFP-

PIPL tag and introduced mutations using primers flanking the positions of performed sequence modifications. Finally, the recombinant pGAP-AKIN10-GFP-PIPL constructs were conjugated into Agrobacterium GV3101 (pMP90RK) and then back-conjugated into E. coli DH5α for verifying the stability of vectors in Agrobacterium by diagnostic restriction endonuclease digestion of plasmid DNAs isolated from several back-conjugants. The verified Agrobacterium stocks were subsequently used for Agrobacterium-mediated transformation of Arabidopsis plants.

2.2.1.13.Gene expression analysis by quantitative RT-PCR

2.2.1.13.1. Large-scale tissue grinding using MixerMill

Plant tissue was collected in 2 mL Eppendorf tubes and immediately frozen in liquid nitrogen. A metal bead was added to each tube. MixerMill was used to grind the tissues in groups of 48 samples at 30 Hz for 45 seconds. Mixing was repeated until the samples were completely ground.

2.2.1.13.2. RNA isolation and DNase-treatment

RNA extractions were performed using Trizol reagent (Invitrogen), except when an RNeasy plant RNA miniprep kit (Qiagen) was used. 800 µL Trizol was added to each homogenized sample and vortexed. The samples were kept at RT for 5 min and 200 µL chloroform was added. After centrifugation for 15 min with 12,000 rpm at 4 ºC, the supernatant (containing RNA) was transferred to a new tube. One volume of i-propanol was added and the samples were incubated for 10 min at RT. After centrifugation for 10 min using the same conditions, the supernatant was discarded and the RNA pellet was washed with 75% ethanol (made with DEPC (diethylpyrocarbonate)-treated water). After another centrifugation of 5 min, the pellet was dried at RT and resuspended in 30 µL of DEPC-treated water. The samples were denatured at 55ºC for 3 min. After RNA quantification using Nanodrop and quality checking by performing gel electrophoresis, 1 or 2 µg RNA was treated with DNase I (NEB BioLabs). 1 µL buffer (NEB BioLabs), 1 µL enzyme and water was added to the samples to a final volume of 10 µL, and the DNase treatment was performed at 65ºC for 5 min.

2.2.1.13.3. Reverse transcription

To each reaction tube, 0.5 µL oligo-dT and 0.5 µL random hexamers were added, and the samples were incubated at 65°C for 5 min. Subsequently, the tubes were chilled on ice and 4 µL 5xRT buffer, 1 µL dNTPs and 2 µL 0.1M DTT were added. The samples were incubated for 2 min at 25°C and then 1 µL Superscript II or IV (Invitrogen) reverse transcriptase was added, and the samples were sequentially incubated for 10 min at 25°C, 50 min at 42°C and 15 min at 70°C. The obtained cDNA samples were stored at -80°C and, before using them as templates in qRT-PCR, were diluted 1:20.

2.2.1.13.4. Design and testing the efficiency of qRT-PCR primers

Oligonucleotide primers were designed using the DNASTAR Primer Select software and tested for their specificity by performing Blast searches against the Arabidopsis genome sequence at TAIR, as well as for the absence of primer dimer formation using the PerlPrimer open-source software. The concentration of cDNA samples was measured using PCR primers designed for the UBQ5 (AT3G62250) transcript and adjusted close to the same as the concentration of control wt cDNA used for generation of internal standard of serial dilutions (1:1, 1:2, 1:4, 1:8, 1:16, 1:32 and 1:64) in each measurement. Subsequently, using the control wt cDNA and standard dilution series, the efficiency of each primer was tested by recurrent PCR combined with melting curve analysis using a Biorad IQ5 real-time PCR equipment and IQ5 Optical System Software. For quantification of cDNA levels, the standard curve method was followed according to the Biorad PCR Application Guide Bulletin 5279 and User Bulletin #2. For quantification of lower cDNA concentrations, alternative primers for the control reference genes *PDF2* (At1g13320) and TIP41 (At4g34270) were used (Czechowski et al., 2005). The dilution standards were always run in the same reaction plates. The expression value from each sample was thus normalized to the internal reference. The standard condition for the qRT-PCR reactions was: 95°C 2 min, followed by 40 cycles (95°C, 15 sec; 60°C, 30 s; and 68°C, 20 sec). The qRT-PCR measurements were performed with triplicates and repeated three times with different biological replicates.

2.2.2. Protein methods

2.2.2.1. *Protein purification from E.coli using Ni-affinity chromatography*

cDNAs encoding the proteins destined for purification from *E. coli* were cloned into the pET201 expression vector (Bhalerao et al., 1999) in frame with coding sequences of an N-terminal thioredoxin and a C-terminal His_6 tag. To purify the full length and C-terminally truncated AKIN10 versions carrying the M119G and T175A/D/E amino acid exchanges, the pET201 vectors carrying the corresponding kinase cDNA sequences were introduced into the *E. coli* strain BL21 Rosetta by electroporation and selection for ampicillin (Amp) resistant transformants. After confirmatory plasmid isolation, the transformed strains were gown in LB-broth containing Amp (100 mg/l) at 37°C to an optical density OD600: 1.0, and then protein expression was induced by addition of 1 mM isopropyl-thio-galactose (1 mM IPTG) for 3h. Cells collected by centrifugation (4,000g, 4°C, 20 min) were resuspended (5 ml/l culture) in lysis buffer and sonicated (time: Branson Sonifier, 2 minutes; Duty cycle 50; Output control 5; repeat 3-4 times) to prepare clear extracts by centrifugation (20 min; 12,000 g; 4°C; Beckmann centrifuge; rotor JA-20). The cleared lysates were loaded onto a NTA (0.2 to 1.0 ml Ni^{2+}-nitrilotriacetic acid agarose matrix, Qiagen) column, which was equilibrated with NTA-buffer (lysis buffer without DNase and lysozyme). After washing with 100 column volume of NTA-buffer containing 50 mM imidazole, the bound proteins were eluted with NTA-buffer (2 x column volume) containing 100, 150, 200, 250 and 300 mM imidazol. Aliquots from each eluted fraction were separated

on an SDS-polyacrylamide gel (10%) to identify the peak fractions, which were then dialysed against kinase buffer (25 mM Tris·HCl (pH 7.8), 15 mM $MgCl_2$, 10% glycerol) or subjected to buffer exchange using PD-10 desalting columns (GE Healthcare). The PD-10 column was equilibrated with 20 mL of exchange buffer prior loading the sample. Then, the protein was eluted by 9 x 500 µL buffer. Following determination of protein concentration, fractions containing the peak of eluted protein were collected, supplemented with 10% glycerol and stored at -80°C or at -20°C.

Lysis buffer: 50 mM HEPES (pH 7.4); 300 mM KCl; 10% glycerol; 40 mM imidazole; 1% Triton X-100; 1mM EDTA; 1mM PMSF; Sigma Bacterial Protease Inhibitor Cocktail 20 µL/mL; 5mM $MgCl_2$; 5mM 2-mercaptoethanol; DNase 3U/mL (Worthington, electrophoretically homogeneous); and lysozyme 0.5mg/mL.

Washing buffer: 50 mM HEPES (pH 7.4); 300 mM KCl; 10% glycerol; 50 mM imidazole; 1% Triton X-100; 1 mM EDTA; 1 mM PMSF; Sigma Bacterial Protease Inhibitor Cocktail 20 µL/mL; 5 mM $MgCl_2$; 5 mM 2-mercaptoethanol.

Elution buffer: 50 mM HEPES (pH 7.4); 100 mM KCl; 250 mM imidazole; 10% glycerol, 1 mM PMSF; 20 µL/mL Sigma Protease Inhibitor Cocktail; 5 mM $MgCl_2$; 5mM β-mercaptoethanol.

Exchange buffer: 50mM Tris.HCl (pH 7.5); 5mM $MgCl_2$; 50 mM KCl.

2.2.2.2. Measurement of protein concentration by Bradford assay

Protein concentration was measured using the Bradford assay (Bradford, 1976). Aliquots (1 to 10 µl) of protein samples were mixed with 1 ml BioRad Protein Assay Concentrated Dye Reagent, which was previously diluted 5 times in water. After 5 min incubation at RT, OD_{595} value was measured with a spectrophotometer. The protein amount was determined by the help of a standard curve obtained previously using a series of dilutions of bovine serum albumin (BSA).

2.2.2.3. Protein kinase assays

His_6-affinity purified wild type and mutant proteins were used in *in vitro* protein kinase assays. The kinase reactions contained 1-2 µg substrate and 0.25-0.5 µg kinase protein in kinase-buffer (50 mM Tris-HCl [pH 7.8], 15 mM $MgCl_2$, 1mM DTT, and 5 to 20 µCi [γ-^{32}P] ATP (Perkin-Elmer, 10 mCi/ml; 6000Ci/mmol), or 1µM ATP). The kinase reactions were incubated for 2 hours at room temperature or at 37°C. The reactions were separated by SDS-PAGE (when using TRX-SPS-KD substrate on 14% SDS-PAGE). When performing the kinase reactions with [γ-^{32}P] ATP, the SDS-PAGE gel was fixed for 30 min in 45% methanol, 10% acetic acid, and then dried and placed into an autoradiography cassette with an X-ray film and exposed for 15 min up to 4 h.

Thiophosphorylation kinase reactions were performed with 0.5 µg purified wild type AKIN10 and AS-AKIN10 kinases and 2 µg Trx- KD or SAMS peptide as standard substrates (Bhalerao et al., 1999; carrying a consensus SnRK1 phosphorylation site from spinach sucrose phosphate synthase) or other purified candidate substrate proteins in a total volume of 20 µl of kinase buffer (25mM Tris.HCl (pH 7.8), 15mM $MgCl_2$) containing either 0.5 mM ATPγS or N^6-phenyl- ATPγS or N^6benzyl-ATPγS at room temperature for 2h. Subsequently, the pH was adjusted to 4.0 by addition of 3µl 3M K-acetate (pH 4.0), and 2 µl PNBM (25 mM p-nitrobenzyl mesylate stock dissolved in 5% DMSO) was added to selectively alkylate the phosphothiol groups for 30 min at room temperature (Lee et al., 2011). Proteins from the kinase assays were resolved by 10% or 14% SDS-PAGE (for TRX-SPS-KD substrate) and subjected to western blotting. The thiophosphorylated kinase and substrate proteins were reacted with rabbit anti-PNBM-thioester antibody (Epitomics, 1:5000 dilution) and visualized with peroxidase conjugated goat anti-rabbit secondary antibody (Vector Co., 1:10,000 dilution) and Enhanced Chemoluminescence detection as described in sections (2.2.2.4 and 5).

2.2.2.4. Size separation of proteins by SDS-polyacrylamide gel electrophoresis (SDS-PAGE)

Protein samples are size separated by SDS-polyacrylamide gel electrophoresis (SDS-PAGE) according to their molecular weight. Between pre-casted Biorad Mini Protean Gel glass plates 4.5 ml of 12% separating gel solution was pipetted and overlayed with H_2O. After polymerization, the H_2O was carefully removed, a stacking gel layer poured on the top of the separating gel and casted with a 10 or 15-well comb. The gel was placed into an electrophoresis chamber and protein samples were loaded using a pipette and separated in SDS-PAGE by applying 30 mA current. The size of separated proteins was estimated using a parallel slot with pre-stained protein markers (Bio-Rad). Before loading, the proteins samples were supplemented wint 1/5 volume of 5 x Laemmli sample buffer (2% SDS, 10% glycerol, 50 mM Tris.HCl (pH 6.8), 5% β-mercaptoethanol, 0.1% bromophenol blue) and denatured at 95°C for 5 min.

Components for two 12% SDS-PAGE gels

Separation gel (12%)	Stacking gel (4 %)	SDS-running buffer
5.4 ml ddH_2O	2.4 ml ddH_2O	25 mM Tris
2.5 ml 1.5 M Tris.HCl (pH 8.8)	1 ml 1 M Tris.HCl (pH 6.8)	192 mM glycine
3.0 ml 29:1 acrylamide to bisacrylamide (40%)	0.5 ml 29:1 acrylamide to bisacrylamide (40%)	0.1% SDS
0.1 ml 10% SDS	40 µl 10% SDS	
50 µl 10% APS	30 µl 10% APS	
5 µl TEMED	5 µl TEMED	

2.2.2.5. Western blotting

2.2.2.5.1. Transfer of proteins from SDS-PAGE gels onto membranes

In order to detect proteins with specific antibodies, proteins are transferred from SDS-PAGE onto nitrocellulose or Immobilon-P PVDF (Polyvinylidene fluoride) membranes. The stacking gel is removed and the separating gel is equilibrated in 1 x Transfer buffer for 5 min. Then, a transfer "sandwich" is assembled from the following components: sponge layer, 3xWhatman gel blot paper, SDS-PAGE gel, nitrocellulose/PVDF membrane, 3xWhatman gel blot paper, and sponge layer. This sandwich placed in a wet blotting transfer apparatus such that the membrane faces the anode and the gel sandwich is fully submerged in Transfer buffer. Protein transfer is performed either for 1-2 h at 24 V or overnight at 10V.

1x Transfer buffer (stock is 5x concentrated): Do not adjust pH
50mM boric acid
50mM Tris base

2.2.2.5.2. Antibody probing

After protein transfer, the nitrocellulose/PDVF membrane is incubated in blocking solution for 1 h at room temperature or at 4°C overnight. Then, the membrane in blocking solution is incubated with diluted primary antibody for 2h followed by washing the membrane 3 times for 10 min with washing buffer. Subsequently, the filter is incubated for 1.5 h with a horseradish peroxidase conjugated secondary antibody diluted in blocking solution. The membrane is then washed 3 times for 10 min with washing buffer.

TBS	137 mM NaCl, 2.7 mM KCl, 20 mM Tris.HCl(pH7.4)
Blocking solution:	5% milk powder in 1X TBS with 0.2% Tween-20
Washing buffer:	1X TBS with 0.2% Tween-20

2.2.2.5.3. Detection of chemiluminescent signal

To visualize the position of proteins using horseradish peroxidase conjugated second antibodies, an enhanced chemiluminescence (ECL) detection kit is used. An 1:1 mixture of the two ECL reagents is freshly prepared and applied onto the nitrocellulose/PVDF membrane. Light emission is captured on HyperfilmTM by autoradiography and the films are developed in Optimax X-ray Film Processor.

2.2.2.6. Protein silver staining

The silver staining kits were purchased from Carl Roth. The procedure of protein silver staining were followed the procedures in the manual.

2.2.3. Plant Methods

2.2.3.1. Agrobacterium-mediated plant transformation by vacuum infiltration (Bechtold et al., 1993; Clough and Bent, 1998)

Arabidopsis Col-0 plants are cultivated in short day photoperiod in 10 cm pots (10-12 plants/pot). Prior transformation, the siliques are removed to increase the transformation efficiency. Agrobacterium strains with pPCV/pGAP binary vectors are grown in 500 ml YEB Cb100 medium at 28°C to OD_{600} of 0.8 to 1.0, harvested by centrifugation (4°C, 10,000g) and resuspended in infiltration medium containing 4.3g/l MS basal salt mixture, 1X B5 vitamin, 3% sucrose, 5 mM MES (pH 5.7), 0.05µM BAP, and 0.005%(v/v) Silwet L-77. Arabidopsis plants are submerged in the Agrobacterium suspension followed by application of vacuum for 5 minutes two times. Subsequently, the plants are covered with plastic bags for 2 days to secure slow adaptation to lower humidity. After 12 weeks seeds are collected in paper bags, dried and subjected to selection for the Agrobacterium T-DNA encoded antibiotics resistance markers by germination on MSAR agar medium (Koncz et al., 1994).

2.2.3.2. Seed sterilization

About 100 µl Arabidopsis seed in Eppendorf tube is treated with 1ml of ethanol by turning in a roller for 5 min. After removal of ethanol, 1 mL 5% $Ca(ClO)_2$ containing 0.1% Triton X-100 is added and the tubes are rolled for 15 min. Subsequently, the seeds are pelleted by centrifugation at 6,000 rpm for 1 min in an Eppendorf tabletop centrifuge. The hypochlorite solution is removed and the seed sample is washed three times with 1ml sterile distilled water. Subsequently, the seeds are suspended in 1ml sterile water, and directly plated onto selective MSAR medium. Alternatively, the sterilized seeds are dried after the final washing step leaving open the Eppendorf tubes for overnight in a sterile hood, stored at 4°C and sawn any time within 2-3 weeks. To stimulate germination, the sawn seeds on MSAR plates are subjected to stratification for 24 to 48h at 4°C.

2.2.3.3. Selection of primary transformants

The seeds are sawn on 0.5 MSAR medium containing 0.5% sucrose and appropriate antibiotics to select for the T-DNA encoded resistance marker. The plates are supplemented with ticarcillin/clavulanic acid to kill surviving Agrobacterium that may be protected within the seed coat after sterilization. Resistant seedlings (primary transformants) are transferred to soil and further cultivated in the greenhouse.

2.2.3.4. Segregation analysis of T2 generation seeds

The T2 generation seeds are germinated in 0.5 MSAR medium containing antibiotics to select for the T-DNA encoded resistance marker, and the segregation is counted by screening for lines showing a 3:1 ratio of resistance to sensitivity, in order to identify lines carrying single locus T-DNA insertions.

2.2.3.5. Crossing of Arabidopsis plants

On each floral axis flower buds are accessible for crossing Arabidopsis until they are still closed. Upon removal all open flowers and young siliques from the inflorescence axis selected for crossing, 3 to 5 closed flower buds are emasculated with pointed pairs of forceps taking off the sepals and petals using a magnifying glass headset. An open mature flower is taken from the crossing partner plant and its stamens are used to fertilize the prepared carpel by touching it several times.

2.2.4. Plant protein isolation and purification

***2.2.4.1.** Plant total protein extraction and pull down of GFP and HA tagged AKIN10 kinases with GFP-Trap and anti-HA antibody matrices*

In order to identify target protein complexes *in vivo*, the bait proteins are fused GFP, GFP-PIPL or HA tags and expressed by native gene constructs in transgenic plants. For monitoring the expression of target proteins, and for their subsequent purification and identification of interacting partners, protein extracts are prepared from whole sterile seedlings or shoots of soil grown plants prior onset of flowering. For analytical purposes, 1g plant material is grinded in liquid nitrogen with 1.5 ml extraction buffer. The extract is let to thaw on ice for about 30 min and then subjected to centrifugation for 15 min at a maximum speed (15,000 rpm) for 15 min in an Eppendorf centrifuge at 4°C. The supernatant is transferred into a new tube and protein concentration is measured. At the same time, 25ul GFP-Trap (ChromoTek) bead is equilibrated with 3 x 200 µl Equilibration buffer and then washed with 1ml extraction buffer. Subsequently, the equilibrated GFP-Trap resin is incubated with the protein extract for 2h at 4°C. After removing the supernatant (which is stored as control, along with an aliquot of input extract), the GFP-Trap resin is washed with 3 x 1 ml washing buffer three times. The bound proteins are then eluted from the GFP-Trap resin with 2 x 20 µl 0.1% TFA (each time 2 min incubation time) and the eluted protein fractions are neutralized by addition of 4 µl 1M Tris base. The eluted fractions are resolved by SDS-PAGE and analyzed for the presence of the isolated GFP-tagged protein and its partners by western blotting.

Modified AKIN10 kinase derivatives carrying an HA-tag (i.e., expressed from cDNA constructs or genomic constructs fused to coding sequences of PIP-L tag) were isolated using the above protocol in combination with pull-down using an immobilized anti-HA antibody matrix (Biotool). Total protein extract prepared from 1g starting plant material was incubated for 2h at 4°C with a 30µl aliquot of anti-HA-agarose resin, which was previously equilibrated as described above. For subsequent western blotting and mass spectrometry analysis, the resin was washed as in case of the GFP-Trap, and then bound proteins were eluted with 2 x 30 µl 100 mM glycine-HCl (pH 3.0; each time with 2 min incubation time) and neutralized by immediate addition of 4 µl 1M Tris base. Alternatively, after washing the anti-HA-agarose matrix with bound proteins was suspended in 30 µl kinase buffer containing 2 µg Trx-SPS-KD substrate and 20 µCi (γ-^{32}P)ATP and kinase reactions were performed as described in section 2.2.2.3.

Followed addition of 5 x Laemmli sample buffer, the samples were denatured for 5 min at 95°C, centriguged (13 krpm, Eppendorf centrifuge) and the supernatants were resolved by SDS-PAGE.

For LC/MS mass spectrometry analysis of GFP-Trap isolated protein complexes the protocol is scaled up. 15g of leaf and stem material of about 3 week's old greenhouse grown seedlings or 2 weeks old sterile seedlings is harvested and ground to fine power in liquid nitrogen using 30 ml of extraction buffer with freshly added DTT, PIC and PMSF. After about 1h thawing on ice, the crude extract is subjected to centrifugation in Beckmann JA20 rotor at 12.000 rpm (about 17.000g) for 20 min at 4°C. The supernatant is then divided into 3 equal 10 ml aliquots into Falcon tubes to set up three technical parallels. For each aliquot, 50 µl GFP-Trap (ChromoTek) resin is washed 3 times with extraction buffer in 1.5 mL Eppendorf tubes. Then, the GFP-Trap suspension in 100 µl extraction buffer is added to the 10 ml aliquots of protein extract in Falcon tubes and incubated for 2 hrs at 4°C in the cold room. Next, the GFP-trap resin is pelleted by centrifugation at (500 rpm, Heraeus centrifuge) at 4°C and washed 1 times with 10 ml wash-buffer, 2 times with wash-buffer containing 300 mM NaCl followed each time by centrifugation. Finally, the GFP-trap resin is suspended in 1ml washing buffer and transferred into 1.5ml Eppendorf tube. The bound proteins were eluted by 50 µl 0.1% TFA and the solution is neutralized by addition of 8 µl 1M Tris-base. The eluted protein samples are subsequently submitted for analysis by the Protein Mass Spectrometry Service at the MPIPZ.

Extraction buffer	**Freshly added supplement during extraction:**
50 mM Tris-HCl (pH7.8)	2mM DTT
10% glycerol	0.5mM PMSF
1 mM EDTA	1mM MG132 proteasome inhibitor
1 mM EGTA	20µL/mL Proteinase Inhibitor (Sigma, 100X dilution)
1% Triton-X100	
Equilibration and Wash buffer:	
20 mM Tris-HCl (pH 7.8)	
5 mM $MgCl_2$	
150 mM NaCl	

2.2.4.2. Isolation of nuclei and GFP-Trap purification of SnRK1 complexes from nuclear extracts

For initial optimization of thiophosphorylation with bulky N^6-substituted thio-ATP derivatives, nuclei from 4-weeks-old Arabidopsis seedlings were isolated as described by Németh et al. (1998). Briefly, 220g plant material was harvested, washed twice with cold water and dried between paper towels before homogenizing with an Ultraturax rolling knife homogenizator (3x5 sec. high speed bursts) in the cold room in 440 ml nuclear isolation buffer (NIB; 10 mM HEPES(pH 5.5), 10 mM $MgCl_2$, 25 mM NaCl, 10 mM KCl, 2.5 mM EDTA, 0.15 mM spermine, 0.5 mM spermidine, 0.25% Triton X-100, 0.2 M sucrose, 2.5 mM DTT (freshly added), 1mM PMSF and 2 tablet/l Rosche plant protease inhibitor). The homogenate was filtered through Miracloth and 4 layer of nylon mesh (100, 70, 50 and 20µm), and then nuclei were pelleted by centrifugation in 50ml Flacon tubes at 4°C for 10 min at 5,000g in a Heraus

centrifuge. The pelleted nuclear fraction was resuspended three times in nuclear wash buffer (NWB 10 mM HEPES (pH 5.5), 10 mM $MgCl_2$, 25 mM NaCl, 10 mM KCl, 2.5 mM EDTA, 0.15 mM spermine, 0.5 mM spermidine, 1 mM PMSF, 0.2 M sucrose, 10% glycerol, 0.25% Triton-X, 20 µl/ml Sigma plant protease inhibitor cocktail) and pelleted as above. Finally, the nuclear pellet was resuspended in nuclear storage buffer (NSB, 50 mM HEPES (pH 7.2), 10 mM $MgCl_2$;5 mM KCl; 2 mM DTT, 0.2 mM PMSF and 50% glycerol) and stored in aliquots at -80°C or used freshly in *in situ* phosphorylation assays.

For enrichment of thiophosphorylated AKIN10 substrates and purification of SnRK1 complexes using GFP-Trap pull down of AKIN10-GFP-PIPL and Snf4-FP proteins, nuclei were isolated from shoot tissues of 3 weeks old seedlings grown under short day conditions in soil. Prior harvesting, the plants are covered for 12 h to reduce the starch content of leaves, which might interfere with the isolation of intact nuclei. 150 g of fresh plant material is grinded on ice in the cold room in 300 ml NI-buffer, and then filtrated through 2 layers of miracloth and 20 and 50 µm nylon mesh into a sterile beaker. The nuclei are collected by centrifugation for 10min at 3000 rpm in 50 ml Falcon tubes in a Heraeus centrifuge at 4°C. The crude nuclear pellet is resuspended in 20 ml NWB buffer and pelleted again by centrifugation with 3,000 rpm for 5 min at 4°C. The nuclei are similarly washed 3 times with 20 ml 1 x NWB buffer. Finally, the nuclear pellet is resuspended in 2 ml NLB, sonicated 4 times for 10 sec on ice (Branson Sonifier, 50% output, in a 15mm diameter Corex tube with a rod-shape sonicator head of 12 mm diameter) and cleared by centrifugation in an Eppendorf centrifuge (15 krpm) for 15 min at 4°C. The supernatant was dialysed against binding-buffer (20 mM Tris-HCl (pH 7.8), 5 mM $MgCl_2$, 150 mM NaCl, 2mM DTT). After dialysis, the protein concentration is measured with Bio-Bradford reagent, and the nuclear extract is subjected to affinity purification on GFP-Trap as described in section 2.2.4.1.

Nuclear Isolation Buffer	
10 mM Hepes (NaOH) pH 7.4	Freshly added supplement
10 mM $MgCl_2$	20 µl/ml Sigma plant protease inhibitor
25 mM NaCl	5 mM DTT
10 mM KCl	PMSF 6 µl/ml 400µM PMFS
0.4 M Sucrose	phosphatase inhibitors
0.25% Triton X-100	
Nuclear Wash Buffer 3x	
50 mM Hepes (NaOH) pH 7.4	Freshly added supplement
20 mM $MgCl_2$	20 µl/ml Sigma plant protease inhibitor
100 mM NaCl	5 mM DTT
40% Sucrose	PMSF 6µl/ml 400µM PMFS
40% Glycerol	phosphatase inhibitors
0.75% Triton X-100	
Nuclear Lysis Buffer 1x	
20 mM Hepes(NaOH) pH 7.4	Freshly added supplement
15 mM $MgCl_2$	20 µl/ml Sigma plant protease inhibitor
25 mM NaCl	5 mM DTT

0.4 M $(NH_4)_2SO_4$	PMSF 6 µl/ml 400µM PMFS
10% Glycerol	phosphatase inhibitors (1.0 mM Na_3VO_4, 20mM NaF)
1% Triton X-100	50 µM MG132 (DMSO stock)

2.2.4.3. LC-MS/MS analysis and data acquisition

The proteins eluted from GFP-trap by 0.1% TFA were reduced with dithiothreitol, alkylated with chloroacetamide, and digested with trypsin. The digested samples were desalted using StageTips with C18 Empore disk membranes (3 M), dried in a vacuum evaporator, and dissolved in 2% ACN (acetonitrile), 0.1% TFA. Samples were analyzed using an EASY-nLC 1200 (Thermo Fisher) coupled to a Q Exactive Plus mass spectrometer (Thermo Fisher). Peptides were separated on 16 cm frit-less silica emitters (New Objective, 0.75 µm inner diameter), packed in-house with reversed-phase ReproSil-Pur C18 AQ 1.9 µm resin (Dr. Maisch). Dried peptides were re-dissolved in 2% ACN, 0.1% TFA for analysis and adjusted to a final concentration of 0.1 µg/µl.

The samples were analysed using an EASY-nLC 1200 (Thermo Fisher) coupled to a Q Exactive Plus mass spectrometer (Thermo Fisher). Peptides were separated on 16 cm frit-less silica emitters (New Objective, 0.75 µm inner diameter), packed in-house with reversed-phase ReproSil-Pur C18 AQ 1.9 µm resin (Dr. Maisch). Peptides (0.5 µg) were loaded on the column and eluted for 115 min using a segmented linear gradient of 5% to 95% solvent B (0 min : 5%B; 0-5 min -> 5%B; 5-65 min -> 20%B; 65-90 min ->35%B; 90-100 min -> 55%; 100-105 min ->95%, 105-115 min ->95%) (solvent A 0% ACN, 0.1% FA; solvent B 80% ACN, 0.1% FA) at a flow rate of 300 nL/min. Mass spectra were acquired in data-dependent acquisition mode with a TOP15 method. MS spectra were acquired in the Orbitrap analyzer with a mass range of 300–1750 m/z at a resolution of 70,000 FWHM and a target value of 3×106 ions. Precursors were selected with an isolation window of 1.3 m/z. HCD fragmentation was performed at normalized collision energy of 25. MS/MS spectra were acquired with a target value of 105 ions at a resolution of 17,500 FWHM, a maximum injection time (max.) of 55 ms and a fixed first mass of m/z 100. Peptides with a charge of +1, greater than 6, or with unassigned charge state were excluded from fragmentation for MS2, dynamic exclusion for 30s prevented repeated selection of precursors.

Raw data were processed using MaxQuant software (version 1.5.7.4, http://www.maxquant.org/) with label-free quantification (LFQ) and iBAQ enabled. MS/MS spectra were searched by the Andromeda search engine against a combined database containing the sequences from Arabidopsis (TAIR10_pep_20101214; ftp://ftp.arabidopsis.org/home/tair/Proteins/TAIR10_protein_lists/) and sequences of 248 common contaminant proteins and decoy sequences. Trypsin specificity was required and a maximum of two missed cleavages allowed. Minimal peptide length was set to seven amino acids. Carbamidomethylation of cysteine residues was set as fixed, oxidation of methionine and protein N-terminal acetylation as variable modifications. Peptide-spectrum-matches and proteins were retained if they were below a false discovery rate of 1%.

2.2.5. Kinase assays with nuclear extracts and enrichment of thiophosphorylated peptides

2.2.5.1. *Thiophosphorylation with wild type and AS-AKIN10*

Followed sonication (section 2.2.4.2), the nuclear protein extract is loaded into a dialysis bag without centrifugation and dialyzed against in kinase exchange buffer for two times 20 min with buffer change. Subsequently, the dialysed protein extract (1 to 2 mg protein) is centrifuged for 10min at 12, 000 rpm in 2ml Eppendorf tubes in a centrifuge at 4°C. Subsequently, the combined supernatant is supplemented with N^6-phenyl-ATPγS (10mM stock) at a final concentration of 0.25 mM, and 10µg SAMS added as internal spike to monitor the kinase reaction and enrichment of thiophosphorylated peptides. The kinase reactions are performed at room temperature for 2h. Subsequently, 1/100 or 1/200 aliquots of samples are subjected to PNBM alkylation (section 2.2.2.3) and detection of thiophosphorylated proteins by western blotting.

Kinase exchange buffer
20 mM Tris.HCl (pH 7.4)
5 mM $MgCl_2$
60 mM KCl

2.2.5.1.1. Enrichment of thiophosphorylated peptides

Three volumes of 1 x denaturation buffer (100 mM NH_4HCO_3, 2 mM EDTA, 10 mM TCEP (Tris(2-carboxyethyl)phosphine hydrochloride, Sigma), and 8 M urea) is added to the samples that the final concentration of urea is 6 M. The samples are incubated at 55°C for 1h and then cooled down to room temperature for 10 min. Subsequently, the samples are diluted with 50 mM NH_4HCO_3 to reduce the urea concentration to 2M and 1M TCEP is added to a final concentration of 10 mM. After addition of trypsin (Promega, cat. no. V5113) at a ratio of 1:50 by weight (1:100 would be 10µg trypsin for 1mg of protein), the protein samples are digested at 37°C overnight, and then the samples are acidified by addition of 0.1% final concentration of TFA (trifluoroacetic acid, 2.5% stock).

A C-18 SepPak column is washed with 2 mL of 0.1% TFA and 80% ANC (acetonitrile), followed by 2 mL of 0.5% TFA. The acidified sample is loaded onto the column and recycled five times through the column. Next, the C18 column is washed with 2 mL 0.5% TFA. Finally, the peptides are eluted with 2 x 400 µl 0.5% TFA and 80% ACN, and concentrated near to dryness using a SpeedVac vacuum evaporator.

In the next step, the desalted peptides are bound to iodoacetyl-agarose (Pierce) beads. 300 µl of 50% slurry is pipetted into a 0.5 mL tube and pelleted in a tabletop centrifuge for 30 seconds at 10,000g to remove the supernatant. The resin is washed with 800µl 200 mM HEPES (pH 7.0), and centrifuged to remove the supernatant. Subsequently, 800µl of 20 mM HEPES (pH 7.0) in 80% acetonitrile and 5 µl

10mg/mL BSA are added followed by short vortexing, and the resin is blocked by incubation for 10 min in the dark.

The nearly dried peptide mixture is adjusted to 60µl with H_2O followed by addition of 75 µl acetonitrile, and 15µl 200 mM HEPES (pH 7.0). After removing the supernatant, the blocked iodoacetyl-agarose resin is incubated with this peptide mixture at room temperature in the dark with gentle rocking for 16 hours. After incubation, the supernatant is removed (and stored as LC/MS control) and the resin is washed with 100µL 20 mM HEPES (pH 7.0) in 50% acetonitrile. Subsequently, the resin is washed sequentially with 1 ml of each: i) H_2O, ii) 5M NaCl, iii) 50% acetonitrile and iv) 5% formic acid, each time followed by centrifugation and removal of the supernatant. Next, the resin is treated with 10 mM DTT for 10 min to block the still available free iodoacetyl groups. Finally, the bound thiophosphorylated peptides are eluted by incubating the beads two times for 10 min with 100 µl freshly prepared 1mg/mL Oxone (pH 3.5; DuPont).

The eluted phosphopeptides are immediately desalted using Stage Tips with C18 Empore disk membranes (3 M) , which are previously equilibrated with 60 µl 100% methanol, and then with 60 µl 80% acetonitrile containing 0.5% TFA, and finally with 60 µl 0.5% TFA. The 200 µl peptide solution eluted by oxone from the iodoacetyl-agarose resin is filtered through 4 to 10 times the Stage Tip, which is then washed with 2 x 40 µl 0.5% TFA. Finally, the peptides are eluted with 2 x 30µl 0.5% TFA in 80% acetonitrile and concentrated to about 10 µl for LC/MS mass spectrometry analysis.

2.2.5.2. Identification of phosphopeptides

After performing *in vitro* protein kinase reactions with purified proteins (section 2.2.2.3) and ATP, the samples were reduced with dithiothreitol, alkylated with chloroacetamide, and digested with trypsin. The digested samples were desalted using StageTips with C18 Empore disk membranes (3 M) (Rappsilber et al, 2003), dried in a vacuum evaporator, and dissolved in 2% ACN, 0.1% TFA. After enrichment of thiophosphorylated peptides on idoacetyl-agarose, selective cleavage of the phosphothiol bond by oxone and release of phosphopeptides from the originally thiophosphorylates peptides, the samples were similarly concentrated on StageTips as described in 2.2.5.1.

The phosphopeptide samples were analysed using an EASY-nLC 1200 (Thermo Fisher) coupled to a Q Exactive Plus mass spectrometer (Thermo Fisher). Peptides were separated on 16 cm frit-less silica emitters (New Objective, 0.75 µm inner diameter), packed in-house with reversed-phase ReproSil-Pur C18 AQ 1.9 µm resin (Dr. Maisch). Peptides were loaded on the column and eluted for 50 min using a segmented linear gradient of 5% to 95% solvent B (0 min : 5% B; 0-5 min -> 5% B; 5-25 min -> 20% B; 25-35 min ->35% B; 35-40 min -> 95% B; 40-50 min ->95% B) (solvent A 0% ACN, 0.1% FA; solvent B 80% ACN, 0.1% FA) at a flow rate of 300 nL/min. Mass spectra were acquired in data-dependent acquisition mode with a TOP15 method. MS spectra were acquired in the Orbitrap analyzer with a mass range of 300–1500 m/z at a resolution of 70,000 FWHM and a target value of 3×106 ions.

Precursors were selected with an isolation window of 1.3 m/z. HCD fragmentation was performed at a normalized collision energy of 25. MS/MS spectra were acquired with a target value of 5x105 ions at a resolution of 17,500 FWHM, a maximum injection time of 120 ms and a fixed first mass of m/z 100. Peptides with a charge of 1, greater than 6, or with unassigned charge state were excluded from fragmentation for MS2; dynamic exclusion for 20s prevented repeated selection of precursors.

Raw data from DDA acquisition were processed using MaxQuant software (version 1.5.7.4, http://www.maxquant.org/) (Cox and Mann, 2008). MS/MS spectra were searched by the Andromeda search engine against a database containing the respective proteins used in the *in vitro* kinase reactions. Trypsin specificity was required and a maximum of two missed cleavages allowed. Minimal peptide length was set to seven amino acids. Carbamidomethylation of cysteine residues was set as fixed, phosphorylation of serine, threonine and tyrosine, oxidation of methionine and protein N-terminal acetylation as variable modifications. The match between runs option was disabled. Peptide-spectrum-matches and proteins were retained if they were below a false discovery rate of 1% in both cases. Raw data were analysed on MS1 level using Skyline (Version 4.1.0.18169, https://skyline.ms) (Tyanova et al., 2016) and a database containing the respective proteins used in the *in vitro* kinase reactions. Trypsin specificity was required and a maximum of two missed cleavages allowed. Minimal peptide length was set to seven maximum length to 25 amino acids. Carbamidomethylation of cysteine, phosphorylation of serine, threonine and tyrosine, oxidation of methionine and protein N-terminal acetylation were set as modifications. Results were filtered for precursor charges of 2, 3 and 4.

2.2.6. Confocal-laser-scanning microscopy

The localization of GFP and mCherry tagged proteins in fresh tissue samples was captured by a Leica TCS SP8 confocal microscope (Leica, Bensheim, Germany). GFP was excited with the Argon laser at 488 nm and the emitted fluorescence was detected between 493 and 550 nm. mCherry was excited with the Argon laser at 561 nm and the emitted fluorescence was detected between 576 and 632 nm. The autofluorescence of chlorophyll was detected at 640-720 nm. Simultaneous bright field images were documented by a transmission detector. Merging of images was performed using the Leica LAS X software. Merging of images and calculations of 3D projections are performed with the Leica LCS software. Counterstaining of specimens was performed with 50 µl of 10 x diluted propidium iodine (PI, 1mg/ml stock solution stored in the dark at -20°C) for 10 seconds followed by mounting the tissues in water on microscope glass with cover glass. For PI, the excitation maximum is 535 nm and fluorescence emission maximum 617 nm.

3. Results

3.1. Construction of analog-sensitive and T-loop mutant versions of SnRK1α1/AKIN10

3.1.1. Site-directed mutagenesis of AKIN10 (At3g01090.1) cDNA

Yeast Snf1, human AMPKα1 and 2, and Arabidopsis SnRK1s AKIN10 and AKIN11 show high amino sequence homology in their kinase catalytic domains, but their C-terminal sequences, including the β and γ subunit binding sites, are more divergent (Figure 6).

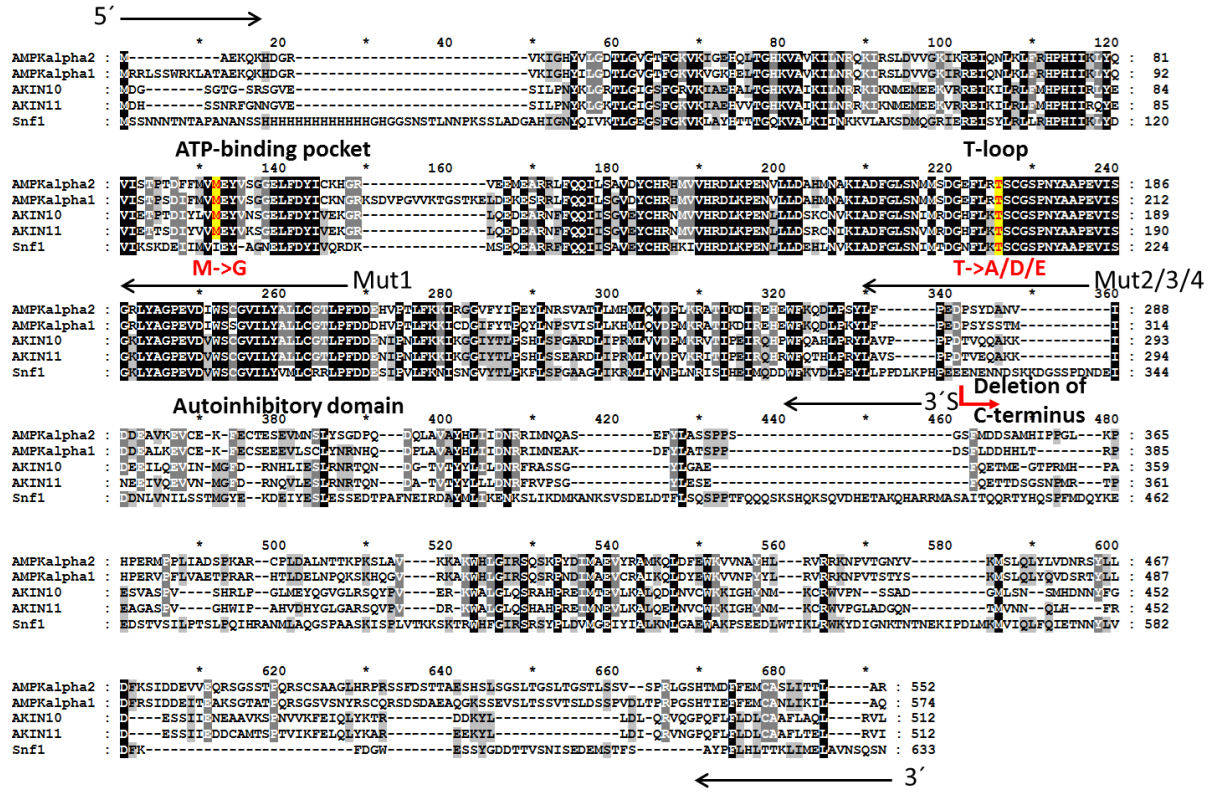

Figure 6. Amino acid sequence alignment of human AMPKα1 and α2, Arabidopsis SnRK1α1/AKIN10 and SnRKα2/AKIN11, and yeast Snf1 kinases.
The positions of conserved gatekeeper M119 residue in the ATP-binding domain and T175 residue in the activation T-loop of AKIN10 kinase are indicated. Red latter label the positions of created M119G and T175A/D/E amino acid exchanges, deleted C-terminus carrying the autoinhibitory domain (AID), whereas arrows show the location of primers used in the PCR-based mutagenesis approach (Figure 7).

The ATP-binding pockets of Arabidopsis SnRK1α1/2 kinases AKIN10/11 carry a conserved "gatekeeper" methionine (M119) residue, which is also present in the human AMPKα1/2 kinases. The exchange of this methionine residue to glycine was used for construction of an analog-sensitive human AMPKα2, which is capable to bind bulky N^6-substituted benzyl or phenyl-ATPγS and catalyze specific thiophosphorylation of substrate proteins. Mass spectrometry analysis of thiophosphorylated peptides enriched by either alkylation with PNBM (p-nitrobenzyl mesylate) and pull-down with anti-PNBM thioester antibody (Banko et al., 2011), or covalent binding to iodoacetyl-agarose (Hertz et al., 2010)

represent currently the only approaches that allow specific identification of *in vivo* kinase substrates. By contrast, routine analysis of phosphopeptide changes evoked by overexpression or antisense inhibition of kinases, or comparison of phosphoproteomes in wild type and kinase mutants cannot exclude that the observed differential regulation is indeed due to the examined kinase and not to other kinases or phosphatases, which represent its regulatory targets. An alternative common approach for assessment of a kinase function is to modify the activation T-loop in order to overexpress an inactivated (nonphosphorylatable T to A exchange) or constitutively active (phosphomimetic T to D/E exchanges) kinase using cDNA constructs. The activation T-loop is very conserved in the Snf1/SnRK1/AMPK family (Figure 6). In AKIN10.1, encoded by the mRNA isoform At3g01090.1, the activation T-loop Thr175 residue is autophosphotylated *in vitro*, and phosphorylated by the upstream activating kinases SnAK1/GIRK2 and SnAK2/GIRK1 *in vivo* (Shen et al., 2009; Crozet et al., 2010; Robertlee et al., 2010).

To construct analogue-sensitive and activation T-loop mutant versions of Arabidopsis SnRK1α1/AKIN10, codon exchanges M119G, Thr175A, Thr175D and Thr175E were first separately introduced into the *AKIN10.1* cDNA isoform, which was originally cloned by Bhalerao et al. (1999) in the *E. coli* protein expression vector pET201. To test inhibitory effect of C-terminal regulatory domain on the kinase activity, the same amino acid codon exchanges were parallel incorporated into a short version of AKIN10 cDNA, from which 3' coding sequence of the C-terminal domain was deleted starting from nucleotide position 873 (corresponding to amino acid position 291 upstream of the Autoinhibitory/UBA (294-331) domain).

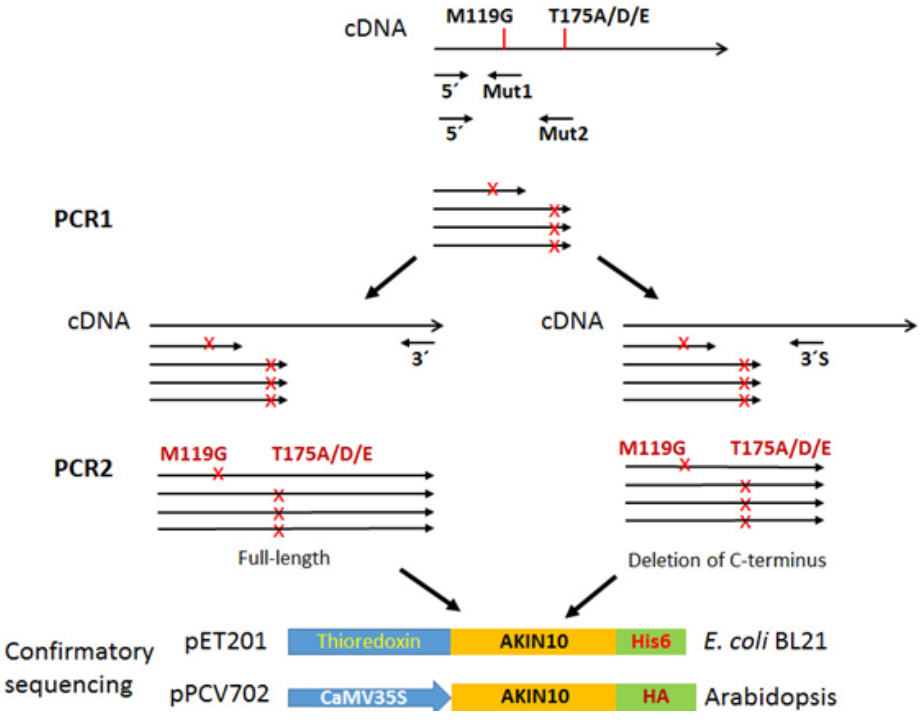

Figure 7. Scheme of PCR-based site-directed mutagenesis approach used for generation of amino acid codon exchanges in the coding regions of ATP binding pocket and T-loop of AKIN10 cDNA.

The resulting cDNA constructs were cloned in pET201 to express in and purify from the *E. coli* BL21 Rosetta strain the modified AKIN10 kinase versions in fusion with N-terminal thioredoxin and C-terminal-His6 tags. The coding regions of same AKIN10 constructs were modified by addition of coding sequences of a HA (hemagglutinin) tag followed by a stop codon and cloned between CaMV35S promoter and NOS (Nopaline synthase) termination & polyadenylation sequences in the plant binary vector pPCV702 (Koncz et al., 1994) for overexpression of corresponding proteins in Arabidopsis plants.

First, cDNA sequences extending from the ATG codon to either the ATP-binding pocket or T-loop were PCR amplified using a 5'-primer and mutagenesis primers Mut1 and Mut2 that carried the M119G, and T175A, T175D and T175E amino acid codon exchanges, respectively (Figure 7). After gel purification, these PCR fragments were used as primers in combination with either the 3' or 3'S primers (section 2.1.5.3.1., primers AKIN10-3-long and AKIN10-3 short No AID) to PCR amplify either the full-length cDNA or its 3'-truncated version lacking the coding region for the C-terminal β and γ subunit-binding domains. The 5' and 3' PCR primers were designed such that they carried suitable enzyme cleavage sites to insert the modified cDNA coding sequences in frame into BamHI and SalI sites of the *E.coli* expression vector pET201. After DNA sequencing with the 5' and 3'S primers, the modified AKIN10 kinases were expressed in *E. coli* BL21 Rosetta cells in fusion with N-terminal thioredoxin and C-terminal His_6 tags. In parallel, all modified versions of AKIN10 cDNAs were PCR amplified from the pET201 plasmid templates with the 5' primer and modified 3' primers (section 2.1.5.3.1., primers AKIN10-5, AKIN10HA-long-3 or AKIN10HA-short-3 primers), which added coding sequences of a HA-epitope tag and a stop codon in frame to the 3' end of mutagenized cDNA sequences. These cDNA versions were cloned into the plant expression vector pPCV702 (Koncz et al., 1994), to ectopically express different versions of modified AKIN10-HA kinase proteins in Arabidopsis plants.

3.1.2. Purification and characterization of AS-AKIN10 and T-loop mutant AKIN10 kinase derivatives

Both long and short versions of modified AKIN10 kinase derivatives were purified by Ni^{2+}-agarose (NTA) affinity chromatography from *E. coli* BL21 as described in section 2.2.2.1, similarly to the standard SnRK1 kinase substrate Trx-SPS-KD described by Bhalerao et al. (1999). The quality of purified proteins was assessed by SDS-PAGE (Figure 8).

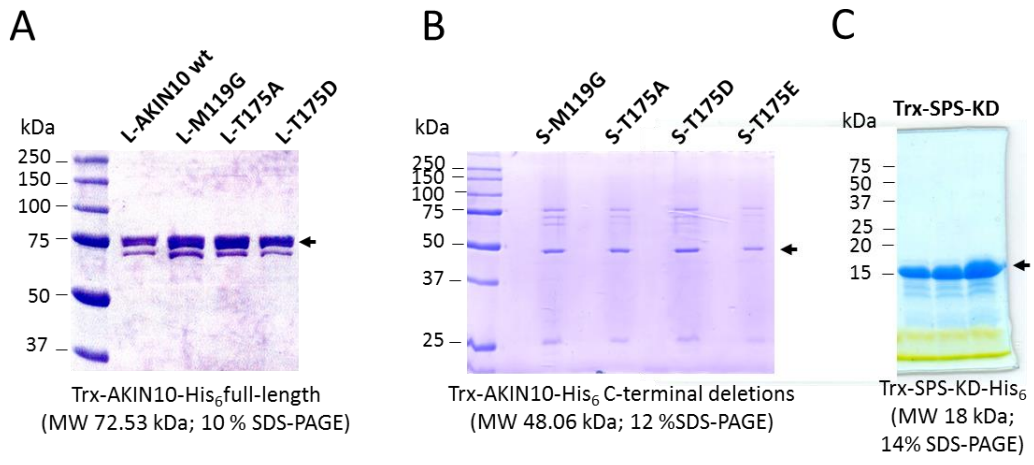

Trx-AKIN10-His_6full-length
(MW 72.53 kDa; 10 % SDS-PAGE)

Trx-AKIN10-His_6 C-terminal deletions
(MW 48.06 kDa; 12 %SDS-PAGE)

Trx-SPS-KD-His_6
(MW 18 kDa;
14% SDS-PAGE)

Figure 8. Purification of full length (L) and C-terminally truncated (S) AKIN10 derivatives carrying the M119G, T175A, T175D and T175E amino acid exchanges.
A) Full-length AKIN10 derivatives (4µg of each) separated in a Coomassie-stained 10% SDS-PAGE. **B**) C-terminally truncated AKIN10 derivatives (1 µg of each) separated in a Coomassie-stained 14% SDS-PAGE. The expected molecular masses of full-length and C-terminally truncated forms of Trx-AKIN10-His_6 were 72.53 and 48.06 kDa, respectively. **C)** Purification of a thioredoxin-fused spinach sucrose phosphate synthase (SPS) peptide (Trx-SPS-KD). The expected molecular mass was 18kDa.

The activities of modified AKIN10 derivatives was compared by performing *in vitro* kinase assays with [γ-^{32}P]ATP using the Trx-SPS-KD substrate. As illustrated in Figure 9, the M119G amino acid exchange in the ATP-binding pocket greatly reduced substrate phosphorylation activity of both full length and C-terminally truncated forms (L and S) of AKIN10 using unmodified ATP, whereas exchange of the T-loop T175 residue to A, E and D resulted in a marginal decrease of activity only in the case of T175A version of full-length AKIN10. Deletion of the C-terminal autoregulatory domain resulted in an increase of kinase activity in case of all mutated T-loop derivatives. Compared to wild type AKIN10, autophoshorylation of all kinase derivatives appeared to be weaker in this assay.

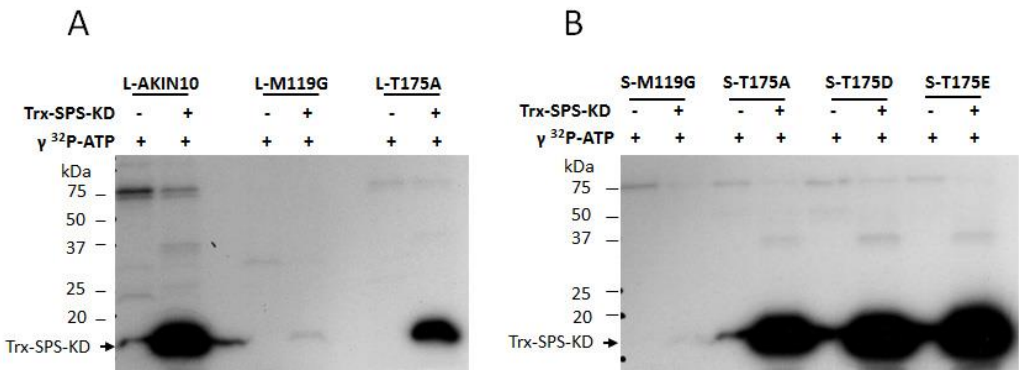

Figure 9. Comparison of substrate and authophosphorylation activities of modified AKIN10 derivatives.
The effects of amino acid exchanges introduced into long (L) and short (S) forms of AKIN10 were tested by comparing the kinase substrate and autophosphorylation activities in radioactive kinase assays with [γ-^{32}P]ATP and Trx-SPS-KD as substrate as described in the text.

Lower, but detectable level of autophosphorylation of AKIN10 derivatives (bands around 75 kDa in Figure 9), which carried A/D/E replacements of T-loop Thr175 residue indicated AKIN10 also undergoes autophosphorylation on other residues in addition to the T-loop threonine. Following autophosphorylation with "cold" ATP, tryptic phosphopeptides in AKIN10 were mapped by LC-MS/MS mass spectrometry (section 2.2.5.2). In fact, two additional positions located at Ser338/339 and Ser364 were identified as autophosphorylation sites in the C-terminal regulatory domain of AKIN10, in addition to the T-loop Thr175 residue (Figure 10). In short forms of AKIN10 (1 to 291aa), two other minor *in vitro* autophosphorylation sites (Ser29 and Ser238) were identified. Functional significance of these autophosphorylation sites in the regulation of activity and assembly of SnRK1 remains to be determined by further studies.

To monitor autophosphorylation of the T-loop, *in vitro* kinase assays were performed with the wild type, M119G, T175A and T175D derivatives of full length AKIN10. After SDS-PAGE separation

and western blotting, the samples were probed with an antibody raised against the phosphorylated T172 T-loop residue of human AMPKα2 (Figure 11).

AKIN10.1

```
MDGSGTGSRSGVESILPNYKLGRTLGIGSFGRVKIAEHALTGHKVAIKILNRRKIKNMEM 60
EEKVRREIKILRLFMHPHIIRLYEVIETPTDIYLVMEYVNSGELFDYIVEKGRLQEDEAR 120
NFFQQIISGVEYCHRNMVVHRDLKPENLLLDSKCNVKIADFGLSNIMRDGHFLKTSCGSP 180
NYAAPEVISGKLYAGPEVDVWSCGVILYALLCGTLPFDDENIPNLFKKIKGGIYTLPSHL 240
SPGARDLIPRMLVVDPMKRVTIPEIRQHPWFQAHLPRYLAVPPPDTVQQAKKIDEEILQE 300
VINMGFDRNHLIESLRNRTQNDGTVTYYLILDNRFRASSGYLGAEFQETMEGTPRMHPAE 360
SVASPVSHRLPGLMEYQGVGLRSQYPVERKWALGLQSRAHPREIMTEVLKALQDLNVCWK 420
KIGHYNMKCRWVPNSSADGMLSNSMHDNNYFGDESSIIENEAAVKSPNVVKFEIQLYKTR 480
DDKYLLDLQRVQGPQFLFLDLCAAFLAQLRVL 512
```

Figure 10. *In vitro* autophosphorylation sites identified in AKIN10.
Amino acids labelled by green color represent major autophosphorylation sites in full-length AKIN10, while sites marked by blue color indicate additional candidate phospho-sites detected in short forms of AKIN10, which carried a C-terminal truncation starting at amino acid position 291.

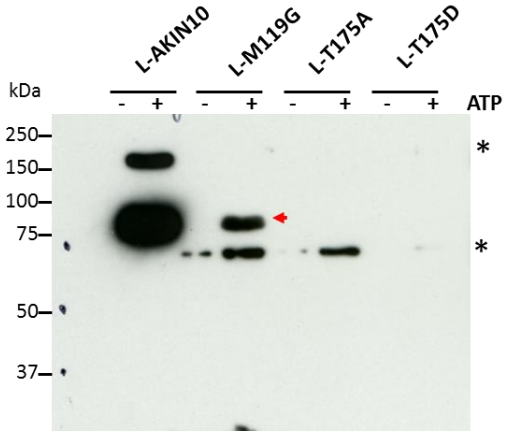

Figure 11. Detection of T-loop phosphorylation with an antibody recognizing the phosphorylated T-loop Thr172P peptide of human AMPKα2.
The phospho-Thr172 antibody (Millipore 15-115; 1:5000 dilution) detects autophosphorylation of the T-loop in wild type AKIN10 and AS-AKIN10 carrying the M119G amino acid exchange in the ATP-binding pocket, but fails to react with the T-loop mutated T175A and T175D versions of AKIN10. This indicates that the antibody is potentially useful to detect T-loop phosphorylation of Arabidopsis SnRK1. Yet, the appearance of several nonspecific cross-reacting bands indicates that the use of proper controls, such as T-loop mutants is necessary in such analyses.

Despite the fact that the human AMPKα2 peptide epitope (MSDG**E**FL**R**TSCGSPNYAAP) differs in two amino acid residues (MRDG**H**FL**K**TSCGSPNYAAP) from the corresponding Arabidopsis AKIN10 peptide, the antibody recognized the phosphorylated T-loop wild type AKIN10 (Figure 11). Lower signal obtained with the M119G version indicated that modification of the ATP-binding pocket also reduced *in vitro* autophosphorylation of the kinase T-loop with non-substituted ATP. As control, the antibody failed to detect the T175A and T175D T-loop mutant versions of AKIN10, which lacked the Thr175 residue.

To optimize nonradioactive detection of SnRK1 phosphorylated substrates, kinase assays were performed with thio-ATP, and long and short versions of modified AKIN10 derivatives (section 2.2.2.3). As recommended by Banko et al. (2011), thiophosphorylation of AKIN10 T-loop and TRX-SPS-KD

substrate was detected by addition of 2.5 mM PNBM after termination of kinase reactions. The PNBM-alkylated proteins were then detected by western blotting with a commercial monoclonal anti-thioester antibody (Epitomics 51-8, Abcam ab92570). The results shown in Figures 12 and 13 indicated that thiophosphorylation of AKIN10 and Trx-SPS-KD could be well detected. However, alkylation with PNBM also highlighted several minor contaminating proteins present in our purified kinases, as PNBM alkylated Cys-residues of these contaminants. As observed in the kinase assays with [γ-^{32}P]ATP (Figure 9), the M119G and to less extent the T175A amino acid exchanges in full-length L-AKIN10 decreased both autophosphorylation and substrate phosphorylation activity the kinase with thio-ATP.

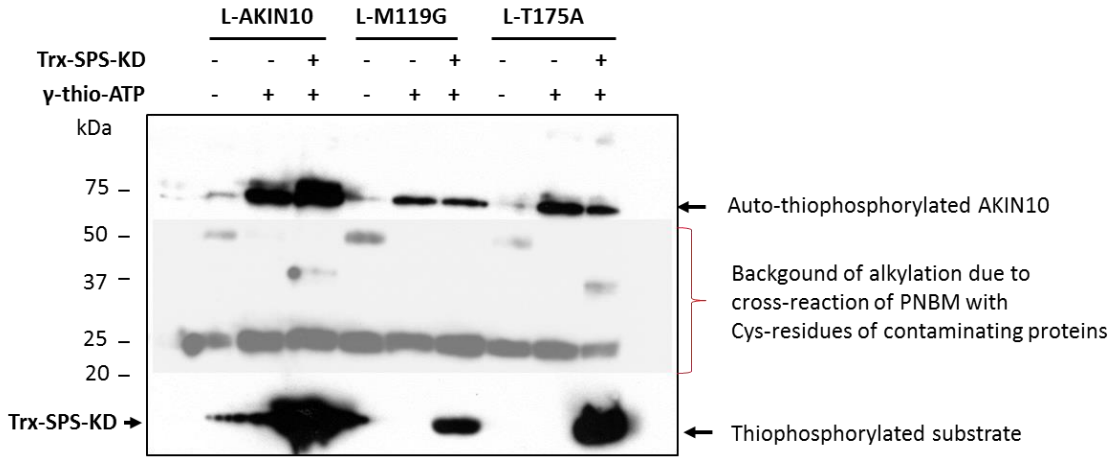

Figure 12. Thiophosphorylation assays with full-length derivatives of AKIN10.
Alkylation with 2.5mM PNBM at pH 7.8 for 30 min at room temperature results in a cross-reaction with Cys-containing contaminating proteins. The M119G and to less extent the T175A amino acid exchanges decrease both autophosphorylation and substrate phosphorylation activities of the kinase. The kinase reactions were performed with 2µg of each AKIN10 kinase derivative, Trx-SPS-KD substrate (2µg) and 1mM thio-ATP for 2h at 37°C.

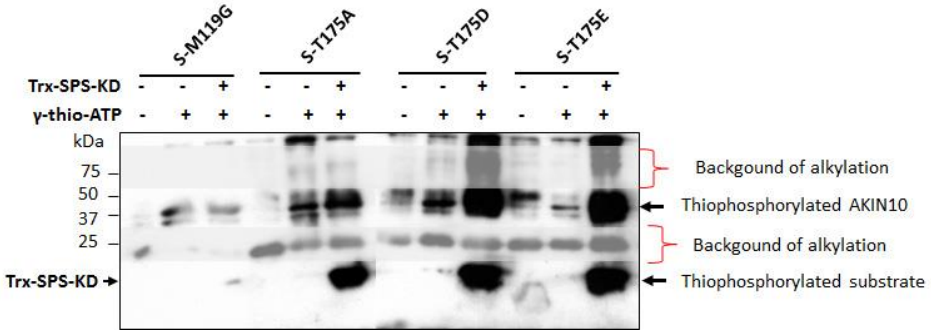

Figure 13. Thiophosphorylation assays with C-terminally truncated versions of AKIN10.
The M119G mutation dramatically decreases the kinase activity with non-substituted thioATP, whereas kinase versions carrying the T-loop amino acid exchanges are equally active. Addition of Trx-SPS-KD substrate appears to increase the autophosphorylation activity of latter kinase derivatives.

In comparison, the M119G mutation dramatically reduced the activity of C-terminally truncated AKIN10, whereas kinase derivatives with the T-loop amino acid exchanges T175A/D/E showed comparable high substrate phosphorylation activity with non-substituted thio-ATP. Labelling of T-loop mutant versions of AKIN10 in the kinase assays confirmed our notion that AKIN10 is

autophosphorylated not only on its T-loop (i.e., which is mutated in the T175A/D/E kinase versions) but also at other positions.

To determine whether M119G modification of the ATP-binding pocket indeed allows selective thiophosphorylation with bulky-ATP derivatives, kinase assays were performed with N^6-phenyl-ATP and N^6-benzyl-thio-ATP followed by PNBM-alkylation for 30 min. Compared to wild type and T-loop mutant versions, the ATP-binding pocket mutant AKIN10-M119G and its C-terminally truncated version showed remarkably high substrate thiophosphorylation activity with both bulky thio-ATP derivatives in contrast to wild type and T-loop mutant versions of AKIN10 (Figure 14).

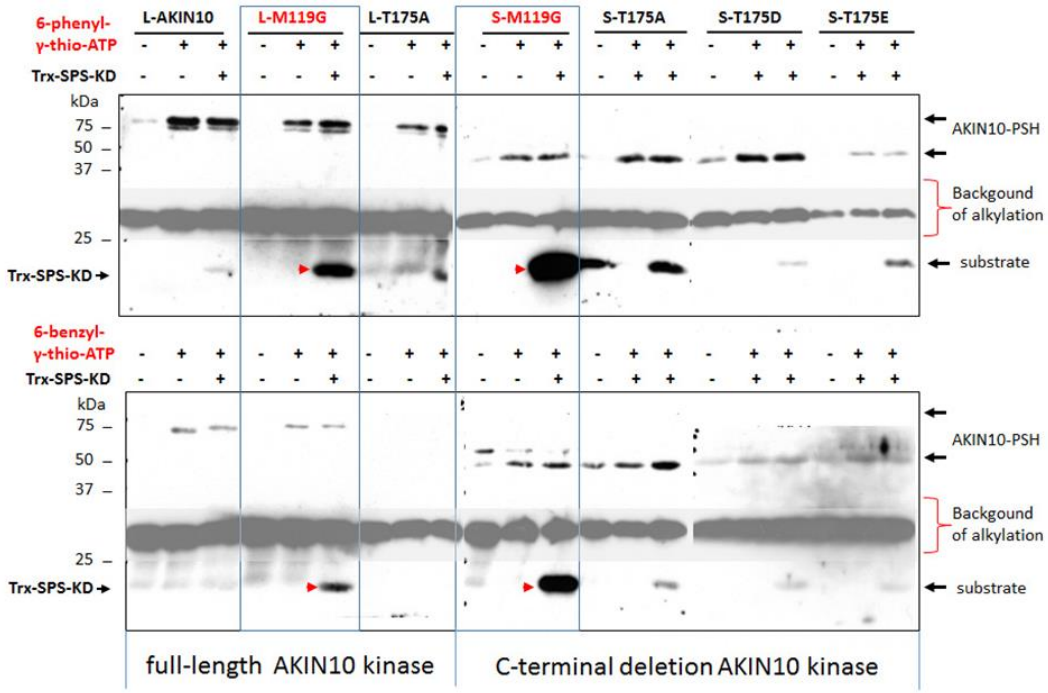

Figure 14. *In vitro* kinase assays with modified AKIN10 kinase derivatives using N^6-phenyl-ATP and N^6-benzyl-thioATP.
Compared to wild type and T-loop mutated versions, the ATP-binding pocket modified AKIN10-M119G kinase shows high substrate thiophosphorylation activity with N^6-phenyl-ATP and N^6-benzyl-thioATP.

In order to decrease or eliminate the background of unspecific PNBM alkylation, the alkylation conditions were optimized using different concentrations of PNBM and lowering the pH to 4.0 according to Lee et al. (2011). Optimal detection of thiophosphorylated TRX-SPS-KD substrate was achieved using 1mM PNBM alkylation for 20 min at pH 4.0 (Figure 15A). Using this condition, the kinase assays with non-substituted thioATP detected no substrate phosphorylation with the ATP-binding pocket M119G mutant AS-AKIN10 kinase and revealed significantly lower activity of T175A nonphosphorylatable version of AKIN10 compared to the phospho-mimicking (constitutively activated) T175D and T175E T-loop derivatives (Figure 15B).

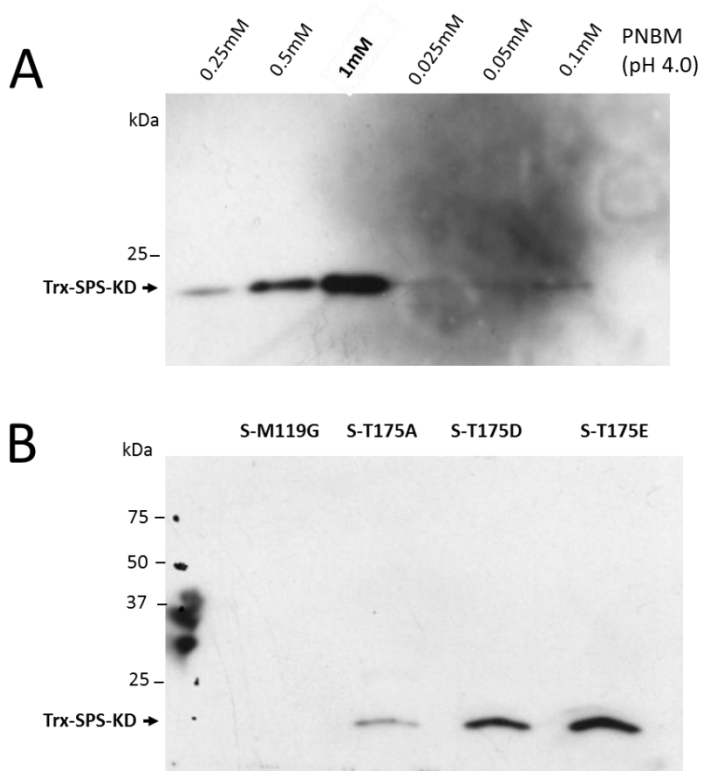

Figure 15. Optimization of PNBM alkylation.
A) Optimization of detection of thiophosphorylated AKIN10 substrate TRX-SPS-KD using different concentrations of PNBM for alkylation at pH 4.0, to decrease the cross-reaction with Cys-containing contaminating proteins. **B)** Detection of thiophosphorylated TRX-SPS-KD in kinase assays with C-terminally truncated short versions of AKIN10 followed by alkylation with 1mM PNBM at pH 4.

For application of the M119G ATP-pocket mutant AS-AKIN10 kinase to specifically detect its thiophosphorylated substrates in plant protein extracts, it was important to demonstrate that wild type protein kinases in Arabidopsis plants cannot utilize bulky N^6-substituted versions of thio-ATP. For this purpose, nuclei were purified from shoot material of 4-weeks-old soil-grown Arabidopsis plants. Equal aliquots of isolated nuclei were pelleted and resuspended in kinase buffer (section 2.2.2.3, containing 5µM MG132 proteasome inhibitor but no DTT) and subjected to *in situ* phosphorylation by incubation for 2h at room temperature with either 1mM ATP, or thio-ATP, or N^6-benzyl-thioATP or N^6-phenyl-thio-ATP using a control sample without ATP. After digestion for 1h with DNase and RNase (both 100 µg/ml), the samples were disrupted by sonication (in a Diagenode water bath at 4°C for 3 x 5 min), cleared by centrifugation and subjected to alkylation with 1mM PNBM with or without acidifying the pH to 4.0 [i.e., using 1/10 volume of 3M potassium acetate (pH4.0)]. Finally, the alkylated nuclear proteins were resolved by SDS-PAGE and detected by western blotting with the anti-thioester antibody. As illustrated in Figure 15, alkylation at pH 7.8 resulted in a considerable background due to cross-reaction of PNBM with Cys-rich proteins in the nuclear protein extracts. By contrast, PNBM alkylation at pH 4.0 reduced this background and revealed specific thiophosphorylation of nuclear proteins only with non-substituted thioATP. This demonstrated that wild type protein kinases in Arabidopsis nuclei

can only utilize non-substituted thio-ATP but cannot phosphorylate their substrates using bulky N^6-substituted ATP derivatives, such as N^6-benzyl-thio-ATP and N^6-benzyl-thio-ATP.

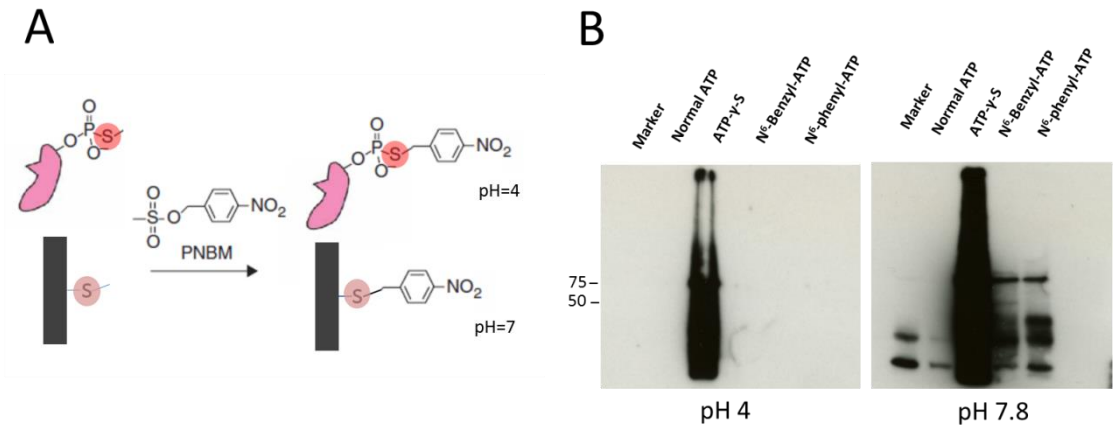

Figure 16. Detection of *in situ* thiophosphorylation in wild type nuclei using thio-ATP and N^6-substituted thio-ATP derivatives by alkylation at neutral and acidic pH.
A) Schematic presentation of PNBM alkylation reaction of protein Cys residues and thiophosphate (-PO_3SH) groups transferred by protein kinases on Ser/Thr residues of their substrates. Cross-reaction of PNBM with Cys residues is largely reduced at pH 4.0. **B)** Detection of *in situ* thiophosphorylated kinase substrates in nuclear protein extracts by PNBM alkylation at pH 4.0 versus pH 7.8

3.2. Expression of wild type and T-loop mutant versions of AKIN10 in transgenic plants using CaMV 35S promoter-driven cDNA constructs

cDNAs encoding the modified AKIN10 kinase derivatives were introduced in CaMV 35S promoter expression cassettes of the binary vector pPCV702 (Koncz et al., 1994) into Arabidopsis (Col-0) plants by Agrobacterium-mediated transformation. For each construct, at least 20 T1 transformed lines were isolated and their T2 progeny was tested for 3:1 segregation of the kanamycin resistance marker of pPCV702 T-DNA. At least 3 independent T3 families homozygous for the transgene T-DNA insertions were further characterized by comparison of *in planta* expression levels and activities of wild type, M119G, T175A and T175D AKIN10 derivatives, as well as phenotypes of transgenic plants. The expression of modified AKIN10 kinases was first monitored by western blotting with anti-AKIN10 antibody (Agrisera) followed by specific detection of HA-tagged kinases using affinity binding to anti-HA antibody matrix.

Due to alternative splicing of the first intron and use of two alternative transcript initiation sites, three transcript isoforms are transcribed from the *AKIN10* gene in Arabidopsis. Isoforms AKIN10.1 and 3 encode a shorter kinase (58 kDa) that lacks 23 N-terminal amino acids compared to the longer kinase isoform (61 kDa) encoded by the transcript isoform AKIN10.2. As the molecular mass of HA-tagged forms of modified AKIN10 derivatives is 60.28 kDa, it was expected that they co-migrate on SDS-PAGE with the longer form of AKIN10.2 isoform, if this form was similarly expressed in plants as the short isoform. In fact, western blotting detected two 61 and 58 kDa bands in all transgenic plants carrying

the HA-tagged wild type, M119G, T175A and T175D modified AKIN10 kinase versions (Figure 16A). Although the ratio between the amounts of two bands varied in transgenic lines expressing different versions of modified AKIN10, due to similar molecular mass of HA-tagged AKIN10 versions and the longer AKIN10 isoform, no clear conclusion could be drawn, as we had no information about the expression levels of short and long AKIN10 isoforms.

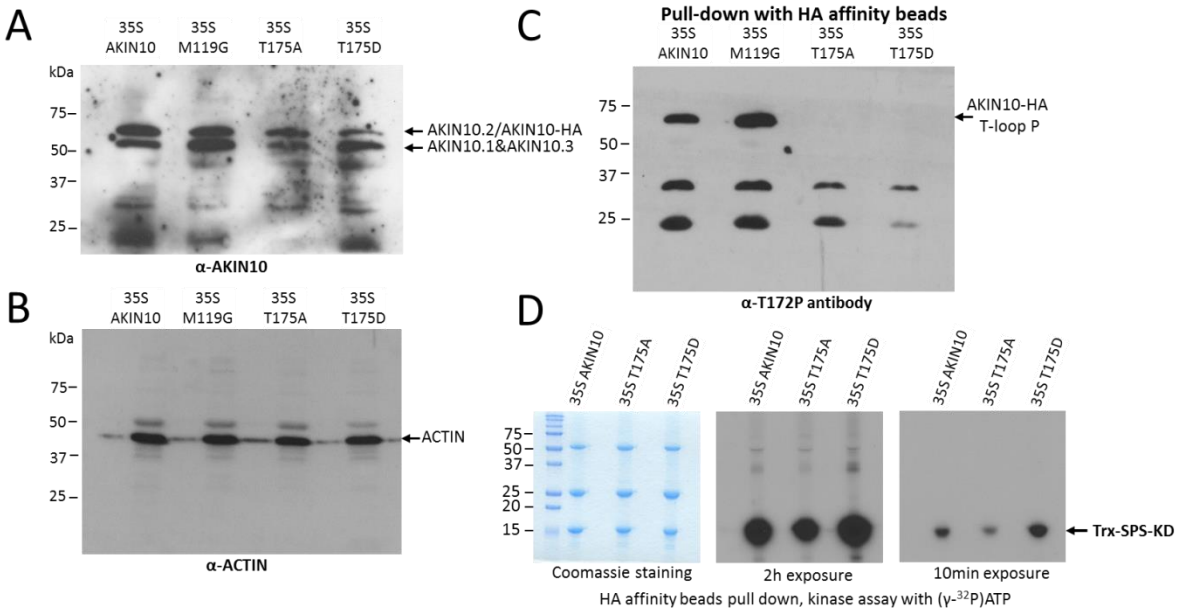

Figure 17. Characterization of expression and activities of modified AKIN10 derivatives expressed by CaMV 35S promoter driven cDNA constructs in transgenic plants.
A) Detection of AKIN10 protein isoforms by western blotting with anti-AKIN10 antibody (Agrisera, 1:5000 dilution) in transgenic plants carrying cDNA expression constructs of wild type, M199G, T175A and T175D AKIN10 derivatives. **B)** Equal loading of protein samples in A) was controlled by western blotting with anti-α-ACTIN antibody (Agrisera, 1:3000 dilution). **C)** Western blotting of protein samples purified by anti-HA-agarose affinity with anti-phospho-Thr172 antibody. **D)** On bead protein kinase assays performed with anti-HA-agarose purified wild type, T175A and T175 derivatives of AKIN10 using (γ-^{32}P)ATP and TXR-SPS-KD substrate. To the left: Coomassie stained gel of kinase assays shows three visible protein bands: the heavy (50 kDa) and light (25 kDa) chains of eluted anti-HA IgG and Trx-SPS-KD (18 kDa). The autoradiographs at the middle and to the right show two different exposures of Trx-SPS-KD phosphorylation by comparable amounts (tested in B) of anti-HA affinity purified wild type, T175A and T175D derivatives of AKIN10.

To examine the transcript levels of different AKIN10 isoforms, specific primers for the first two alternatively spliced exons were designed, and the levels of different isoforms were compared to the total level of all isoforms using the common exon 10 and 11, and exon 9 and 10 specific primers. In the qRT-PCR measurements, we also determined the AKIN10 mRNA isoform levels in the GABI_579E09 T-DNA insertion mutant. In the GABI mutant, a T-DNA insertion in the 3' intron10-exon 11 region resulted in the deletion of 37 C-terminal amino acid codons of AKIN10, which were replaced by 23 T-DNA encoded codons. The GABI *akin10* insertion was defined as null mutation in several recent publications (Mair et al., 2015; Nukarinen et al., 2016; Pedrotti et al., 2018). The qRT-PCR measurements (Figure 18) indicated that the isoform-specific primers detected comparable expression of mRNAs of long AKIN10.2 and short AKIN10.1 and AKIN10.3 isoforms. As the T-DNA insertion in

the GABI mutant was located between the primer sites in exons 10 and 11, no transcript was detected with these primers in the GABI mutant. However, the upstream exon 9 and 10 specific primers, as well as the exon 9 primer combined with a T-DNA specific primer (GABI_T-DNA fused in Figure 18) detected normal transcription of the *akin10* mutant allele in the GABI mutant. Compared to wild type, the total level of AKIN10 mRNA level, as well as the amount of individual AKIN10 mRNA isoforms was slightly higher in the GABI mutant indicating that this T-DNA insertion line is not a null mutant. Subsequent expression of reconstituted GABI mutant AKIN10 coding sequence in *E. coli* by Ajit Gosh in our laboratory revealed that the Agrisera antibody cannot recognize the C-terminally truncated AKIN10 protein made in the GABI mutant because the T-DNA insertion deleted the coding sequence of the peptide epitope, which was used for generation of Agrisera anti-AKIN10 antibody. In addition to wild type, we used this weak GABI *akin10* mutant as control to compare growth-related phenotypes of plants expressing the modified AKIN10 derivatives.

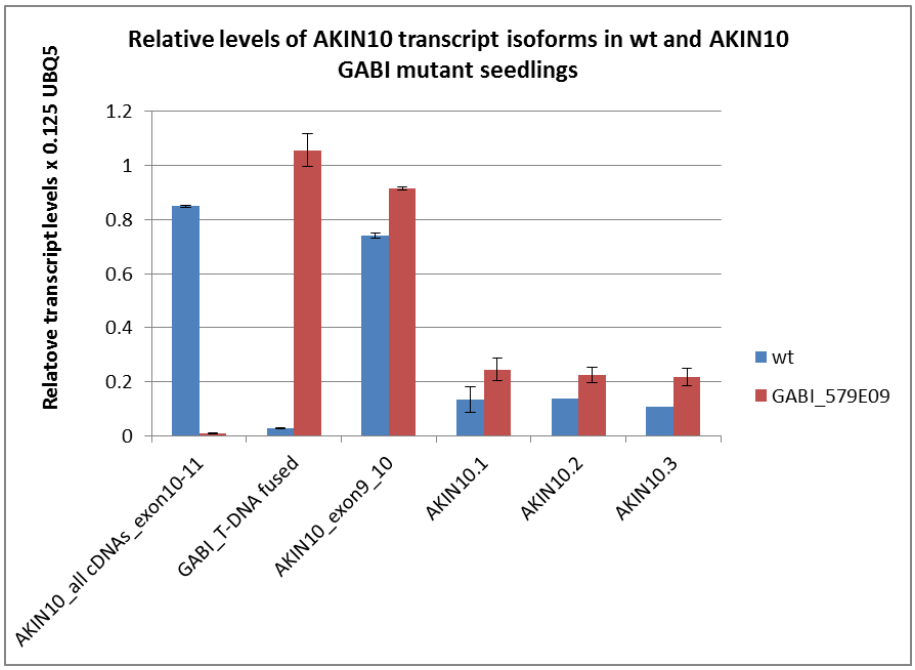

Figure 18. qRT-PCR measurement of total transcript and isoform specific AKIN10 mRNA levels in wild type and GABI_579E09 *akin10* T-DNA insertion mutant plants.

The HA-tagged AKIN10 derivatives were purified from plant protein extracts with anti-HA immunoaffinity pull-down. After controlling that the beads carried comparable amounts of kinase proteins by western blotting with anti-HA antibody, the eluted fractions were subjected to western blotting with anti-Thr172P antibody to monitor phosphorylation of the T-loop of AKIN10 derivatives (Figure 17C). As expected, the AKIN10 Thr175A and Thr175D derivatives lacking the phosphorylated T-loop threonine 175 were not detected by the antibody. By contrast, comparable amounts of T-loop Thr175 phosphorylation were detected in the ATP pocket mutant M119G and wild type AKIN10 kinases. This indicated that the T-loop of the AS-AKIN10 M119G kinase derivative was equally well phosphorylated *in vivo* as the wild type kinase, in contrast with the T-loop autophosphorylation data

obtained *in vitro*. Finally, comparison of the activity of anti-HA-agarose bound wild type, T175A and T175D AKIN10 derivatives using the Trx-SPS-KD substrate in phosphorylation assays *in vitro* indicated that Ala exchange of phosphorylated Thr175 in the AKIN10 T-loop somewhat reduced but did not completely abolish the kinase activity. By contrast, the phosphomimicking Thr175 to aspartate exchange conferred only slightly higher activity compared to wild type suggesting that the expression of phosphatase resistant T-loop derivatives of AKIN10 might not increase dramatically the kinase activity in plants.

Examination of growth related phenotypes of transgenic plants expressing the modified AKIN10 derivatives also failed to reveal dramatic differences. When germinated under 12h light/12h dark conditions in MSAR seed medium with 0.5% sucrose for 6 days, seedlings expressing the wild type, T175A and T175D AKIN10 derivatives showed comparable size, including hypocotyl and root lengths (Figure 19A and B). Upon 12 days of germination seedlings expressing the T175D phosphomimicking T-loop mutant version of AKIN10 displayed however about 15 to 20% longer hypocotyls and roots, compared to wt, GABI mutant and T175A AKIN10 expressing plants (Figure 19C).

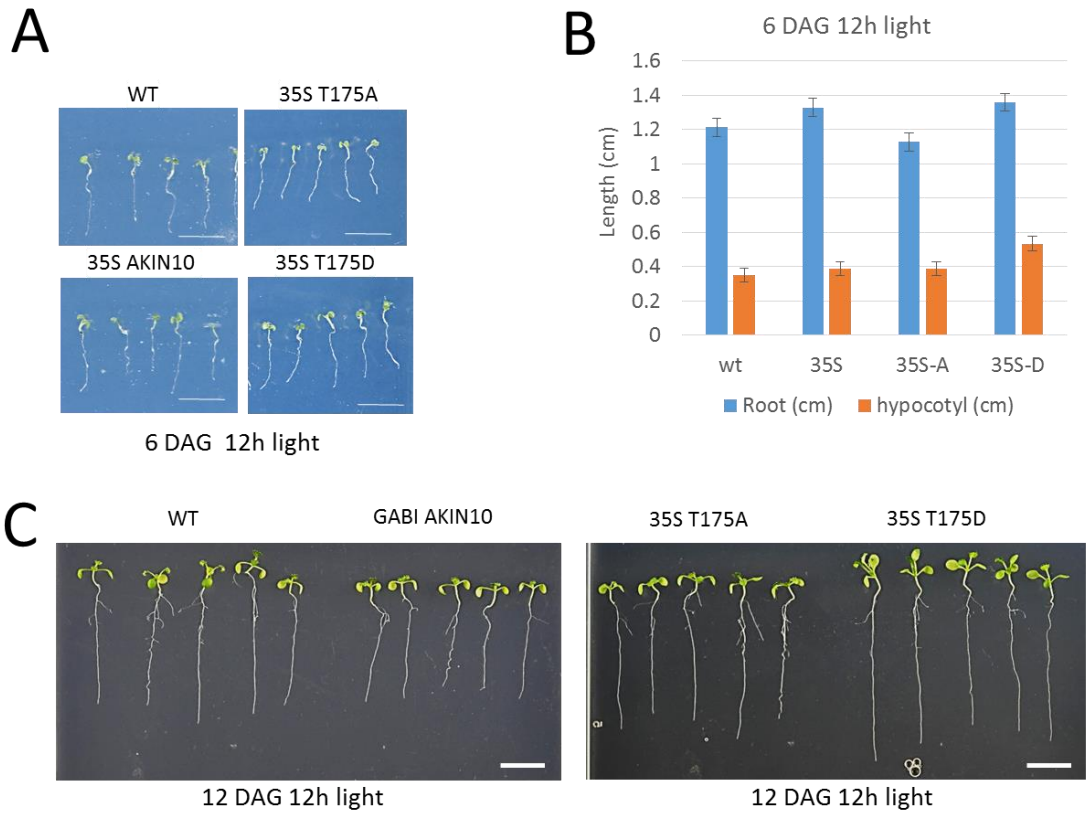

Figure 19. Expression of phosphomimicking T175D T-loop mutant version of AKIN10 confers enhanced root and hypocotyl growth of seedlings.
A) Upon germination for 6 days on 0.5 MASR medium with 0.5% sucrose under 12h light/12 h dark conditions seedlings expressing the AKIN10 derivatives developed similarly to wild type. **B)** Compared to wt control and 35S-wt and T175A AKIN10 expressing plants, the hypocotyls of Thr175D AKIN10 expressing plants were about 5-10% longer 6 days after germination (DAG). **C)** At 12 DAG, the difference between root lengths of T175D AKIN10 expressing plants exceeded by about 15 to 20% those of control wt, GABI mutant and T175A AKIN expressing seedlings. Bars: 1cm.

In addition to metabolic factors, such as sucrose export to roots, auxin plays a key role in regulating root growth and elongation in a concentration dependent fashion, where increasing concentrations are inhibitory (see for review Tanimoto, 2005). Therefore, plants carrying the AKIN10 cDNA expression constructs in homozygous form were crossed with lines expressing GFP-tagged forms of PIN1 and PIN2 auxin import carriers (Benková et al., 2003; Xu and Scheres, 2005) and the DR5-GFP auxin-inducible reporter gene (Liao et al., 2015), to monitor potential changes in auxin transport and auxin-induced transcription in the roots of resulting F1 hybrids. Compared to wild type and T175A AKIN10 expressing seedlings, the T175D AKIN10 lines had slightly higher levels of DR5-GFP in the columella cells of root meristem and DR5-GFP expression was also detectable in the central stele upstream of the meristem. The expression pattern of PIN2-GFP in their roots extended into the endodermis cell layers suggesting possibly higher rate of acropetal auxin transport (i.e., from root to shoot direction) towards the upstream root elongation zone (Figure 20).

Figure 20. Confocal microscopy analysis of PIN1-GFP, PIN2-GFP and DR5-GFP expression patterns in roots of modified AKIN10 expressing seedlings.

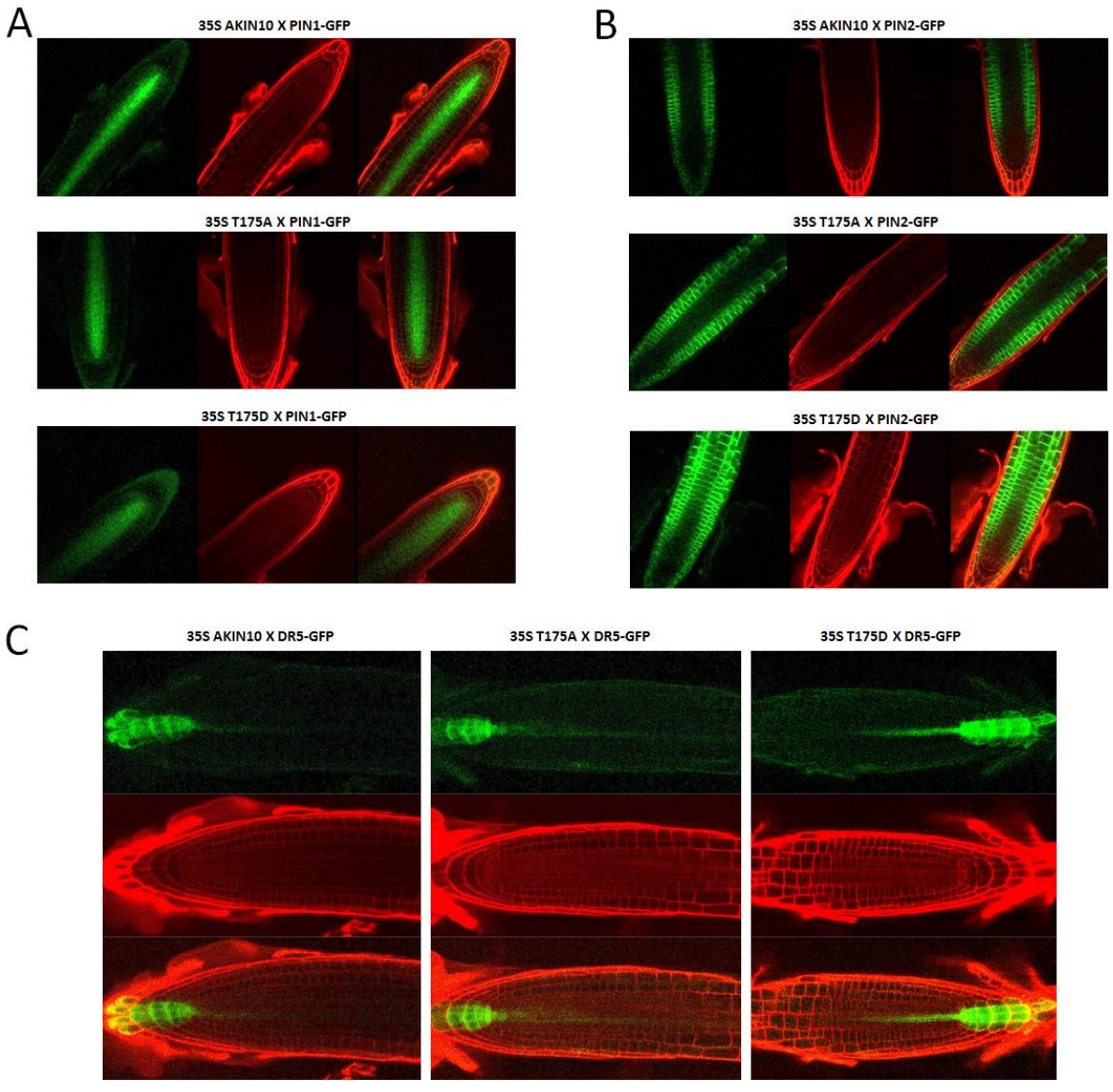

A) PIN1-GFP expression patters in roots of wild type, T175A and T175D AKIN10 expressing 7-days-old seedlings. **B)** PIN2-GFP localization in roots of seedlings of same age. **C)** Expression patters of auxin inducible DR5-GFP reporter. Each panel shows GFP images to the left, counterstaining of cell walls with propidium iodine (PI) at the middle, and overlay of GFP and PI images to the right.

Whether the observed changes in PIN2-GFP and DR5-GFP expression patterns correlate with enhancement of root elongation and are due to expression of phosphomimicking T175D version of AKIN10 should be confirmed by further studies using inducible root specific expression of AKIN10 derivatives.

It is generally accepted that enhanced activity of AKIN10 results in a late flowering phenotype, especially in the *tps1* (TREHALOSE-6-PHOSPHATE SYNTHASE 1) mutant, in which proposed inhibition of SnRK1 by T6P is abolished (Gómez et al., 2010, Wahl et al., 2013). By growing 20 individual plants in separate pots under inducing long day (16h light/8h dark) condition, plants expressing wild type, T175A and T175D AKIN10 derivatives harbored 2 to 4 more normal and cauline leaves compared to wild type plants. However, plants expressing the phosphomimicking T175D AKIN10 version started to flower at least 3 to 4 days earlier, and the onset of flowering occurred 1 and 2 days earlier in case of plants ectopically expressing wild type and T175A AKIN10 respectively, compared to the control Arabidopsis Col-0 line. In recurrent flowering time assays, 50 and 100 wild type control and 35S-AKIN10 transgenic plants were assayed respectively under short (8h light/16h dark) and long day condition by growing plants at somewhat higher density (i.e., 3 plants per pot). This repeated flowering time test failed to reveal a significant difference in leaf number between wt and 35S-AKIN10 plants under inductive long day condition. However, under short day, 35S-AKIN10 plants flowered significantly earlier, at least with 10 leaves fewer compared to wild type (Figure 21).

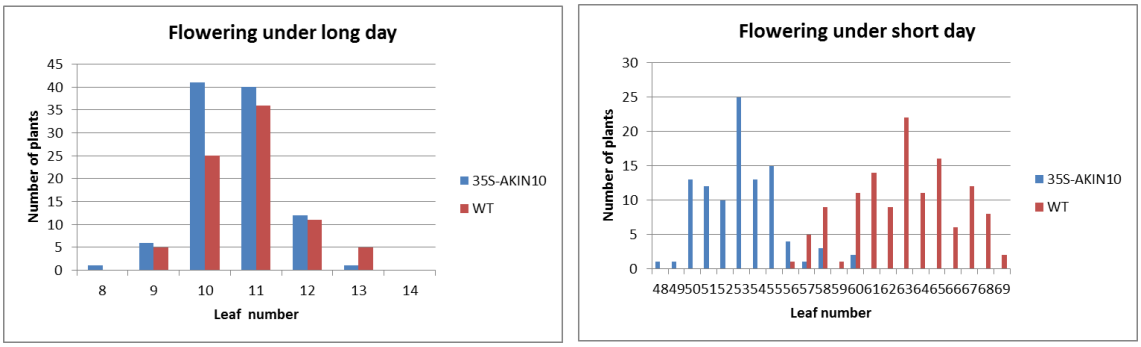

Figure 21. Comparison of flowering time of 35S-AKIN10 transgenic and wild type plants under short and long day conditions.

Although similar flowering time data are still missing for the CaMV35S promoter expressed T175A and T175D AKIN10 constructs, the results shown in Figure 20 indicate that the effect of ectopic expression of AKIN10 on flowering time is clearly day-length dependent. This suggests that ectopic AKIN10 expression could alter circadian clock-dependent regulation of the photoperiod-dependent flowering time pathway. Recently, Shin et al. (2017) reported that CaMV35S promoter driven ectopic expression of AKIN10 lengthened the clock light period and delayed the peak of GIGANTEA (GI)

expression in the dark period. GI is a direct activator of FT (Mizoguchi et al., 2005), the key transcription activator of transition to flowering. GI also stimulates stabilization of CO (CONSTANS) and CO-mediated activation of FT (Mishra and Panigrahi, 2015). Accordingly to Frank et al. (2018), ectopic expression of AKIN10 enhances the activation of bZIP83, which in turn stimulates the expression of PPR7 (PSEUDO RESPONSE REGULATOR7), a repressor of morning clock genes (CCA1/LHY; Nakamichi et al., 2010). PRR7 also interacts with and stabilizes CO (Hayama et al., 2017). Whereas these reports provide an evidence for that ectopic expression of AKIN10 influences the regulation of circadian clock, it is so far unknown how changes in the length of light and dark periods (short versus long day) affect the transcription of AKIN10 and other SnRK1 subunit genes. To examine this question, we monitored changes in the transcript levels of SnRK1 subunit genes in leaves of short day grown plants for 1 day at every 4 hours and then, after exposing the plants for 2 days to inductive long day condition, at 4 hours intervals for 48 hours (Figure 22).

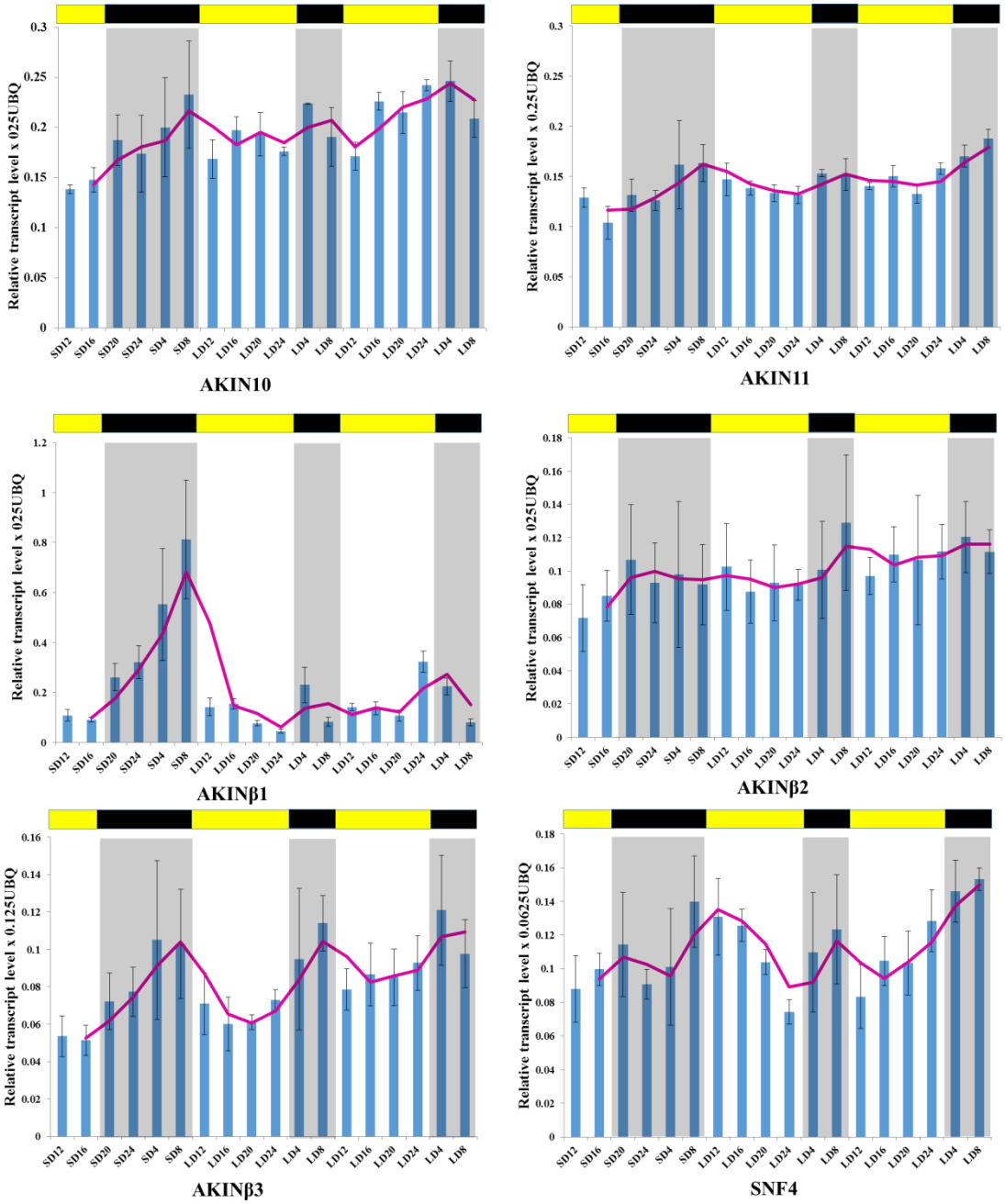

Figure 22. qRT-PCR measurement of transcript levels of SnRK1 subunit genes under short and long day conditions.
RNA samples were prepared at 4h intervals starting in the light period (Zeitgeber time 12h) under short (8h light/12h dark) day from leaves of 3-weeks-old plants. The plants were then exposed for 2 days to inductive long (16g light/8h dark) day condition, and then from the start of the light period (ZT 12h) samples were collected at every 4h for 2 days. Yellow and dark bars above the graphs mark the light and dark periods. UBQ5 mRNA was used as internal control for standardization. Standard deviation between measurements is indicated by error bars. The trend line in purple indicates moving average of consecutive samples.

The qRT-PCR measurements revealed that transcript levels of SnRK1 AKINβ1 and β3 subunits are increasing in darkness during the night and decline in the light period under short day. However, circadian peaking of the AKIN10β1 transcription is abolished under long day condition, while is still present but dampened in its amplitude in case of the AKINβ3 transcript. The amplitude of changes in the dark and light transcript levels is much less in case of all other SnRK1 subunit genes, which show

minimal (e.g., SNF4), if any (e.g., AKIN10/11/β2), cycling during the day. In case of ectopic expression, the overexpressed AKIN10 subunit will increase SnRK1 activity only if it was incorporated into trimeric complexes with the β and γ subunits. So far, no data is available about cell type specific regulation of SnRK1 subunits except for AKIN10 and SNF4 (Bitrán et al., 2011) and about the stability and incorporation of ectopically overexpressed AKIN10 into complexes with various β-subunits. Furthermore, it is suggested that only AKIN10 affects the regulation of circadian clock and flowering time but not its paralog AKIN11 (Shin et al., 2017). Therefore, for further analysis of regulatory interactions, signaling partners and substrates of SnRK1 kinases, it is more desirable to use precisely tagged native gene constructs to avoid artificial change of transcription regulation of SnRK1 subunits.

3.3. Purification of SnRK1 complexes using precisely modified native AKIN10 gene constructs

3.3.1. Site-directed modifications of the AKIN10 *gene by BAC recombineering and expression of tagged wild type and AS-kinase versions in plants*

As described in section 2.2.1.12, recombineering (i.e., λ-phage Red recombinase-mediated recombination between short homologous sequences) is a facile tool for precise site-directed modification of large eukaryotic genes, which are cloned in BACs (bacterial artificial chromosomes) in *E. coli*. The *AKIN10* and *SNF4* SnRK1 subunit genes were previously tagged in our laboratory by Bitrián et al. (2011), who used a *galK* positive/negative selectable marker for replacing their stop codons by recombineering with coding sequences of the green and yellow fluorescent (GFP and YFP) proteins, respectively. Because the application of *galK*$^+$ (galactokinase) marker is based on the complementation of chromosomal *galK*$^-$ mutation by selecting for galactose auxotrophy on minimal medium at 32°C, the time requirement of such recombineering experiments is several weeks. We replaced therefore the *galK*$^+$ marker with a new selectable/counter-selectable marker, which is composed of a kanamycin resistance gene (KmR) fused to a conditionally inducible *ccdB* gyrase inhibitor killer gene that is controlled by an arabinose-inducible promoter through the AraC repressor. The KmR-AraC-ccdB cassette was PCR amplified by primers, which carried 50 nucleotides homology to DNA sequences flanking the stop codon of the *AKIN10* gene. Following recombination induced by short heat-activation of the λ-phage Red genes, the cassette was incorporated into the *AKIN10* gene by replacing its stop codon. To facilitate the purification of AKIN10-containing SnRK1 kinase complexes, the KmR-AraC-ccdB cassette was replaced in the next step with coding sequences of the PIPL affinity tag without or in fusion with the GFP coding region. The PIPL tag developed in our laboratory is composed of a fusion of 38 His residues from the high affinity Co^{2+}/Ni^{2+} binding domain of Arabidopsis Cobw/PIP-L protein, two streptactin-binding StrepII motives, and a HA epitope. DNA fragments encoding the PIPL, GFP and GFP-PIL tags with C-terminal stop codons were similarly PCR amplified with primers providing 50 nucleotide flanks for replacement of the KmR-AraC-ccdB killer gene, which was induced by arabinose to select for its loss. On this way, without any nucleotide change or deletion, the tags were integrated in frame into the *AKIN10* gene.

The same work-flow was used for exchanging the codon M119 gate-keeper amino acid in the ATP-binding pocket of AKIN10 for a Gly codon, in order to construct an analog-sensitive AS-*AKIN10* kinase gene. The KmR-AraC-ccdB cassette inserted into the place of M119 codon was replaced in this case with a synthetic double stranded oligonucleotide, which carried the M119G codon exchange and suitable homology arms flanking the exchanged codon position. The modified genes were finally transferred by gap-repair into the Agrobacterium binary vectors pGAP-Km and pGAP-Hyg and transformed into wild type Arabidopsis plants. At least 20 T1 transformants were screened in the T2 generation for 3:1 segregation of pGAP vector T-DNA insertions followed by isolation of homozygous T3 progeny. The expression of AKIN10_GFPPIPL and AS(M119G)-AKIN10-GFPPIPL (as well as GFP-tagged versions) was monitored in the T2 and T3 lines by confocal microscopy in the roots of seedlings (Figure 23A).

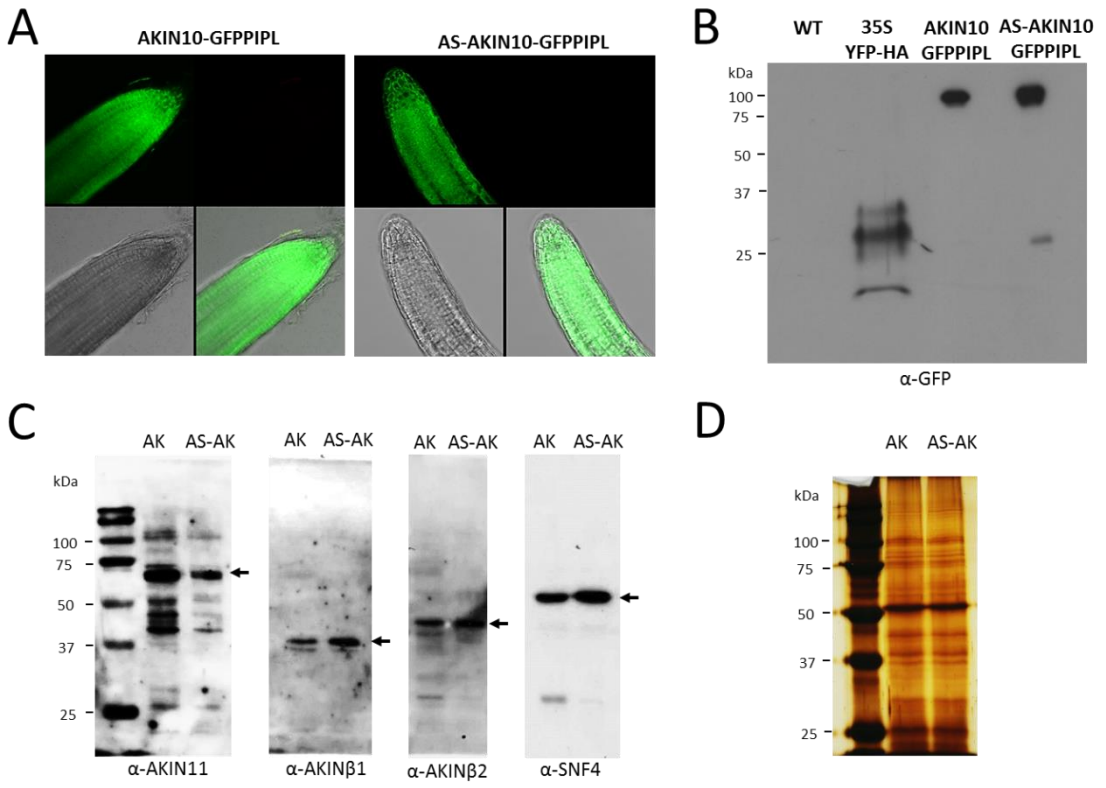

Figure 23. Expression of GFPPIPL-tagged of wild type and AS-kinase versions of AKIN10 in plants and detection of their association with AKIN11, AKINβ1/2 and SNF4 SnRK1 subunits.
A) Expression patterns of GFPPIPL-tagged wild type AKIN10 and AS-AKIN10 in roots of 3-weks old seedlings grown under short day condition in 0.5 MSAR medium with 0.5% sucrose. The bulk of GFPPIPL tagged kinase proteins is located in the cytoplasm and around the plasma membranes, and nuclei in the upper root elongation zone. **B)** The presence of intact AKIN10-GFPPIPL and AS-AKIN10-GFPPIPL proteins in total protein extracts from seedlings (expected molecular mass for the GFPPIPL-tagged AKIN10.1 isoform is 94 kDa) was confirmed by western blotting with anti-GFP antibody using control wild type (WT) and YFP-HA expressing seedlings grown under the same conditions as in A). AKIN10-GFPPIPL and AS-AKIN10-GFPPIL were purified by GFP-Tap affinity pull-down and subjected to western blotting with anti-AKIN11, anti-AKINβ1, anti-AKINβ2 and anti-SNF4 antibodies from Agrisera. AK: AKIN10-GFPPIPL, AS-AK: analog-sensitive AS-AKIN10-GFPPIPL. D) Silver stained SDS-PAGE of GFP-TRAP purified AKIN10-GFPPIPL and AS-AKIN10-GFPPIPL samples derived total protein extracts of 1g whole seedling material grown for 3 weeks under short day condition in 0.5 MSAR medium with 0.5% sucrose.

GFPPIPL-tagged versions of AKIN10 and its analog-sensitive AS-AKIN10 derivative showed identical localization patterns in roots. Both proteins were mainly detected in the cytoplasm and along the plasma membranes of cells in the root tip, while their localization around nuclei was only observed in cells of the root elongation zone. Both proteins were detected by anti-GFP western blotting in total protein extracts of seedlings confirming the expected molecular mass of 94 kDa (Figure 23B). The GFP-PIPL tagged AKIN10 and AS-AKIN10 proteins were purified on analytical scale from 1g aliquots of 3-weeks-old seedlings by GFP-Trap to examine their association with other SnRK1 subunits by western blotting with Agrisera anti-AKIN11, AKINβ1, AKINβ2 and SNF4 antibodies (Figure 23 C and D). As expected, both AKIN10 and AS-AKIN10 were detected in association of both AKINβ1 and AKINβ2, as well as with the activating subunits SNF4. However, surprisingly the second SnRK1α2 catalytic subunit AKIN11 was also identified by immunoblotting in the purified AKIN10 and AS-AKIN10 complexes suggesting that the AKIN10 and AKIN11 catalytic subunits might form dimeric kinase complexes. To determine whether this is indeed the case or the Agrisera anti-AKIN11 antibody is not specific (i.e., as it also cross-react with other proteins, Figure 23C), we GFP-Trap purified AKIN10-GFP complexes from total seedling protein extracts and analyzed their subunits by LC-MS/MS mass spectrometry.

3.3.2. Purification of AKIN10-containing SnRK1 complexes from total cell extracts and identification of associated interacting proteins by LC-MS/MS mass spectrometry

AKIN10-GFP, AKIN10-GFPPIL and AS-AKIN10-GFPPIPL were purified using 3 independent replicates for each sample in 5 experiments (Table 1). In experiment 1, we used the exclusively nuclear localized PRL1-GFP protein, which is a core subunit of the spliceosome activation NTC (Nineteen) complex (Koncz et al., 2012) as control for pull-down of nuclear proteins. In all other experiments, the SnRK1 activating subunit SNF4-YFP was used as a control. SNF4-YFP was reported by Bitrián et al. (2011) to show predominant nuclear localization. On this way, we monitored the pull down of common partners by the SnRK1α1 subunit AKIN10 and its activating SNF4 subunit. In experiment 5, we compared the interacting partners of wild type AKIN10 and AS-AKIN10 derivatives. In all experiments, protein extracts from wild type and 35S-YFP-HA expressing plants were used as positive and negative controls. Table 2 shows a short data output of Experiments 4 and 5, including the log2 values of enrichment factors and their standard errors based on comparison to wild type and YFP-HA controls. Table 3 provides a list of proteins identified to interact with AKIN10 and AS-AKIN10 compared to SNF4 in the analyzed samples.

Table 1 GFP-Trap purification of AKIN10 baits.
Protein extracts in experiments 1 and 2 were prepared from rosettes of 4-weeks-old plants grown under 12 h/12 h dark condition in soil. In experiment 3, protein extract was prepared from roots of 5-weks old plant grown in Erlenmeyer bottles in liquid MSAR medium with 3% sucrose. In experiments 4 and 5, 3-weeks-old seedlings grown under heterotrophic conditions in short day (8hlight/16h dark) in 0.5 MASR medium with 0.5% sucrose in Petri dishes were used for total protein extraction.

Experiment	**1**	**2**	**3**	**4**	**5**
Plant tissue	seedling	seedling	roots	seedling	seedling

Bait	AKIN10-GFP	AKIN10-GFP	AKIN10-GFP	AKIN10-GFPPIPL	AS-AKIN10-GFPPIPL
Control 1	PRL1-GFP	SNF4-YFP	SNF4-YFP	-	-
Control 2	YFP-HA	YFP-HA	YFP-HA	YFP-HA	YFP-HA
Control 3	wild type	wild type	wild type	wild type	wild type

Table 2. LC/MS analysis of AKIN10-GFPPIPL and AS-AKIN10-GFPPIPL associated proteins after GFP-Trap pull-down.
LFQ, integral of peptide peak areas proportional with the amount of peptides detected in 3 biological replicates; Log2 ratio: 2^{log2} enrichment of a given protein in the sample; p-value of log2. NaN: no detection.

				AKIN10			AS-AKIN10			YFP			wt			AKIN10 vs		AKIN10 vs wt		AS-AKIN10		AS-AKIN10	
TAIR IDs	Gene	Peptide No	MS/MS count	LFQ 1	LFQ 2	LFQ 3	LFQ 1	LFQ 2	LFQ 3	LFQ 1	LFQ 2	LFQ 3	LFQ 1	LFQ 2	LFQ 3	log2 ratio	p-value	log2 ratio	p-value	log 2 ratio	p-value	log2 ratio	p-value
AT3G01090	AKIN10	43	1108	34.38	33.09	33.53	34.064	33.96	33.91	25.6	26.05	25.18	21.231	20.61	21.11	**8.057**	4.231	**12.682**	5.139	**8.371**	5.29	**13**	6.5
AT1G09020	SNF4	29	634	34.18	32.69	33.31	33.791	33.64	33.6	24.37	24.74	24.44	24.808	24.34	24.34	**8.881**	4.418	**8.8993**	4.374	**9.163**	6.64	**9.181**	6.2
AT5G21170	AKINβ1	8	218	31.12	30.12	30.59	30.886	31.2	30.81	20.26	20.65	21.15	20.938	19.88	21.04	**9.924**	4.862	**9.9896**	4.54	**10.28**	5.47	**10.35**	4.9
AT4G16360	AKINβ2	8	142	31.38	29.92	30.49	30.694	30.62	30.72	NaN	NaN	NaN	NaN	NaN	NaN	**30.6**	0	**30.596**	0	**30.68**	0	**30.68**	0
AT3G29160	AKIN11	14	64	29.97	28.78	29.29	30.328	30.04	29.46	NaN	18.87	NaN	NaN	NaN	NaN	**10.48**	0	**29.349**	0	**11.07**	0	**29.94**	0
AT1G06410	TPS7 class II trehalose phosphate synthase	35	146	28.4	27.67	28.18	27.863	27.94	27.94	21.92	NaN	22.38	21.221	23.82	22.81	**5.929**	3.434	**5.4627**	2.644	**5.763**	4.21	**5.297**	2.7
AT2G18700	TPS11 class II trehalose phosphate synthase	27	75	27.89	27.13	27.33	26.914	26.36	27.01	22.61	21.82	NaN	25.424	24.22	20.93	**5.235**	2.962	**3.9274**	1.346	**4.544**	2.85	**3.236**	1.1
AT2G28060	AKINβ3	3	22	26.39	25.93	26.23	25.531	25.52	25.31	NaN	NaN	NaN	NaN	NaN	NaN	**26.18**	0	**26.183**	0	**25.45**	0	**25.45**	0
AT1G70290	TPS8 class II trehalose phosphate synthase	20	55	26.11	26.2	26.23	26.772	26.74	26.61	21.41	21.53	22.76	21.024	22	22.28	**4.278**	3.233	**4.4085**	3.488	**4.808**	3.42	**4.938**	3.7
AT2G44670	DUF581 domain protein	5	17	27.08	24.49	25.72	25.252	25.32	25.5	NaN	NaN	NaN	23.016	NaN	NaN	**25.76**	0	**2.7446**	0	**25.36**	0	**2.34**	0
AT1G60140	TPS10 class II trehalose phosphate synthase	32	144	27.25	24.62	25.39	31.075	30.31	30.57	17.32	18.47	17.76	18.821	18.01	18.06	**7.901**	3.131	**7.4559**	3.087	**12.8**	5.22	**12.35**	5.4
AT1G23870	TPS9class II trehalose phosphate synthase	13	27	24.64	24.28	25.03	25.916	25.79	25.35	NaN	NaN	NaN	NaN	19.94	NaN	**24.65**	0	**4.7139**	0	**25.68**	0	**5.746**	0
AT2G40000	HSPRO2 | ortholog of sugar beet HS1 PRO-1 2	14	40	26.77	23.9	24.41	26.549	26.24	25.88	NaN	NaN	NaN	19.238	NaN	21.47	**25.03**	0	**4.6704**	1.343	**26.22**	0	**5.866**	2.2
AT4G17770	TPS5 class II trehalose phosphate synthase	5	14	23.78	22.46	22.83	23.725	24.08	23.8	NaN	NaN	NaN	NaN	NaN	NaN	**23.02**	0	**23.024**	0	**23.87**	0	**23.87**	0
AT1G22160	DUF581 domain protein	3	12	23.48	21.6	22.67	24.223	23.92	24.47	NaN	NaN	NaN	NaN	NaN	NaN	**22.58**	0	**22.585**	0	**24.2**	0	**24.2**	0
AT1G78020	DUF581 domain protein	2	2	21.21	21.14	22.6	22.257	21.99	21.99	NaN	NaN	NaN	NaN	NaN	NaN	**21.65**	0	**21.65**	0	**22.08**	0	**22.08**	0
AT5G47060	DUF581 domain protein	*1*	*5*	*21.55*	*21.1*	*22.3*	*22.03*	*21.85*	*22.14*	*NaN*	*NaN*	*NaN*	*NaN*	*NaN*	*NaN*	***21.65***	*0*	***21.646***	*0*	***22***	*0*	***22.01***	*0*

In all purification experiments using either AKIN10 or AS-AKIN10 as baits, the SnRK1α1 subunit pulled down the activating SNF4 and all three AKINβ subunits. Similarly, the SNF4-YFP bait co-purified with the catalytic SnRK1α subunits AKIN10 and AKIN11, and with the AKINβ1, 2 and 3 subunits, from which AKINβ3 was detected at the lowest amount. Except for AKIN10-GFP complexes purified from roots, AKIN11 was detected in all other AKIN10 and SNF4 pull-down samples, indicating that indeed the two catalytic SnRK1α subunits occurred in dimeric kinase complexes. The fact that the nuclear PRL1 protein was not detected in the total protein extract indicated that the identified protein complexes likely represent cytotosolic SnRK1 kinases and their associated partners. Among the latter, several DUF581 domain proteins were identified, which were previously shown to interact in yeast two-hybrid assays with AKIN10 or AKIN11. Jamsheer and Laxmi (2014) found that the DUF581 domain is a conserved plant-specific FCS-like zinc finger involved in protein-protein interactions. Nietzsche et al. (2016) suggested that the DUF581 proteins might target SnRK1 kinases to important signaling factors, as they interact in yeast 2H assays with TCP transcription factors and DELLA repressors of gibberellin signaling (Nietzsche et al., 2014; 2016). However, none of the previously reported two-hybrid interacting partners of DUF581 proteins was identified in the pull-down samples by mass spectrometry.

At relatively low representation, Arabidopsis homolog HSPRO2 of the sugar beet HS1 PRO-1 leucine-rich-repeat protein was detected in both AKIN10 and SNF4 pull-downs. HSPRO2 was identified to interact with the CBM-domain of SNF4 in yeast 2H assays (Gissot et al., 2004) and is involved in resistance response to Pseudomonas (Murray et al., 2007; Schuck et al., 2013). Our mass spectrometry data thus provided evidence for *in vivo* association of these factors with SnRK1 complexes in Arabidopsis seedlings, although they were not detected in roots.

Table 3.The lists of AKIN10, AS-AKIN10 and SNF4 associated factors identified in five independent experiments using three biological replicates for each GFP-Trap purified sample from total protein extracts prepared from whole seedlings and roots (in experiment 3).

Proteins identified in at least 4 x 3 pull-down samples are marked by grey color. Others, which represent statistically weaker candidates, found only in two experiments, are printed in yellow background. Factors represented by 1 or 2 peptides at very low abundance are marked by letters in italics.

Experiment		1		2		3		4	5
TAIR IDs	Gene	AKIN10	PRL1	AKIN10	SNF4	AKIN10	SNF4	AKIN10	AS-AKIN10
AT3G01090	**AKIN10**	+	-	+	+	+	+	+	+
AT1G09020	**SNF4**	+	-	+	+	+	+	+	+
AT4G16360	**AKINβ2**	+	-	+	+	+	+	+	+
AT5G21170	**AKINβ1**	+	-	+	+	+	+	+	+
AT3G29160	**AKIN11**	+	-	+	+	-	+	+	+
AT2G28060	**AKINβ3**	+	-	+	+	+	+	+	+
AT1G60140	**TPS10 classII trehalose phosphate synthase**	+	-	+	+	+	+	+	+
AT4G17770	**TPS5 classII trehalose phosphate synthase**	+	-	+	+	+	+	+	+
AT1G68020	**TPS6 classII trehalose phosphate synthase**	+	-	+	+	-	-	-	-
AT1G06410	**TPS7 classII trehalose phosphate synthase**	-	-	+	+	+	+	+	+
AT1G70290	**TPS8 classII trehalose phosphate synthase**	+	-	+	+	+	+	+	+
AT1G60140	**TPS10 classII trehalose phosphate synthase**	+	-	+	+	+	+	+	+
AT1G23870	**TPS9 classII trehalose phosphate synthase**	+	-	+	+	+	+	+	+
AT2G18700	**TPS11 classII trehalose phosphate synthase**	+	-	+	+	-	-	+	+
AT5G47060	**DUF581 domain protein**	+	-	+	-	-	-	+	+
AT2G44670	**DUF581 domain protein**	+	-	+	+	-	-	+	+
AT1G78020	**DUF581 domain senescence-associated family protein**	-	-	+	+	-	-	+	+
AT2G40000	**HSPRO2 ortholog of sugar beet HS1 PRO-1 2**	-	-	+	+	-	-	+	+
AT3G23570	*yeast AIM2-like alpha/beta-Hydrolases superfamily protein*	-	-	+	+	-	-	+	+
AT1G68580	*agenet / bromo-adjacent homology (BAH) domain protein*	+	-	+	+	-	-	-	-
AT1G01610	GPAT4 glycerol-3-phosphate acyltransferase 4	+	-	+	+	-	-	-	-
AT1G08050	Zinc finger (C3HC4-type RING finger) family protein	+	-	+	+	-	-	-	-
AT3G52750	FTSZ2-2 | Tubulin/FtsZ family protein	+	-	+	+	-	-	-	-
AT1G13320	PP2AA3 | protein phosphatase 2A subunit A3	+	-	+	+	-	-	-	-
AT4G19710	AK-HSDH II, aspartate kinase-homoserine dehydrogenase II	+	-	+	+	-	-	-	-
AT1G60780	HAP13 Clathrin adaptor complexes medium subunit	+	-	+	+	-	-	-	-
AT1G70510	*KNAT2, ATK1 | KNOTTED-like homeobox TF*	+	-	+	+	-	-	-	-
AT5G65840	*Thioredoxin superfamily protein |*	+	-	+	+	-	-	-	-
AT3G12050	Aha1 domain-containing protein	+	-	+	+	-	-	-	-
AT3G42170	DAYSLEEPER BED zinc finger;hAT dimerisation domain	+	-	+	+	-	-	-	-
AT4G15110	*CYP97B3 | cytochrome P450, family 97, subfamily B,*	+	-	-	+	-	-	-	-

Surprisingly, our results demonstrated that in at least 4 out of 5 experiments the AKIN10 and SNF4 containing, likely dimeric SnRK1 complexes occurred in association with members of the class II trehalose 6-phosphate synthase/phosphatase (TPS) family. TPS5, 8, 9 and 10, which were more abundant in the samples were consistently detected in all 5 experiments using AKIN10 and AS-AKIN10 as baits, as well as in 2 experiments with the SNF4-YFP bait (Table 3). TPS11 was not present in root samples, and TPS6 appeared to have the lowest abundance in the samples. Although the LC-MS/MS data are not quantitative, the differences in the LFQ peptide peak intensity values suggested that only about $1/2^6$ (1/64) to 0.1% proportion of SnRK1 complexes were associated with individual class II TPS proteins in the purified samples, although these ratios varied between the different purification experiments.

The Arabidopsis class II TPS proteins are considered as inactive enzymes because they cannot complement the yeast *Δtps1Δtpp* mutations (Ramon et al., 2009). Nonetheless, class II TPS proteins carry conserved catalytic domains of TPS (trehalose-6-phosphatase synthase) and TPP (T6P phosphatase) enzymes. Therefore, they could theoretically function of T6P receptors or T6P-dependent effectors as speculated by Broeckx et al. (2016), or alternatively as sensors of T6P precursors including glucose-6-phosphate (G6P) and UDP-glucose. NADPH was reported to bind to and activate TPS1, which was therefore proposed to act as redox sensor controlling the activation of virulence gene repressors in the rice blast disease fungus *Magnaporthe oryzae* (Wilson et al., 2010). Therefore, we

performed an assay to determine whether association of class II TPS proteins with SnRK1 enzymes would influence the kinase activity in response to the availability of TPS substrates and NADPH. AKIN10-GFPPIPL was purified from seedlings by standardizing the protein input to prepare parallel samples of GFP-Trap bound SnRK1 kinase complexes. The beads were extensively washed as in case of LC-MS sample preparations, and then were subjected to on-bead kinase reactions using (γ^{32}P)ATP and Trx-SPS-KD kinase substrate in the presence of glucose-6-phosphate (G6P, 100µM), UDP-glucose (UDPG, 100µM) and NADPH (1mM) applied alone or in combinations.

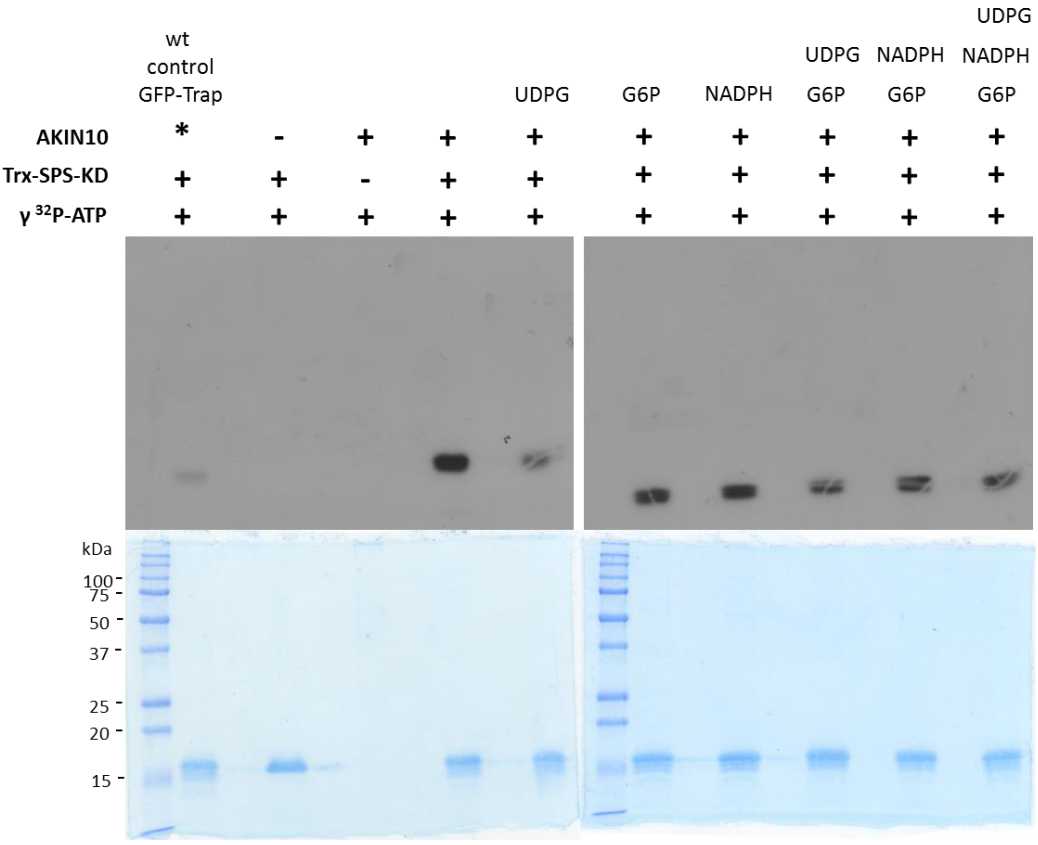

Figure 24. On bead protein kinase assays with GFP-Trap bound purified AKIN10-GFPPIPL complexes in the presence of TPS substrates and NADPH.
The upper panel shows phosphorylation of SnRK1 substrate Trx-SPS-DK in the presence of TSP substrates and NADPH alone or in combinations detected by autoradiography. The first column shows a control pull down assay with wild type protein extract, indicating the background of aspecifically bound protein kinases. The lower panels show Coomassie staining of SDS-PAGE gels on which the kinase reactions were size separated.

The results of kinase assays shown in Figure 24 indicated that phosphorylation of the SnRK1 substrate Trx-SPS-KD protein was reduced by about 30-40% whenever the kinase reactions were performed in the presence of UDP-glucose. This suggested that binding of the TPS substrate UDP-glucose to AKIN10-GFPPIPL-associated class II TPS proteins resulted in an inhibition of SnRK1 substrate phosphorylation.

In collaboration, Dr. Ajit Ghosh in our laboratory expressed the class II TPS protein TPS8 in fusion with a C-terminal mCherry tag in AKIN10-GFP expressing plants. Followed purification of

AKIN10-GFP on GFP-Trap, TPS8-mCherry was detected in association with AKIN10-GFP by western blotting with anti-RFP antibody. At the same time, association of TPS8 with AKIN10-GFP was detected by reciprocal pull-down of TPS8-mCherry with RFP-trap followed by western blotting with anti-GFP antibody (Figure 25A).

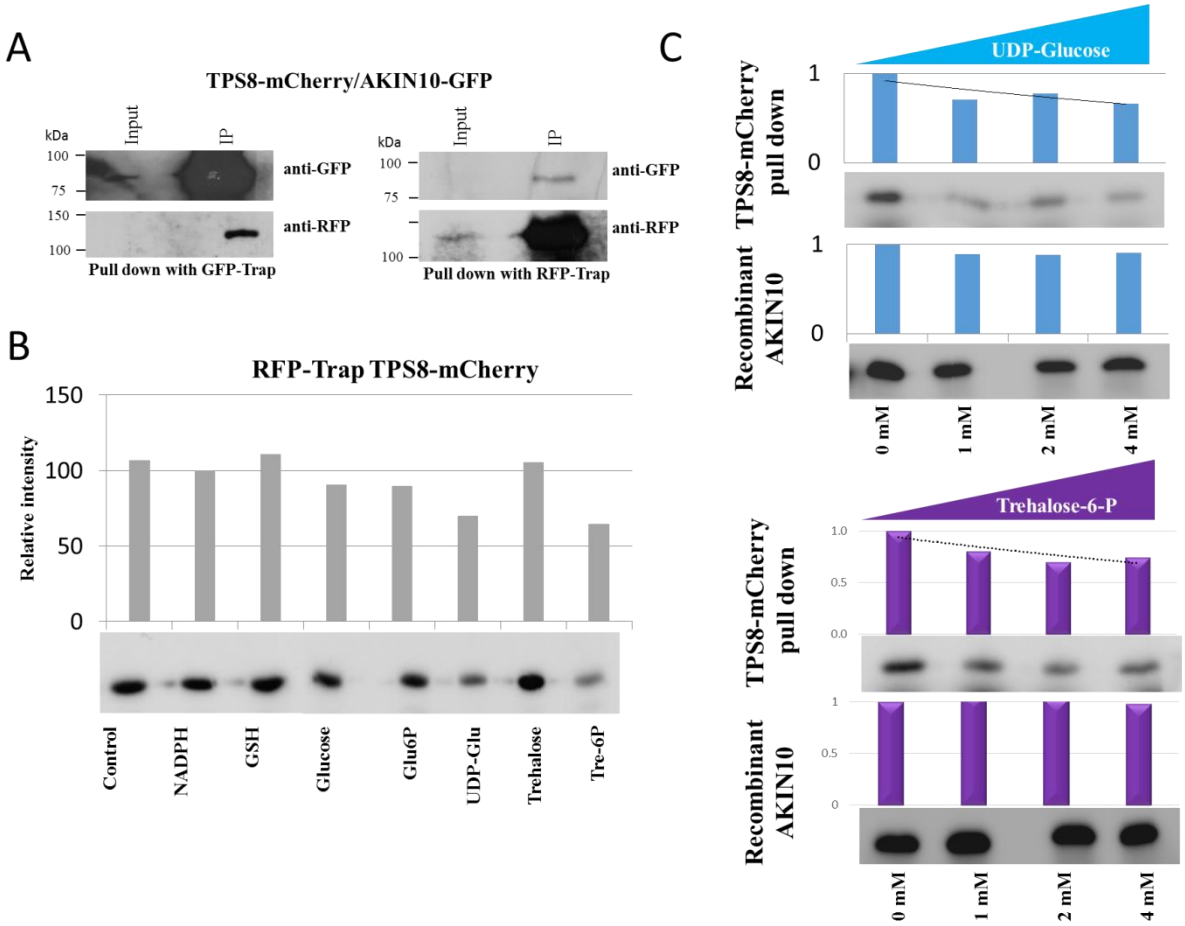

Figure 25. UDP-glucose and trehalose-6-P inhibit phosphorylation of the SnRK1 kinase substrate Trx-SPS-KD by the TPS8-associated kinase.
A) Protein extract was prepared from AKIN10-GFP and TPS8-mCherry expressing 3-weeks-old seedlings grown in short day on 0.5MSAR medium with 0.5% sucrose. Half of the extract was bound to GFP-Trap and followed elution subjected to western blotting with anti-RFP antibody to detect AKIN10-association with TPS8-mCherry. Equivalent aliquot of protein extract was bound to RFP-Trap and after elution subjected to western blotting with ant-GFP antibody to reciprocally confirm association of AKIN10-GFP with the TPS8-mCherry bait. **B)** Protein kinase assays with the RFP-bound TPS8-mCherry protein complex using (γ ^{32}P)ATP and SnRK1 substrate Trx-SPS-KD in the presence of 1mM NADPH, 5 mM glutathione (GSH), 50mM glucose (Gluc), 0.5mM glucose-6-phosphate (Gluc6P), 0.5 mM UDP-glucose (UDP-Glu), 50mM trehalose and 0.5mM trehalose-6-phosphate (Tre-6P). **C)** Comparative protein kinase assays using RFP-Trap bound purified TPS8-mCherry protein complex, (γ^{32}P)ATP, SnRK1 substrate Trx-SPS-KD and increasing concentrations of UDP-glucose and T6P. Control kinase assays were parallel performed with purified AKIN10 *in vitro*.

These reciprocal pull-down experiments confirmed that part of AKIN10 was associated with TPS8 and *vice versa* part of TPS8 pulled down AKIN10. In collaboration with Dr. Zsuzsa Koncz, next a repeated kinase assays was performed using a reciprocal TPS8 pull-down. The TPS8-mCherry protein complex was purified from total protein extract on RFP-Trap and used in phosphorylation assays with

the SnRK1 substrate Trx-SPS-KD in the presence of NAPDH, glutathione, glucose, glucose-6-phosphate, UDP-glucose, trehalose and trehalose-6-phosphate (T6P). In addition to UDP-glucose, these assays indicated that trehalose-6-P can similarly inhibit the activity of TPS8-associated kinase to phosphorylate the SnRK1 substrate Trx-SPS-KD (Figure 25B). Finally, kinase assays were performed with the RFP-Trap bound TPS8-mCherry protein complex using increasing concentrations of UDP-glucose and T6P (1 to 4 mM) by performing parallel control assays with the SnRK1α1 kinase subunit AKIN10 purified from *E. coli*. While both increasing concentrations of UDP-glucose and T6P resulted in a gradual (though not linear) decrease of kinase activity associated with TPS8-mCherry, the activity of purified SnRK1α1 kinase subunit AKIN10 was not inhibited by these compounds (Figure 25C), in contrast to a recent report by Zhai et al. (2018). These results suggest that class II TPS proteins in SnRK1-associated cytoplasmic protein complexes might function as UDP-glucose and T6P sensors to negatively modulate the activity of SnRK1. Nonetheless, these results should be further corroborated by double affinity purification of TPS-SnRK1 complexes.

3.3.3. Purification of SnRK1 complexes from isolated nuclei

For isolation of SnRK1 protein complexes, cell nuclei were partially purified from leaves of 4-weeks-old soil grown seedlings as described in section 2.2.4.2. For initial optimization of nuclear protein extraction protocol, we compared two extraction buffers, one containing 0.1% SDS (A: used for IP in ChIP-Seq experiments) and another with 1% Triton X100 (B). Nuclei were isolated from 200g leaf material of AS-AKIN10-GFPPIPL expressing 4-weeks-old plants grown in soil under short day condition, lysed in nuclear extraction buffers A and B followed by centrifugation and the extracted proteins were comparatively analysed by SDS-PAGE separation and Coomassie staining, as well as by western blot detection of extracted AS-AKIN10-GFPPIPL protein with anti-GFP antibody. Surprisingly, the results indicated that in the absence of subsequent sonication step, the efficiency of nuclear protein extraction using 0.1% SDS as detergent is very low compared to nuclear lysis with 1% Triton X100-containing extraction buffer (Figure 26).

For chromatin-IP of DNA cross-linked protein complexes (see e.g., Reimer and Turck, 2010), Arabidopsis nuclei are usually sonicated in NLBA or similar buffer containing no $(NH_4)_2SO_4$, until the DNA is fragmented to mono-nucleosome size (about 145 bp).

Nuclear Lysis Buffer A (1x)

20mM	Hepes(NaOH) pH 7.4
15mM	$MgCl_2$
25mM	NaCl
0.4 M	$(NH_4)_2SO_4$
10%	Glycerol
0.1%	SDS

Nuclear Lysis Buffer B (1x)

20mM	Hepes(NaOH) pH 7.4
15mM	$MgCl_2$
25mM	NaCl
0.4 M	$(NH_4)_2SO_4$
10%	Glycerol
1%	Triton X-100

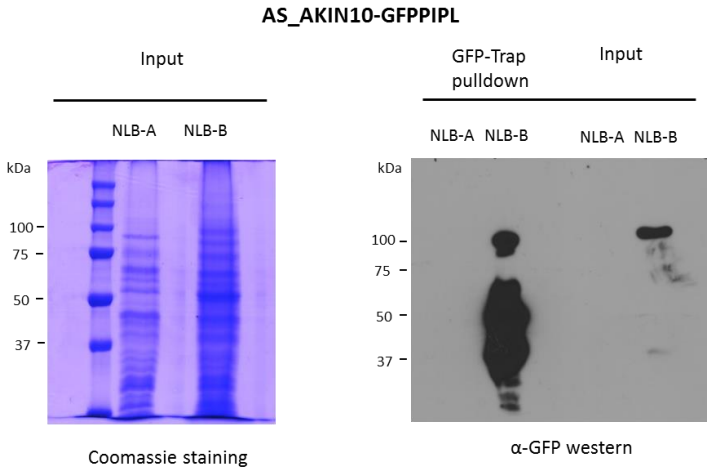

Figure 26. Comparison of efficiency of nuclear protein isolation using nuclear extraction buffers with different detergents.
Nuclear lysis buffer A (NLBA) containing 0.1% SDS results in a much lower yield of extracted proteins compared to NLB containing 1% Triton X-100. The amount of extracted nuclear protein was monitored by SDS-PAGE followed by Coomassie staining. Specific recovery of AS-AKIN10-GFPPIPL protein in the nuclear extract was monitored by western blotting using anti-GFP antibody.

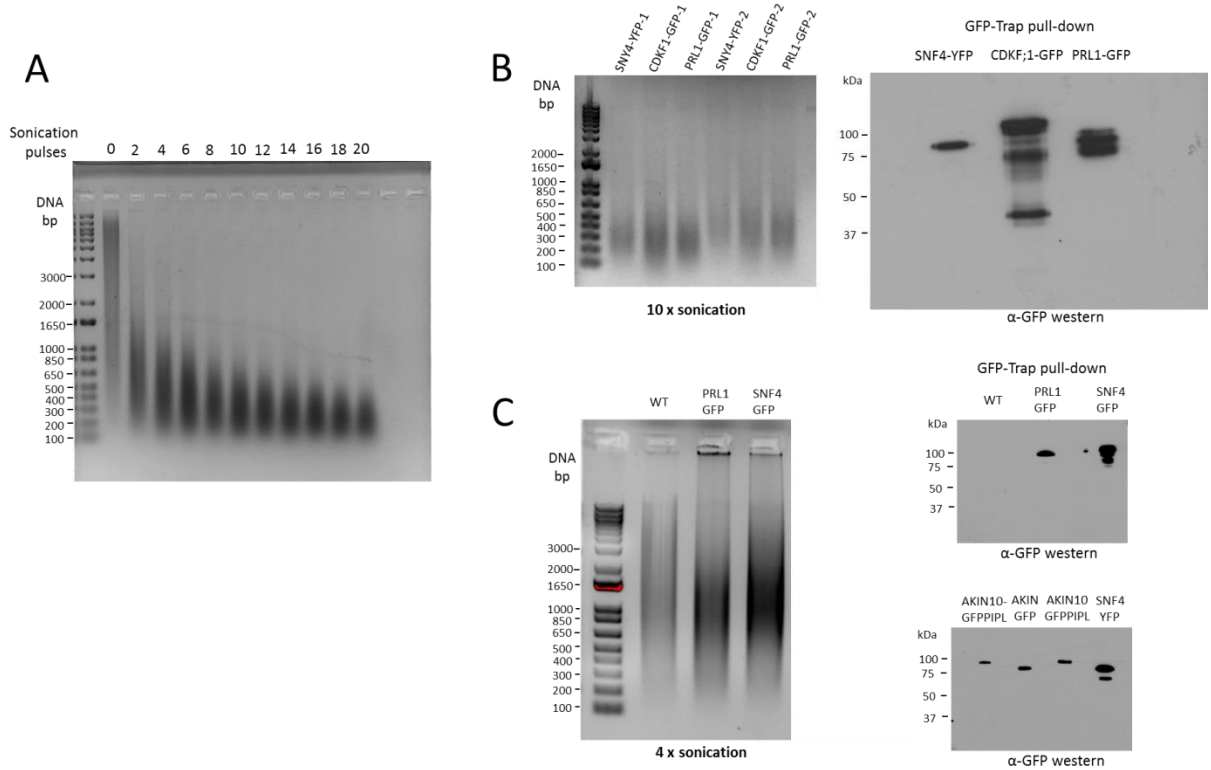

Figure 27. Optimization of sonication conditions for extraction of nuclear proteins.
A) Titration of chromatin DNA fragmentation by increasing the number of sonication pulses (each pulse 10 sec). **B)** Upon 10 x 10sec sonication, the DNA fragment size corresponds to 1-2 nucleosome size. Under these conditions three nuclear proteins, the SNF4 activating subunit of SnRK1, the CDKF;1 activating kinase of RNA polymerase II general transcription factor TFIIH-associated CDKD kinases, and the PRL1 subunit of spliceosome activating NTC complex are efficiently extracted as confirmed by western blotting of their GFP and YFP tagged versions.

C) After 4 x 10 sec sonication the chromatin DNA is fragmented to 6-8 nucleosome size, which might better preserve larger protein complexes. PRL1, AKIN10, AS-AKIN10 and SNF4 are similarly extracted as monitored by western blotting of their GFP, GFPPIPL and YFP tagged forms.

Alternatively, the nuclei are lysed using the chaotropic salt $(NH_4)_2SO_4$, which was introduced originally for preparation of nuclear protein lysates used in DNA-binding gel retardation assays to study various transcription factors (see e.g., Foster et al., 1992). To titrate the nucleosome fragmentation by sonication, the nuclei isolation was standardized using NLBB (Figure 26) and the decrease of DNA size during increasing the number of sonication pulses was monitored by gel electrophoresis (Figure 27A). In the next step, nuclei prepared from plants expressing three nuclear proteins (PRL1, CDKF;1 and SNF4; Figure 27B) were subjected to DNA fragmentation to about 2-3 nucleosome size and the recovery of GFP/YFP tagged forms of these nuclear proteins were monitored by western blotting. Each of the three nuclear proteins was equally well extracted using this protocol. Similarly, 4 sonication cycles were used to prepare protein extracts, in which the DNA was fragmented to 6-8 nucleosome size to facilitate the recovery of larger protein complexes. This was tested by extraction of AKIN10-GFP, AS-AKIN10-GFPPIPL, PRL1-GFP and SNF4-YFP from nuclei. Somewhat lower yield of all four proteins was confirmed by western blotting using anti-GFP antibody (Figure 27C).

An alternative approach to degrade nucleic acids in nuclear protein samples is offered by treating the nuclear extracts with DNase and RNase. As nuclear lysis was enhanced by using 0.4M $(NH_4)_2SO_4$ in the NLBB extraction buffer, prior application of nucleases the samples had to be desalted by dialysis or gel filtration. The disadvantage of this step is that during dialysis a continuous protease protection must be maintained (i.e., by addition of protease inhibitors and proteasome inhibitor of MG132), which is not practical (i.e., due to the high cost). Another problem is that the applied DNase and RNase enzymes must be of high quality (such as homogeneous Worthington DNase and similar quality of RNase, or recombinant benzonase from Merck). Even using high quality enzymes, DNase and RNase have their temperature optima at 37°C, where proteolysis in plant nuclear extracts is extremely fast. By contrast, treating the extract with DNase and RNase at 4°C, providing parallel inhibition of proteasome and protease activities, might not be sufficient for efficient fragmentation of nucleosome and nuclear RNAs. This could result in the isolation of large nucleic acid bound protein complexes preventing the identification of specific interacting partners of bait proteins. A final problem in LS-MS/MS analysis of nuclear protein complexes is the choice of internal nuclear protein control, which should be a protein that cannot form common complexes with the purified bait.

Table 4. Comparative LC-MS/MS mass spectrometry analysis of GFP-Trap purified AKIN10-GFP, SNF4-YFP and PRL1-GFP nuclear protein complexes purified by four different nuclear extraction protocols.

Experiment		1: 4°C DNase & RNase			2: 37°C DNase & RNase			3: 10 x sonication			4: 4 x sonication		
Protein IDs	Gene	AKIN10	SNF4	PRL1	AKIN10	SNF4	PRL1	AKIN10	SNF4	PRL1	AKIN10	SNF4	PRL1
AT1G09020	**SNF4**	27	31	NaN	30	29	16	29	32	14	32	33	20
AT3G01090	**AKIN10**	29	31	NaN	32	29	19	31	30	NaN	33	30	18
AT3G29160	**AKIN11**	NaN	29	NaN	25	30	NaN	22	30	NaN	28	29	20
AT5G21170	**AKINbeta1**	23	27	NaN	26	27	NaN	28	29	NaN	30	30	NaN
AT4G16360	**AKINbeta2**	24	25	NaN	27	25	NaN	26	26	NaN	27	27	NaN
AT2G28060	**AKINbeta3**	20	22	NaN	21	19	NaN	23	25	NaN	25	25	NaN
AT1G07840	Sas10/Utp3/C1D family neuroguidin, EIF4E binding protein	27	27	NaN	-	20	NaN	-	-	-	-	-	-
AT3G50590	Transducin/WD40 repeat-like superfamily protein	26	23	NaN	-	-	-	22	22	20	-	-	-
AT5G38640	NagB/RpiA/CoA transferase-like superfamily protein	27	24	21	-	-	-	20	20	20	-	-	-
AT2G35940	BLH1 | BEL1-like homeodomain 1	22	23	20	-	-	-	-	-	-	20	22	24
AT2G24590	SR protein RSZ22a RNA recognition motif CCHC-type zinc finger domain	23	24	21	-	-	-	22	21	22	23	NaN	NaN
AT5G05230	RING/U-box superfamily protein	23	24	22	NaN	18	NaN	-	-	-	20	21	NaN
AT3G06610	DNA-binding enhancer protein-related	-	-	-	NaN	19	NaN	-	-	-	23	23	NaN
AT1G53720	CYP59 | cyclophilin 59	-	-	-	NaN	18	NaN	NaN	NaN	21	NaN	NaN	NaN
AT5G48160	OBE2 | Protein of unknown function (DUF1423)	-	-	-	NaN	18	NaN	-	-	-	NaN	23	NaN
AT1G60140	TPS10 classII trehalose phosphate synthase 10	-	-	-	22	22	NaN	-	-	-	21	21	NaN
AT4G17770	TPS5 class II trehalose phosphatase/synthase 5	-	-	-	19	19	NaN	-	-	-	21	NaN	NaN
AT2G25560	DNAJ heat shock N-terminal domain-containing protein	-	-	-	-	-	-	NaN	NaN	23	NaN	NaN	NaN
AT2G37340	RSZ33 arginine/serine-rich zinc knuckle-containing protein 33	-	-	-	-	-	-	21	21	21	22	NaN	NaN
AT5G15210	HB30, ZHD8 homeobox protein 30	-	-	-	-	-	-	NaN	20	21	22	NaN	NaN
AT1G70770	Protein of unknown function DUF2359, transmembrane	-	-	-	-	-	-	20	20	19	NaN	21	NaN
AT4G15900	**NTC PRL1 | pleiotropic regulatory locus 1 PRL1**	30	29	34	20	24	33	26	25	33	26	25	36
AT1G09770	**NTC CDC5 (MOS4 PRL1 interactor) Cef1** cell division cycle 5	32	30	34	21	25	28	26	25	33	26	24	36
AT1G04510	**NTC PRP19A MOS4-associated complex 3A (MAC3A), PRP19A**	30	28	34	19	22	27	25	25	32	26	25	35
AT1G77180	**NTC subunit SKIP**	32	29	34	21	25	26	26	26	32	27	26	35
AT3G18165	**NTC MOS4, atSPF27 , SPF27, BCAS2, NTC25 modifier of snc1,4**	29	27	32	20	22	26	24	24	31	24	23	34
AT2G33340	**NTC PRP19b MOS4-associated complex 3A (MAC3B)**	31	29	34	-	-	-	26	26	33	27	27	36
AT5G28740	**NTC subunit SYF1 pre-mRNA-splicing factor**	29	27	33	-	-	-	24	23	32	26	25	35
AT5G41770	**NTC subunit atCRN1c putative crooked neck protein**	28	27	33	-	-	-	23	24	32	26	24	35
AT3G18790	**NTC atlsy1 pre-mRNA-splicing factor ISY1 , fSap33, NTC30**	29	27	32	-	-	-	24	22	31	23	19	34
AT2G36130	**NTR NTC-associated CyPL1a, CPR3a, PPIL1a, peptidyl-prolyl cis-trans isomer**	30	29	32	NaN	21	25	24	25	31	24	24	34
AT3G16650	**NTC PRL1 subunit paralog PRL2 Transducin/WD40 repeat-like superfamily pr**	26	23	30	NaN	NaN	27	NaN	NaN	28	NaN	NaN	25
AT2G38770	**NTR NTC-associated atAquarius EMB2765 fSAP164, KIAA0560**	29	27	34	-	-	-	25	25	33	27	27	36
AT1G10580	**NTR NTC-associated PRP17a pre-mRNA-processing factor 17**	30	27	33	-	-	-	25	25	32	25	24	35
AT3G13200	**NTR NTC-associated atAD-002 AD-002, CCAP2, CWC15 EMB2769**	32	31	33	-	-	-	25	25	32	25	25	34
AT1G07360	**NTR NTC-associated atECM2-1a pre-mRNA-splicing factor fSAP47, ECM2**	30	28	33	-	-	-	24	24	32	24	23	34
AT3G05070	**NTR NTC-associated cwf18 coiled-coil domain-containing protein 12**	30	30	32	-	-	-	24	22	30	24	24	33
AT4G21110	**NTR NTC-associated AtBud31 bud site selection protein 31, fSAP17, G10, Bud**	29	26	31	-	-	-	23	23	30	23	22	33
AT1G80930	**NTR NTC-associated pre-mRNA-splicing factor CWC22, nucampholin, KIAA16(**	27	26	31	-	-	-	23	23	30	26	25	32
AT2G29580	**NTR NTC-associated atECM2-1b zinc finger CCCH domain-protein 25, fSAP47**	25	21	28	-	-	-	NaN	17	28	16	15	30
AT1G25682	**NTR NTC-associated Yju2, CCDC130, Cwc16, coiled-coil domain-containing p**	22	22	27	-	-	-	NaN	NaN	26	NaN	NaN	29
AT1G32490	**NTR atPrp2-1a ESP3 ENHANCED SILENCING PHENOTYPE 3 DHX16 ESP3 | RN**	-	-	-				17	17	24	18	NaN	24
AT4G16680	**NTR tPrp2-2 putative RNA helicase P-loop containing nucleoside triphosphate**	-	-	-	-	-	-	NaN	NaN	22	NaN	NaN	26
AT1G80070	**U5 snRNP U5-220 kDa Prp8a, SUS2; ABNORMAL SUSPENSOR 2**	30	28	35	19	23	20	26	26	34	29	29	38
AT1G06220	**U5 snRNP U5-116 kDa MEE5, CLOTHO/GAMETOPHYTIC FACTOR**	33	28	34	-	-	-	28	27	33	28	28	36
AT2G43770	**U5 snRNP U5-40 kDa Prp8 binding WD40 protein**	31	29	33	-	-	-	25	25	32	25	24	35
AT1G20960	**U5 snRNP U5-200 kDa atU5-200-2a EMB1507**	29	26	34	-	-	-	27	26	32	29	29	34
AT5G25230	**U5 snRNP U5-116 kDa atU5-116-1b elongation factor EF-2**	27	25	30	-	-	-	23	22	29	24	23	31
AT3G49601	**U5 snRNP SUS2 interacting pre-mRNA-splicing factor**	-	-	-	-	-	-	18	18	29	20	20	30
AT1G13690	**Novel RRM RNA-binding domain coiled coil ATE1 | ATPase E1**	31	30	32	-	-	-	25	25	31	26	25	33
AT1G20580	**Sm core atSmD3-b Small nuclear ribonucleoprotein**	-	-	-	-	-	-	24	24	30	25	25	33
AT4G20440	**Sm core atSmB-b Small nuclear ribonucleoprotein**	-	-	-	-	-	-	23	23	30	26	24	33
AT3G62840	**Sm core atSmD2-b Small nuclear ribonucleoprotein**	-	-	-	-	-	-	23	24	30	25	25	32
AT4G02840	**Sm core atSmD1-b Small nuclear ribonucleoprotein**	-	-	-	-	-	-	25	24	29	25	26	32
AT4G30220	**Sm core subunit atSmF; small nuclear ribonucleoprotein F RUXF**	26	25	29	-	-	-	22	23	29	21	21	31
AT4G30330	**Sm core AtSmE-a Small nuclear ribonucleoprotein**	-	-	-	-	-	-	23	24	29	NaN	NaN	29
AT3G11500	**Sm core subunit atSmG-b Small nuclear ribonucleoprotein**	29	27	30	-	-	-	23	23	28	26	25	32
AT2G23930	**Sm core subunit atSmG-a, SNRNP-G**	23	23	23	-	-	-	20	19	28	19	19	30
AT1G76300	**Sm core subunit atSmD3-a Small nuclear ribonucleoprotein SmD3**	28	28	28	-	-	-	18	19	27	20	23	30
AT3G07590	**Sm core atSmD1-a Small nuclear ribonucleoprotein**	-	-	-	-	-	-	NaN	NaN	25	NaN	NaN	28
AT2G18740	**Sm core atSmE-b Small nuclear ribonucleoprotein**	-	-	-	-	-	-	-	-	-	25	24	32
AT3G07790	**C-complex associated protein DGCR14|**	27	25	29	-	-	-	15	12	29	18	NaN	31
AT4G18465	**C-complex associated ATP-dependent RNA helicase DDX35**	26	25	31	-	-	-	18	18	29	18	18	30
AT5G23080	**C-complex associated TOUGH (TGH) G patch protein 1 TGH, SWAP**	26	25	29	-	-	-	NaN	13	29	20	18	30
AT5G64270	**U2 snRNP SF3b155, SAP155 atSAP155 putative splicing factor |**	27	28	29	-	-	-	20	22	29	24	24	30
AT3G55220	**U2 snRNP atSAP130b Cleavage and polyadenylationfactor (CPSF) A**	-	-	-	-	-	-	25	25	29	23	23	30
AT4G21660	**U2 snRNP atSF3b150 splicing factor 3B subunit 2 proline-rich spliceosome-a**	-	-	-	-	-	-	21	22	27	24	22	29
AT5G12190	**U2 snRNP atP14-1 pre-mRNA branch site protein p14 (RRM/RBD/RNP motifs) p**	-	-	-	-	-	-	22	21	26	23	22	28
AT1G27650	**Splice site selection atU2AF35a/AUSa splicing factor U2af small subunit A**	-	-	-	-	-	-	-	-	-	22	22	28
AT5G06160	**U2 snRNP atSAP61 splicing factor 3A subunit 3; ATROPOS (ATO) ATO | splicir**	-	-	-	-	-	-	19	NaN	24	NaN	NaN	27
AT1G14650	**U2 snRNP atSAP114-1a splicing factor 3A subunit 1 SWAP (Suppressor-of-Wh**	-	-	-	-	-	-	19	17	26	20	NaN	27
AT2G18510	**U2 snRNP atSAP49a splicing factor 3B subunit 4, emb2444 emb2444**	-	-	-	NaN	18	NaN	-	-	-	19	19	28
AT4G14342	**U2 snRNP SF3b10a splicing factor 3B subunit 5**	-	-	-	-	-	-	NaN	19	26	22	20	26
AT2G32600	**U2 snRNP atSAP62 splicing factor 3A subunit 2**	-	-	-	-	-	-	16	19	25	21	19	27
AT5G42820	**Splice site selection U2 snRNP atU2AF35a/AUSa splicing factor U2af small su**	24	24	21	NaN	20	NaN	22	22	22	NaN	NaN	23
AT5G64730	**C-complex MORG1 WDR83| transducin/WD40 domain-containing protein**	23	20	26	-	-	-	NaN	17	27	20	NaN	27
AT3G63400	**C-complex PPIG cyclophilin-like peptidyl-prolyl cis-trans isomerase family pr**	-	-	-	-	-	-	NaN	18	25	23	24	28
AT4G02720	**C-complex human NKAP homolog**	25	24	25				NaN	NaN	22	NaN	NaN	24
AT4G02720	**C-complex human NKAP homolog**	25	24	25				NaN	NaN	22	NaN	NaN	24
AT3G20550	**RES complex DAWDLE; DDL SMAD/FHA domain-containing protein**	-	-	-	-	-	-	14	14	27	20	NaN	27
AT1G31870	**RES complex pre-mRNA-splicing factor CWC26**	-	-	-	-	-	-	18	18	26	21	20	28
AT3G47120	**RES complex interacting protein GDS1, GROWTH, DEVELOPMENT AND SPLIC**	23	21	24	-	-	-	NaN	17	26	NaN	NaN	26
AT3G62310	Disassembly factor atPrp43-2a ATP-dependent RNA helicase DHX15	-	-	-	-	-	-	-	-	-	17	20	28
AT1G24706	**TREX complex subunot THO2, AtTHO2**	24	25	25	-	-	-	NaN	NaN	19	20	19	27
AT5G42920	THO/TREX complex THO5, AtTHO5 | THO complex, subunit 5	-	-	-							NaN	NaN	24
AT1G04080	**U1 snRNP atPrp39a late flowering PRP39 | Tetratricopeptide repeat (TPR)-like**	-	-	-	-	-	-	-	-	-	NaN	16	28
AT4G32420	**U1 snRNP Cyclophilin-like peptidyl-prolyl cis-trans isomerase family protein**	-	-	-	-	-	-	18	17	24	21	22	27
AT4G36980	**CLK4-associating serine/arginine-rich protein**	-	-	-	NaN	NaN	27	NaN	NaN	NaN	NaN	NaN	31
AT3G49430	SRp34a| SER/ARG-richSR- protein 34A	-	-	-	-	-	-	23	23	27	26	25	29
AT2G29210	**SRm160 serine/arginine repetitive matrix protein 1 splicing factor**	-	-	-				17	NaN	24	NaN	NaN	24
AT3G26560	**2nd step factot Prp22-1 ATP-dependent RNA helicase DHX8**	-	-	-				NaN	NaN	23	NaN	NaN	25
AT2G06990	**Exosome HEN2 DExH-box RNA helicase**	21	21	NaN	-	-	-	NaN	20	21	20	22	28
AT1G15200	**EJC complex atPinin protein-protein interaction regulator family protein**	-	-	-	-	-	-	21	22	26	25	23	28
AT5G11200	**EJC complex atUAP56a DEAD-box ATP-dependent RNA helicase 56**	-	-	-	-	-	-	-	-	-	25	25	28
AT1G80670	**RNA export factor 1 RAE1 Transducin/WD40 repeat protein**	28	28	24	-	-	-	NaN	NaN	NaN	22	23	27
AT1G73720	**Bact complex Smu-1/fSAP57 SMU1 | transducin family protein / WD-40 repeat**	-	-	-	-	-	-	NaN	19	NaN	NaN	20	27
AT2G41500	U4/U6 snRNP atSAP60 LACHESIS (LIS); EMB2776 LIS, EMB2776 WD-40 repeat f	-	-	-	-	-	-				NaN	NaN	26
AT1G60170	U4/U6 snRNP U4/U6-61 kDa (Prp31p) emb1220 pre-mRNA processing ribonucleop	23	23	NaN							NaN	NaN	25
AT2G13540	CAP binding complex ENS, ABH1, CBP80, ATCBP80 | ARM repeat superfamily pro	-	-	-	-	-	-				NaN	NaN	26
AT3G09100	mRNA capping enzyme family protein CAP1A, RNGTT RNA guanylyltransferase and	-	-	-							NaN	NaN	24
AT3G06400	Spliceosome-asscociated CHR11, chromatin-remodeling protein 11 CHR11	26	28	29	-	-	-	25	25	26	26	27	30
AT5G13480	**Polyadenylation cleavage complex Flowering time control protein FY | Transc**	-	-	-	-	-	-	-	-	-	17	17	27
AT1G65440	GTB1 | global transcription factor group B1	23	25	25	-	-	-	-	-	-	20	20	29
AT2G17930	Human TRRAP jomolog of SAGA histone acetyltransferase (HAT) complex subunit	-	-	-	NaN	20	NaN	NaN	NaN	18	20	22	28
AT5G14170	CHC1 SWI/SNF chromatin remodeling complex BAF60A subunit	28	27	27	-	-	-	-	-	-	25	26	28
AT1G18450	SWI/SNF chromatin remodeling complex ARP4 actin-related protein 4	-	-	-	-	-	-	-	-	-	25	23	28
AT3G57300	SWI/SNF chromatin remodeling DNA helicase INO80	-	-	-	-	-	-	-	-	-	19	23	27
AT3G60830	SWI/SNF chromatin remodeling ATARP7, ARP7 | actin-related protein 7	-	-	-	-	-	-				21	19	26
AT5G44800	CHR4, PKR1 (PICKLE RELATED 1) SNF2 ATPase of SWI/SNF chromatiin remode	-	-	-	NaN	19	NaN	NaN	21	21	22	23	26
AT2G46020	SWI/SNF chromatin remodelling complex CHR2, ATBRM, BRM, CHA2 SNF2 ATPas	25	26	26	-	-	-	NaN	20	23	23	24	26

To test these conditions, we prepared four experiments. In the first and second experiments, the nuclear extracts were DNase/RNase treated for 2h at 4°C and at 37°C, respectively, followed by purification of AKIN10-GFP and SNF4-YFP baits using PRL1-GFP as nuclear control, in addition to the regular control extracts from wild type and YFP-HA expressing plants. In the third and fourth experiments, the nuclei were sonicated 10 and 4 times to reduce the size of nucleic acids and then treated with DNase and RNase during incubation of the samples with GFP-Trap for 2h at 4°C. Three biological repeats from all samples were analyzed by LC-MS/MS mass spectrometry (Table 4). As illustrated by arbitrary intensity values of detected peptide peaks in Table 4, in the first experiments no great difference was identified between the representations of bait-associated nuclear proteins compared to the internal nuclear protein control PRL1. This indicated that nuclease digestion at 4°C was not sufficient to disrupt large DNA/RNA associated complexes. The results suggest that AKIN10 and SNF4 are likely part of protein complexes that during transcription are associated through the undigested pre-mRNAs with the spliceosome and its activating NTC complex including PRL1. Therefore, the difference in the representation of AKIN10/SNF4 versus PRL1 associated proteins is maximum 8 to 16-fold, which excludes safe identification of their specific interacting partners.

Although recommended in several plant protocols, DNase/RNase digestion of nuclear extracts at 37°C in the second experiment efficiently disrupted the protein interactions. As in the first experiment, AKIN10 and SNF4 were only identified in core trimeric complexes with AKINβ1 and β2, and at much lower representation with AKINβ3. Compared to SNF4, AKIN11 was detected at much lower representation in the AKIN10-GFP pull-downs, indicating that the amount of dimeric (i.e., 2 x 3 hexameric) kinase complexes is lower in the nuclear samples compared to kinase forms detected in the total protein extracts. Nuclease digestion at 37°C also largely disrupted the activated spliceosome associated NTC complex. In the second experiment, therefore only the basic core of five closely associated PRL1-binding NTC proteins were identified.

Chromatin fragmentation to 2-3 nucleosome size by 10 x sonication did not improve the detection of AKIN10 and SNF4 interacting partners. By contrast, this protocol resulted in the identification of most components of so-called activated spliceosome C-complex, which contains the U5-snRNP-bound NTC, NTC-associated NTR (NTC-related), and Sm-core protein complexes identified in the crystal structure of spliceosome C-complex (Liu et al., 2017; Shi, 2017; Yan et al., 2017). Through the U5 snRNP, this megacomplex of over 50 proteins is bound to the U2 snRNP and other C-complex specific proteins, few of which are represented in the sample at lower peptide peak intensities.

Finally, reducing the number of sonication cycles to 4 further enhanced the detection of proteins, which are peripherally associated with the NTC-NTR-U5-snRNA complex, including more components of U2-snRNP, the TREX/THO mRNA export and RES (retention) complex. However, even under this gentle extraction condition, which proved to be ideal for identification of over 150 components of NTC-

associated large protein complex(es), no novel partners were detected with the AKIN10 and SNF4 baits. The reason to this failure is probably the implication of $(NH_4)_2SO_4$ in the extraction buffer, which likely interrupts those RNA polymerase II associated protein complexes, which are not kept tightly together by RNA-binding and U-snRNP interactions. This conclusion is supported by the fact that parallel purification of TFIIH kinases CDKF;1 and CDKD;2 also failed to result in pull-down of known TFIIH components, which were however detected by GFP-Trap affinity binding from $(NH_4)_2SO_4$-free total cell extracts. Consequently, the optimization of extraction of nuclear SnRK1 complexes has to be continued by returning to the use of alternative salt fractionation protocols.

3.4. Exploitation of analogue sensitive AS-AKIN10 for enrichment of SnRK1 substrates

The final goal of the present Ph.D. work was the use of analogue sensitive AS-AKIN10 kinase characterized in section 3.1, for enrichment of SnRK1 substrate proteins, which are specifically thiophosphorylated by the modified kinase using bulky N^6-substituted thioATP derivatives. When constructing and expressing the AS-AKIN10 kinase, which carries an M119G amino acid replacement in its ATP-binding pocket, we demonstrated that AS-AKIN10 can accept N^6-benzyl and phenyl thioATP analogues and catalyze efficient thiophosphorylation of SnRK1 substrate protein Trx-SPS-KD *in vitro*. To determine that AS-AKIN10 is also active with these bulky thioATP analogues *in vivo*, first total cell extracts were prepared from AKIN10-GFPPIPL and AS-AKIN10-GFPPIPL expressing homozygous T3 seedlings and used in phosphorylation assays (Figure 28A). Upon incubation with N^6-phenyl-thioATP and alkylation with PNBM, only few, likely Cys-rich proteins were detected in total protein extract from AKIN10-GFPPIPL expressing plants compared to AS-AKIN10-GFPPIPL containing extracts. One of the prominent proteins labelled in the latter extracts corresponded in molecular mass to the AS-AKIN10 kinase.

The same protein extracts were subjected to purification on GFP-Trap affinity resin, and then thiophosphorylation assays were performed with the bead-bound proteins followed by PNBM alkylation and western blotting with the anti-thioester antibody (Figure 28B). The background of PNBM-alkylated Cys-rich proteins detected in the total protein extract was largely reduced resulting in barely any detectable thiophosphorylation with GFP-Trap purified AKIN10. By contrast, several prominent thiophosphorylated proteins, including one with the same molecular mass as the GFPPIPL-tagged kinase, were detected in the GFP-Trap purified AS-AKIN10 complex. This suggested that in addition to autophosphorylation, the AS-AKIN10 kinase mediated thiophosphorylation of several proteins with N^6-phenyl-thioATP, which were bound to the GFP-Trap beads in association with the kinase. Western blotting of proteins eluted from the GFP-Trap with anti-GFP antibody indeed confirmed that the prominent thiophosphorylated protein of about 98 kDa indeed corresponded to the purified kinase (Figure 28C).

To demonstrate that the wild type AKIN10-GFPPIPL kinase detected by western blotting was also active when bound to GFP-Trap, kinase reactions were performed with both thioATP and bulky N^6-phenyl-thioATP (Figure 28D). These kinase assays demonstrated that the GFP-Trap bound purified AKIN10-GFPPIPL kinase thiophosphorylated the same associated proteins with unmodified thioATP as the analog-sensitive AS-AKIN10 kinase version with N^6-phenyl-thioATP, but the wild type kinase had greatly reduced activity with the latter bulky ATP derivative. Finally, the GFP-Trap purified kinases were demonstrated to thiophosphorylate the SnRK1 kinase substrate Trx-SPS-KD indicating that the bead-bound kinases can also be used for testing specific phosphorylation of candidate substrates (Figure 28 E).

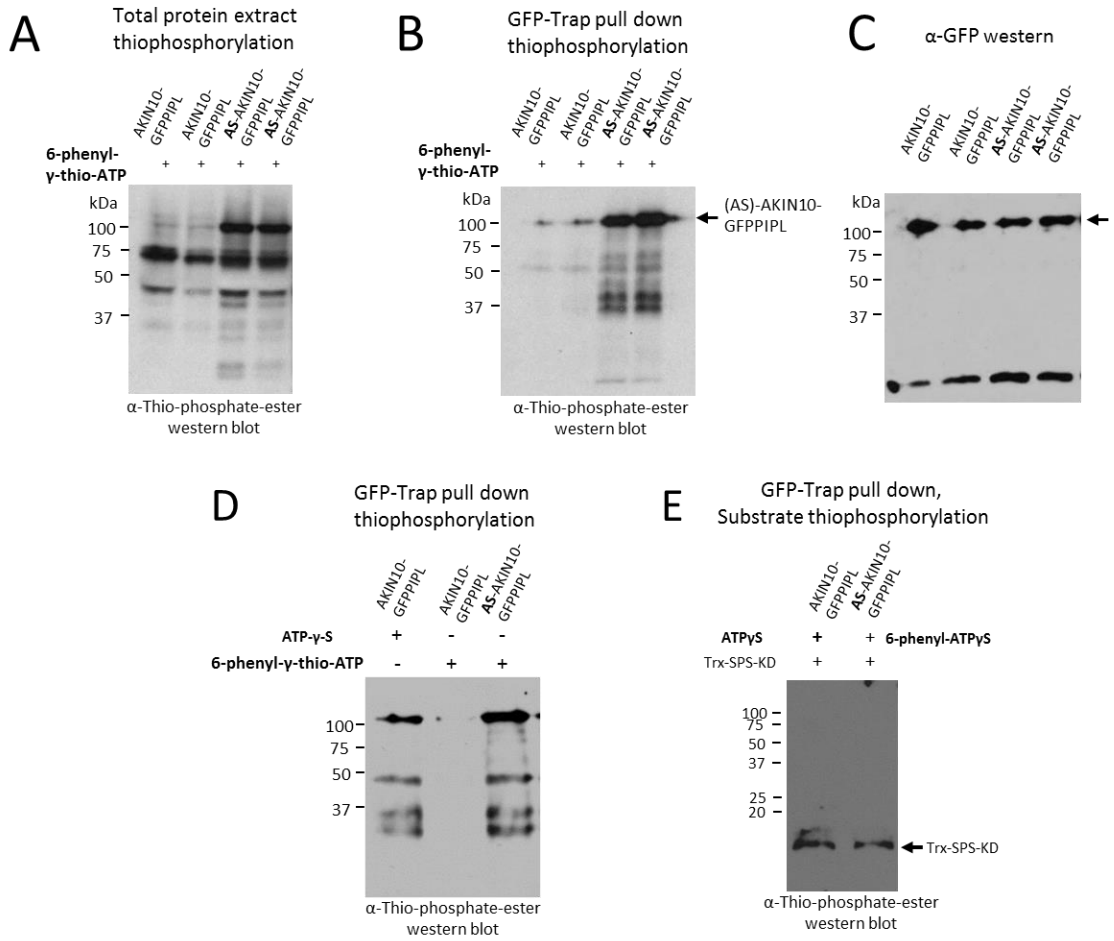

Figure 28. Thiophoshorylation of substrates in total cell extracts and upon GFP-Trap purification of kinase associated proteins with wild type and analog-sensitive AKIN10 kinases.
A) Total protein extracts prepared from 3-weeks-old seedlings expressing AKIN10-GFPPIPL and AS-AKIN10-GFPPIPL were supplemented with 0.5mM N^6-phenyl-γthioATP, incubated for 2h at room temperature, alkylated with PNBM, separated with SDS-PAGE, and subjected to wester blotting with anti-thioester antibody to detect thiophosphorylated substrate proteins. **B)** GFPPIPL tagged AKIN10 and AS-AKIN10 were purified on GFP-Trap and subjected to self-thiophosphorylation as described above. **C)** Western blotting of samples shown in B with anti-GFP antibody. **D)** Comparison of patterns of proteins, which are thiophosphorylated in GFP-Trap purified AKIN10 complexes using unmodified thioATP and by AS-AKIN10 using 6-phenyl-thioATP. **E)** Kinase assays demonstrate thiophosphorylation of SnRK1 substrate Trx-SPS-KD by AKIN10 and AS-AKIN10 using thioATP and 6-phenyl-thioATP, respectively.

As we had no information on nuclear uptake of bulky thioATP-derivatives and could not determine this in the absence of available ^{32}P-labelled compounds, two different strategies were tested for performing *in situ* thiophosphorylation reactions with cell nuclei isolated from AS-AKIN10-GFPPIPL expressing plants. In the first approach (Figure 29, protocol A), purified nuclei were resuspended in nuclear lysis buffer NLBB, sonicated and then dialysed against kinase buffer prior performing kinase reactions. In the second approach, isolated nuclei were directly resuspended in kinase buffer and supplemented with thioATP or N^6-phenyl-thioATP for AS-AKIN10, to perform *in situ* kinase reactions with intact but swelling nuclei. After the kinase reactions, the nuclei were sonicated and lysed, and the thiophosphorylated kinase substrates were alkylated with PNBM as in protocol A. As illustrated by Figure 29, kinase reactions with nuclear lysates containing AKIN10-GFPPIPL and unmodified thioATP, as well as AS-AKIN10-GFPPIPL and N^6-phenyl-thioATP, provided a higher yield of PNBM alkylated substrates in protocol A, compared to *in situ* phosphorylation reactions with intact nuclei in protocol B. In addition, background thiophosphorylation by the wild type AKIN10 kinase with N^6-phenyl-thioATP appeared to be lower in protocol A compared to B.

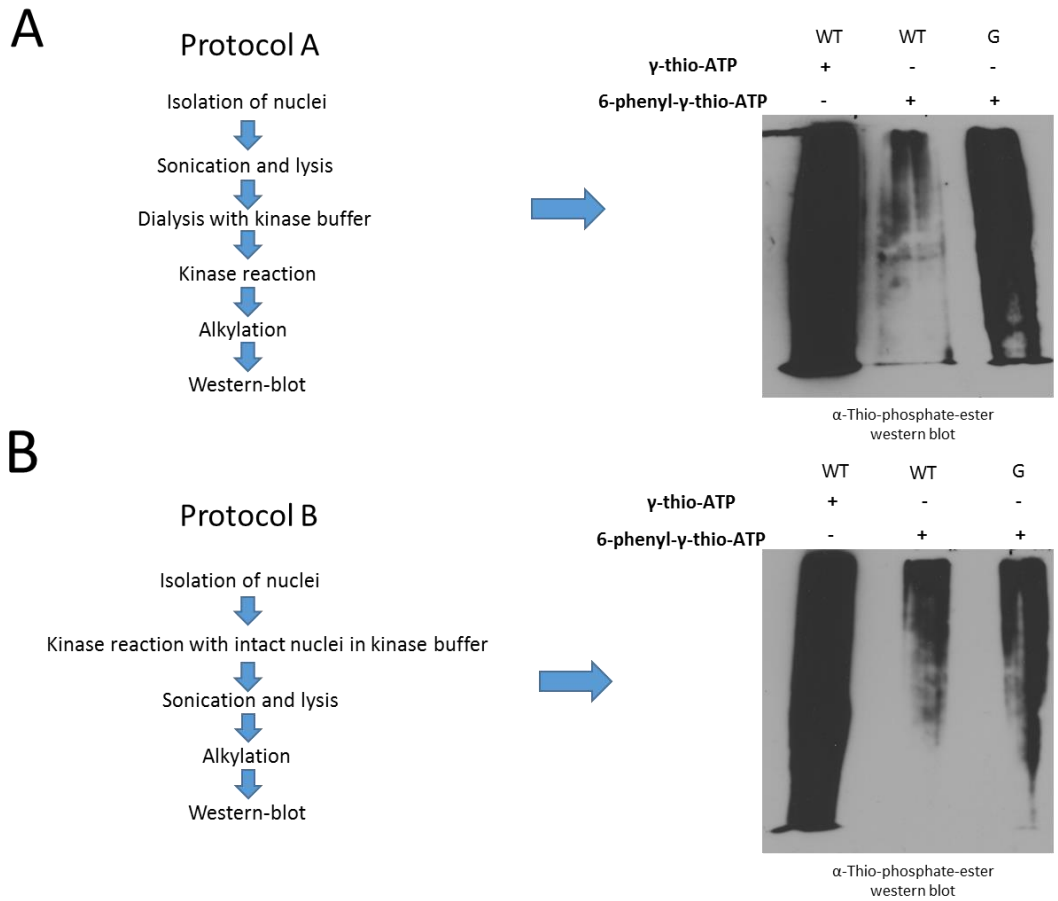

Figure 29. Comparison of efficiencies of thiophosphorylation reactions using nuclear lysates and intact nuclei.
A) In protocol A, isolated nuclei were first sonicated and lysed in nuclear lysis buffer NLB, and then the lysate was dialyzed against kinase buffer before performing thiophosphorylation with AKIN10 using ATPγS and N^6-phenyl-thioATP, and with AS-AKIN10 using N^6-phenyl-thioATP. The samples were then alkylated by PNBM,

separated by SDS-PAGE, and thiophosphorylated proteins were detected by western blotting with anti-thioester antibody. **B)** In protocol B, intact nuclei prepared from AKIN10 and AS-AKIN10 expressing plants were incubated with ATPγS and N^6-phenyl-thioATP as described in A) and after this *in situ* thiophoshorylation step the nuclear samples were sonicated and lysed, alkylated and subjected to western blot detection of kinase substrate proteins.

3.4.1. Iodoacetyl-agarose enrichment and mass spectrometry analysis of peptides thiophosphorylated by AS-AKIN10 using N^6-phenyl-thioATP

To identify substrates specifically thiophosphorylated by AS-AKIN10, proteins from the kinase assays were digested by trypsin, desalted and covalently bound to iodoacetyl-agarose (SulfoLink™ Coupling Resin) as described by Hertz et al. (2010). The matrix-bound peptides were released by specific cleavage of the PO_3-S bond by oxone, desalted and analysed by LS-MS/MS mass spectrometry. As control, nuclear extracts from wild type and AKIN10 expressing plants were similarly subjected to thiophosphorylation with N^6-phenyl-thioATP and processed. As control for Sulfolink-binding of thiophosphorylated peptides and subsequent recovery of phosphopeptides, to each sample 5 to 10 µg of AKIN10 thiophosphorylated SAMS peptide was added as spike after performing the kinase reactions and prior trypsin digestion. Detection of the SAMS peptide by mass spectrometry thus provided an internal control for the enrichment procedure. So far, 3 independent small scale peptide enrichment experiments were performed. The identified AS-AKIN10 phosphorylated peptides, which were absent from the control samples, are listed in Table 5.

Table 5. The list of candidate AS-AKIN10 substrates based on enrichment of peptides thiophosphorylated with N^6-phenyl-thioATP in nuclear extracts.
Proteins with confirmed nuclear localization are highlighted in bold letters.

Experient 1		
TAIR ID	**Gene**	**Phospho (STY) Probabilities**
AT3G57150	**NAP57, CBF5, DYSKERIN pseudouridine synthase**	**RPPLIS(1)AVKRQLRIR**
AT3G57150	**NAP57, CBF5, DYSKERIN pseudouridine synthase**	**RALESLT(1)GAVFQR**
AT3G09480	**Histone H2B.5**	**REIQT(1)AVRLVLP**
AT5G51280	**DEAD-box ATP-dependent RNA helicase 35, ABSTRAKT, Dbp2p, DDX41, Spliceosome complex C**	**EPLLTGWKPPLHIR**
AT4G23640	ATKT3, KUP4, TINY ROOT HAIR 1, TRH1 Potassium transporter PM	**LSRSIS(1)EANIAGS**
AT1G68260	ACYL-LIPID THIOESTERASE 3, ALT3 chloroplast	**WRRPLS(1)IPLRS(1)VKTFKP**
AT4G36440	unknown transmembrane protein ER/PM	**RVFKGFT(1)VGLHPR**
Experiment 2		
AT1G03110	**TRM82 WD40 repeat-like superfamily protein, tRNA MODIFICATION 82**	**LFVS(1)AGDDKLVK**
AT1G61730	**DNA-binding storekeeper protein-related transcriptional regulator**	**IKS(0.982)PS(0.014)AT(0.002)T(0.002)AAAPPAK**
AT1G70770	Unknown DUF2359 domain transmembrane protein	**MTAIDS(1)DDDGVVR**
AT1G80930	**NTC-associated NTR protein KIAA1606 (fSAPb) pre-mRNA-splicing factor CWC22**	**VIADKPS(1)DEEDDRQR**
AT3G28920	**Homeobox protein 34 AtHB34; ZHD9; ZINC FINGER HOMEODOMAIN 9**	**SMDMT(0.047)PKS(0.949)PEPES(0.003)ET(0.001)PT(0.001)R**
AT4G20520	RNA-directed DNA polymerase	**RS(1)ALDKMAELVQK**
AT5G08130	**BIM1 basic helix-loop-helix (bHLH) DNA-binding superfamily BHLH46**	**FQMLRQLIPNS(1)DQKR**
AT5G08180	**NHP2 ribonucleoprotein DKCB2; NHP2P; NOLA2**	**GS(0.981)DT(0.019)EAEKSIQKEK**
AT5G24740	SHORT-ROOT interacting VSP13 vacuolar protein sorting-associated protein SHRUBBY Protein (DUF1162)	**IMS(0.021)IDVGILS(0.979)DK**
AT5G39570	Phosphatidic acid-binding PLD REGULATED PROTEIN1, PLDRP1	**SES(0.003)EY(0.004)ERKPS(0.968)Y(0.025)GR**
AT5G45210	Disease resistance protein (TIR-NBS-LRR class)	**LMDVS(1)KK**
AT5G52040	**HYL1-binding spliceosome RS41 protein arginine/serine-rich splicing factor 41; At-RS41 involved in miRNA biogenesis**	**VAS(1)PENGAVRNRS(1)PR**
Experiment 3		
AT4G19500	WRKY19 interacting nucleoside-triphosphatase/transmembrane receptor/nucleotide binding/ATP binding protein	**VLDLGAVEQS(1)LMHKK**
AT2G28780	P-hydroxybenzoic acid efflux pump subunit, miR395 target	**IGKET(1)REIEEMVK**
AT5G40360	**MYB115 myb domain protein 115 TF regulator of vegetative to embryonic transition and benzoyloxy glucosinolate synthesis**	**S(0.001)ENIVKNHWNAT(0.999)K**
AT2G13370	**CHR5 chromatin remodeling 5, Arabidopsis homolog of human CHD2 SNF2 ATPase of SWI/SNF chromatin remodeling complex**	**GFQFQRLDGS(0.5)T(0.5)K**
Control		
SAMS_peptide	Known substrate peptide of AMPK	**RSAMSGLHLVKRR**

The short list of candidate AS-AKIN10 substrates in the first experiment included three proteins with known nuclear localization. NAP57, named also CBF5 or DYSKERIN is a pseudouridine synthase, which interacts in Cajal bodies and nucleoli with the H/ACA snoRNP assembly factor NAF1 regulating ribosome biogenesis (Lermontova et al., 2007). Dyskerin also binds the H/ACA box of Arabidopsis telomerase RNA and interacts with AtPOT1a component of telomerase controlling telomere elongation. Therefore, null mutation of *NAP57* is lethal (Kannan et al., 2008). Histone H2B.5 is an Arabidopsis homolog of yeast histone H2B, which is involved in Sir4-mediated regulation of telomeric silencing in

response to DNA damage (Kyriss et al., 2010). Finally, Abstract is an activated spliceosome C-complex DDX41 helicase, which is involved also in the recognition of invading viral RNAs in human viral leukemia diseases. The majority of phosphorylation sites appeared to confirm the Rxxx(x)S/R consensus site suggested for mammalian AMPKs (Schaffer et al., 2015; Lin and Hardie, 2017) in the first experiment. For initial confirmation of phosphorylation of candidate substrates by AKIN10, NAP57 and the ACYL-LIPID THIOESTERASE 3, ALT3 proteins, which carried the RPPLIS and RRPLS AS-AKIN10 phosphorylated motives respectively were expressed in *E. coli* upon cloning their full-length coding sequences in the pET201 vector. ALT3 is annotated as potential chloroplast targeted protein, but it is likely located in the cytosole in Arabidopsis cells. The proteins fused to N-terminal thioredoxin and C-terminal His_6-tags were purified by Ni^{2+}-agarose chromatography and subjected to western blotting using an anti-His_6 antibody (Figure 30A). Although both proteins showed relative instability in *E. coli*, the production of full-length products with an expected molecular mass was achieved. NAP57 and ATR3 were then used as substrates with purified AKIN10 in kinase assays with (γ^{32}P) ATP (Figure 30B and C). Both proteins were effectively phosphorylated by AKIN10 *in vitro* indicating that they are indeed SnRK1 kinase substrates.

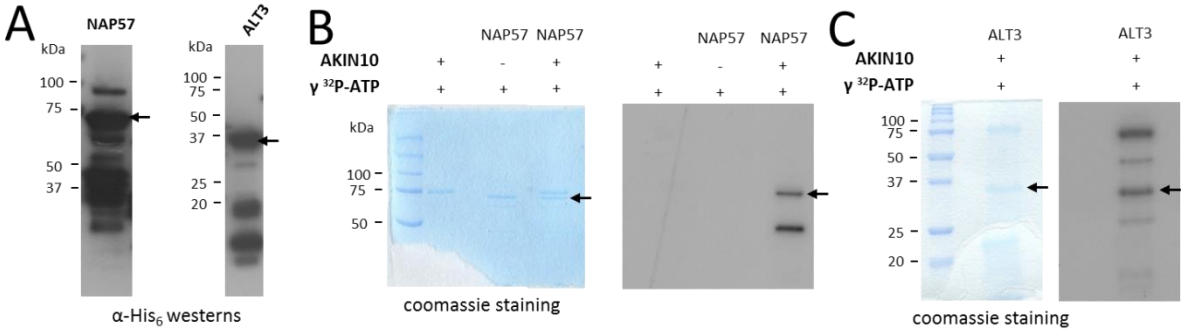

Figure 30. Confirmation of phosphorylation of identified candidate AS-AKIN10 substrates by wild type AKIN10 in kinase assays using (γ^{32}P)ATP.
A) NAP57 and ALT3 were expressed in *E. coli* by insertion of their coding sequences into pET201, purified by Ni^{2+}-agarose chromatography and subjected to western blotting with anti-His_6 antibody. **B)** Phosphorylation of NAP57 by AKIN10 in kinase assays with (γ^{32}P)ATP. Proteins in the kinase assays were separated by SDS-PAGE (Coomassie-stained gel is shown to the left), and then phosphorylated NAP57 was detected by autoradiography (to the right). **C)** Phosphorylation of ALT3 by AKIN10 in kinase assays with (γ^{32}P)ATP. Left: Coomassie-stained gel, right: autoradiography.

Further analysis of identified candidate AS-AKIN10 substrates could not be carried out in the time frame of this PhD study. The so far available list of candidate substrates contains several other proteins, which play essential functions in the regulation of chromatin remodeling (e.g. CHR5), developmental phase specific transcription (e.g. MYB115, Wang et al., 2009), brassinosteroid/UV-B signaling (e.g. BIM1, Liang et al., 2018), telomere length (TRM82) etc., which provide a good basis for follow up studies. Together with scaled-up enrichment of AS-AKIN10 substrates, future studies are expected to open a new avenue to uncovering yet unknown regulatory functions of SnRK1 in plants.

4. Discussion

Since the reference publication of Baena-González et al. (2007) describing transcription changes resulting from overexpression of the SnRK1α AKIN10/11 subunits in leaf protoplasts and stimulatory effects of co-expression of SnRK1α and S1-group of bZIP transcription factors on the expression of some dark-induced DIN genes it is accepted as general model that SnRK1 in plants is activated by darkness causing sugar starvation. However, the same report showed that inhibition of photosynthesis by DCMU (3-(3,4-dichlorophenyl)-1,1-dimethylurea) results in a fast increase of SnRK1 activity, which suggests that declining ATP production or redox signals might also contribute to SnRK1 activation, or that SnRK1 is required for safe-guarding the chloroplast function in leaves. The roles of AMP and ADP in the regulation of SnRK1 is still questionable as the activity of in vitro assembled trimeric SnRK1 complexes does not appear to be modulated by these compounds (Emanuelle et al., 2015), although AMP is reported to inhibit T-loop dephosphorylation of purified SnRK1 by a human PP2C phosphatase in vitro (Sugden et al., 1999a). Similarly to yeast Snf1 and human AMPKs, Arabidopsis SnRK1 was found to be phosphorylated on its activation T-loop by the SnAK1/GIRK2 and SnRK2/GIRK1 kinases that complement mutations of the yeast Snf1-activating kinases Pak1, Elm1 and Tos1 (Hey et al., 2007; Shen et al., 2009; Crozet et al., 2010; Robertlee et al., 2010). However, expression of SnAK1/2 kinases appears to be confined to the apical meristem (Shen et al., 2009) and it was thus questioned whether they are essential and sole activating kinases of SnRK1 in Arabidopsis (Crozet et al., 2014, Margalha et al., 2016). Recent reports indicate that the snak1snak2 double mutant is only viable in glucose-supplemented medium similarly to the snf1ab double mutant of Physcomitrella (Thelander et al., 2004) and shows largely reduced activating T-loop phosphorylation of SnRK1α1 subunit AKIN10 (Glab et al., 2017). However, it is still unknown whether expression of phosphomimicking version of SnRK1α subunits would rescue the growth defect of snak1snak2 double mutant or its lethality is independent of the failure of SnRK1 activation. In contrast to these results, Baena-González et al. (2007) found that viral siRNA silencing of the SnRK1α subunits results in seedling lethality, which cannot be compensated by glucose or sucrose feeding. Whereas the AMPK-activating kinase LKB is found in common complexes with AMPK (e.g., Zhang et al., 2017), in vivo interaction of SnAK1/2 with SnRK1 is not yet confirmed convincingly. SnAK1/2 were not detected either in any of our AKIN10 and SNF4 pull-down experiments by mass spectrometry. In all studies so far, SnAK1/2 were shown to mediate T-loop phosphorylation of monomeric SnRKα subunits in vitro. In comparison, association of mammalian AMPKα subunits with activating γ-subunits is essential for their T-loop phosphorylation by LKB, while the CAMKK2 kinase is found to phosphorylate monomeric AMPKα subunits (Woods et al., 2005).

4.1. Comparison of in vitro and in vivo activities of wild type, T-loop and ATP-binding pocket mutant versions of Arabidopsis SnRKα1/AKIN10

There are considerable contradictions in the literature concerning in vitro activities of SnRK1α subunits AKIN10/11 purified from E. coli. AKIN10 fused to an N-terminal His6-tag is reported to be

inactive in vitro unless its T-loop is phosphorylated by SnAK2/GIRK1 (Zhai et al., 2018). The same authors found that sugar feeding and T6P in vitro inhibits interaction of AKIN10 with GIRK1, and that T6P directly binds to AKIN10 and inhibits its activity. In our experiments, we purified the shorter isoform of AKIN10 encoded by the transcript isoform At3g01090.1 in fusion with N-terminal thioredoxin and C-terminal His6 tags. When tested in kinase assays with both (γ32P)ATP and ATPγS, purified AKIN10 was found to undergo autophosphorylation of its T-loop and phosphorylated the GRMRRISSVEMMDNW peptide of spinach sucrose-phosphate synthase (SPS) used by Bhalerao et al. (1999) as specific SnRK1 substrate. The SnRK1 phosphorylation motive of spinach SPS peptide is conserved in Arabidopsis SPS2F/A2 (GRMRRISSVEMMDNW), which is a candidate SnRK1 substrate. Large majority of eukaryotic protein kinases show similar autoactivation as through their catalytic domains are capable for dimerization, and in the dimeric stucture phosphorylate the T-loop of their partner (Beenstock et al., 2016). Probably this is the case for AKIN10 following purification from E. coli, although we did not test dimeric combinations of in vitro assembled wild type, T-loop and catalytically inactive mutant versions of AKIN10. Phosphorylation of the T-loop of purified SnRK1α subunits and SnRK1 complexes is detectable by a monoclonal anti-Thr172P AMPKα2 antibody developed for monitoring activating T-loop phosphorylation of human AMPKs (Sugden et al., 1999a). However, the backgound of phospho-T-loop antibodies is considerable when using total cell extracts, so application of proper controls, such as T-loop mutant kinase versions are necessary. Our data show that AKIN10 is autophosphorylated in vitro at three major positions, on its T-loop Thr175 and C-terminal Ser338/339 and Ser364 residues. Exchange of the T-loop Thr175 residue to Ala prevented T-loop phosphorylation but not autophosphorylation of C-terminal Ser residues suggesting that phosphorylation of the T-loop is not absolutely necessary for in vitro activity of purified AKIN10.

During initial characterization of SnRK1α subunits and their interacting partners, Farrás et al. (2001) reported that the α-subunits of Arabidopsis SnRK1 carry ubiquitin-associated UBA-domains between their catalytic and C-terminal regulatory domains. Similar UBA domains were subsequently identified in the α-subunits of mammalian AMPKs. By contrast, sequences of autoinhibitory domains (AIDs) are less conserved between plant SnRK1 and animal AMPK kinases. Recently, Emanuelle et al. (2018) reported that deletion of the UBA domain decreases SnAK/GIRK-mediated activation (i.e., T-loop phosphorylation) of SnRK1α subunits AKIN10/11, and also accelerates in vivo inactivation of phosphomimetic T-loop Thr175E version of AKIN10. Our data show that C-terminally truncated versions of AKIN10, lacking the UBA domain and carrying Thr175A, Thr175D and Thr175E amino acid exchanges show comparably higher activity compared to full-length versions of AKIN10 in vitro using the Trx-SPS-KD substrate. In support of the conclusion that in vitro autoactivation is due cross-phosphorylation of dimerized kinase subunits, we found that the M119G amino acid exchange in the ATP-binding pocket of AKIN10, which enables the kinase to use bulky N6-substituted thioATP derivatives, largely abolishes auto- and substrate phosphorylation activities of AKIN10 with unmodified ATP.

The T-loop and M119G mutant versions of AKIN10 tagged by a C-terminal HA-epitope were ectopically expressed from cDNA constructs by the CaMV35S promoter in transgenic plants. Following the purification of SnRK1 complexes using their HA-tagged AKIN10 subunits on anti-HA-agarose matrix, we found that T-loop phosphorylation of the M119G pocket mutant version of AKIN10 was similar to wild type AKIN10 in the isolated SnRK1 kinase complexes. This indicated that in contrast to the in vitro situation, in complex with other SnRK1 subunits the M119G analog-sensitive AS-AKIN10 kinase is similarly activated by T-loop phosphorylation as its unmodified version. HA-pulled-down SnRK1 complexes carrying the nonphosphorylatable Thr175A T-loop mutant version of AKIN10 showed about 30-40% lower substrate phosphorylation activity, whereas purified SnRK1 carrying the phosphomimetic Thr175D T-loop mutant version of AKIN10 displayed about 30-40% higher activity compared to wild type. The analysis of AKIN10 protein levels in these transgenic plants did not reveal remarkable overexpression of wild type and modified AKIN10 subunits. This indicated that AKIN10 overexpressed ectopically in transgenic plants might not increase considerably the total level of SnRK1 activity, possibly due to degradation of overexpressed kinase subunit in the absence of complex formation with other subunits. In the light of recent data from Emanuelle et al. (2018), it will be interesting to determine the in vivo effect of UBA domain deletion using wild type and T-loop mutant versions of C-terminally truncated AKIN10.

In all analyzed AKIN10-HA transgenic plants, we identified two isoforms of AKIN10 kinase, a full length and a shorter form carrying a deletion of 28 N-terminal amino acids, due to alternative splicing of AKIN10 pre-mRNA in the transcripts isoforms At3g01090.1 and 3. As the molecular mass of full-length AKIN10 was close to the same of ectopically expressed HA-tagged versions, we could not directly determine the ratio of resident wild type and HA-tagged modified AKIN10 kinases. Our data show that all three splicing isoforms of AKIN10 mRNA are expressed at similar level, so if translated similarly, the expected ratio of full-length and shorter protein isoforms should be about 1:2. Despite observing minor variations in the amounts of these two protein isoforms, our western blotting data failed to reveal overproduction of HA-AKIN10 having the same molecular mass as the full length isoforms. These results indicate that when using overexpression lines, it is absolutely necessary to confirm that overexpression of a kinase construct verified by transcript measurements indeed leads to an increase (or decrease, in case of inactive kinase versions) of in vivo SnRK1 activity.

Characterization of AKIN10-HA expressing transgenic plants has also led to two intriguing side observations. As several recent articles reported on the existance of an akin10 null mutation in the GABI_346E09 T-DNA insertion line (Mair et al., 2015; Nukarinen et al., 2016; Pedrotti et al., 2018), we intended to use this line as control to characterize the effects of ectopic expression of different versions of AKIN10-HA kinase in transgenic plants. By analysing the transcription of akin10 mutant allele in the GABI_346E09 mutant, however we found that the mutant gene is normally transcribed and thus probably results in the synthesis of a protein, in which 37 C-terminal amino acid codons of AKIN10

are replaced by 23 T-DNA-encoded codons. In collaboration with Dr. Ajit Ghosh, we have reconstructed the cDNA coding region of GABI akin10 mutant allele and expressed the corresponding protein in E. coli. Surprisingly, we found that in contrast to AKIN10 kinase derivatives used in our experiments, the GABI version of C-terminally truncated AKIN10 was not recognized in western blotting by the anti-AKIN10 antibody used in the previous reports to support the conclusion that the GABI_346E09 line carries an akin10 null mutation. As many important conclusions in the mentioned reports were based on differential phosphoproteome and gene expression data observed in the GABI mutant compared to wild type, it should be further investigated how the GABI mutation influences the stability and/or cellular localization of C-terminally truncated AKIN10 in vivo. In any case, our data indicate that the GABI mutation did not cause a gene knockout but could represent a partial loss of function mutation.

The second side product of qRT-PCR analysis of SnRK1 subunit mRNAs was the observation that transcription of the AKINβ1 and AKINβ3 subunit genes is increased during the dark period under short day condition suggesting that their transcription is regulated in a circadian fashion. Intriguingly, the amplitude of circadian change in AKINβ1 mRNA levels was largely reduced under long days, while cycling of AKINβ3 mRNA levels was less affected. The qRT-PCR measurements also revealed that AKINβ3 is expressed at the lowest levels among all SnRK1 subunit genes. In comparison to AKINβ1 and AKINβ3, circadian changes in the dark and light transcript levels were minimal in the case of SNF4 and barely detectable in case of AKIN10/11 and AKINβ2 genes.

Several recent reports implicated AKIN10 in the regulation of circadian clock suggesting that AKIN10 overexpression prolongs the clock light period and delays the peak of GI expression in the dark (Shin et al., 2017). In addition, activation of bZIP83 by AKIN10 overexpression was reported to stimulate expression of PPR7 (Frank et al., 2018) and thereby enhance stabilization of CO (Hayama et al., 2017) suggesting enhanced transition to flowering. However, most other reports claim that enhanced AKIN10 activity (i.e., due to lack of SnRK1 inhibitions by T6P) in the tsp1 mutant results in late flowering (Wahl et al., 2013). By contrast, Avonce et al. (2004) found that TPS1 overexpression causes late flowering and down-regulation of ABI4 in ABA signalling. Despite the fact that we failed to demonstrate overexpression of the AKIN10-HA constructs in our transgenic lines, we have examined their flowering time characteristics. In the initial test experiment, we found that wild type AKIN10-HA lines flower with 1 or 2 leaves more compared to wild type on long day, whereas Thr175D T-loop mutant AKIN10-HA expressing lines had 3 or 4 more leaves at the onset of flowering. However, lines carrying either unmodified or Thr175D T-loop mutant versions of AKIN10-HA flowered several days earlier than wild type under long day conditions. As these initial assays were performed only with 20 plants, we increased the sample size to 50 and 100 plants and repeated the flowering time measurements under both short and long days. The repeated experiments revealed no significant difference in flowering time between wild type and AKIN10 transgenic plants under long day, however, surprisingly showed that plants ectopically expressing AKIN10 carried about 10 leaves less, thus flowered earlier compared to

wild type during short day. These data appear to be consistent with those of Avonce et al. (2004). In accordance, ectopic expression of AKIN10 is found to increase ABA sensitivity in contrast to overexpression of TPS1 (see for reviews Crozet et al., 2014, Margalha et al., 2016).

In support of our conclusion that ectopic expression of AKIN10-HA derivatives did not result in dramatic alterations of AKIN10 kinase levels, we observed only slight differences in overall development of our transgenic plants. Lines expressing the phosphomimetic Thr175D T-loop mutant version of AKIN10-HA were found to show somewhat higher rate of root elongation. In the roots of these plants, we detected slightly altered pattern of auxin-induced DR5-GFP reporter, which extended into the central stele above the root meristem. At the same time, expression of PIN2-GFP auxin influx carrier was somewhat higher in the epidermal and cortex cells, and also extended into the endodermis layer suggesting enhanced acropetal auxin transport towards the root elongation zone. Whether these minor changes were indeed due to altered SnRK1 activity in the roots of Thr175D AKIN10 plants requires further confirmatory studies using locally inducible AKIN10 constructs.

4.2. Evidence for SnRK1 dimerization and occurrence in common complexes with class II trehalose synthase/phosphatase metabolic sensors

A major goal of our work was to use native gene constructs for expression and cellular localization SnRK1 subunits promoting further purification of SnRK1 complexes and analysis of their composition. Plants expressing AKIN-GFP and SNF4-YFP constructs were previously generated in our laboratory by Bitrián et al. (2011) using a BAC recombineering technology with galK selectable marker. We improved this recombineering technology by replacing galK with an antibiotic resistance (KmR) selectable marker gene, which was fused to an arabinose-inducible conditionally lethal ccdB gyrase inhibitor gene. The use of the KmR-araC-ccdB cassette did not only allow a much faster selection for modified BAC clones in E. coli, but also simple introduction of site-directed mutations, such as codon exchanges, into any position of target genes carried by BACs. To facilitate the purification of SnRK1 complexes from plants, we have used a new combined tag, which carried coding sequences of GFP, 38 His residues from the high affinity Co2+/Ni2+-binding domain of PIPL protein, two Streptactin-binding StrepII motives, and a HA-epitope tag. This combined GFPPIPL tag, as well as the GFP and PIPL tags alone, were introduced into the AKIN10 gene by replacing in frame of its stop codon. Subsequently, the M199G codon exchange was introduced by site-directed mutagenesis into AKIN10 to express a pocket mutant analog-sensitive AS-AKIN10 kinase in plants using Agrobacterium transformation after transferring the modified gene constructs into pGAP binary vectors Bitrián et al. (2011).

SnRK1 complexes were purified from protein extracts prepared from either shoot material of AKIN10-GFP, SNF4-YFP, AKIN10-GFPPIPL and AS-AKIN10-GFPPIPL expressing plants, which were grown in soil, or from whole seedlings, or roots cultured in in sterile growth media with 0.5% or 3% (i.e., in case of roots) sucrose by affinity capture on GFP-Trap resin. In 5 experiments, 3 biological replicates for each sample were then analyzed by LC-MS/MS mass spectrometry. Compilation of LC-

MS identified proteins found in association with at least 3 different baits revealed that AKIN10 and AS-AKIN10 interacted similarly with SNF4 (and vice versa) and all three AKINβ subunits, from which AKINβ3 was represented at the lowest abundance. Except the root sample, the second SnRK1α2 subunit AKIN11 was also surprisingly identified in all purified complexes of AKIN10 and SNF4 baits indicating dimer formation between the AKIN10 and AKIN11 containing SnRK1 complexes. This observation suggests that AKIN10 and AKIN11 could form a dimer also in vivo either by direct interaction between their catalytic domains or dimerization of the interacting SNF4 γ-activating subunit, as observed in yeast (Rudolph et al., 2007). Whether two different AKINβ subunits are found in these dimeric complexes or AKIN10/11 and SNF4 could form dimeric (i.e. 2x2) SnRK1 complexes also in their absence of the β-subunits remains to be determined by studying the composition of kinases isolated from the available akinβ1akinβ2 double mutant. In any case, detection of AKIN10 association with AKIN11 suggests that in the dimeric complex AKIN10 could activate AKIN11 by T-loop phosphorylation (and vica versa) even in the absence of an upstream activating kinase, which might explain the fact why no SnAK1/2 kinase was detected in any of the purified SnRK1 complexes. The fact that the GFP-Trap bound SnRK1 complexes were active in kinase assays with both (γ-32P)ATP and ATPγS demonstrates that the dimeric forms of SnRK1 complexes contain active kinases. The fact that the nuclear control PRL1 protein bait did not pull-down any of its known partners in these experiments suggests that the identified SnRK1 complexes are probably localized in the cytoplasm. This conclusion is supported at the meanwhile by co-localization of AKIN10-GFP and SNF4-YFP baits with mCherry tagged versions of their identified interacting partners.

As prominent interacting partners, class II trehalose synthase/phosphatases (TPS) were identified in the purified SnRK1 complexes. In this work, we provided evidence for that one of them, TPS8 tagged with mCherry co-immunoprecipitates with AKIN10-GFP when purified with RFP-Trap, and reciprocally AKIN10-GFP co-immunoprecipitates TPS8-mCherry when bound to GFP-Trap. At the meanwhile, similar data are available for all other members of class II TPS family from collaboration studies with Dr. Ajit Ghosh. Although the available LC-MS data are not quantitative, based on the intensities of detected peptide peaks it is estimated that each TPS protein might represent 0.1 to 2% of the amount of AKIN10 and SNF4 subunits in the purified SnRK1 complexes. Although class II TPS enzymes cannot complement the yeast Δtps1Δtpp mutation (Delorge et al., 2015), they carry conserved domains of TPS and TPP enzymes, and thus might interact with and sense TPS/TPP enzyme substrates, including UDP-glucose (UDP-Gluc), glucose-6-phosphate (Gluc-6-P) and trehalose-6-phosphate (T6P).

T6P was proposed to act as specific inhibitor of SnRK1 as metabolic signal of sucrose availability (Zhang et al., 2009; Lunn et al., 2014; Figueroa and Lunn, 2016). Therefore, we have tested whether the activity of TPS-associated SnRK1 complexes was affected by metabolites derived from sucrose. First, SnRK1 complexes were isolated using the AKIN10-GFPPIPL bait on GFP-Trap and kinase reactions were performed with resin bound protein complexes in the presence of UDP-Gluc,

Gluc-6-P and NAPDH. The reason to include NADPH in these assays was the observation indicating that TPS1 in the fungus Magnaporthe oryzae functions as redox sensor directly binding NADPH (Wilson et al., 2010). The results showed that UDP-Gluc (i.e., the degradation product of sucrose by sucrose synthase and a precursor of T6P) decreased by about 30-40% of purified SnRK1 activity in phosphorylation assays with the Trx-SPS-KD substrate. In a reciprocal pull-down experiment, the activity RFP-Trap purified TPS8-mCherry-associated kinase was assayed in the presence of T6P, including glucose, trehalose and glutathione as additional controls. In addition to UDP-Gluc, in these assays T6P was also found to inhibit Trx-SPS-KD phosphorylation by the TPS8mCherry-associated kinase. Next, we showed that increasing concentrations of UDP-Gluc and T6P in the range of 1 to 4 mM result in proportional, although not completely linear increase in the inhibition of the SnRK1 kinase. These results strongly suggest that the protein factors hypothesized by Zhang et al. (2009) and Emanuelle et al. (2015) to inhibit SnRK1 activity in T6P-dependent fashion correspond to members of the class II TPS family, which appear to confer inhibition of SnRK1 activity as metabolite sensors of UDP-Gluc and T6P. This conclusion is supported by parallel experiments of Dr. Ajit Ghosh using RFP-Trap purified TPS10-mCherry-associated kinase complexes, which lead to similar results as with TPS8. Further double affinity purification of AS-AKIN10-GFPPIPL complexes on anti-HA agarose or Ni2+-agarose followed by RFP-Trap pull-down of associated TPS-mCherry proteins and kinase assays with these complexes should further corroborate these observations.

In addition to class II TPS proteins, several other partners were identified in the SnRK1 complexes purified by the help of AKIN10GFP/PIPL and SNF4-YFP baits. These included several FCS-like zinc finger DUF581 domain proteins (Jamsheer and Laxmi, 2014) that were previously identified in yeast two-hybrid screens as AKIN10 interacting partners. In two-hybrid assays the DUF581 domain proteins interact with TCP transcription activators of sucrose-stimulated genes involved in ribosome biogenesis and DELLA repressors of gibberellin signaling (Nietzsche et al., 2014; 2016). However, none of these DUF581 protein interactors were observed in the purified SnRK1 complexes. At lower abundance, a two-hybrid interacting partner of SNF4, the HSPRO2 homolog of the sugar beet HS1 PRO-1 leucine-rich-repeat protein was however detected in both AKIN10 and SNF4 pull-downs. Thus, our mass spectrometry studies confirmed in vivo association of these factors with SnRK1 complexes in Arabidopsis.

We have performed extensive optimization of nuclear isolation and protein extraction protocols using the PRL1-GFP bait, a known subunit of nuclear spliceosome-activating NTC complex. In conclusion, it was found that inclusion of 1% Tritox X-100 detergent and 0.4M (NH4)2SO4 as chaotropic salt enhancing protein extraction is optimal for the isolation of nuclear PRL1-NTC complex, if the DNA was degraded by sonication to 2-3 or 6-8 nucleosome length prior affinity binding of proteins to GFP-Trap. DNase and RNase digestion at 4°C without sonication did not yield sufficient disruption of large nucleic acid-bound protein complexes, excluding conclusive identification of specific

interactors of AKIN10, SNF4 and PRL1. On the other hand, combined DNase and RNase digestion at 37°C lead to the destruction of otherwise remarkably stable PRL1-NTC complex. By performing 4 independent purification experiments with nuclear extracts prepared under these conditions, we could identify over 50 components of the core NTC and NTR (NTC-related) complexes bound to the U5-SnRNP particle. When fragmenting the DNA to 6-8 nucleosome followed by GFP-Trap binding and on-beads nuclease digestion, the size of isolated PRL1-NTC protein complex was considerable increased. This resulted in the identification of over 150 proteins, including more loosely associated components of co-transcriptionally formed spliceosome-NTC complexes, such as subunits of U2-snRNP, THO/TREX RNA exports and RES, transcription elongation PAF1 and SWI/SNF chromatin remodeling complexes. By contrast, under the conditions optimized for the isolation of the PRL1-NTC complex, only components of trimeric SnRK1 kinases were recovered by purification from nuclear extracts. In the nuclear AKIN10-GFP complexes, the proportion of associated AKIN11 subunit was lower compared to SnRK1 complexes purified from total cell extracts indicating lower abundance of dimeric SnRK1 complexes in nuclei. In conclusion, the results suggested that nuclear lysis and protein extraction using (NH4)2SO4 likely disrupts the chromatin associated SnRK1 complexes. Thus, successful isolation of nuclear SnRK1 complexes requires further optimization of the extraction protocol.

4.3. Identification of candidate SnRK1 substrates by enrichment of peptides thiohosphorylated in nuclei by the analog-sensitive AS-AKIN10 kinase

Another major goal of this Ph.D. study was the application and optimization of analog-sensitive kinase technology for identification of *in vivo* substrates of SnRK1. Towards this goal, we constructed an analog-sensitive version of AKIN10-GFPPIPL by replacing the gatekeeper M119 amino acid by Gly in the ATP-binding pocket by introducing a codon exchange into the corresponding gene using site-directed mutagenesis with BAC recombineering. The AS-AKIN10 kinase was initially expressed in *E. coli* and purified to optimize the thiophosphorylation kinase assays. We showed that the M119G mutation largely reduces the kinase activity with unmodified ATP, but allowes the kinase to use bulky N6-substituted thioATP derivatives, such as N6-benzyl and phenyl-thioATP.

Thiophosphorylated kinase substrates are detected by alkylation with PNBM (p-nitrobenzyl mesylate) followed by western blotting with a monoclonal antibody recognizing the PNBM alkylated thioester (Allen et al., 2005, 2007; Banko et al., 2011). Maximum alkylation with PNBM is achieved at pH 8.0. However, under this condition Cys-groups of proteins also react with PNBM. Consequently, Cys-rich contaminating proteins disturb the detection of thiophosphorylated kinase substrates by western blotting. At pH 4.0, PNBM reactivity with Cys-residues is largely reduced, but it still alkylates the phosphothiol groups of kinase substrates, although at considerable lower efficiency. While PNBM alkylation at pH 4.0 dramatically improves the specificity of detection of thiophosphorylated kinase substrates, under this condition the efficiency of enrichment of thiophosphorylated proteins by immunoprecipitation with the anti-thioester antibody is low. To overcome this problem,

thiophosphorylated peptides obtained by trypsin digestion of proteins after the kinase reaction are captured by covalent binding to iodoacetyl-agarose (Sulfolink) through an alkylation reaction. The iodoacetyl group also alkylates Cys-residues of peptides, which are therefore parallel bound to the matrix. However, in contrast to the S-S-bond of alkylated Cys residues, strong oxidizing agents, such as oxone specifically cleave the PO3-S bond resulting in a release of phosphopeptides (Hertz et al., 2010). This technology is widely applied for enrichment of AS-AMPK kinase substrates that are thiophosphorylated in cell extracts, permeabilized cells or cell nuclei in mammalian and human cell lines (see e.g., Schaffer et al., 2015).

In our experiments, we compared thiophosphorylation of proteins in nuclei, which were isolated from leaves of AS-AKIN10-GFPPIPL plants. The nuclei were purified with a protocol, which is compatible with performing subsequent nuclear run-on assays (Logemann et al., 1996; Németh et al., 1998). Thus, the thiophosporylation reactions were assayed in transcription competent nuclei. Compared to nuclear extracts, the efficiency of thiophosphorylation by incubating intact nuclei with N6-phenyl-thioATP was considerable lower. Therefore, for iodoacetyl-agarose enrichment of AS-AKIN10 thiophosphorylated nuclear proteins, we used sonicated nuclear extracts in three independent experiments followed by LC-MS mass spectrometry detection of phosphopeptides. The yield of these experiments was rather low indicating that further optimization of the protocol is necessary. Nevertheless, 22 thiophosphorylated peptides were detected, which identified 12 nuclear proteins as candidate SnRK1 substrates. In the first enrichment experiment (Table 4), all 6 detected thiophosphorylated peptides confirmed the (L)x(x)Rxx(x)S/T consensus suggested for phosphorylation site preference of human AMPKs (Hardie at al., 2016). Therefore, we arbitrarily chosen two of these candidate SnRK1 substrates and expressed the corresponding NAP57 (DYSKERIN pseudouridine synthase) and ATL3 (ACYL-LIPID THIOESTERASE 3) proteins in *E. coli*. Subsequent kinase assays with the purified proteins confirmed that both of them were efficiently phosphorylated by AKIN10 *in vitro*.

The list of identified candidate SnRK1 substrates includes three nuclear factors with known roles in the regulation of ribosome biogenesis and telomere length. NAP57 interacts with the POT1a component of telomerase controlling telomere elongation (Kannan et al., 2008). Histone H2B.5 is a homolog of yeast histone H2B, which is involved in the control telomeric silencing (Kyriss et al., 2010). Similarly to NAP57, NHP2 is also a component of telomerase and H/ACA snoRNP required for 18S rRNA production, rRNA pseudouridylation and telomere elongation, mutation of which in humans causes the premature ageing syndrome dyskeratosis congenital (Vulliamy et al., 2008). Three other candidate SnRK1 substrates represent spliceosome-associated proteins. ABSTRACT functions as helicase (Dbp2p, DDX41) in the activated spliceosome complex C, but is also required for ribosome assembly and immunity signaling (Jiang et al., 2017). The KIAA1606 (fSAPb) pre-mRNA-splicing factor CWC22 is a component of the PRL1-NTC complex (Deng et al., 2016), whereas RS41

(ARGININE/SERINE-RICH SPLICING FACTOR 41) interacts with FIERY2 RNA polymerase II CTD phosphatase and HYL1 proteins, and is involved in the control of microRNA biogenesis in Arabidopsis (Chen et al., 2013; 2015). Finally, the list of candidate nuclear SnRK1 partners includes the CHD5 Snf2-like chromodomain ATPase of SWI/SNF chromatin remodelling complex and three transcription factors. From the latter, AtHB34 (ZHD9; ZINC FINGER HOMEODOMAIN 9) is a homolog of Mediator-interacting ZHD1 transcription factor involved in osmotic stress and ABA signaling (Tran et al., 2007). The basic helix-loop-helix (bHLH) transcription factor BIM1 interacts with BES1 in brassinosteroid signaling to regulate transcription of genes by binding to E-box (CANNTG) promoter elements in concert with the UVR8 UV-B photoreceptor. BIM1 functions in the control of embryonic pattern formation, photomorphogenesis, root stele development, shade avoidance and other basic processes (Yin et al., 2005; Ohashi-Ito and Bergmann, 2007; Chandler et al., 2009; Cifuentes-Esquivel et al., 2013; Liang et al., 2018). Last but not least, Myb115 and its homolog MYB158 act as activators of BABY BOOM, LEAFY COTYLEDON1 (LEC1) inducing somatic embryogenesis from root cells (Wang et al., 2009). Further study of SnRK1 association of these nuclear factors and replacement of their observed thiophosphorylated sites with Ala and phosphomimetic D/E amino acid exchanges is required to confirm that they are genuine kinase substrates. This and additional scaled-up enrichment of thiophosphorylated AS-AKIN10 substrates and their similar analysis is expected to provide more insight into yet unknown regulatory functions of SnRK1.

5. Reference

Ahuatzi, D., Riera, A., Peláez, R., Herrero, P., and Moreno, F. (2007) Hxk2 regulates the phosphorylation state of Mig1 and therefore its nucleocytoplasmic distribution. J Biol Chem. 282, 4485-4493.

Alaimo, P.J., Shogren-Knaak, M.A., and Shokat, K.M. (2001) Chemical genetic approaches for the elucidation of signaling pathways. Curr Opin Chem Biol. 5, 360-367.

Alderson, A., Sabelli, P.A., Dickinson, J.R., Cole, D., Richardson, M., Kreis, M., Shewry, P.R., and Halford, N.G. (1991) Complementation of snf1, a mutation affecting global regulation of carbon metabolism in yeast, by a plant protein kinase cDNA. Proc Natl Acad Sci USA. 88, 8602-8605.

Alessi, D.R., Sakamoto, K., and Bayascas, J.R. (2006) LKB1-dependent signaling pathways. Annu Rev Biochem. 75, 137-163.

Allen, J.J., Lazerwith, S.E., and Shokat, K.M. (2005) Bio-orthogonal affinity purification of direct kinase substrates. J Am Chem Soc. 127, 5288-5289.

Allen, J.J., Li, M., Brinkworth, C.S., Paulson, J.L., Wang, D., Hübner ,A., Chou, W.H., Davis, R.J., Burlingame, A.L., Messing, R.O., Katayama, C.D., Hedrick, S.M., and Shokat, K.M. (2007) A semisynthetic epitope for kinase substrates. Nat Methods. 4, 511-516.

Alonso, R., Oñate-Sánehez, L., Weltmeier, F., Ehlert, A., Diaz, I., Dietrich, K., Vicente-Carbajosa, J., and Dröge-Laser, W. (2009). A pivotal role of the basic leucine zipper transcription factor bZIP53 in the regulation of Arabidopsis seed maturation gene expression based on heterodimerization and protein complex formation. Plant Cell. 21, 1747-1761.

Amodeo, G.A., Rudolph, M.J., and Tong. L. (2007) Crystal structure of the heterotrimer core of Saccharomyces cerevisiae AMPK homologue SNF1. Nature. 449, 492–495.

Ananieva, E.A., Gillaspy, G.E., Ely, A., Burnette, R.N., and Erickson, F.L. (2008). Interaction of the WD40 domain of a myoinositol polyphosphate 5-phosphatase with SnRK1 links inositol, sugar, and stress signaling. Plant Physiol.148, 1868–1882.

Arden, C., Hampson, L.J., Huang, G.C., Shaw, J.A., Aldibbiat, A., Holliman, G., Manas, D., Khan, S., Lange, A.J,, and Agius, L. (2008) A role for PFK-2/FBPase-2, as distinct from fructose 2,6-bisphosphate, in regulation of insulin secretion in pancreatic beta-cells. Biochem J. 411, 41-51.

Avila, J., Gregory, O.G., Su, D., Deeter, T.A., Chen, S., Silva-Sanchez, C., Xu, S., Martin, G.B., and Devarenne, T,P. (2012). The β-subunit of the SnRK1 complex is phosphorylated by the plant cell death suppressor Adi3. Plant Physiol. 159, 1277–1290.

Avonce, N., Leyman, B., Mascorro-Gallardo, J.O., Van Dijck, P., Thevelein, J.M., and Iturriaga, G. (2004) The Arabidopsis trehalose-6-P synthase AtTPS1 gene is a regulator of glucose, abscisic acid, and stress signaling. Plant Physiol. 136, 3649-3659.

Baena-González, E., Rolland, F., Thevelein, J.M., and Sheen, J. (2007) A central integrator of transcription networks in plant stress and energy signalling. Nature. 448, 938–942.

Balazadeh, S., Siddiqui, H., Allu, A.D., Matallana-Ramirez, L.P., Caldana, C., Mehrnia, M., Zanor, M.I., Köhler, B., and Mueller-Roeber, B. (2010) A gene regulatory network controlled by the NAC transcription factor ANAC092/AtNAC2/ORE1 during salt-promoted senescence. Plant J. 62, 250-264.

Barajas-Lopez, J.D., Moreno, J.R., Gamez-Arjona, F.M., Pardo, J.M., Punkkinen, M., Zhu, J.K., Quintero, F.J., and Fujii, H. (2018) Upstream kinases of plant SnRKs are involved in salt stress tolerance. Plant J. 93, 107-118.

Banko, M.R., Allen, J.J., Schaffer, B.E., Wilker, E.W., Tsou, P., White, J.L., Villén, J., Wang, B., Kim, S.R., Sakamoto, K., Gygi, S.P., Cantley, L.C., Yaffe, M.B., Shokat, K.M., and Brunet, A. (2011) Chemical genetic screen for AMPKα2 substrates uncovers a network of proteins involved in mitosis. Mol Cell. 44, 878-892.

Bechtold, N., Ellis, J., and Pelletier, G. (1993) In planta Agrobacterium-mediated gene transfer by infiltration of adult Arabidopsis thaliana plants. C R Acad Sci Paris, Life Sci. 316, 1194–1199.

Beczner, F., Dancs, G., Sós-Hegedűs, A., Antal, F., and Bánfalvi, Z. (2010). Interaction between SNF1-related kinases and a cytosolic pyruvate kinase of potato. J Plant Physiol. 167, 1046–1051.

Beenstock, J., Mooshayef, N., and Engelberg, D. (2016) How do protein kinases take a selfie (Autophosphorylate)? (2016) Trends Biochem Sci. 41, 938-953.

Benková, E., Michniewicz, M., Sauer, M., Teichmann, T., Seifertová, D., Jürgens, G., and Friml, J. (2003). Local, efflux-dependent auxin gradients as a common module for plant organ formation. Cell. 115, 591-602.

Bhalerao, R.P., Salchert, K., Bakó, L., Ökrész, L., Szabados, L., Muranaka, T., Machida, Y., Schell, J., and Koncz, C. (1999) Regulatory interaction of PRL1 WD protein with Arabidopsis SNF1-like protein kinases. Proc Natl Acad Sci USA. 96, 5322-5327.

Birnboim, H.C., and Doly, J. (1979) A rapid alkaline extraction procedure for screening recombinant plasmid DNA. Nucleic Acids Res. 7, 1513-1523.

Bitrián, M. (2009) Regulation of plant stress responses by AMP-activated protein kinases. PhD. Thesis, University Cologne.

Bitrián, M., Roodbarkelari, F., Horváth, M., and Koncz, C. (2011). BAC-recombineering for studying plant gene regulation: developmental control and cellular localization of SnRK1 kinase subunits. Plant J 65, 829-842.

Blazquez, M.A., Lagunas, R., Gancedo, C. and Gancedo, J.M. (1993) Trehalose-6-phosphate, a new regulator of yeast glycolysis that inhibits hexokinases. FEBS Lett 329, 51–54.

Blethrow, J.D., Glavy, J.S., Morgan, D.O., and Shokat, K.M. (2008). Covalent capture of kinase-specific phosphopeptides reveals Cdk1-cyclin B substrates. Proc Natl Acad Sci USA 105, 1442–1447.

Bonini, B.M., Van Dijck. P.and Thevelein, J.M. (2003) Uncoupling of the glucose growth defect and the deregulation of glycolysis in Saccharomyces cerevisiae Tps1 mutants expressing trehalose-6-phosphate-insensitive hexokinase from Schizosaccharomyces pombe. Biochim Biophys Acta. 1606, 83–93.

Bradford, M. M. (1976). A rapid and sensitive method for the quantitation of microgram quantities of protein utilizing the principle of protein-dye binding. Anal Biochem. 72, 248–254.

Broach, J.R. (2012) Nutritional control of growth and development in yeast. Genetics. 192, 73-105.

Broeckx, T., Hulsmans, S., and Rolland, F. (2016) The plant energy sensor: evolutionary conservation and divergence of SnRK1 structure, regulation, and function. J Exp Bot. 67, 6215-6252.

Bultot, L., Guigas, B., Von Wilamowitz-Moellendorff, A., Maisin, L., Vertommen, D., Hussain, N., Beullens, M., Guinovart, J.J., Foretz, M., Viollet, B., Sakamoto, K., Hue, L., and Rider, M.H. (2012) AMP-activated protein kinase phosphorylates and inactivates liver glycogen synthase. Biochem J. 443, 193-203.

Busti, S., Coccetti, P., Alberghina, L., and Vanoni, M. (2010) Glucose signaling-mediated coordination of cell growth and cell cycle in Saccharomyces cerevisiae. Sensors. 10, 6195-6240.

Cao, L., Tang, Y., Quan, Z., Zhang, Z., Oliver, S.G., and Zhang, N. (2016) Chronological lifespan in yeast is dependent on the accumulation of storage carbohydrates mediated by Yak1, Mck1 and Rim15 kinases. PLoS Genet. 12, e1006458.

Cantó, C., Gerhart-Hines, Z., Feige, J.N., Lagouge, M., Noriega, L., Milne, J.C., Elliott, P.J., Puigserver, P., and Auwerx, J. (2009). AMPK regulates energy expenditure by modulating NAD+ metabolism and SIRT1 activity. Nature. 458, 1056–1060.

Carling, D. (2004) The AMP-activated protein kinase cascade--a unifying system for energy control. Trends Biochem Sci. 29, 18-24.

Carling, D., Aguan, K., Woods, A., Verhoeven, A.J., Beri, R.K., Brennan, C.H., Sidebottom, C., Davison, M.D., and Scott. J. (1994) Mammalian AMP-activated protein kinase is homologous to yeast

and plant protein kinases involved in the regulation of carbon metabolism. J Biol Chem. 269, 11442-11448.

Carling, D., Mayer, F.V., Sanders, M.J., and Gamblin, S.J. (2011) AMP-activated protein kinase: nature's energy sensor. Nat Chem Biol. 7, 512-518.

Carlson, M. (1999) Glucose repression in yeast. Curr Opin Microbiol. 2, 202-207.

Carlson, S.M., and White, F.M. (2012) Labeling and identification of direct kinase substrates. Sci Signal. 5, pl3.

Carroll, B., and Dunlop, E.A. (2017) The lysosome: a crucial hub for AMPK and mTORC1 signalling. Biochem J. 474, 1453-1466.

Castermans, D., Somers, I., Kriel, J., Louwet, W., Wera, S., Versele, M., Janssens, V., and Thevelein, J.M. (2012) Glucose-induced posttranslational activation of protein phosphatases PP2A and PP1 in yeast. Cell Res. 22, 1058-1077.

Celenza, J.L., and Carlson, M. (1984) Cloning and genetic mapping of SNF1, a gene required for expression of glucose-repressible genes in Saccharomyces cerevisiae. Mol Cell Biol. 4, 49–53.

Chandler, J.W., Cole, M., Flier, A., and Werr, W. (2009) BIM1, a bHLH protein involved in brassinosteroid signalling, controls Arabidopsis embryonic patterning via interaction with DORNROSCHEN and DORNROSCHEN-LIKE. Plant Mol Biol. 69, 57-68.

Chang, A.C., and Cohen, S.N. (1978) Construction and characterization of amplifiable multicopy DNA cloning vehicles derived from the P15A cryptic miniplasmid. J Bacteriol. 134, 1141-1156.

Chary, S.N., Hicks, G.R., Choi, Y.G., Carter. D., and Raikhel, N.V. (2008) Trehalose-6-phosphate synthase/phosphatase regulates cell shape and plant architecture in Arabidopsis. Plant Physiol. 146, 97-107.

Chen, Q., Behar, K.L., Xu, T., Fan, C., and Haddad, G.G. (2003) Expression of Drosophila trehalose-phosphate synthase in HEK-293 cells increases hypoxia tolerance. J Biol Chem. 278, 49113-49118.

Chen, T., Cui, P., Chen, H., Ali, S., Zhang, S., and Xiong, L. (2013) A KH-domain RNA-binding protein interacts with FIERY2/CTD phosphatase-like 1 and splicing factors and is important for pre-mRNA splicing in Arabidopsis. PLoS Genet. 9, e1003875.

Chen, T., Cui, P., and Xiong, L. (2015). The RNA-binding protein HOS5 and serine/arginine-rich proteins RS40 and RS41 participate in miRNA biogenesis in Arabidopsis. Nucleic Acids Res. 43, 8283-8298.

Chen, L., Peng, Y., Tian, J., Wang, X., Kong, Z., Mao, T., Yuan, M., and Li, Y. (2016) TCS1, a microtubule-binding protein, interacts with KCBP/ZWICHEL to Regulate trichome cell shape in Arabidopsis thaliana. PLoS Genet. 12, e1006266.

Cheng, W.H., Endo, A., Zhou, L., Penney, J., Chen, H.C., Arroyo, A., Leon, P., Nambara, E., Asami, T., Seo, M., Koshiba, T., and Sheen. J. (2002) A unique short-chain dehydrogenase/reductase in Arabidopsis glucose signaling and abscisic acid biosynthesis and functions. Plant Cell. 14, 2723-2743.

Cherkasova, V., Qiu, H., and Hinnebusch, A.G. (2010) Snf1 promotes phosphorylation of the alpha subunit of eukaryotic translation initiation factor 2 by activating Gcn2 and inhibiting phosphatases Glc7 and Sit4. Mol Cell Biol. 30, 2862–2873.

Cho, Y.H., and Yoo, S.D. (2011) Signaling role of fructose mediated by FINS1/FBP in Arabidopsis thaliana. PLoS Genet. 7, e1001263.

Cho, H.Y., Wen, T.N., Wang, Y.T., and Shih. M.C. (2016). Quantitative phosphoproteomics of protein kinase SnRK1 regulated protein phosphorylation in Arabidopsis under submergence. J Exp Bot. 67, 2745–2760.

Cifuentes-Esquivel, N., Bou-Torrent, J., Galstyan, A., Gallemí, M., Sessa, G., Salla Martret. M,, Roig-Villanova. I,, Ruberti. I., an Martínez-García, J.F. (2013) The bHLH proteins BEE and BIM positively modulate the shade avoidance syndrome in Arabidopsis seedlings. Plant J. 75, 989-1002.

Clement, S.T., Dixit, G., and Dohlman, H.G. (2013) Regulation of yeast G protein signaling by the kinases that activate the AMPK homolog Snf1. Sci Signal. 6, ra78.

Clough, S.J., and Bent, A.F. (1998) Floral dip: a simplified method for Agrobacterium-mediated transformation of Arabidopsis thaliana. Plant J. 16, 735-743.

Cookson, S.J., Yadav, U.P., Klie, S., Morcuende, R., Usadel, B., Lunn, J.E., and Stitt, M. (2016). Temporal kinetics of the transcriptional response to carbon depletion and sucrose readdition in Arabidopsis seedlings. Plant Cell Environ. 39, 768–786.

Conrad, M., Schothorst, J., Kankipati, H.N., Van Zeebroeck, G., Rubio-Texeira, M., and Thevelein, J.M. (2014) Nutrient sensing and signaling in the yeast Saccharomyces cerevisiae. FEMS Microbiol Rev. 38, 254-299.

Cordero, M.D., and Violett, B. (eds). (2016) AMP-activated protein kinase. Springer, Experimentia Supplementum 107.

Coughlan, K.A., Valentine, R.J., Sudit, B.S., Allen, K., Dagon, Y., Kahn, B.B., Ruderman, N.B., and Saha, A.K. (2016). PKD1 inhibits AMPKα2 through phosphorylation of serine 491 and impairs insulin signaling in skeletal muscle cells. J Biol Chem. 291, 5664–5675.

Cox, J., and Mann, M. (2008). MaxQuant enables high peptide identification rates, individualized p.p.b.-range mass accuracies and proteome-wide protein quantification. Nat Biotechnol. 26, 1367-1372.

Craig, P.M., Moyes, C.D., and LeMoine, C.M.R. (2018) Sensing and responding to energetic stress: Evolution of the AMPK network. Comp Biochem Physiol B Biochem Mol Biol. 224, 156-169.

Crozet, P., Jammes, F., Valot, B., Ambard-Bretteville, F., Nessler, S., Hodges, M., Vidal, J., and Thomas, M. (2010). Cross-phosphorylation between Arabidopsis thaliana sucrose nonfermenting 1-related protein kinase 1 (AtSnRK1) and its activating kinase (AtSnAK) determines their catalytic activities. J Biol Chem. 285, 12071-12077.

Crozet, P., Margalha, L., Confraria, A., Rodrigues, A., Martinho, C., Adamo, M., Elias, C.A., and Baena-González. E. (2014) Mechanisms of regulation of SNF1/AMPK/SnRK1 protein kinases. Front Plant Sci. 5, 190.

Crozet, P., Margalha, L., Butowt, R., Fernandes, N., Elias, C.A., Orosa, B., Tomanov, K., Teige, M., Bachmair, A., Sadanandom, A., and Baena-González, E. (2016). SUMOylation represses SnRK1 signaling in Arabidopsis. Plant J. 85, 120-133.

Cullen, P.J., and Sprague, G.F. (2000). Glucose depletion causes haploid invasive growth in yeast. Proc Natl Acad Sci USA 97, 13619–13624.

Cutler, S.R., Rodriguez, P.L., Finkelstein, R.R., and Abrams, S.R. (2010). Abscisic acid: Emergence of a core signaling network. Annu Rev Plant Biol. 61, 651–679.

Czechowski, T., Stitt, M., Altmann, T., Udvardi, M.K., and Scheible, W.R. (2005) Genome-wide identification and testing of superior reference genes for transcript normalization in Arabidopsis. Plant Physiol. 139, 5-17.

Dasgupta, B., and Milbrandt, J. (2009). AMP-activated protein kinase phosphorylates retinoblastoma protein to control mammalian brain development. Dev. Cell 16, 256–270.

Datta, M., Kaushik, S., Jyoti, A., Mathur, N., Kothari, S.L., and Jain, A. (2018) SIZ1-mediated SUMOylation during phosphate homeostasis in plants: Looking beyond the tip of the iceberg. Semin Cell Dev Biol. 74, 123-132.

Davies, S.P., Carling, D., and Hardie, D.G. (1989). Tissue distribution of the AMP-activated protein kinase, and lack of activation by cyclic-AMP-dependent protein kinase, studied using a specific and sensitive peptide assay. Eur J Biochem. 186, 123-128.

Delorge, I., Figueroa, C.M., Feil, R., Lunn, J.E., and Van Dijck. P. (2015) Trehalose-6-phosphate synthase 1 is not the only active TPS in Arabidopsis thaliana. Biochem J. 466, 283-290.

Deng, X., Lu, T., Wang, L., Gu, L., Sun, J., Kong, X., Liu, C., and Cao, X. (2016) Recruitment of the NineTeen Complex to the activated spliceosome requires AtPRMT5. Proc Natl Acad Sci USA. 113, 5447-5552.

DeRan, M., Yang, J., Shen, C.-H., Peters, E.C., Fitamant, J., Chan, P., Hsieh, M., Zhu, S., Asara, J.M., Zheng, B., Bardeesy, N., Liu, J., and Wu, X.. (2014). Energy stress regulates hippo-YAP signaling involving AMPK-mediated regulation of angiomotin-like 1 protein. Cell Rep. 9, 495–503.

Deroover, S., Ghillebert, R., Broeckx, T., Winderickx, J., and Rolland, F. (2016) Trehalose-6-phosphate synthesis controls yeast gluconeogenesis downstream and independent of SNF1. FEMS Yeast Res. 16, fow036.

Deutscher, J. (2008) The mechanisms of carbon catabolite repression in bacteria. Curr Opin Microbiol. 11, 87-93.

Dobrenel, T., Caldana, C., Hanson, J., Robaglia, C., Vincentz, M., Veit, B., and Meyer, C. (2016). TOR signaling and nutrient sensing. Annu Rev Plant Biol. 67, 261-285.

Dong, Z., Yu, Y., Li, S., Wang, J., Tang, S., and Huang, R. (2016) Abscisic acid antagonizes ethylene production through the ABI4-mediated transcriptional repression of ACS4 and ACS8 in Arabidopsis. Mol Plant. 9, 126-135.

Dower, W.J., Miller, J.F., and Ragsdale, C.W. (1988) High efficiency transformation of E. coli by high voltage electroporation. Nucleic Acids Res. 16, 6127-6145.

Dröge-Laser, W., and Weiste, C. (2018) The C/S1 bZIP network: A regulatory hub orchestrating plant energy homeostasis. Trends Plant Sci. 23, 422-433.

Dröge-Laser, W., Snoek, B.L., Snel, B., and Weiste, C. (2018) The Arabidopsis bZIP transcription factor family-an update. Curr Opin Plant Biol. 45, 36-49.

Eguchi, S., Oshiro, N., Miyamoto, T., Yoshino, K.I., Okamoto, S., Ono, T., Kikkawa, U., and Yonezawa, K. (2009). AMP-activated protein kinase phosphorylates glutamine: Fructose-6-phosphate amidotransferase 1 at Ser243 to modulate its enzymatic activity. Genes Cells. 14, 179–189.

Elrouby, N., and Coupland, G. (2010). Proteome wide screens for small ubiquitin like modifier (SUMO) substrates identify Arabidopsis proteins implicated in diverse biological processes. Proc Natl Acad Sci USA. 107, 17415–17420.

Emanuelle, S., Hossain, M.I., Moller, I.E., Pedersen, H.L., van de Meene, A.M., Doblin, M.S., Koay, A., Oakhill, J.S., Scott, J.W., Willats, W.G., Kemp, B.E., Bacic, A., Gooley, P.R., and Stapleton. D.I. (2015) SnRK1 from Arabidopsis thaliana is an atypical AMPK. Plant J. 82, 183-192.

Emanuelle, S., Doblin, M.S., Stapleton, D.I., Bacic, A., and Gooley, P.R. (2016) Molecular insights into the enigmatic metabolic regulator, SnRK1. Trends Plant Sci. 21, 341-353.

Emanuelle, S., Doblin, M.S., Gooley, P.R., and Gentry, M.S. (2018) The UBA domain of SnRK1 promotes activation and maintains catalytic activity. Biochem Biophys Res Commun. 497, 127-132.

Faller, W.J., Jackson, T.J., Knight, J.R.P., Ridgway, R.A., Jamieson, T., Karim, S.A., Jones, C., Radulescu, S., Huels, D.J., Myant, K.B., et al. (2015). mTORC1-mediated translational elongation limits intestinal tumour initiation and growth. Nature. 517, 497–500.

Farrás, R., Ferrando, A., Jásik, J., Kleinow, T., Ökrész, L., Tiburcio, A., Salchert, K., Del Pozo, C., Schell, J., and Koncz. C. (2001). SKP1–SnRK protein kinase interactions mediate proteasomal binding of a plant SCF ubiquitin ligase. EMBO J. 20, 2742–2756.

Feng, C.Z., Chen, Y., Wang, C., Kong, Y.H., Wu, W.H., and Chen, Y.F. (2014) Arabidopsis RAV1 transcription factor, phosphorylated by SnRK2 kinases, regulates the expression of ABI3, ABI4, and ABI5 during seed germination and early seedling development. Plant J. 80, 654-668.

Fernández-García, P., Peláez, R., Herrero, P., and Moreno, F. (2012) Phosphorylation of yeast hexokinase 2 regulates its nucleocytoplasmic shuttling. J Biol Chem. 287, 42151-42164.

Figueroa, C.M., and Lunn, J.E. (2016) A Tale of Two Sugars: Trehalose 6-Phosphate and Sucrose. Plant Physiol. 172, 7-27.

Flores-Pérez, U., Pérez-Gil, J., Closa, M., Wright, L.P., Botella-Pavía, P., Phillips, M.A., Ferrer, A., Gershenzon, J., and Rodríguez-Concepción. M. (2010) Pleiotropic regulatory locus 1 (PRL1) integrates the regulation of sugar responses with isoprenoid metabolism in Arabidopsis. Mol Plant. 3, 101-112.

François, J., and Parrou, J.L. (2001) Reserve carbohydrates metabolism in the yeast Saccharomyces cerevisiae. FEMS Microbiol Rev. 25, 125-145.

Foster, R., Gasch, A., Kay, S. And Chua, N.H. (1992) Analysis of protein/DNA interactions. In: Methods in Arabidopsis research. (eds. Koncz, C., Chua, N.-H. and Schell, J.), World Scientific, pp. 378-392.

Frank, A., Matiolli, C.C., Viana, A.J.C., Hearn, T.J., Kusakina, J., Belbin, F.E., Wells Newman. D., Yochikawa, A., Cano-Ramirez, D.L., Chembath, A., Cragg-Barber, K., Haydon, M.J., Hotta, C.T., Vincentz, M., Webb, A.A.R., and Dodd. A.N. (2018) Circadian entrainment in arabidopsis by the sugar-responsive transcription factor bZIP63. Curr Biol. 28, 2597-2606.

Fujii, H., Verslues, P.E., and Zhu, J.K. (2011) Arabidopsis decuple mutant reveals the importance of SnRK2 kinases in osmotic stress responses in vivo. Proc Natl Acad Sci USA. 108, 1717-2172.

Gao, X.Q., Liu, C.Z., Li, D.D., Zhao, T.T, Li, F., Jia, X.N., Zhao, X.Y., and Zhang, X.S. (2016) The Arabidopsis KINβγ subunit of the SnRK1 complex regulates pollen hydration on the stigma by mediating the level of reactive oxygen species in pollen. PLoS Genet. 12, e1006228.

Gancedo, J.M. (1998) Yeast carbon catabolite repression. Microbiol Mol Biol Rev. 62, 334-361.

Garapati, P., Feil, R., Lunn, J.E., Van Dijck, P., Balazadeh, S., and Mueller-Roeber, B.. (2015). Transcription factor Arabidopsis activating factor 1 integrates carbon starvation responses with trehalose metabolism. Plant Physiol. 169, 379-390.

Garcia, D., and Shaw, R.J. (2017) AMPK: Mechanisms of cellular energy sensing and restoration of metabolic balance. Mol Cell. 66, 789-800.

García-Salcedo, R., Lubitz, T., Beltran, G., Elbing, K., Tian, Y., Frey, S., Wolkenhauer, O., Krantz, M., Klipp, E., and Hohmann. S. (2014) Glucose de-repression by yeast AMP-activated protein kinase SNF1 is controlled via at least two independent steps. FEBS J.281, 1901-1917.

Gómez, L.D., Gilday, A., Feil, R., Lunn, J.E., and Graham, I.A. (2010) AtTPS1-mediated trehalose 6-phosphate synthesis is essential for embryogenic and vegetative growth and responsiveness to ABA in germinating seeds and stomatal guard cells. Plant J. 64, 1-13.

Gissot, L., Polge, C., Bouly, J.P., Lemaitre, T., Kreis, M., and Thomas, M. (2004) AKINbeta3, a plant specific SnRK1 protein, is lacking domains present in yeast and mammals non-catalytic beta-subunits. Plant Mol Biol. 56, 747-759.

Gissot, L., Polge, C., Jossier, M., Girin, T., Bouly, J.P., Kreis, M., and Thomas, M. (2006) AKINbetagamma contributes to SnRK1 heterotrimeric complexes and interacts with two proteins implicated in plant pathogen resistance through its KIS/GBD sequence. Plant Physiol. 142, 931-944.

Glab, N., Oury, C., Guérinier, T., Domenichini, S., Crozet, P., Thomas, M., Vidal, J., and Hodges, M. (2017) The impact of Arabidopsis thaliana SNF1-related-kinase 1 (SnRK1)-activating kinase 1 (SnAK1) and SnAK2 on SnRK1 phosphorylation status: characterization of a SnAK double mutant. Plant J. 89, 1031-1041.

Görke, B., and Stülke, J. (2008) Carbon catabolite repression in bacteria: many ways to make the most out of nutrients. Nat Rev Microbiol. 6, 613-624.

Granot, D., Kelly, G., Stein, O., and David-Schwartz, R. (2014) Substantial roles of hexokinase and fructokinase in the effects of sugars on plant physiology and development. J Exp Bot. 65, 809-819.

Greer, E.L., Oskoui, P.R., Banko, M.R., Maniar, J.M., Gygi, M.P., Gygi, S.P., and Brunet, A. (2007). The energy sensor AMP-activated protein kinase directly regulates the mammalian FOXO3 transcription factor. J Biol Chem. 282, 30107–30119.

Guigas, B., and Viollet B. (2016) Targeting AMPK: From ancient drugs to new small-molecule activators. EXS. 107, 327-350.

Guzmán, P., and Ecker, J.R. (1990) Exploiting the triple response of Arabidopsis to identify ethylene-related mutants. Plant Cell. 2, 513-523.

Gwinn, D.M., Shackelford, D.B., Egan, D.F., Mihaylova, M.M., Mery, A., Vasquez, D.S., Turk, B.E., and Shaw, R.J. (2008). AMPK phosphorylation of Raptor mediates a metabolic checkpoint. Mol Cell 30, 214-226.

Halford, N.G., Vicente-Carbajosa, J., Sabelli, P.A., Shewry, P.R., Hannappel, U., and Kreis, M. (1992) Molecular analyses of a barley multigene family homologous to the yeast protein kinase gene SNF1. Plant J. 2, 791-797.

Hao, L., Wang, H., Sunter, G., and Bisaro, D.M. (2003) Geminivirus AL2 and L2 proteins interact with and inactivate SNF1 kinase. Plant Cell. 15, 1034-1048.

Hayama, R., Sarid-Krebs, L., Richter, R., Fernández, V., Jang, S., and Coupland, G. (2017) PSEUDO RESPONSE REGULATORs stabilize CONSTANS protein to promote flowering in response to day length. EMBO J. 36, 904-918.

Hardie, D.G. (2004) The AMP-activated protein kinase pathway--new players upstream and downstream. J Cell Sci. 117, 5479-5487.

Hardie, D.G. (2007) AMP-activated/SNF1 protein kinases: conserved guardians of cellular energy. Nat Rev Mol Cell Biol. 8, 774-785.

Hardie, D.G. (2010). Hot stuff: thyroid hormones and AMPK. Cell Res. 20, 1282–1284.

Hardie, D.G. (2014). AMPK–sensing energy while talking to other signaling pathways. Cell Metab. 20, 939-952.

Hardie, D.G., and MacKintosh, R.W. (1992) AMP-activated protein kinase--an archetypal protein kinase cascade? Bioessays. 14, 699-704.

Hardie, D.G., and Carling, D. (1997) The AMP-activated protein kinase--fuel gauge of the mammalian cell? Eur J Biochem. 246, 259-273.

Hardie, D.G., Carling, D., and Carlson, M. (1998) The AMP-activated/SNF1 protein kinase subfamily: metabolic sensors of the eukaryotic cell? Annu Rev Biochem. 67, 821-855.

Hardie, D.G., Carling, D., and Gamblin, S.J. (2011) AMP-activated protein kinase: also regulated by ADP? Trends Biochem Sci. 36, 470-477.

Hardie, D.G., Schaffer, B.E., and Brunet, A. (2016) AMPK: An energy-sensing pathway with multiple inputs and outputs. Trends Cell Biol. 26, 190-201.

Hardin, S.C., Tang, G.Q., Scholz, A., Holtgraewe, D., Winter, H., and Huber, S.C. (2003). Phosphorylation of sucrose synthase at serine 170: Occurrence and possible role as a signal for proteolysis. Plant J. 35, 588-603.

Harthill, J.E., Meek, S.E., Morrice, N., Peggie, M.W., Borch, J., Wong, B.H., and Mackintosh, C. (2006) Phosphorylation and 14-3-3 binding of Arabidopsis trehalose-phosphate synthase 5 in response to 2-deoxyglucose. Plant J. 47, 211-223.

Hasenour, C.M., Berglund. E.D., and Wasserman. D.H. (2013) Emerging role of AMP-activated protein kinase in endocrine control of metabolism in the liver. Mol Cell Endocrinol. 366,152-1+62.

Hawley, S.A., Boudeau, J., Reid, J.L., Mustard, K.J., Udd, L., Mäkelä, T.P., Alessi, D.R., and Hardie D.G. (2003) Complexes between the LKB1 tumor suppressor, STRAD alpha/beta and MO25 alpha/beta are upstream kinases in the AMP-activated protein kinase cascade. J Biol. 2, 28.

Hawley, S.A., Pan, D.A., Mustard, K.J., Ross, L., Bain, J., Edelman, A.M., Frenguelli, B.G., and Hardie, D.G. (2005). Calmodulin-dependent protein kinase kinase-b is an alternative upstream kinase for AMP-activated protein kinase. Cell Metab. 2, 9–19.

Hawley, S.A., Ross, F.A., Chevtzoff, C., Green, K.A., Evans, A., Fogarty, S., Towler, M.C., Brown, L.J., Ogunbayo, O.A., Evans, A.M., and Hardie, D.G. (2010). Use of cells expressing gamma subunit variants to identify diverse mechanisms of AMPK activation. Cell Metab. 11, 554–565.

Hawley, S.A., Ross, F.A., Gowans, G.J., Tibarewal, P., Leslie, N.R., and Hardie, D.G. (2014). Phosphorylation by Akt within the ST loop of AMPK-a1 down-regulates its activation in tumour cells. Biochem J. 459, 275–287.

He, G., Zhang, Y.-W., Lee, J.-H., Zeng, S.X., Wang, Y.V., Luo, Z., Dong, X.C., Viollet, B., Wahl, G.M., and Lu, H. (2014). AMP-activated protein kinase induces p53 by phosphorylating MDMX and inhibiting its activity. Mol Cell Biol. 34, 148–157.

Heathcote, H.R., Mancini, S.J., Strembitska, A., Jamal, K., Reihill, J.A., Palmer, T.M., Gould, G.W., and Salt, I.P. (2016). Protein kinase C phosphorylates AMP-activated protein kinase α1 Ser487. Biochem. J. 473, 4681–4697.

Hedbacker, K., and Carlson, M. (2008) SNF1/AMPK pathways in yeast. Front Biosci. 13, 2408–2420.

Hedbacker, K., Hong, S.-P., and Carlson, M.(2004a).Pak1protein kinase regulates activation and nuclear localization of Snf1-Gal83protein kinase. Mol Cell Biol 24, 8255–8263.

Hedbacker, K., Townley, R., and Carlson, M. (2004b).Cyclic AMP-dependent protein kinase regulates the subcellular localization of Snf1-Sip1 protein kinase. Mol Cell Biol. 24, 1836-1843.

Henriques, R., Magyar, Z., Monardes, A., Khan, S., Zalejski, C., Orellana, J., Szabados, L., de la Torre, C., Koncz, C., and Bögre, L. (2010) Arabidopsis S6 kinase mutants display chromosome instability and altered RBR1-E2F pathway activity. EMBO J. 29, 2979-9293.

Hertz, N.T., Wang, B.T., Allen, J.J., Zhang, C., Dar, A.C., Burlingame, A.L., and Shokat, K.M. (2010) Chemical genetic approach for kinase-substrate mapping by covalent capture of thiophosphopeptides and analysis by mass spectrometry. Curr Protoc Chem Biol. 2, 15-36.

Hey, S., Mayerhofer, H., Halford, N.G., and Dickinson, J.R. (2007) DNA sequences from Arabidopsis, which encode protein kinases and function as upstream regulators of Snf1 in yeast. J Biol Chem. 282, 10472-10479.

Hey, S.J., Byrne, E., and Halford. N.G. (2010) The interface between metabolic and stress signalling. Ann Bot. 105, 197-203.

Hong, S. P., Leiper, F. C., Woods, A., Carling, D., and Carlson, M. (2003a) Activation of yeast Snf1 and mammalian AMP-activated protein kinase by upstream kinases. Proc Natl Acad Sci USA. 100, 8839-8843.

Hong, Y.H., Varanasi, U.S., Yang, W., and Leff, T. (2003b). AMP-activated protein kinase regulates HNF4alpha transcriptional activity by inhibiting dimer formation and decreasing protein stability. J Biol Chem. 278, 27495–27501.

Honigberg, S.M., and Lee, R.H. (1998). Snf1 kinase connects nutritional pathways controlling meiosis in Saccharomyces cerevisiae. Mol Cell Biol. 18, 4548–4555.

Hoppe, S., Bierhoff, H., Cado, I., Weber, A., Tiebe, M., Grummt, I., and Voit, R. (2009). AMP-activated protein kinase adapts rRNA synthesis to cellular energy supply. Proc Natl Acad Sci USA 106, 17781-17786.

Horman, S., Morel, N., Vertommen, D., Hussain, N., Neumann, D., Beauloye, C., El Najjar, N., Forcet, C., Viollet, B., Walsh, M.P., et al. (2008). AMP-activated protein kinase phosphorylates and desensitizes smooth muscle myosin light chain kinase. J. Biol. Chem. 283, 18505–18512.

Hrabak, E.M., Chan, C.W., Gribskov, M., Harper, J.F., Choi, J.H., Halford, N., Kudla, J., Luan, S., Nimmo, H.G., Sussman, M.R., Thomas, M., Walker-Simmons, K., Zhu, J.K., and Harmon, A.C. (2003).The Arabidopsis CDPK-SnRK superfamily of protein kinases. Plant Physiol. 132, 666–680.

Hulsmans, S., Rodriguez, M., De Coninck, B., and Rolland, F. (2016) The SnRK1 energy sensor in plant biotic interactions. Trends Plant Sci. 21, 648-661.

Hurley, R.L., Anderson, K.A., Franzone, J.M., Kemp, B.E., Means, A.R., and Witters, L.A. (2005). The Ca2+/calmodulin-dependent protein kinase kinases are AMP-activated protein kinase kinases. J. Biol. Chem. 280, 29060-29066.

Hurley, R.L., Barré, L.K., Wood, S.D., Anderson, K.A., Kemp, B.E., Means, A.R., and Witters, L.A. (2006). Regulation of AMP-activated protein kinase by multisite phosphorylation in response to agents that elevate cellular cAMP. J. Biol. Chem. 281, 36662–36672.

Iglesias-Fernández, R., Barrero-Sicilia, C., Carrillo-Barral ,N., Oñate-Sánchez, L., and Carbonero, P. (2013). Arabidopsis thaliana bZIP44: a transcription factor affecting seed germination and expression of the mannanase-encoding gene AtMAN7. Plant J. 74, 767-780.

Im, J.H., Cho, Y.H., Kim, G.D., Kang, G.H,, Hong, J.W., and Yoo, S.D. (2014). Inverse modulation of the energy sensor Snf1-related protein kinase 1 on hypoxia adaptation and salt stress tolerance in Arabidopsis thaliana. Plant Cell Environ. 37, 2303-2312.

Imamura, K., Ogura, T., Kishimoto, A., Kaminishi, M., and Esumi, H. (2001). Cell cycle regulation via p53 phosphorylation by a 50-AMP activated protein kinase activator, 5-aminoimidazole- 4-carboxamide-1-beta-D-ribofuranoside, in a human hepatocellular carcinoma cell line. Biochem Biophys Res Commun. 287, 562–567.

Inoki, K., Zhu, T., and Guan, K.L. (2003). TSC2 mediates cellular energy response to control cell growth and survival. Cell. 115, 577–590.

Jamsheer, M.K. and Laxmi, A. (2014) DUF581 is plant specific FCS-like zinc finger involved in protein-protein interaction. PLoS One. 9, e99074.

Jeong, E.Y., Seo, P.J., Woo, J.C. and Park, C.M. (2015). AKIN10 delays flowering by inactivating IDD8 transcription factor through protein phosphorylation in Arabidopsis. BMC Plant Biol. 15, 110.

Jäger, S., Handschin, C., St-Pierre, J., and Spiegelman, B.M. (2007). AMP-activated protein kinase (AMPK) action in skeletal muscle via direct phosphorylation of PGC-1alpha. Proc Natl Acad Sci USA 104, 12017-12022.

Jiang, R., and Carlson, M. (1996) Glucose regulates protein interactions within the yeast SNF1 protein kinase complex. Genes Dev. 10, 3105-3115.

Jiang, Y., Zhu, Y., Liu, Z.J., and Ouyang, S. (2017) The emerging roles of the DDX41 protein in immunity and diseases. Protein Cell. 8, 83-89.

Jones, R.G., Plas, D.R., Kubek, S., Buzzai, M., Mu, J., Xu, Y., Birnbaum, M.J., and Thompson, C.B. (2005). AMP-activated protein kinase induces a p53-dependent metabolic checkpoint. Mol Cell 18, 283–293.

Joo, M.S., Kim, W.D., Lee, K.Y., Kim, J.H., Koo, J.H., and Kim, S.G. (2016). AMPK facilitates nuclear accumulation of Nrf2 by phosphorylating at serine 550. Mol Cell Biol 36, 1931–1942.

Jossier, M., Bouly, J.-P., Meimoun, P., Arjmand, A., Lessard, P., Hawley, S., Hardie G. D., and Thomas, M. (2009) SnRK1 (SNF1-related kinase 1) has a central role in sugar and ABA signalling in Arabidopsis thaliana. Plant J 59, 316–328.

Ju, C., Yoon, G.M., Shemansky, J.M., Lin, D.Y., Ying, Z.I., Chang, J., Garrett, W.M., Kessenbrock, M., Groth, G., Tucker, M.L., Cooper, B., Kieber, J.J., and Chang, C. (2012) CTR1 phosphorylates the central regulator EIN2 to control ethylene hormone signaling from the ER membrane to the nucleus in Arabidopsis. Proc Natl Acad Sci USA. 109, 19486-19491.

Kang, S.G., Price, J., Lin, P.C., Hong, J.C., and Jang, J.C. (2010). The Arabidopsis bZIP1 transcription factor is involved in sugar signaling, protein networking, and DNA binding. Mol Plant. 3, 361-373.

Kannan, K., Nelson, A.D., and Shippen, D.E. (2008) Dyskerin is a component of the Arabidopsis telomerase RNP required for telomere maintenance. Mol Cell Biol. 28, 2332-2341.

Kawaguchi, T., Osatomi, K., Yamashita, H., Kabashima, T., and Uyeda, K. (2002). Mechanism for fatty acid ‘‘sparing’’ effect on glucose-induced transcription: regulation of carbohydrate-responsive element-binding protein by AMP-activated protein kinase. J Biol Chem. 277, 3829–3835.

Kayikci, Ö. and Nielsen, J. (2015) Glucose repression in Saccharomyces cerevisiae. FEMS Yeast Res. 15, fov068.

Kazan, K., and Manners, J.M. (2013). MYC2: the master in action. Mol Plant. 6, 686-703.

Kemp, B.E., Mitchelhill, K.I., Stapleton, D., Michell, B.J., Chen, Z.P., and Witters, L.A. (1999) Dealing with energy demand: the AMP-activated protein kinase. Trends Biochem Sci. 24, 22-5.

Kim, J., Kundu, M., Viollet, B., and Guan, K.-L. (2011). AMPK and mTOR regulate autophagy through direct phosphorylation of Ulk1. Nat Cell Biol. 13, 132–141.

Kim, J., Kim, Y.C., Fang, C., Russell, R.C., Kim, J.H., Fan, W., Liu, R., Zhong, Q., and Guan, K.-L. (2013). Differential regulation of distinct Vps34 complexes by AMPK in nutrient stress and autophagy. Cell. 152, 290–303.

Kim, G.D., Cho, Y.H., and Yoo, S,D. (2017) Regulatory functions of cellular energy sensor SNF1-related kinase1 for leaf senescence delay through ETHYLENE- INSENSITIVE3 repression. Sci Rep. 7, 3193.

Kleinow, T., Bhalerao, R., Breuer, F., Umeda, M., Salchert, K., and Koncz, C. (2000) Functional identification of an Arabidopsis snf4 ortholog by screening for heterologous multicopy suppressors of snf4 deficiency in yeast. Plant J. 23, 115-122.

Kleinow, T., Himbert, S., Krenz, B., Jeske, H., and Koncz, C. (2009). NAC domain transcription factor ATAF1 interacts with SNF1-related kinases and silencing of its subfamily causes severe developmental defects in Arabidopsis. Plant Sci. 177, 360–370.

Knupp, J., Martinez-Montañés, F., Van Den Bergh, F., Cottier, S., Schneiter, R., Beard, D., and Chang, A. (2017) Sphingolipid accumulation causes mitochondrial dysregulation and cell death. Cell Death Differ. 24, 2044-2053.

Koncz, C., and Schell, J. (1986). The promoter of TL-DNA gene 5 controls the tissue specific expression of chimaeric genes carried by a novel type of Agrobacterium binary vector. Mol Gen Genet 204, 383-396.

Koncz, C., and Rédei G.P. (1994) Genetic studies with Arabidopsis: A historical view. In: Arabidopsis. (Meyerowitz E.M., and Somerville, C.R., eds.), Cold Spring Harbor Laboratory Press.

Koncz, C., Martini, N., Szabados, L., Hrouda, M., Bachmair, A., and Schell, J. (1994) Specialized vectors for gene tagging and expression studies. In: Plant Molecular Biology Manual, Gelvin S and Schilperoort B (eds.), Kluwer Academic, Dordrect, B2, 1-22.

Koncz, C., Dejong, F., Villacorta, N., Szakonyi, D., and Koncz, Z. (2012) The spliceosome-activating complex: molecular mechanisms underlying the function of a pleiotropic regulator. Front Plant Sci. 3, 9.

Kong, L.J., and Hanley-Bowdoin, L. (2002) A geminivirus replication protein interacts with a protein kinase and a motor protein that display different expression patterns during plant development and infection. Plant Cell. 14, 1817-1832.

Koo, S.-H., Flechner, L., Qi, L., Zhang, X., Screaton, R.A., Jeffries, S., Hedrick, S., Xu, W., Boussouar, F., Brindle, P., Takemori, H., and Montminy, M. (2005). The CREB coactivator TORC2 is a key regulator of fasting glucose metabolism. Nature 437, 1109–1111.

Kulma, A., Villadsen, D., Campbell, D.G., Meek, S.E.M., Harthill, J.E., Nielsen, T.H., and MacKintosh, C. (2004). Phosphorylation and 14-3-3 binding of Arabidopsis 6-phosphofructo-2-kinase/ fructose-2,6-bisphosphatase. Plant J. 37, 654–667.

Kyriss, M.N., Jin, Y., Gallegos, I.J., Sanford, J.A., and Wyrick, J.J. (2010) Novel functional residues in the core domain of histone H2B regulate yeast gene expression and silencing and affect the response to DNA damage. Mol Cell Biol. 30, 3503-3518.

Laera, L., Guaragnella, N., Ždralević, M., Marzulli, D., Liu, Z., and Giannattasio, S. (2016) The transcription factors ADR1 or CAT8 are required for RTG pathway activation and evasion from yeast acetic acid-induced programmed cell death in raffinose. Microb Cell. 3, 621-631.

Lamia, K.A., Sachdeva, U.M., DiTacchio, L., Williams, E.C., Alvarez, J.G., Egan, D.F., Vasquez, D.S., Juguilon, H., Panda, S., Shaw, R.J., Thompson, C.B., and Evans, R.M. (2009). AMPK regulates the circadian clock by cryptochrome phosphorylation and degradation. Science 326, 437–440.

Lamia, K.A., Papp, S.J., Yu, R.T., Barish, G.D., Uhlenhaut, N.H., Jonker, J.W., Downes, M., and Evans, R.M. (2011). Cryptochromes mediate rhythmic repression of the glucocorticoid receptor. Nature 480, 552–556.

Lastdrager, J., Hanson, J., and Smeekens, S. (2014). Sugar signals and the control of plant growth and development. J Exp Bot. 65, 799-807.

Lee, E.C., Yu, D., Martinez de Velasco, J., Tessarollo, L., Swing, D.A., Court, D.L., Jenkins, N.A., and Copeland, N.G. (2001) A highly efficient Escherichia coli-based chromosome engineering system adapted for recombinogenic targeting and subcloning of BAC DNA. Genomics. 73, 56-65.

Lee, J.-H., Terzaghi, W., Gusmaroli, G., Charron, J.-B.F., Yoon, H.-J., Chen, H., He, Y.J., Xiong, Y., and Deng, X.W. (2008). Characterization of Arabidopsis and rice DWD proteins and their roles as substrate receptors for CUL4-RING E3 ubiquitin ligases. Plant Cell. 20, 152–167.

Lee, M.N., Ha, S.H., Kim, J., Koh, A., Lee, C.S., Kim, J.H., Jeon, H., Kim, D.H., Suh, P.G., and Ryu, S.H. (2009). Glycolytic flux signals to mTOR through glyceraldehyde-3-phosphate dehydrogenase-mediated regulation of Rheb. Mol Cell Biol. 29, 3991–4001.

Lee, S.E., Elphick, L.M., Kramer, H.B., Jones, A.M., Child, E.S., Anderson, A.A., Bonnac, L., Suwaki, N., Kessler. B.M., Gouverneur. V., and Mann, D.J. (2011) The chemoselective one-step alkylation and isolation of thiophosphorylated cdk2 substrates in the presence of native cysteine. Chembiochem. 12, 633-640.

Lee, J.O., Lee, S.K., Kim, N., Kim, J.H., You, G.Y., Moon, J.W., Jie, S., Kim, S.J., Lee, Y.W., Kang, H.J., Lim, Y., Park ,S.H., and Kim, H.S. (2013). E3 ubiquitin ligase, WWP1, interacts with AMPKα2 and down-regulates its expression in skeletal muscle C2C12 cells. J Biol Chem. 288, 4673–4680.

Lee, M.E., Rusin, S.F., Jenkins, N., Kettenbach, A.N., and Moseley, J.B. (2018). Mechanisms connecting the conserved protein kinases Ssp1, Kin1, and Pom1 in fission yeast cell polarity and division. Curr Biol. 28, 84-92.

Le Guen, L., Thomas, M., Bianchi, M., Halford, N.G., and Kreis, M. (1992) Structure and expression of a gene from Arabidopsis thaliana encoding a protein related to SNF1 protein kinase. Gene. 120, 249-254.

Lemoine, R., La Camera, S., Atanassova, R., Dédaldéchamp, F., Allario, T., Pourtau, N., Bonnemain, J.L., Laloi, M., Coutos-Thévenot, P., Maurousset, L., Faucher, M., Girousse, C., Lemonnier, P., Parrilla,

J., and Durand, M. (2013) Source-to-sink transport of sugar and regulation by environmental factors. Front Plant Sci. 4, 272.

Leprivier, G., Remke, M., Rotblat, B., Dubuc, A., Mateo, A.-R.F., Kool, M., Agnihotri, S., El-Naggar, A., Yu, B., Somasekharan, S.P., et al. (2013). The eEF2 kinase confers resistance to nutrient deprivation by blocking translation elongation. Cell 153, 1064–1079.

Lermontova, I., Schubert, V., Börnke, F., Macas,J., and Schubert, I. (2007) Arabidopsis CBF5 interacts with the H/ACA snoRNP assembly factor NAF1. Plant Mol Biol. 65, 615-626.

Le Roux, F., Binesse, J., Saulnier, D., and Mazel, D. (2007) Construction of a Vibrio splendidus mutant lacking the metalloprotease gene vsm by use of a novel counterselectable suicide vector. Appl Environ Microbiol. 73, 777-784.

Li, X.F., Li, Y.J., An, Y.H., Xiong, L.J., Shao, X.H., Wang, Y., and Sun, Y. (2009). AKINβ1 is involved in the regulation of nitrogen metabolism and sugar signaling in Arabidopsis. J Integr Plant Biol. 51, 513-520.

Li, Y., Xu, S., Mihaylova, M.M., Zheng, B., Hou, X., Jiang, B., Park, O., Luo, Z., Lefai, E., Shyy, J.Y.J., Gao, B., Wierzbicki, M., Verbeuren, T.J., Shaw, R.J., Cohen, R.A., and Zang, M. (2011). AMPK phosphorylates and inhibits SREBP activity to attenuate hepatic steatosis and atherosclerosis in diet-induced insulin-resistant mice. Cell Metab. 13, 376-388.

Li, Z., Peng, J., Wen, X., and Guo, H. (2013) Ethylene-insensitive3 is a senescence-associated gene that accelerates age-dependent leaf senescence by directly repressing miR164 transcription in Arabidopsis. Plant Cell. 25, 3311-3328.

Li, J., Li, S., Wang, F., and Xin, F. (2017) Structural and biochemical insights into the allosteric activation mechanism of AMP-activated protein kinase. Chem Biol Drug Des. 89, 663-669.

Liang, J., Shao, S.H., Xu, Z.X., Hennessy, B., Ding, Z., Larrea, M., Kondo, S., Dumont, D.J., Gutterman, J.U., Walker, C.L., et al. (2007). The energy sensing LKB1-AMPK pathway regulates p27(kip1) phosphorylation mediating the decision to enter autophagy or apoptosis. Nat Cell Biol. 9, 218–224.

Liang, T., Mei, S., Shi, C., Yang, Y., Peng, Y., Ma, L., Wang, F., Li, X., Huang, X., Yin, Y., and Liu, H. (2018). UVR8 Interacts with BES1 and BIM1 to regulate transcription and photomorphogenesis in Arabidopsis. Dev Cell. 44, 512-523.

Liao, C.Y., Smet, W., Brunoud, G., Yoshida, S., Vernoux, T., and Weijers, D. (2015) Reporters for sensitive and quantitative measurement of auxin response. Nat Methods. 12, 207-110.

Lillo, C., Meyer, C., Lea, U.S., Provan, F., and Oltedal, S. (2004) Mechanism and importance of post-translational regulation of nitrate reductase. J Exp Bot. 55, 1275-1282.

Lim, C.T., Kola, B., and Korbonits, M. (2010). AMPK as a mediator of hormonal signalling. J Mol Endocrinol. 44, 87-97.

Lin, S.C., and Hardie, D.G. (2017) AMPK: Sensing glucose as well as cellular energy status. Cell Metab. 27, 299-313.

Liu, Y., and Bassham, D.C. (2010). TOR is a negative regulator of autophagy in Arabidopsis thaliana. PLoS One. 5, e11883.

Liu, J., Ishitani, M., Halfter, U., Kim, C.S., and Zhu. J.K. (2000) The Arabidopsis thaliana SOS2 gene encodes a protein kinase that is required for salt tolerance. Proc Natl Acad Sci USA. 97, 3730-3734.

Liu, S., Li, X., Zhang, L., Jiang, J., Hill, R.C., Cui, Y., Hansen, K.C., Zhou, Z.H., and Zhao, R. (2017) Structure of the yeast spliceosomal postcatalytic P complex. Science. 358, 1278-1283.

Lo, W.S., Duggan, L., Emre, N.C., Belotserkovskya, R., Lane, W.S., Shiekhattar, R., and Berger, S.L. (2001) Snf1–a histone kinase that works in concert with the histone acetyltransferase Gcn5 to regulate transcription. Science 293, 1142–1146.

Lo, W.S., Gamache, E.R., Henry, K.W., Yang, D., Pillus, L., and Berger, S.L. (2005) Histone H3 phosphorylation can promote TBP recruitment through distinct promoter-specific mechanisms. EMBO J. 24, 997–1008.

Logemann, E., Wu, S.C., Schröder, J., Schmelzer, E., Somssich, I.E., and Hahlbrock, K. (1995) Gene activation by UV light, fungal elicitor or fungal infection in Petroselinum crispum is correlated with repression of cell cycle-related genes. Plant J. 8, 865-876.

Lovas, A.,Sós-Hegedűs,A.,Bimbó, A.,and Bánfalvi, Z.(2003).Functional diversity of potato SNF1-related kinases tested in Saccharomyces cerevisiae. Gene 321, 123-129.

Lumbreras, V., Alba, M.M., Kleinow, T., Koncz, C., and Pagès, M. (2001) Domain fusion between SNF1-related kinase subunits during plant evolution. EMBO Rep. 2, 55-60.

Lu, C.-A., Lin, C.-C., Lee, K.-W., Chen, J.-L., Huang, L.-F., Ho, S.-L., Liu, H.-J., Hsing. Y.-I., and Yu. S.-M. (2007). The SnRK1A protein kinase plays a key role in sugar signaling during germination and seedling growth of rice. Plant Cell 19, 2484–2499.

Lu, J.Y., Lin, Y.Y., Sheu, J.C., Wu, J.T., Lee, F.J., Chen, Y., Lin, M.I., Chiang, F.T., Tai, T.Y., Berger, S.L., Zhao, Y., Tsai, K.S., Zhu, H., Chuang. L.M., and Boeke, J.D. (2011) Acetylation of yeast AMPK controls intrinsic aging independently of caloric restriction. Cell. 146, 969-979.

Lumba, S., Tsuchiya, Y., Delmas, F., Hezky, J., Provart, N.J., Shi Lu. Q., McCourt, P., and Gazzarrini, S. (2012) The embryonic leaf identity gene FUSCA3 regulates vegetative phase transitions by negatively modulating ethylene-regulated gene expression in Arabidopsis. BMC Biol. 10, 8.

Lunn, J.E., Delorge, I., Figueroa, C.M., Van Dijck. P, and Stitt. M. (2014). Trehalose metabolism in plants. Plant J. 79, 544–567.

Ma, X.M., and Blenis, J. (2009). Molecular mechanisms of mTOR-mediated translational control. Nature Rev Mol Cell Biol. 10, 307-318.

Ma, J., Hanssen, M., Lundgren, K., Hernández, L., Delatte, T., Ehlert, A., Liu, C.M., Schluepmann, H., Dröge-Laser, W., Moritz, T., Smeekens, S., and Hanson, J. (2011) The sucrose-regulated Arabidopsis transcription factor bZIP11 reprograms metabolism and regulates trehalose metabolism. New Phytol. 191, 733-745.

Mack, H.I.D., Zheng, B., Asara, J.M., and Thomas, S.M. (2012). AMPK-dependent phosphorylation of ULK1 regulates ATG9 localization. Autophagy. 8, 1197–1214.

Mahfouz, M.M., Kim, S., Delauney, A.J., and Verma, D.P.S. (2006). Arabidopsis TARGET of RAPAMYCIN interacts with RAPTOR, which regulates the activity of S6 kinase in response to osmotic stress signals. Plant Cell 18, 477-490.

Mair, A., Pedrotti, L., Wurzinger, B., Anrather, D., Simeunovic, A., Weiste, C., Valerio, C., Dietrich, K., Kirchler, T., Nägele, T., Vicente Carbajosa, J., Hanson, J., Baena-González, E., Chaban, C., Weckwerth, W., Dröge-Laser, W., and Teige, M. (2015) SnRK1-triggered switch of bZIP63 dimerization mediates the low-energy response in plants. 4, e05828.

Margalha, L., Valerio, C., and Baena-González, E. (2016) Plant SnRK1 kinases: Structure, regulation, and function. EXS. 107, 403-438.

Mayer, F.V., Heath, R., Underwood, E., Sanders, M.J., Carmena, D., McCartney, R.R., Leiper ,F.C., Xiao, B., Jing, C., Walker, P.A., Haire, L.F., Ogrodowicz, R., Martin, S.R., Schmidt, M.C., Gamblin, S.J., and Carling, D. (2011) ADP regulates SNF1, the Saccharomyces cerevisiae homolog of AMP-activated protein kinase. Cell Metab. 14, 707-714.

McCartney, R.R., and Schmidt, M.C. (2001) Regulation of Snf1 kinase. Activation requires phosphorylation of threonine 210 by an upstream kinase as well as a distinct step mediated by the Snf4 subunit. J Biol Chem. 276, 36460-36466.

McCartney, R.R., Rubenstein, E.M., and Schmidt, M.C. (2005). Snf1kinase complexes with different beta subunits display stress-dependent preferences for the threeSnf1-activatingkinases. Curr Genet. 47, 335-344.

McCormick, A.J., and Kruger, N.J. (2015). Lack of fructose 2,6-bisphosphate compromises photosynthesis and growth in Arabidopsis in fluctuating environments. Plant J. 81, 670–683.

Mihaylova, M.M., Vasquez, D.S., Ravnskjaer, K., Denechaud, P.-D., Yu, R.T., Alvarez, J.G., Downes, M., Evans, R.M., Montminy, M., and Shaw, R.J. (2011). Class IIa histone deacetylases are hormone-activated regulators of FOXO and mammalian glucose homeostasis. Cell. 145, 607–621.

Miranda, J.A., Avonce, N., Suárez, R., Thevelein, J.M., Van Dijck, P., and Iturriaga, G. (2007) A bifunctional TPS-TPP enzyme from yeast confers tolerance to multiple and extreme abiotic-stress conditions in transgenic Arabidopsis. Planta. 226, 1411-1421.

Mishra, P., and Panigrahi, K.C. (2015) GIGANTEA - an emerging story. Front Plant Sci. 6, 8.

Mizoguchi, T., Wright, L., Fujiwara, S., Cremer, F., Lee, K., Onouchi, H., Mouradov, A., Fowler, S., Kamada, H., Putterill, J., and Coupland. G. (2005) Distinct roles of GIGANTEA in promoting flowering and regulating circadian rhythms in Arabidopsis. Plant Cell. 17, 2255-2270.

Mo, J.-S., Meng, Z., Kim, Y.C., Park, H.W., Hansen, C.G., Kim, S., Lim, D.-S., and Guan, K.-L. (2015). Cellular energy stress induces AMPK-mediated regulation of YAP and the Hippo pathway. Nat Cell Biol. 17, 500–510.

Mohannath, G., Jackel, J.N., Lee, Y.H., Buchmann, R.C., Wang, H., Patil, V., Adams, A.K., and Bisaro, D.M. (2014) A complex containing SNF1-related kinase (SnRK1) and adenosine kinase in Arabidopsis. PLoS One. 9, e87592.

Momcilovic, M., Iram, S.H., Liu, Y., and Carlson, M (2008) Roles of the glycogen-binding domain and Snf4 in glucose inhibition of SNF1 protein kinase. J Biol Chem. 283, 19521–19529.

Moore, B., Zhou, L., Rolland, F., Hall, Q., Cheng, W.H., Liu, Y.X., Hwang, I., Jones, T., and Sheen, J. (2003) Role of the Arabidopsis glucose sensor HXK1 in nutrient, light, and hormonal signaling. Science. 300, 332-336.

Moreno, F., Ahuatzi, D., Riera, A., Palomino, C.A., and Herrero, P. (2005) Glucose sensing through the Hxk2-dependent signalling pathway. Biochem Soc Trans. 33, 265-268.

Mouchiroud, L., Eichner, L.J., Shaw, R.J., and Auwerx, J. (2014). Transcriptional coregulators: fine-tuning metabolism. Cell Metab. 20, 26–40.

Mönke, G., Seifert, M., Keilwagen, J., Mohr, M., Grosse, I., Hähnel, U., Junker, A., Weisshaar, B., Conrad, U., Bäumlein, H., and Altschmied, L. (2012) Toward the identification and regulation of the Arabidopsis thaliana ABI3 regulon. Nucleic Acids Res. 40, 8240-8254.

Muranaka, T., Banno, H., and Machida, Y. (1994) Characterization of tobacco protein kinase NPK5, a homolog of Saccharomyces cerevisiae SNF1 that constitutively activates expression of the glucose-repressible SUC2 gene for a secreted invertase of S. cerevisiae. Mol Cell Biol. 14, 2958-2965.

Murray, S.L., Ingle, R.A., Petersen, L.N., and Denby, K.J. (2007) Basal resistance against Pseudomonas syringae in Arabidopsis involves WRKY53 and a protein with homology to a nematode resistance protein. Mol Plant Microbe Interact. 20, 1431-1438.

Nakamichi, N., Kiba, T., Henriques, R., Mizuno, T., Chua, N.H., and Sakakibara, H. (2010) PSEUDO-RESPONSE REGULATORS 9, 7, and 5 are transcriptional repressors in the Arabidopsis circadian clock. Plant Cell. 22, 594-605.

Németh, K., Salchert, K., Putnoky, P., Bhalerao, R., Koncz-Kálmán, Z., Stankovic-Stangeland, B., Bakó, L., Mathur, J., Ökrész, L., Stabel, S., Geigenberger, P., Stitt, M., Rédei, G.P., Schell, J., and Koncz, C. (1998). Pleiotropic control of glucose and hormone responses by PRL1, a nuclear WD protein, in Arabidopsis. Genes Dev. 12, 3059–3073.

Nietzsche, M., Landgraf, R., Tohge, T., and Börnke, F. (2016). A protein–protein interaction network linking the energy-sensor kinase SnRK1 to multiple signaling pathways in Arabidopsis thaliana. Curr Plant Biol. 5, 36–44.

Noubhani, A., Bunoust, O., Bonini. B.M., Thevelein, J.M., Devin, A., and Rigoulet, M. (2009) The trehalose pathway regulates mitochondrial respiratory chain content through hexokinase 2 and cAMP in Saccharomyces cerevisiae. J Biol Chem. 284, 27229-27234.

Nukarinen, E., Nägele, T., Pedrotti, L., Wurzinger, B., Mair, A., Landgraf, R., Börnke, F., Hanson, J., Teige, M., Baena-Gonzalez, E., Dröge-Laser, W., and Weckwerth, W. (2016) Quantitative phosphoproteomics reveals the role of the AMPK plant ortholog SnRK1 as a metabolic master regulator under energy deprivation. Sci Rep. 6, 31697.

Nunes, C., Primavesi, L.F., Patel, M.K., Martinez-Barajas, E., Powers, S.J., Sagar, R., Fevereiro, P.S., Davis, B.G., and Paul. M.J. (2013) Inhibition of SnRK1 by metabolites: tissue-dependent effects and cooperative inhibition by glucose 1-phosphate in combination with trehalose 6-phosphate. Plant Physiol Biochem. 63, 89–98.

Oakhill, J.S., Chen, Z.P., Scott, J.W., Steel, R., Castelli, L.A., Ling, N., Macaulay, S.L., and Kemp, B.E. (2010). Beta-subunit myristoylation is the gatekeeper for initiating metabolic stress sensing by AMP-activated protein kinase (AMPK). Proc Natl Acad Sci USA. 107, 19237–19241.

O'Brien, M., Kaplan-Levy, R.N., Quon, T., Sappl, P.G., and Smyth, D.R. (2015). PETAL LOSS, a trihelix transcription factor that represses growth in Arabidopsis thaliana, binds the energy-sensing SnRK1 kinase AKIN10. J. Exp Bot. 66, 2475-2485.

Ohashi-Ito, K., and Bergmann, D.C. (2007) Regulation of the Arabidopsis root vascular initial population by LONESOME HIGHWAY. Development. 134, 2959-2968.

Ohta, M., Guo, Y., Halfter, U., and Zhu, J.K. (2003) A novel domain in the protein kinase SOS2 mediates interaction with the protein phosphatase 2C ABI2. Proc Natl Acad Sci USA. 100, 11771-11776.

Paul, M.J. (2008) Trehalose 6-phosphate: a signal of sucrose status. Biochem J. 412, e1-2.

Paul, M.J., and Foyer, C.H. (2001) Sink regulation of photosynthesis. J Exp Bot. 52, 1383-1400.

Pedrotti, L., Weiste, C., Nägele, T., Wolf, E., Lorenzin, F., Dietrich, K., Mair, A., Weckwerth, W., Teige, M., Baena-González, E., and Dröge-Laser. W. (2018) Snf1-RELATED KINASE1-controlled C/S1-bZIP signaling activates alternative mitochondrial metabolic pathways to ensure plant survival in extended darkness. Plant Cell. 30, 495-509.

Peeters, K., Van Leemputte, F., Fischer, B., Bonini, B.M., Quezada, H., Tsytlonok, M., Haesen, D., Vanthienen, W., Bernardes, N., Gonzalez-Blas, C.B., Janssens, V., Tompa, P., Versées, W., and Thevelein, J.M. (2017) Fructose-1,6-bisphosphate couples glycolytic flux to activation of Ras. Nat Commun. 8, 922.

Pfeiffer, A., Janocha, D., Dong, Y., Medzihradszky, A., Schöne, S., Daum, G., Suzaki, T., Forner, J., Langenecker, T., Rempel, E., Schmid, M., Wirtz, M., Hell, R., and Lohmann. J.U. (2016). eLife. 5, e17023.

Piattoni, C.V., Bustos, D.M., Guerrero, S.A., and Iglesias. A.A. (2011). Nonphosphorylating glyceraldehyde-3-phosphate dehydrogenase is phosphorylated in wheat endosperm at serine-404 by an Snf1-related

protein kinase allosterically inhibited by ribose-5-phosphate. Plant Physiol. 156, 1337–1350.

Pierre, M., Traverso, J.A., Boisson, B., Domenichini, S., Bouchez, D., Giglione, C., and Meinnel, T. (2007). N-myristoylation regulates the SnRK1 pathway in Arabidopsis. Plant Cell. 19, 2804–2821.

Pineda, C.T., Ramanathan, S., Fon Tacer, K., Weon, J.L., Potts, M.B., Ou, Y.-H., White, M.A., and Potts, P.R. (2015). Degradation of AMPK by a cancer-specific ubiquitin ligase. Cell. 160, 715–728.

Petitjean, M., Teste, M.A., François, J.M., and Parrou, J.L. (2015) Yeast tolerance to various stresses relies on the trehalose-6P synthase (Tps1) protein, not on trehalose. J Biol Chem. 290, 16177-16190.

Petitjean, M., Teste, M.A., Léger-Silvestre, I., François, J.M., and Parrou, J.L. (2017) A new function for the yeast trehalose-6P synthase (Tps1) protein, as key pro-survival factor during growth, chronological ageing, and apoptotic stress. Mech Ageing Dev. 161, 234-246.

Pulsifer, I.P., Lowe, C., Narayaran, S.A., Busuttil, A.S., Vishwanath, S.J., Domergue, F., and Rowland, O. (2014) Acyl-lipid thioesterase1-4 from Arabidopsis thaliana form a novel family of fatty acyl-acyl carrier protein thioesterases with divergent expression patterns and substrate specificities. Plant Mol Biol. 84, 549-563.

Qiao, H., Shen, Z., Huang, S.S., Schmitz, R.J., Urich, M.A., Briggs, S.P., and Ecker, J.R. (2012) Processing and subcellular trafficking of ER-tethered EIN2 control response to ethylene gas. Science. 338, 390-393.

Radchuk, R., Radchuk, V., Weschke, W., Borisjuk, L., and Weber, H. (2006) Repressing the expression of the SUCROSE NONFERMENTING-1-RELATED PROTEIN KINASE gene in pea embryo causes pleiotropic defects of maturation similar to an abscisic acid-insensitive phenotype. Plant Physiol 140,263-278.

Ramon, M., De Smet, I., Vandesteene, L., Naudts, M., Leyman, B., Van Dijck, P., Rolland, F., Beeckman, T., and Thevelein, J.M. (2009) Extensive expression regulation and lack of heterologous enzymatic activity of the class II trehalose metabolism proteins from Arabidopsis thaliana. Plant Cell Environ. 32, 1015-1032.

Rappsilber, J., Ishihama, Y., and Mann, M. (2003) Stop and go extraction tips for matrix-assisted laser desorption/ionization, nanoelectrospray, and LC/MS sample pretreatment in proteomics. Anal Chem. 75, 663-670.

Reimer, J.J., and Turck, F. (2010) Genome-wide mapping of protein-DNA interaction by chromatin immunoprecipitation and DNA microarray hybridization (ChIP-chip). Part A: ChIP-chip molecular methods. Methods Mol Biol. 631, 139-160.

Robertlee, J., Kobayashi, K., Suzuki, M., and Muranaka, T. (2010) AKIN10, a representative Arabidopsis SNF1-related protein kinase 1 (SnRK1), phosphorylates and downregulates plant HMG-CoA reductase. FEBS Lett. 591, 1159-1166.

Rodrigues, A., Adamo, M., Crozet, P., Margalha, L., Confraria, A., Martinho, C., Elias, A., Rabissi, A., Lumbreras, V., González-Guzmán, M., Antoni, R., Rodriguez, P.L., and Baena-González. E. (2013) ABI1 and PP2CA phosphatases are negative regulators of Snf1-related protein kinase1 signaling in Arabidopsis. Plant Cell. 25, 3871-3884.

Rødkaer, S.V., and Faergeman, N.J. (2014) Glucose- and nitrogen sensing and regulatory mechanisms in Saccharomyces cerevisiae. FEMS Yeast Res. 14, 683-696.

Ross, F.A,, MacKintosh. C., and Hardie, D.G. (2016) AMP-activated protein kinase: a cellular energy sensor that comes in 12 flavours. FEBS J. 283, 2987-3001.

Rudolph, M.J., Amodeo, G.A., Iram, S.H., Hong, S.P., Pirino, G., Carlson, M., and Tong, L. (2007) Structure of the Bateman2 domain of yeast Snf4: dimeric association and relevance for AMP binding. Structure. 15, 65-74.

Rourke, J.L., Hu, Q., and Screaton, R.A. (2018) AMPK and friends: central regulators of β cell biology. Trends Endocrinol Metab. 29, 111-122.

Ruiz, A., Xu, X., and Carlson, M. (2011) Roles of two protein phosphatases, Reg1-Glc7 and Sit4, and glycogen synthesis in regulation of SNF1 protein kinase. Proc Natl Acad Sci USA. 108, 6349-5634.

Ruiz, A., Xu, X., and Carlson, M. (2013) Ptc1 protein phosphatase 2C contributes to glucose regulation of SNF1/AMP-activated protein kinase (AMPK) in Saccharomyces cerevisiae. J Biol Chem. 288, 31052-31058.

Sancak, Y., Bar-Peled, L., Zoncu, R., Markhard, A.L., Nada, S., and Sabatini, D.M. (2010). Ragulator-Rag complex targets mTORC1 to the lysosomal surface and is necessary for its activation by amino acids. Cell. 141, 290–303.

Sanz, P., Viana, R., Garcia-Gimeno, M.A. (2016) AMPK in yeast: The SNF1 (Sucrose Non-fermenting 1) protein kinase complex. EXS. 107, 353-374.

Schaffer, B.E., Levin, R.S., Hertz, N.T., Maures, T.J., Schoof, M.L., Hollstein, P.E., Benayoun, B.A., Banko, M.R., Shaw, R.J., Shokat, K.M., and Brunet, A. (2015). Identification of AMPK phosphorylation sites reveals a network of proteins involved in cell invasion and facilitates large-scale substrate prediction. Cell Metab. 22, 907–921.

Schepetilnikov, M., Dimitrova, M., Mancera-Martínez, E., Geldreich, A., Keller, M., and Ryabova, L.A. (2013) TOR and S6K1 promote translation reinitiation of uORF-containing mRNAs via phosphorylation of eIF3h. EMBO J. 32, 1087-1102.

Schuck, S., Baldwin, I.T., and Bonaventure, G. (2013) HSPRO acts via SnRK1-mediated signaling in the regulation of Nicotiana attenuata seedling growth promoted by Piriformospora indica. Plant Signal Behav. 8, e23537.

Scott, J.W., Oakhill, J.S., and van Denderen, B.J. (2009) AMPK/SNF1 structure: a menage a trois of energy-sensing. Front Biosci. 14, 596-610.

Seo, P.J., Ryu, J., Kang, S.K., and Park, C. M. (2011) Modulation of sugar metabolism by an INDETERMINATE DOMAIN transcription factor contributes to photoperiodic flowering in Arabidopsis. Plant J. 65, 418-429.

Shao, D., Oka, S., Liu, T., Zhai, P., Ago, T., Sciarretta, S., Li, H., and Sadoshima, J. (2014). A redox-dependent mechanism for regulation of AMPK activation by Thioredoxin1 during energy starvation. Cell Metab. 19, 232–245.

Shen, W., and Hanley-Bowdoin, L. (2006) Geminivirus infection up-regulates the expression of two Arabidopsis protein kinases related to yeast SNF1- and mammalian AMPK-activating kinases. Plant Physiol. 142, 1642-1655.

Shen, W., Reyes, M.I., and Hanley-Bowdoin, L. (2009) Arabidopsis protein kinases GRIK1 and GRIK2 specifically activate SnRK1 by phosphorylating its activation loop. Plant Physiol. 150, 996-1005.

Shen, W., Dallas, M.B., Goshe, M.B., and Hanley-Bowdoin, L. (2014) SnRK1 phosphorylation of AL2 delays Cabbage leaf curl virus infection in Arabidopsis. J Virol. 8, 10598-10612.

Shi, Y. (2017) Mechanistic insights into precursor messenger RNA splicing by the spliceosome. Nat Rev Mol Cell Biol. 18, 655-670.

Shimobayashi, M., and Hall, M,N, (2014) Making new contacts: the mTOR network in metabolism and signalling crosstalk. Nat Rev Mol Cell Biol. 15, 155–162.

Shin, H.-J.R., Kim, H., Oh, S., Lee, J.-G., Kee, M., Ko, H.-J., Kweon, M.-N., Won, K.-J., and Baek, S.H. (2016). AMPK-SKP2-CARM1 signalling cascade in transcriptional regulation of autophagy. Nature, 534, 553–557.

Shin, J., Sánchez-Villarreal, A., Davis, A.M., Du, S.X., Berendzen, K.W., Koncz, C., Ding, Z., Li, C., and Davis, S.J. (2017) The metabolic sensor AKIN10 modulates the Arabidopsis circadian clock in a light-dependent manner. Plant Cell Environ. 40, 997-1008.

Shukla, V.(2005). Characterization of regulatory roles of DPBF4 and SNF4 in sugar and stress signaling in Arabidopsis. PhD thesis, Universität zu Köln.

Slocombe, S.P., Beaudoin, F., Donaghy, P.G., Hardie, D.G., Dickinson, J.R., and Halford, N.G. (2004). SNF1-related protein kinase (SnRK1) phosphorylates class I heat shock protein. Plant Physiol. Biochem. 42, 111–116.

Son, S., Oh, C.J., and An, C.S. (2014) Arabidopsis thaliana remorins interact with SnRK1 and play a role in susceptibility to Beet Curly Top Virus and Beet Severe Curly Top Virus. Plant Pathol J. 30, 269-278.

Soto-Burgos, J., and Bassham, D.C. (2017) SnRK1 activates autophagy via the TOR signaling pathway in Arabidopsis thaliana. PLoS One. 12, e0182591.

Steinhorst, L., and Kudla, J. (2013). Calcium and reactive oxygen species rule the waves of signaling. Plant Physiol. 163, 471–485.

Stitt, M., and Zeeman, S.C. (2012) Starch turnover: pathways, regulation and role in growth. Curr Opin Plant Biol. 15, 282-292.

Sugden, C., Crawford, R.M., Halford, N.G., and Hardie, D.G (1999a) Regulation of spinach SNF1-related (SnRK1) kinases by protein kinases and phosphatases is associated with phosphorylation of the T loop and is regulated by 5'-AMP. Plant J. 19, 433–439.

Sugden, C., Donaghy, P.G., Halford, N.G., and Hardie, D.G. (1999b). Two SNF1-related protein kinases from spinach leaf phosphorylate and inactivate 3-hydroxy-3-methylglutaryl-coenzyme A reductase, nitrate reductase, and sucrose phosphate synthase in vitro. Plant Physiol. 120, 257–274.

Suttangkakul, A., Li, F., Chung, T., and Vierstra, R.D. (2011). The ATG1/ATG13 protein kinase complex is both a regulator and a target of autophagic recycling in Arabidopsis. Plant Cell. 23, 3761-3779.

Szczesny, R., Büttner, D., Escolar, L., Schulze, S., Seiferth, A., and Bonas, U. (2010) Suppression of the AvrBs1-specific hypersensitive response by the YopJ effector homolog AvrBsT from Xanthomonas depends on a SNF1-related kinase. New Phytol. 187, 1058-1074.

Suzuki, T., Bridges, D., Nakada, D., Skiniotis, G., Morrison, S.J., Lin, J.D., Saltiel, A.R., and Inoki, K. (2013). Inhibition of AMPK catabolic action by GSK3. Mol. Cell 50, 407–419.

Swisa, A., Granot, Z., Tamarina, N., Sayers, S., Bardeesy, N., Philipson, L., Hodson, D.J., Wikstrom, J.D., Rutter, G.A., Leibowitz, G., Glaser, B., and Dor. Y. (2015) Loss of liver kinase B1 (LKB1) in beta cells enhances glucose-stimulated insulin secretion despite profound mitochondrial defects. J Biol Chem. 290, 20934-20946.

Tanimoto, E. (2005) Regulation of root growth by plant hormones - Roles for auxin and gibberellin. Crit Rev Plant Sci. 24, 249–265.

Thalmann, M., Pazmino, D., Seung, D., Horrer, D., Nigro, A., Meier, T., Kolling, K., Pfeifhofer, H.W., Zeeman, S.C., and Santelia. D. (2016). Regulation of leaf starch degradation by abscisic acid is important for osmotic stress tolerance in plants. Plant Cell 28, 1860–1878.

Thelander, M., Olsson, T., and Ronne, H. (2004) Snf1-related protein kinase 1 is needed for growth in a normal day-night light cycle. EMBO J. 23, 1900–1910.

Toroser, D., Plaut, Z., and Huber, S.C. (2000) Regulation of a plant SNF1-related protein kinase by glucose-6-phosphate. Plant Physiol 123,403–412.

Toyama, E.Q., Herzig, S., Courchet, J., Lewis, T.L., Jr., Losón, O.C., Hellberg, K., Young, N.P., Chen, H., Polleux, F., Chan, D.C., and Shaw, R.J. (2016). AMP-activated protein kinase mediates mitochondrial fission in response to energy stress. Science. 351, 275–281.

Tran, L.S., Nakashima, K., Sakuma, Y., Osakabe, Y., Qin, F., Simpson, S.D., Maruyama, K., Fujita, Y., Shinozaki, K., and Yamaguchi-Shinozaki, K. (2007) Co-expression of the stress-inducible zinc finger homeodomain ZFHD1 and NAC transcription factors enhances expression of the ERD1 gene in Arabidopsis. Plant J. 4, 46-63.

Tsai, A.Y., and Gazzarrini, S. (2012) AKIN10 and FUSCA3 interact to control lateral organ development and phase transitions in Arabidopsis. Plant J. 69, 809-821.

Tsugama, D., Liu, S., and Takano, T. (2012) A putative myristoylated 2C-type protein phosphatase, PP2C74, interacts with SnRK1 in Arabidopsis. FEBS Lett. 586, 693-698.

Tyanova, S., Temu, T., Sinitcyn, P., Carlson, A., Hein, M.Y., Geiger, T., Mann, M., and Cox, J. (2016). The Perseus computational platform for comprehensive analysis of (prote)omics data. Nat Methods. 13, 731-740.

Um, J.H., Yang, S., Yamazaki, S., Kang, H., Viollet, B., Foretz, M., and Chung, J.H. (2007). Activation of 50-AMP-activated kinase with diabetes drug metformin induces casein kinase Iε (CKI-epsilon)-dependent degradation of clock protein mPer2. J Biol Chem. 282, 20794–20798.

Umezawa, T., Nakashima, K., Miyakawa, T., Kuromori, T., Tanokura, M., Shinozaki, K., Yamaguchi-Shinozaki, K. (2010). Molecular basis of the core regulatory network in ABA responses: sensing, signaling and transport. Plant Cell Physiol. 51, 1821–1839.

Usadel, B., Bläsing, O.E., Gibon, Y., Retzlaff, K., Höhne, M., Günther, M., and Stitt, M. (2008). Global transcript levels respond to small changes of the carbon status during progressive exhaustion of carbohydrates in Arabidopsis rosettes. Plant Physiology 146, 1834–1861.

Usaite, R., Jewett, M.C., Oliveira, A.P., Yates, J.R. III., Olsson, L., and Nielsen, J. (2009) Reconstruction of the yeast Snf1 kinase regulatory network reveals its role as a global energy regulator. Mol Syst Biol. 5, 319.

Vandesteene, L., López-Galvis, L., Vanneste, K., Feil, R., Maere, S., Lammens, W., Rolland, F., Lunn, J.E., Avonce, N., Beeckman, T., and Van Dijck, P. (2012) Expansive evolution of the trehalose-6-phosphate phosphatase gene family in Arabidopsis. Plant Physiol. 160, 884-896.

Vila, I.K., Yao, Y., Kim, G., Xia, W., Kim, H., Kim, S.-J., Park, M.-K., Hwang, J.P., González-Billalabeitia, E., Hung, M.-C., Song, S.J., and Song, M.S. (2017). A UBE2O-AMPKα2 axis that promotes tumor initiation and progression offers opportunities for therapy. Cancer Cell 31, 208–224.

Vincent, O., Townley, R., Kuchin, S., and Carlson, M. (2001) Subcellular localization of the Snf1 kinase is regulated by specific beta subunits and a novel glucose signaling mechanism. Genes Dev. 15, 1104-1114.

Vulliamy, T., Beswick, R., Kirwan, M., Marrone, A., Digweed, M., Walne, A., and Dokal, I. (2008) Mutations in the telomerase component NHP2 cause the premature ageing syndrome dyskeratosis congenita. Proc Natl Acad Sci USA. 105, 8073-8078.

Wahl, V., Ponnu, J., Schlereth, A., Arrivault, S., Langenecker, T., Franke, A., Feil, R., Lunn, J.E., Stitt, M., and Schmid, M. (2013) Regulation of flowering by trehalose-6-phosphate signaling in Arabidopsis thaliana. Science. 339, 704-707.

Walther, T., Mtimet, N., Alkim, C., Vax, A., Loret, M.O., Ullah, A., Gancedo, C., Smits, G.J., and François, J.M. (2013) Metabolic phenotypes of Saccharomyces cerevisiae mutants with altered trehalose 6-phosphate dynamics. Biochem J. 454, 227-237.

Wan, L., Xu, K., Wei, Y., Zhang, J., Han, T., Fry, C., Zhang, Z., Wang, Y.V., Huang, L., Yuan, M., Xia, W., Chang, W.C., Huang, W.C., Liu, C.L., Chang ,Y.C., Liu, J., Wu, Y., Jin, V.X., Dai, X., Guo, J., Liu, J., Jiang, S., Li, J., Asara, J.M., Brown, M., Hung, M.C., and Wei, W. (2018) Phosphorylation of EZH2 by AMPK suppresses PRC2 methyltransferase activity and oncogenic function. Mol Cell. 69, 279-291.

Wang, H., Hao, L., Shung, C.Y., Sunter, G., and Bisaro, D.M. (2003) Adenosine kinase is inactivated by geminivirus AL2 and L2 proteins. Plant Cell. 15, 3020-3032.

Wang, X., Niu, Q.W., Teng, C., Li, C., Mu, J., Chua, N.H., and Zuo, J. (2009) Overexpression of PGA37/MYB118 and MYB115 promotes vegetative-to-embryonic transition in Arabidopsis. Cell Res. 19, 224-235.

Wang, W., Xiao, Z.-D., Li, X., Aziz, K.E., Gan, B., Johnson, R.L., and Chen, J. (2015). AMPK modulates Hippo pathway activity to regulate energy homeostasis. Nat Cell Biol. 17, 490–499.

Warden, S.M., Richardson, C., O'Donnell, J. Jr., Stapleton, D., Kemp, B.E., and Witters, L.A. (2001). Post-translational modifications of the β-1 subunit of AMP-activated protein kinase affect enzyme activity and cellular localization. Biochem J. 354, 275–283.

Warming, S., Costantino, N., Court, D.L., Jenkins, N.A., and Copeland, N.G. (2005). Simple and highly efficient BAC recombineering using galK selection. Nucleic Acids Res 33, e36.

Weiste, C., and Dröge-Laser, W. (2014). The Arabidopsis transcription factor bZIP11 activates auxin-mediated transcription by recruiting the histone acetylation machinery. Nature Commun. 5, 3883.

Williams, T., and Brenman, J.E. (2008) LKB1 and AMPK in cell polarity and division. Trends Cell Biol. 18, 193-198.

Wilson, R.A., Gibson, R.P., Quispe, C.F., Littlechild, J.A., and Talbot, N.J. (2010) An NADPH-dependent genetic switch regulates plant infection by the rice blast fungus. Proc Natl Acad Sci USA. 107, 21902-21907.

Wingler, A., Delatte, T.L., O'Hara, L.E., Primavesi, L.F., Jhurreea, D., Paul, M.J., and Schluepmann, H. (2012) Trehalose 6-phosphate is required for the onset of leaf senescence associated with high carbon availability. Plant Physiol. 158, 1241–1251.

Winter, H., and Huber, S.C. (2000) Regulation of sucrose metabolism in higher plants: localization and regulation of activity of key enzymes. Crit Rev Biochem Mol Biol. 35, 253-289.

Woods, A., Dickerson, K., Heath, R., Hong, S.-P., Momcilovic, M., Johnstone, S.R., Carlson, M., and Carling, D. (2005). Ca2+/calmodulin-dependent protein kinase kinase-beta acts upstream of AMP-activated protein kinase in mammalian cells. Cell Metab. 2, 21–33.

Wu, N., Zheng, B., Shaywitz, A., Dagon, Y., Tower, C., Bellinger, G., Shen, C.-H., Wen, J., Asara, J., McGraw, T.E., Kahn, B.B., and Cantley, L.C. (2013). AMPK-dependent degradation of TXNIP upon energy stress leads to enhanced glucose uptake via GLUT1. Mol Cell. 49, 1167–1175.

Wurzinger, B., Nukarinen, E., Nägele, T., Weckwerth, W., and Teige, M. (2018) The SnRK1 kinase as central mediator of energy signaling between different organelles. Plant Physiol. 176, 1085-1094.

Xiao, B., Sanders, M.J., Underwood, E., Heath, R., Mayer, F.V., Carmena, D., Jing, C., Walker, P.A., Eccleston, J.F., Haire, L.F., Saiu, P., Howell, S.A., Aasland, R., Martin, S.R., Carling, D., and Gamblin, S.J. (2011) Structure of mammalian AMPK and its regulation by ADP. Nature. 472, 230-233.

Xiong Y, Sheen J. (2012). Rapamycin and glucose–target of rapamycin (TOR) protein signaling in plants. J Biol Chem 287, 2836-2842.

Xiong, Y., McCormack, M., Li, L., Hall, Q., Xiang, C., and Sheen, J. (2013). Glucose–TOR signalling reprograms the transcriptome and activates meristems. Nature. 496, 181-186.

Xiong, Y., and Sheen, J. (2014). The role of target of rapamycin signaling networks in plant growth and metabolism. Plant Physiol. 164, 499-512.

Xu, J., and Scheres, B. (2005). Dissection of Arabidopsis ADPRIBOSYLATION FACTOR 1 function in epidermal cell polarity. Plant Cell. 17, 525-536.

Xu, X., Chi, W., Sun, X., Feng, P., Guo, H., Li, J., Lin, R., Lu, C., Wang, H., Leister, D., and Zhang, L. (2016) Convergence of light and chloroplast signals for de-etiolation through ABI4-HY5 and COP1. Nat Plants. 2, 16066.

Yadav, U.P., Ivakov, A., Feil, R, Duan, G.Y., Walther, D., Giavalisco, P., Piques, M., Carillo, P. Hubberten, H.-M., Stitt, M., and Lunn, E.J. (2014). The sucrose–trehalose 6-phosphate (Tre6P) nexus: specificity and mechanisms of sucrose signalling by Tre6P. J Exp Bot. 65, 1051–1068.

Yan, C., Wan, R., Bai, R., Huang, G., and Shi, Y. (2017) Structure of a yeast step II catalytically activated spliceosome. Science. 355, 149-155.

Yanagisawa, S., Yoo, S.D., and Sheen, J. (2003) Differential regulation of EIN3 stability by glucose and ethylene signalling in plants. Nature. 425, 521-525.

Yang, W., Hong, Y.H., Shen, X.Q., Frankowski, C., Camp, H.S., and Leff, T. (2001) Regulation of transcription by AMP-activated protein kinase: phosphorylation of p300 blocks its interaction with nuclear receptors. J Biol Chem. 276, 38341-38344.

Yasuda, S., Sato, T., Maekawa, S., Aoyama, S., Fukao, Y., and Yamaguchi, J. (2014). Phosphorylation of Arabidopsis ubiquitin ligase ATL31 is critical for plant carbon/nitrogen nutrient balance response and controls the stability of 14-3-3 proteins. J Biol Chem. 289, 15179–15193.

Yasumura, Y., Pierik, R., Kelly, S., Sakuta, M., Voesenek, L.A., and Harberd, N.P. (2015). An ancestral role for CONSTITUTIVE TRIPLE RESPONSE1 proteins in both ethylene and abscisic acid signaling. Plant Physiol. 169, 283-298.

Yi, C., Tong, J.J., and Yu L. (2018) Mitochondria: The hub of energy deprivation-induced autophagy. Autophagy. 14, 1084-1085.

Yin, Y., Vafeados, D., Tao ,Y., Yoshida, S., Asami, T., and Chory, J. (2005) A new class of transcription factors mediates brassinosteroid-regulated gene expression in Arabidopsis. Cell. 120, 249-259.

Young, N.P., Kamireddy, A., Van Nostrand, J.L., Eichner, L.J., Shokhirev, M.N., Dayn, Y., and Shaw, R.J. (2016). AMPK governs lineage specification through Tfeb-dependent regulation of lysosomes. Genes Dev. 30, 535-552.

Zhai, Z., Liu, H., and Shanklin, J. (2017) Phosphorylation of WRINKLED1 by KIN10 results in its proteasomal degradation, providing a link between energy homeostasis and lipid biosynthesis. Plant Cell. 29, 871-889.

Zhai, Z., Keereetaweep, J., Liu, H., Feil, R., Lunn, J.E., and Shanklin, J. (2018) Trehalose 6-phosphate positively regulates fatty acid biosynthesis by stabilizing WRINKLED1. Plant Cell. 30, 2616-2627.

Zhang, Y., Shewry, P.R., Jones, H., Barcelo, P., Lazzeri, P.A., and Halford, N.G. (2001) Expression of antisense SnRK1 protein kinase sequence causes abnormal pollen development and male sterility in transgenic barley. Plant J. 28, 431-441.

Zhang, N., and Cao L. (2017) Starvation signals in yeast are integrated to coordinate metabolic reprogramming and stress response to ensure longevity. Curr Genet. 63, 839-843.

Zhang, Y., Primavesi, L.F., Jhurreea, D., Andralojc, P.J., Mitchell, R.A., Powers. S.J., Schluepmann. H., Delatte, T., Wingler, A., and Paul, M.J. (2009) Inhibition of SNF1-related protein kinase1 activity and regulation of metabolic pathways by trehalose-6-phosphate. Plant Physiol. 149, 1860–1871.

Zhang, Y.L., Guo, H., Zhang, C.S., Lin, S.Y., Yin, Z., Peng, Y., Luo, H., Shi, Y., Lian, G., Zhang, C., Li, M., Ye, Z., Ye, J., Han, J., Li, P., Wu, J.W., and Lin, S.C. (2013). AMP as a low-energy charge signal autonomously initiates assembly of AXIN-AMPK-LKB1 complex for AMPK activation. Cell Metab. 18, 546–555.

Zhang, C.S., Li, M., Ma, T., Zong, Y., Cui, J., Feng, J.W., Wu, Y.Q., Lin, S.Y., and Lin, S.C. (2016). Metformin activates AMPK through the lysosomal pathway. Cell Metab. 24, 521–522.

Zhang, F., Wang, L., Qi, B., Zhao, B., Ko, E.E., Riggan, N.D., Chin, K., and Qiao, H. (2017) EIN2 mediates direct regulation of histone acetylation in the ethylene response. Proc Natl Acad Sci USA. 114, 10274-10279.

Zeng, P.Y., and Berger, S.L. (2006) LKB1 is recruited to the p21/WAF1 promoter by p53 to mediate transcriptional activation. Cancer Res. 66, 10701–10708.

Zheng, Z., Xu, X., Crosley, R.A., Greenwalt, S.A., Sun, Y., Blakeslee, B., Wang, L., Ni, W., Sopko, M.S., Yao, C., Yau, K., Burton, S., Zhuang, M., McCaskill, D.G., Gachotte, D., Thompson, M., and Greene, T.W. (2010) The protein kinase SnRK2.6 mediates the regulation of sucrose metabolism and plant growth in Arabidopsis. Plant Physiol. 153, 99-113.

Zhou, L., Jang, J.C., Jones ,T.L., and Sheen, J. (1998) Glucose and ethylene signal transduction crosstalk revealed by an Arabidopsis glucose-insensitive mutant. Proc Natl Acad Sci USA. 95, 10294-10299.

Zibrova, D., Vandermoere, F., Göransson, O., Peggie, M., Mariño, K. V., Knierim, A., Spengler, K., Weigert, C., Viollet, B., Morrice, N.A., Sakamoto, K., and Heller, R. (2017). GFAT1 phosphorylation by AMPK promotes VEGF-induced angiogenesis. Biochem J. 474, 983–1001.

Zmijewski, J.W., Banerjee, S., Bae, H., Friggeri, A., Lazarowski, E.R., and Abraham, E. (2010). Exposure to hydrogen peroxide induces oxidation and activation of AMP-activated protein kinase. J Biol Chem. 285, 33154-33164.

6. ACKNOWLEDGEMENTS

I would like to thank Dr. Csaba Koncz for his supervision and guidance of my Ph.D. project. I appreciate his many ideas and suggestions in critical experiments. I am thankful to Prof. Dorothea Bartels for her support to finish my degree successfully. I am thankful to Prof. George Coupland for allowing me to accomplish my Ph.D. project in Max Planck Institute for Plant Breeding Research.

I am grateful to Dr. Hirofumi Nakagami, Dr. Sara Stolze and Anne Harzen for their professional and patient advices in protein isolation and mass spectrometry technologies. I am grateful to my former colleague Dr. Mihály Horváth for his guidance and helpfulness in BAC recombineering. I thank my colleague Dr. Ajit Ghosh for his help with the TPS constructs. I am grateful to Sabine Schäfer for her help in RT-PCR screen. Special thanks to Dr. Zsuzsa Koncz for her education and assistance in scientific activities and life in Germany.

I would like to express my special thanks to Simone Zündorf for the German translation of the Ph.D. abstract. Many thanks to our group members Dr. Ravikumar Mayakrishnan and Dr. Zhoubo Hu and all members of the Department of Plant Developmental Biology at MPIPZ for nice working atmosphere in every aspect.

And last but not least, I will always be in debt with of parents Fulin Bai and Guifen Yin for their love and constant support.